MECHANISM OF PROGRAMMED CELL DEATH IN *XANTHOMONAS*

By

Surbhi Wadhawan

(LIFE01200904005)

Bhabha Atomic Research Centre, Mumbai

A thesis submitted to the

Board of Studies in Life Sciences

In partial fulfilment of requirements

for the Degree of

DOCTOR OF PHILOSOPHY

of

HOMI BHABHA NATIONAL INSTITUTE

October, 2014

Homi Bhabha National Institute

Recommendations of the Viva Voce Committee

As members of the Viva Voce Committee, we certify that we have read the dissertation prepared by Surbhi Wadhawan entitled "Mechanism of Programmed Cell Death In *Xanthomonas*" and recommend that it may be accepted as fulfilling the thesis requirement for the award of Degree of Doctor of Philosophy.

Doctoral committee

S. No.	Name	Designation	Signature	Date
1.	Dr. S. K. Apte	Chairman		
2.	Dr. A. K. Sharma	Guide & Convener		
3.	Dr. S Gautam	Co-Guide		
4.	Dr. Vinay Kumar	Member		
5.	Dr. H. S. Misra	Member		
6.	Dr. Santosh Kumar	Member		
7.	Dr. Rakesh Bhatnagar	External examiner		

Final approval and acceptance of this thesis is contingent upon the candidate's submission of the final copies of the thesis to HBNI.

I/We hereby certify that I/we have read this thesis prepared under my/our direction and recommend that it may be accepted as fulfilling the thesis requirement.

Date:

Place:

GUIDE **CO-GUIDE**

STATEMENT BY AUTHOR

This dissertation has been submitted in partial fulfilment of requirements for an advanced degree at Homi Bhabha National Institute (HBNI) and is deposited in the Library to be made available to borrowers under rules of the HBNI.

Brief quotations from this dissertation are allowable without special permission, provided that accurate acknowledgement of source is made. Requests for permission for extended quotation from or reproduction of this manuscript in whole or in part may be granted by the Competent Authority of HBNI when in his or her judgment the proposed use of the material is in the interests of scholarship. In all other instances, however, permission must be obtained from the author.

SURBHI WADHAWAN

DECLARATION

I, hereby declare that the investigation presented in the thesis has been carried out by me. The work is original and has not been submitted earlier as a whole or in part for a degree / diploma at this or any other Institution / University.

SURBHI WADHAWAN

List of Publications Arising from the Thesis

Journal

1. **Wadhawan S**, Gautam S, Sharma A. Involvement of Proline Oxidase (PutA) in Programmed Cell Death of *Xanthomonas.* PLoS ONE, 2014, 9(5):e96423.

2. **Wadhawan S**, Gautam S, Sharma A. Bacteria undergo programmed cell death upon low dose gamma radiation exposure. Int.J.Curr.Microbiol.App.Sci. 2014, 3(12):276-283.

3. **Wadhawan S**, Gautam S, and Sharma A. A component of gamma radiation induced cell death in *E. coli* is programmed and interlinked with activation of caspase-3 and SOS response. Archives of Microbiology, 2013, 195(8):545-57.

4. **Wadhawan S**, Gautam S, and Sharma A. Metabolic stress induced programmed cell death in *Xanthomonas*. FEMS Microbiology Letters, 2010, 312(2): 176-183.

Chapter(s) in Book

1. Sharma A, Gautam S., and **Wadhawan S**. *Xanthomonas*. In: Batt, C.A., Tortorello, M.L. (Eds.), Encyclopedia of Food Microbiology, vol 3. Elsevier Ltd, Academic Press, pp. 811–817.

BARC Newsletter

1. **Wadhawan S,** Gautam S., and Sharma, A. Radiation induced cell death in bacteria is partially programmed. BARC Newsletter. Oct. 2013, 348-354.

Conferences

- **Wadhawan S,** Gautam S., and Sharma, A. Does UV radiation induce programmed cell death in *E. coli*? Life Science Symposium on "Advances in Microbiology of Food, Agriculture, Health and Environment", NPCIL, Mumbai, Feb. 2015.

- **Wadhawan S,** Gautam S., and Sharma, A. Radiation induced cell death in bacteria is partially programmed. XXXVI All India Cell Biology Conference and International Symposium on "Stress Adaptive Response and Genome Integrity (SARGI)", Mumbai, Oct. 2012, 130 ***(Best poster award)*****.**

- Sharma A, Gautam S, and **Wadhawan S.** Reactive oxygen species: Role in bacterial Programmed Cell Death. The International conference SFRR 2011, Recent Trends in Therapeutic Advancement of Free Radical Science, Chennai, Jan. 2011, 44.

- **Wadhawan S,** Gautam S, and Sharma A. Involvement of oxidative stress during programmed cell death in *Xanthomonas*. Proceedings of "50th Annual Conference of Association of Microbiologists of India (Third Golden Era of Microbiology)" Pune, Dec. 2009, 175.

- **Wadhawan S,** Gautam S, and Sharma A. Role of PutA (proline oxidase) in programmed cell death (PCD) of stressed *Xanthomonas campestris* cells. Abstract accepted for poster presentation in the 6th Congress of European Microbiologists (FEMS 2015) to be held in Maastricht, the Netherlands in June, 2015.

DEDICATIONS

I dedicate this work to my family

ACKNOWLEDGEMENTS

I extend my heartfelt gratitude to my guide Dr. A. K. Sharma and co-guide Dr. S. Gautam for their guidance and support throughout the course of this study. I am also immensely grateful to all my doctoral committee members - Dr. S. K. Apte, Dr. H.S. Misra, Dr. Vinay Kumar, Dr. Santosh Kumar, Dr. M. V. Hosur and Dr. T. P. A. Devasagayam for their valuable suggestions, constructive criticism and feedback which helped in improving this work.

I sincerely acknowledge Dr. J Maxwell Dow, Department of Microbiology, National University of Ireland for gifting us *Xanthomonas campestris* pv. *campestris* strain 8004.

I appreciate and thank all my friends and colleagues - Dr. S. N. Hajare, Mr. S. Saxena, Mr. S. Kumar, Mrs. V. More, Dr. R. Shashidhar, Dr. M. N. Karani, Mr. A. P. Janardhan, Dr. A. K. Shrivastav, Mrs. A. Rai and Mrs. N. C. Bandyopadhyay who have helped me in some way or other. I also thank our technical team – Mrs. V. B. Gaonkar, Mrs. N. V. Bhadrige and Mr. A. K. Chaubey.

I can never thank enough my better half, Akshay, for his constant support and encouragement. I would also like to thank my loving daughter, Mrigakshi, whose unconditional love and beautiful smile is a perpetual source of rejuvenation for me. Last but not the least, I express my gratitude to my parents, sisters and in-laws for their love and unrelenting support.

CONTENTS

Homi Bhabha National Institute

SYNOPSIS OF Ph. D. THESIS

1. Name of student:	Ms. Surbhi Wadhawan
2. Name of the Constituent Institution:	Bhabha Atomic Research Centre
3. Enrolment no.:	LIFE01200904005
4. Title of the thesis:	Mechanism of programmed cell death in *Xanthomonas*
5. Board of studies:	Life Sciences

Introduction

In the past couple of decades, several studies have demonstrated existence of programmed cell death (PCD) in a number of unicellular eukaryotes including *Trypanosoma*, *Leishmania*, *Plasmodium* and *Sacharromyces*, as well as, in some prokaryotic organisms (Gautam et al.,2005; Gautam and Sharma, 2005; Bayles, 2014). Among prokaryotes, PCD is known to occur during sporulation and mother cell lysis of *Bacillus*, myxobacterial fruiting body formation, under salt stress in *Anabaena*, and metabolic stress in *Xanthomonas campestris* (Gautam and Sharma, 2002a,b; Gautam and Sharma, 2005; Gautam et al., 2005; Raju et al., 2006; Bayles, 2014). PCD has been reported to play a vital role in bacterial stress response (Bayles, 2014).

Xanthomonas is a Gram negative, aerobic plant pathogenic bacterium having a capsular envelop of xanthan, composed of pentasaccharide repeat units of glucose, mannose and

glucuronic acid (García-Ochoa et al., 2000). Xanthan has wide industrial applications in food and oil industry. In an earlier study from this laboratory, *Xanthomonas* displayed atypical growth in protein rich Luria Bertani (LB) medium where it showed rapid cell death just after log phase without any noticeable stationary phase, whereas, in a carbohydrate rich starch medium it showed the usual bacterial growth pattern with lag, log, and a prolonged stationary phase followed by death (Gautam and Sharma, 2002a,b). Later, while studying this medium dependent differential survival, *Xanthomonas* was found to undergo PCD in LB medium, where it displayed many important markers of apoptosis as reported in eukaryotic cells (Gautam and Sharma, 2002a,b; Gautam and Sharma, 2005). In the due course of study, some metabolites like alanine, glycine, pyruvate, citrate and malate were found to induce PCD in non-inducing conditions, whereas, others like glucose, starch and cAMP inhibited this process (Raju et al., 2006).

The objectives of the study were:

a) To investigate the mechanism of PCD induction in *Xanthomonas* under certain nutrient conditions.

b) Study the impact of different physico-chemical stresses on the PCD profile of *Xanthomonas* and other bacteria.

MATERIALS AND METHODS

Bacterial strains and growth conditions

Xanthomonas strains were grown at 26 ± 2° C in a rotary shaker at 150 rpm in Luria-Bertani (LB) broth {PCD inducing medium (PIM)}, or starch broth (SB) {PCD non-inducing medium (PNIM}. All *E. coli* strains, *Bacillus subtilis* (ATCC6633), *Bordetella*

bronchiseptica (NCIM 2267) and *Salmonella enterica* sv. Typhimurium were grown in LB medium on a rotary shaker (150 rpm) at 37± 2 ºC for 3-5 h. The cell number was enumerated by the standard plate count method.

Quantification of intracellular NADH, ADP and ATP

Alkaline extraction of NADH was carried out using the protocol of Caruso *et al*., 2004. Acid extraction of ATP and ADP was carried out based on the method described previously (Giannattasio et al., 2003). The samples in both the cases were filtered through 0.22 μm filter (Millipore, USA) and analyzed using HPLC.

Analysis of reactive oxygen species (ROS) generation

(A) 2',7'-Dichlorohydrofluorescein diacetate (H_2DCFDA) staining of cells: This dye gets oxidized inside the cells upon ROS generation, forming an intracellular fluorescent DCF (dichlorofluorescein) molecule and the brightly fluorescent cells were observed under a fluorescent microscope.

(B) Electron Spin Resonance (ESR) spectroscopy: Hydroxyl radical ($OH^{\cdot}$) formation inside the cells during the course of PCD was detected with an ESR based spin trapping system, which contained 10 mM α-(4-pyridyl-1-oxide)-N-tert-butyl-nitrone (POBN). The POBN adduct displays a spectrum consisting of triplet of a doublet.

(C) Scopoletin assay: Intracellular H_2O_2 level was measured using fluorogenic substrate scopoletin (2.5 μM) and horseradish peroxidase (5 U/ml) as detected by the decrease in fluorescence intensity.

Measurement of intracellular proline levels and proline oxidase (PutA) activity

Intracellular proline levels were determined in Xcc cells as mentioned before (Bates et al., 1973) using acidic ninhydrin and glacial acetic acid. The reaction mixture was extracted with 2 ml toluene and the absorbance was read at 520 nm using UV–visible spectrophotometer. The proline oxidase activity was assayed in 24 h culture of Xcc according to the method described earlier (Dendinger and Brill, 1970). Cells were permeabilized using toluene and the reaction was performed in the presence of L-proline (1M) and 200 µl o-aminobenzaldehyde (50 mM in 20% ethanol) at 26 ± 2 °C for 1h and terminated with trichloroacetic acid (20%). The absorbance of the clear supernatant was measured at 443 nm. PutA activity was also analyzed in the presence of its inhibitor, tetrahydro-2-furoic acid (THFA), and electron transport chain inhibitors rotenone and antimycin.

Construction of *putA* knockout in *Xanthomonas*

A *putA* knockout was constructed by insertional mutagenesis using pKNOCK-Km suicide plasmid (2 kbp) vector (Alexeyev, 1999) in Xcc8004 which was preferred over Xcg because complete genome sequence of Xcc is available. An internal 600 bp region of *putA* gene (complete size ~ 3 kbp) was amplified and cloned in pKNOCK plasmid. This pKNOCK-putA plasmid was used to transform competent *E. coli* PIR1 and later Xcc cells using electroporation. The integration of pKNOCK-putA into the Xcc genome was confirmed by PCR amplification of full length *putA* from the transformed Xcc colony.

Cloning of Xcc *putA* in a broad host range (bhr) shuttle vector and complementation of Xcc Δ*putA* strain

The full length *putA* gene from Xcc was PCR amplified by colony PCR and the PCR product was cloned in pBBR1MCS5-Gm plasmid (Kovach et al., 1995) which was used to transform

E. coli DH5α cells. The transformants were selected on LB-gentamycin plate. XccΔ*putA* strain was further complemented with pPutA purified from transformed *E.coli* cells.

Analysis of PCD markers

a) **TUNEL (Terminal deoxynucleotidyl transferase dUTP nick end labeling) assay:** It was performed according to the manufacturer's guidelines (APO-Direct Kit, BD Pharmingen) to detect DNA nicks.

b) **Phosphatidylserine (PS) externalization:** PS externalization was detected by AnnexinV-FITC labeling followed by Fluorescence Activated Cell Sorting (FACS) analysis. AnnexinV is a 36 kDa Ca^{2+} dependent phospholipid binding protein having high affinity for PS.

c) **Caspase-3 activity assay:** It was performed using synthetic flurogenic substrate Ac-DEVD-AMC as per the method described earlier (Gautam and Sharma, 2002b). The effect of ROS scavengers and an ETC (electron transport chain) uncoupler (2, 4-dinitrophenol) on PCD profile and caspase-3 activity was also monitored.

d) **Analysis of *in situ* active caspase 3-like protein by FITC-DEVD-FMK staining**

The assay was carried out using Caspase-3 detection kit (Catalog no. QIA91, Calbiochem) where cells were labeled with cell permeable FITC-DEVD-FMK stain and visualized by fluorescence microscopy.

Cell filamentation assay

Gamma radiation exposed *E.coli* cells were smeared on a glass slide, air dried, heat fixed, stained with crystal violet and examined under a microscope (Carl Zeiss, Germany) using oil immersion objective (100X). The cells having a length of more than 1µM were considered as filaments.

Immunoblotting

Protein samples for detection of LexA and caspase-3-like protein were subjected to SDS-PAGE followed by Western blotting as described earlier (Gautam and Sharma, 2002b).

RESULTS AND DISCUSSION

Enhanced level of NADH in *Xanthomonas* cells undergoing PCD exhibited metabolic stress

Xanthomonas campestris pv. *glycines* (Xcg) grown in LB medium, hence after referred to as PCD inducing medium or PIM, accumulated intracellular NADH and ATP. This was revealed by comparative HPLC analysis of intracellular NADH and ATP levels in PIM and PNIM grown cells. High intracellular NADH resulted in enhanced reactive oxygen species (ROS) generation in cells grown in PIM as confirmed by 2', 7'- dichlorohydrofluorescein diacetate (H_2DCFDA) labeling and ESR spectroscopy. This eventually resulted in the activation of caspase-3-like protein in Xcg leading to PCD. ROS scavengers like dimethylsulfoxide, glutathione, n-propyl gallate and catalase significantly inhibited PCD, caspase biosynthesis as well as caspase-like enzyme activity in this organism. Enhanced ROS level was conferred as one of the possible reasons contributing to caspase activation. This was confirmed by the addition of an electron transport chain (ETC) uncoupler, 2, 4-dinitrophenol, that reduced ROS generation and increased the cell survival. Thus, these results indicated that Xcg cells grown in PIM experience metabolic stress leading to electron leakage during electron transfer in ETC which leads to generation of ROS and subsequent activation of caspase-3-like protein, resulting in PCD.

Role of proline oxidase (PutA) in regulating PCD in *Xanthomonas*

LB medium has glutamate (15%) and proline (6%) in abundance (BD Bionutrients technical manual, 2006; Sezonov et al., 2007). PCD was induced in *Xanthomonas* when it was grown

in PNIM supplemented with proline. However, this was not the case when *Xanthomonas* was grown in PNIM in the presence of glutamate. Proline being a secondary amino acid is not metabolized by transaminases and carboxylases but is oxidized by PutA {also called as proline oxidase (POX) or proline dehydrogenase (PRODH)} (Liu and Phang, 2012). PutA converts proline to glutamate through an intermediate P5C. Notably, *Xanthomonas* cells grown in PIM were found to accumulate proline and have higher proline oxidase activity. Moreover, cells grown in PNIM in the presence of higher levels of proline were also found to undergo PCD. Tetrahydro-2-furoic acid (5mM), an inhibitor of PutA, was found to prevent PCD in PIM growing Xcc cells. ETC inhibitors rotenone and antimycin were also found to inhibit PutA activity in Xcc. To further confirm the role of PutA in PCD, a *putA* knockout was constructed. Interestingly, PCD was abolished in Xcc Δ*putA* cells, and the phenotype could be further restored upon complementation with a plasmid vector carrying wild type PutA (pPutA). Contrary to Xcc wt cells, Xcc Δ*putA* cells showed diminished ROS generation and reduced caspase-3-like activity as well as PCD inhibition. Xcc wt cells also displayed cell filamentation and *in situ* caspase-3-like activity when treated with a fluorophore tagged caspase-3 inhibitor (FITC-DEVD-FMK). PCD markers like DNA damage (determined by TUNEL assay), phosphatidylserine (PS) externalization and membrane depolarization were significantly less in Xcc Δ*putA* cells with respect to wt cells. The findings indicate that the oxidation of proline by PutA is one of the contributing factors leading to an increase in ROS levels and PCD of stressed *Xanthomonas* cells.

PCD in other bacteria and involvement of ROS

To evaluate the conserved existence of PCD-like process in other bacteria besides *Xanthomonas*, the study was performed in *Bacillus subtilis*, *Bordetella bronchiseptica*, *Escherichia coli* and *Salmonella enterica* sv. Typhimurium. Radiation was used as a means to

generate ROS. Irradiating these bacteria at their respective D_{10} in the presence of Ac-DEVD-CMK and 3-aminobenzamide, the cell permeable inhibitors of caspase-3 and poly (ADP ribose) polymerase (PARP) respectively, increased the cell survival significantly. FACS analysis indicated an increase in phosphatidylserine (PS) externalization in the radiation exposed bacteria and was found to be reduced in the cells pre-incubated with the cell permeable caspase-3 inhibitor. Radiation-induced SOS response in *E.coli* was also alleviated in the presence of caspase-3 inhibitor as indicated by decrease in LexA degradation and reduced cell filamentation frequency. This might indicate a probable linkage between SOS response and PCD in radiation exposed *E. coli* cells and needs to be confirmed by additional evidences.

SUMMARY

Xanthomonas campestris was observed to experience metabolic stress when grown in a medium (like Luria Bertani broth) where amino acids are the predominant source of carbon and nitrogen. Reactive oxygen species (ROS) were found to be produced in *Xanthomonas* cells undergoing PCD in PIM (PCD inducing medium) and leakage of electrons from electron transport chain (ETC) was found to be a possible source of ROS generation. PutA was also found to be involved in PCD of *Xanthomonas* growing in PIM. PutA enzyme activity was found to be linked to ETC resulting in ROS generation during oxidation of proline and induction of PCD in *Xanthomonas.* Besides *Xanthomonas,* PCD was also observed in other bacteria like, *B.subtilis, B. bronchiseptica, E.coli* and *S.* Typhimurium when they were exposed to oxidative stress caused by γ-radiation. Bacteria undergoing radiation induced cell death displayed PS externalization and activation of caspase-3-like protein. The presence of cell permeable caspase-3 inhibitor inhibited these processes resulting

in PCD inhibition. Cell filamentation and LexA degradation were observed in radiation exposed *E.coli* cells indicating activation of SOS pathway.

The present understanding of the mechanism of PCD in *Xanthomonas* is depicted in the figure below:

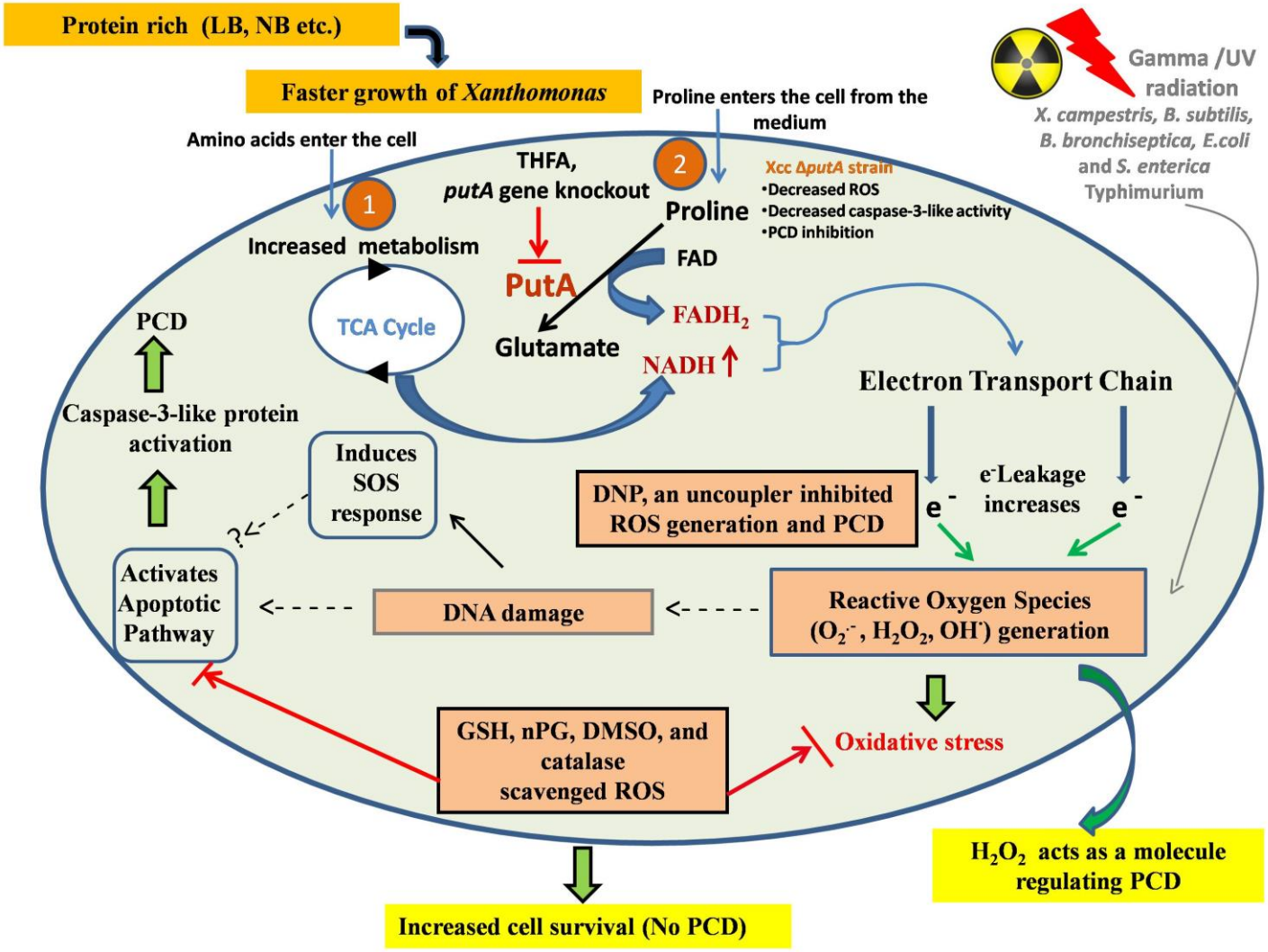

Mechanism of PCD in *Xanthomonas* cells under metabolic stress or *E.coli* and other bacteria upon oxidative stress

CONCLUSION

Metabolism associated stress in *Xanthomonas* cells was found to lead to ROS generation and caspase dependent PCD during which involvement of PutA activity was observed as well. Moreover, other triggers of oxidative stress like radiation treatment also elicited a similar response in different bacteria.

REFERENCES

1. Alexeyev MF (1999) Biotechniques 26: 824-826
2. Bates LS, et al. (1973) Plant soil 39: 205-207
3. Bayles KW (2014) Nat Rev Microbiol 12:63-69
4. BD Bionutrients technical manual (2006) Becton, Dickinson and Company, USA. 53 p
5. Caruso R, et al. (2004) Anal Biochem 330: 43-51
6. Dendinger S, Brill WJ (1970) J Bacteriol 103: 144-152
7. García-Ochoa et al. (2000) Biotechnol Adv 18: 549-579
8. Gautam S, Sharma A (2002a) J Gen Appl Microbiol 48: 67-76
9. Gautam S, Sharma A (2002b) Mol Microbiol 44: 393-401
10. Gautam S, Sharma A (2005) Daya Publishing House, India, pp 122-157
11. Gautam S, et al. (2005) Research Sign Post, India, pp 1-39
12. Giannattasio S, et al. (2003) Brain Res Protoc 10: 168-174
13. Kovach ME, et al. (1995) Gene 166**:** 175-176
14. Liu W, Phang JM (2012) Biofactors 38: 398-406
15. Raju KK, et al. (2006) J Bacteriol 188: 5408-5416
16. Sezonov G, et al. (2007) J Bacteriol 189: 8746-8749

Publications in Refereed Journal:

a. Published

(i) Journals

- **Wadhawan S**, Gautam S, Sharma A. Involvement of Proline Oxidase (PutA) in Programmed Cell Death of *Xanthomonas.* PLoS ONE, 2014, 9(5):e96423.
- **Wadhawan S**, Gautam S, Sharma A. Bacteria undergo programmed cell death upon low dose gamma radiation exposure. 2014, Int.J.Curr.Microbiol.App.Sci. 3(12):276-283.
- **Wadhawan S**, Gautam S, and Sharma A. A component of gamma radiation induced cell death in *E. coli* is programmed and interlinked with activation of caspase-3 and SOS response. Archives of Microbiology, 2013, 195(8):545-57.
- **Wadhawan S**, Gautam S, and Sharma A. Metabolic stress induced programmed cell death in *Xanthomonas*. FEMS Microbiol. Letters., 2010, 312 (2):176-183.

(ii) BARC Newsletter

- **Wadhawan S**, Gautam S., and Sharma, A. Radiation induced cell death in bacteria is partially programmed. BARC Newsletter. Oct. 2013, 348-354.

b. Accepted: Four (published in journals)

c. Communicated: Nil

d. Other Publications: Four (Symposia and Newsletter)

Symposium/ Conference

- **Wadhawan S**, Gautam S., and Sharma, A. Radiation induced cell death in bacteria is partially programmed. XXXVI All India Cell Biology Conference and International Symposium on "Stress Adaptive Response and Genome Integrity (SARGI)", Mumbai, Oct., 2012, 130 ***(Best poster award)***.

- Sharma A, Gautam S, and **Wadhawan S**. Reactive oxygen species: Role in bacterial Programmed Cell Death. The International conference SFRR 2011, Recent Trends in Therapeutic Advancement of Free Radical Science, Chennai, Jan. 2011, 44.
- **Wadhawan S**, Gautam S, and Sharma A. Involvement of oxidative stress during programmed cell death in *Xanthomonas*. Proceedings of "50th Annual Conference of Association of Microbiologists of India (Third Golden Era of Microbiology)" Pune, Dec. 2009, 175.

Signature of Student:

Date:

Doctoral committee

S. No.	Name	Designation	Signature	Date
1.	Dr. S. K. Apte	Chairman		
2.	Dr. A. K. Sharma	Guide & Convener		
3.	Dr. S Gautam	Co-Guide		
4.	Dr. Vinay Kumar	Member		
5.	Dr. H. S. Misra	Member		
6.	Dr. Santosh Kumar	Member		

LIST OF FIGURES

LIST OF TABLES

CHAPTER 1: INTRODUCTION

1.1 Programmed cell death or apoptosis

The term programmed cell death (PCD) refers to the form of cell death which is regulated by intracellular factors. Apoptosis (greek: falling off), considered to be the physiological cell death, is different from accidental or pathological cell death termed necrosis. The process of programmed cell death, or apoptosis, is usually characterized by distinct morphological characteristics (cell membrane blebbing, externalization of phosphatidylserine, and DNA fragmentation) and energy-dependent biochemical mechanisms (activation of caspases).

Programmed cell death (PCD) was first discovered in *C. elegans* by Carl Vogt around the nineteenth century. It was again investigated by Kerr, Wyllie and Currie in 1972 [1]. The Nobel Prize in Physiology or Medicine 2002 was awarded jointly to Sydney Brenner, H. Robert Horvitz and John E. Sulston "for their discoveries concerning genetic regulation of organ development and programmed cell death" in *Caenorhabditis elegans*. Apoptosis is essential for proper development and functioning of the body. It is involved in the embryonic development, functioning of the immune system, and hormone-dependent atrophy. Inappropriate apoptosis (either too little or too much) is a factor in many human ailments including neurodegenerative diseases, ischemic damage, autoimmune disorders and many types of cancer [2] (Elmore, 2007).

In the past couple of decades, several studies have demonstrated the existence of PCD like phenomenon in several unicellular eukaryotes including *Dictyostelium*, *Trypanosoma*, *Leishmania*, *Tetrahymena*, and *Peridinium* as well as in some prokaryotic cells [1,3–5]. Apoptosis associated changes have also been reported in certain groups of fungi like *Aspergillus fumigatus* and yeast, like *Candida albicans* upon oxidative and amphotericin B-mediated stresses [6,7].

PCD has been experimentally proven and established to play vital roles in bacterial developmental processes [3,8]. Some of these include mother cell lysis during sporulation in *Bacillus* [3], vegetative cell lysis during myxobacterial fruiting body formation [3], and salt stress induced PCD in *Anabaena* [9], a cyanobacterium. PCD in bacteria has been proposed to play an altruistic role where defective cells are removed and the nutrients are made accessible to the remaining healthy population.

1.2 Programmed cell death in Archaebacteria

Archaebacteria are the most primitive of all lifeforms and are usually found in extreme environments. They mainly comprise of halophiles, methanogens and thermophiles. Archaebacteria share certain characteristic features with both eubacteria and eukaryotes. They lack a nucleus but their majority proteins involved in replication, transcription and translation have homology to eukaryotic counterparts [10]. Until recently they were considered immortal unless they succumb to death by predators. PCD in archaebacteria like *Haloferax volcanii* under salt stress has recently been reported [11,12]. This archaebacteria exhibits caspase-8 and caspase-4 like activity under salt stress which was inhibited by caspase inhibitor, zVAD-FMK. This activity was also found to be inhibited by EDTA, a metalloprotease inhibitor.

1.3 Programmed cell death in cyanobacteria

Cyanobacteria are photosynthetic microbes, commonly known as 'blue green algae'. They are predominantly present in soil and water bodies as phytoplankton. Cyanobacteria can fix nitrogen as well. Some species (e.g. *Microcystis*) form harmful algal blooms. It has been reported that cyanobacteria like *Microcystis aeruginosa, Trichodesmium,* and *Anabaena*

undergo metacaspase dependent PCD during environmental stress conditions [9,12–15]. *Trichodesmium* forms extensive blooms that may disappear abruptly within 1 to 2 days. Earlier it was thought to be caused by bacteriophage infection, but the work by Berman-Frank et al. [14] has shown that it undergoes autocatalytic PCD due to nutrient deprivation. The deficiency of iron (Fe) and phosphorous (P) was found to initiate PCD in this organism.

1.4 Programmed Cell Death in Eubacteria

Regulation of cell death is essential for living organisms. In eukaryotic cells, apoptotic cell death is essential for embryonic development, for maintenance of normal cell homeostasis, and for elimination of cells damaged by stress or pathogen infection. In bacteria, regulation of cell growth and cell death is also important under various stress conditions [16].

1.5 PCD in *Staphylococcus aureus*: Cid/Lrg Regulatory System

Staphylococcus aureus is a Gram positive cocci commonly found on the skin and in the respiratory tract of humans. The discovery and characterization of the *cid* and *lrg* operons evolved from the initial identification in 1996 of a novel two-component regulatory system from *S. aureus*, termed LytSR, that affected murein hydrolase activity and autolysis. Although the CidA and LrgA proteins are present in most bacteria, their role in PCD of *S. aureus* has been well characterized [17]. They have been recently reported to be integral membrane proteins in this bacterium [18]. *cidA* and *lrgA* encode for holin and anti-holin, respectively [17,18]. One biological function of the *cid* and *lrg* genes is the coordination of cell death and lysis during biofilm development, causing release of genomic DNA (termed as extracellular DNA or eDNA), which eventually becomes a structural component of the biofilm matrix [18]. Rice et al. (2007) reported that the *S. aureus cidA* mutant exhibited

decreased lysis during biofilm formation [19], while the *lrgAB* mutant, as well as the *lytSR* mutant (which exhibits reduced *lrgAB* expression), exhibited increased lysis [20,21]. The consequence of decreased lysis was a decrease in genomic DNA release and biofilm adherence [19]. In contrast, increased cell lysis during biofilm development resulted in increased biofilm adherence [20,21]. Based on their roles in controlling cell death and lysis during biofilm development, it was proposed that these proteins form the regulatory elements of bacterial programmed cell death (PCD). These genes were found to be induced when *S. aureus* was grown in a glucose rich medium that caused production of acetic acid [22]. The murein hydrolase activity of CidA triggers cell lysis. LrgA prevents cell lysis by inhibiting the activity of CidA. It has been reported that the transcription of both *cidABC* and *lrgAB* was induced by growth in the presence of excess glucose, an effect that was shown to be a result of the metabolism of glucose and the subsequent generation of acetic acid (Fig. 1.1 and 1.2) [22]. Interestingly, the *cidC* gene was found to encode a pyruvate oxidase that could contribute to the acetate (and acetic acid) accumulation in the culture medium during growth in excess glucose [22]. Furthermore, cells containing a *cidC* mutation maintained a much higher level of cell viability in stationary phase than did the parental strain when grown in the presence of excess glucose [23]. Recently, it was reported that the drop in pH due to acetic acid production resulted in PCD which was accompanied by ROS generation and DNA damage [22].

Figure 1.1

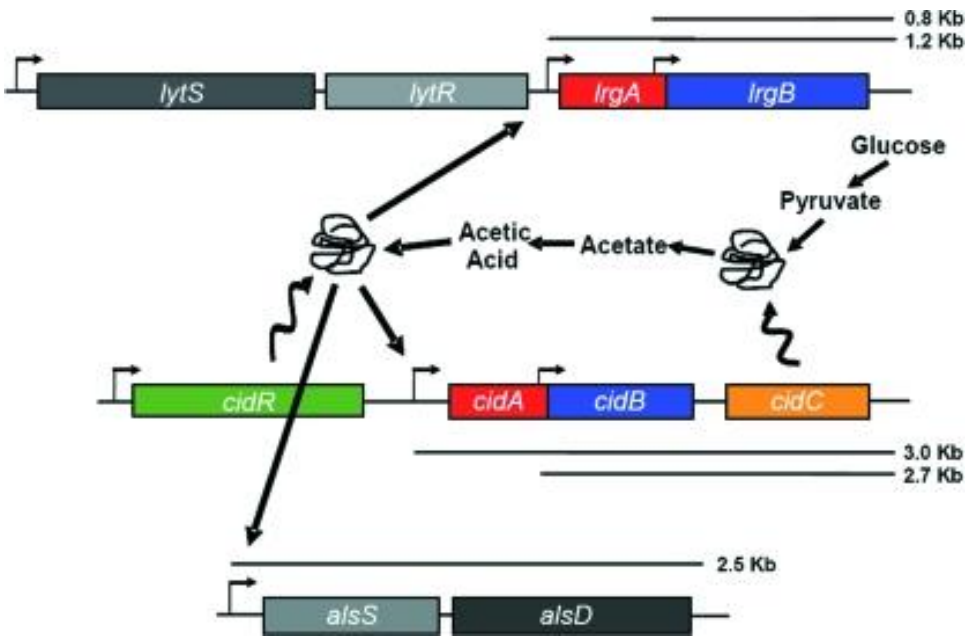

Reference: Rice and Bayles, 2008 [23]

Fig. 1.1: CidR-mediated regulation of holin, antiholin and carbohydrate metabolism. The *cidA* and *lrgA* genes encode homologous hydrophobic proteins believed to function as a holin (toxin) and an antiholin (or antititoxin), respectively. The *cidB* and *lrgB* genes also encode homologous hydrophobic proteins whose functions are unknown. The CidR protein, a LysR-type transcription regulator, enhances the expression of *cidABC*, *lrgAB*, and *alsSD* (encoding acetolactate synthase and acetolactate decarboxylase) in response to carbohydrate metabolism. The *cidC* gene encodes pyruvate oxidase. The transcripts associated with each operon are indicated by black bars [23].

1.6 Analogy of Cid/Lrg Regulatory System with Other Reported Systems

Bax/Bcl-2-mediated control of apoptosis leading to the disruption of mitochondria during the initial stages of apoptosis and the holin/antiholin-mediated control of bacterial death and lysis

have recently led to the hypothesis that these events are analogous, both biochemically and physically, to the events. The Bcl-2 proteins are a large family of proteins that are well conserved in eukaryotic organisms. Similar to holins, Bax can cause mitochondrial membrane permeabilization probably by pore formation involving lipid destabilization (Fig. 1.3). This results in the release of cytochrome c which acts as a trigger to activate the caspase cascade. Like antiholins, Bcl-2 (and related antiapoptotic proteins) can interact with Bax to inhibit the induction of cell death, though the mechanism by which this occurs is still being unravelled (Fig. 1.3) [17,23].

Like many other reported systems of PCD, the Cid/Lrg system has been found to be associated with carbohydrate metabolism. The metabolism of glucose appears to play a central role in the control of cid/lrg expression and in cell death [22,23]. *S. aureus* metabolizes glucose in the presence of oxygen via glycolysis and inhibits the tricarboxylic acid (TCA) cycle, resulting in the secretion of large amounts of acetate into the growth medium (Fig. 1.2) [17,22,23]. The bacteria succumb to acidic milieu. The fate of pyruvate in bacteria (whether it is converted to acetic acid or acetoin) appears to be a key determinant in the decision between life and death (Fig. 1.2), similar to the role that the pyruvate dehydrogenase complex has in controlling the commitment to apoptosis [24–26].

Similar observation has been reported in the case of tumour cells which preferentially metabolize glucose at a higher rate by glycolysis. This observation led to the hypothesis that tumour cells alter metabolism, leading to "aerobic glycolysis" or the "Warburg effect" [25,26]. Recent studies have indicated that the mitochondria in tumour cells undergo a physiological or metabolic "remodelling" that promotes glycolysis rather than mitochondrial glucose oxidation (involving TCA cycle and ETC) [26]. This phenotype of preferential glucose metabolism is used as a marker for detection of cancer cells by PET scan. It is

proposed that the functioning of glycolysis is essential early in the transformation of a cell, which typically occurs in a hypoxic environment prior to vascularisation [27]. Interestingly, it was observed that this glycolytic phenotype is associated with the suppression of apoptosis and resistance to the acidosis produced as a consequence of increased lactic acid generation [28]. Indeed, it is thought that during carcinogenesis, tumour cells "evolve" phenotypic adaptations to the toxic effects of acidosis, culminating in resistance to apoptosis [26].

Thus, in both prokaryotes and eukaryotes, evidence suggests that rapid growth is fuelled by glycolysis and that pyruvate metabolism plays a critical role in the control of cell death (Fig. 1.3) [23].

Figure 1.2

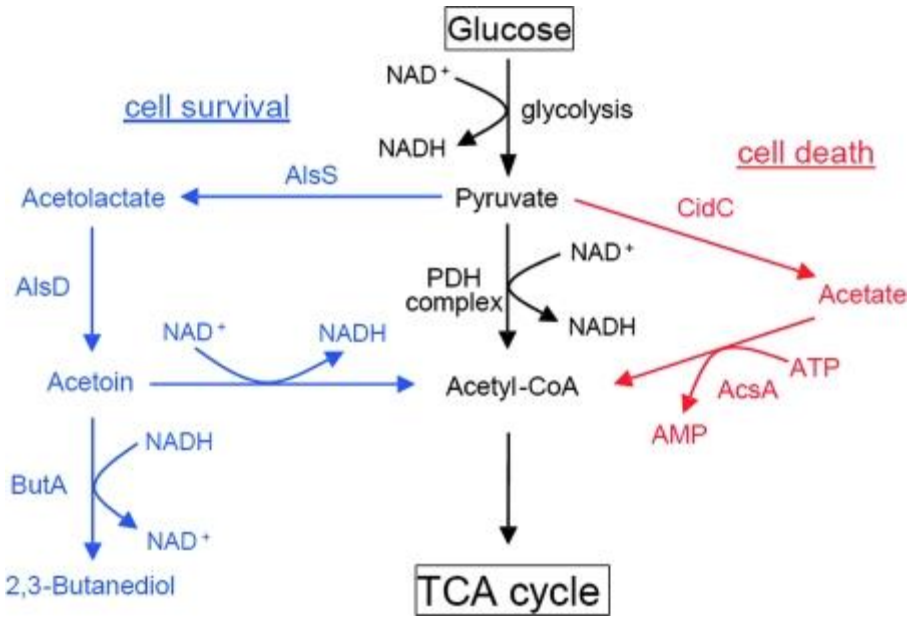

Reference: Rice and Bayles, 2008 [23]

Fig. 1.2: Conversion of pyruvate to acetyl-CoA in *S. aureus*. A major pathway involved in the conversion of pyruvate to acetyl-CoA (shown in black) in bacteria requires the pyruvate dehydrogenase (PDH) complex. Other pathways involved include the AlsSD pathway (blue)

and the CidC pathway (red), which appear to promote cell survival and death, respectively. Enzymes contributing to these pathways include acetolactate synthase (AlsS), acetolactate decarboxylase (AlsD), pyruvate oxidase (CidC), and acetyl-CoA synthetase (AcsA). Also shown is the conversion of acetoin to 2,3-butanediol, requiring the enzyme acetoin reductase (ButA) [23].

Figure 1.3

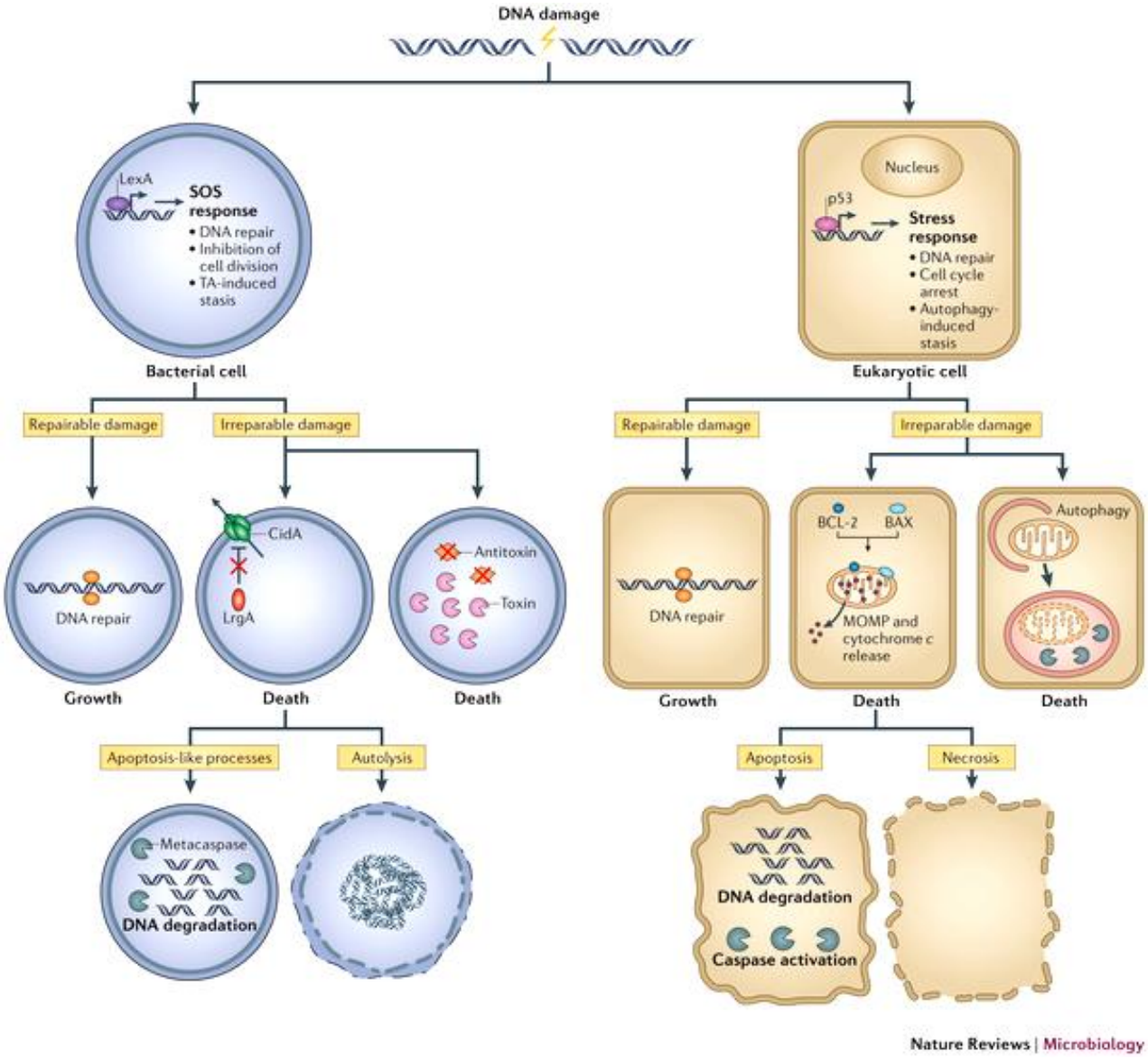

Reference: Bayles, 2014 [17]

Fig. 1.3: Similarities of PCD mechanism in bacteria and eukaryotes: Cell stress, such as that elicited by DNA-damaging agents, induces a response programme that includes DNA-repair mechanisms and cell death pathways. This response includes mechanisms to inhibit cell division, which directs all available resources to repair the damage. If the levels of damage are minimal, the repair mechanisms will be sufficient to restore the cell to working

order. Similar to the role of p53 in assessing the extent of damage in eukaryotic cells and then coordinating an appropriate response, it was thought that the LexA regulator of the SOS response has a role in coordinating the response to DNA damage in bacteria. In both cases, the processes that result in the recycling of cytoplasmic components (such as toxin–antitoxin (TA) systems in bacteria and autophagy in eukaryotes) are supposed to promote DNA repair. If the damage is irreparable, the repair processes will be nullified leading to programmed cell death. CidA–LrgA-induced cell permeabilization and lysis occurs in bacteria and B cell lymphoma 2 (BCL-2) protein family-induced death (including mitochondrial outer membrane permeabilization (MOMP) and cytochrome c release) is induced in eukaryotes. Alternatively, TA system-induced death (in bacteria) or autophagic death (in eukaryotes) can also be triggered. Finally, post-mortem events are activated, such as those that are associated with apoptosis and necrosis in eukaryotes, and those that are associated with apoptosis-like processes and autolysis in bacteria [17].

1.7 Toxin-antitoxin Modules in Bacteria

The role of toxin-antitoxin module has been well established in bacterial PCD. The TA systems are not essential for cell growth but are considered to play important roles in survival under stress conditions. This module comprises of a pair of closely linked genes that encode a toxin and an antitoxin. The toxin is always a protein, whereas, antitoxin can either be a protein or anti-sense RNA. These were first observed in *E. coli* on low copy number plasmids found to be responsible for post-segregational killing. When the cells lose these plasmids, the cured cells are selectively killed by the toxin because the antitoxin is relatively less stable and is degraded faster [29–31]. Thus the cells harbouring such systems were ‘addicted’ to the short-lived antitoxin and their *de novo* synthesis was found to be essential for cell survival

resulting in development of the concept of 'addiction modules' which were implicated in maintaining the stability of extrachromosomal elements. The toxin targets any one of the following cellular processes: DNA replication, mRNA stability, protein synthesis, ATP synthesis or cell wall synthesis [16]. The toxin-antitoxin modules are classified into five types depending on the mechanism of their genetic regulation and also on the nature of antitoxin [32,33]. The antitoxin can prevent the lethal action of toxin in following ways:

(a) Type I

Type I antitoxins are antisense RNAs with short half-life. They work by base pairing with the stable toxin RNA thereby preventing toxin's expression. Examples include *symR/symE, tisB/istR-111, ibs/sib* and hok (host killing)/sok (suppression of killing). The hok/sok genes are encoded by plasmid R1 (Fig. 1.4). In this case regulation is slightly more complex. The RNA antitoxin sok is expressed from a strong promoter but the transcript has a very short half-life of around 30 sec. In contrast, the hok mRNA is expressed from a very weak promoter but has a half-life of ~20 min. The hok transcript shows extensive secondary structure and the 3′ end folds back to the 5′ end. The folded full-length hok mRNA is neither accessible for the ribosome nor the Sok-RNA antitoxin. Processing by RNase II removes a part of the 3′ terminus causing a major structural rearrangement including the 5′ part of the hok mRNA. This allows translation but also binding of the Sok-RNA. However, the Sok antisense-RNA does not show complementarity to the Shine-Dalgarno sequence of hok. Interestingly, the *hok*/*sok* locus contains in addition to the *hok* toxin and *sok* antitoxin a third gene called *mok* for modulator of killing, which overlaps almost the entire *hok* gene. Analysis of point mutations revealed that prevention of *mok* translation abolished efficient expression of *hok*, indicating that the *hok* and *mok* open reading frames are translationally coupled and that the Sok-RNA regulates *hok* translation indirectly by preventing translation of *mok*.

Finally, the hok mRNA/Sok-RNA hybrids are cleaved by RNase III, which is the initial step for decay of the hok mRNA [32]. However, for some type I modules like txpA/ratA18, bsrG/sr419, and yonT/as-yonT18 of *Bacillus subtilis* cleavage of double-stranded RNA regions created by binding of the antitoxin RNA to the toxin mRNA by RNase III is crucial for regulation of toxin expression.

Figure 1.4

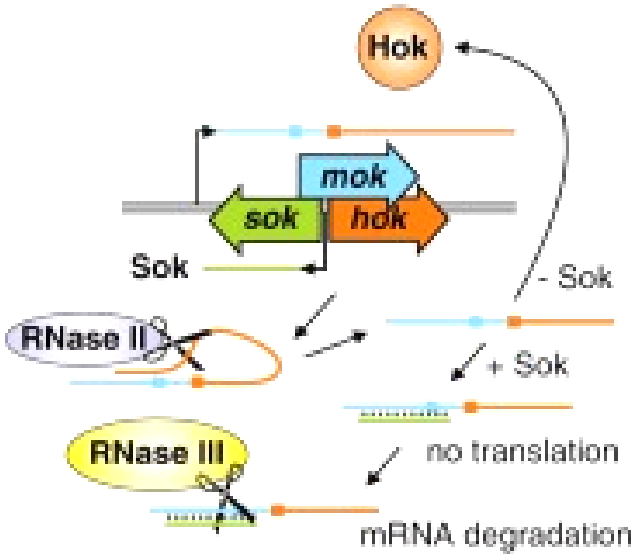

Reference: Unterholzner et al, 2013 [32].

Fig. 1.4: Regulation of the type I system hok/sok of plasmid R1. The toxin and its encoding gene are shown in orange while the antitoxin and its encoding gene are shown in green.

(b) Type II

Unlike Type I, here both toxin as well as antitoxin is protein. This is the best studied type of all TA systems. The antitoxin forms a protein-protein complex with the toxin and inhibits its action. The antitoxin is comparatively labile and is degraded by cellular proteases [Clp (caseinolytic protease) or Lon] under stress conditions, thereby, releasing the toxin leading to either bacteriostasis or cell death. Some examples of type II include *mazE/F, relB/E,*

parD/E, mqsR/A, vapB/C, higA/higB and *yefM/*yoeB [16,32,34,35]. The operon of type II TA modules typically comprises two open reading frames where the upstream gene usually encodes the antitoxin. However, exceptions of this conserved gene organization are known, for instance the *higB/higA* TA module, where the toxin gene higB is located upstream of the antitoxin gene higA. Another TA pair, MazEF has been studied in great detail in *E. coli*. It mediates cell death under various stress conditions like amino acid starvation, antibiotic treatment, inhibition of transcription or translation, DNA damage (by mitomycin C or UV irradiation) and oxidative stress. Under these conditions, MazE (antitoxin) is degraded by cellular proteases releasing MazF to exert its endoribonucleolytic activity on mRNAs (Fig 1.5) [30]. MazF endoribonuclease preferentially cleaves single-stranded mRNAs at ACA sequences [30]. Recently, it was shown that a pentapeptide (Asn-Asn-Trp-Asn-Asn), also known as extracellular death factor (EDF) was required for *mazEF* mediated cell death [36–38]. This pentapeptide was found to induce the endoribonucleolytic activities of two toxins: MazF and ChpBK [39]. It has been reported that the genes specifying MazEF, the glucose-6-phosphate dehydrogenase, and ClpXP protease are critical in EDF production [37].

Figure 1.5

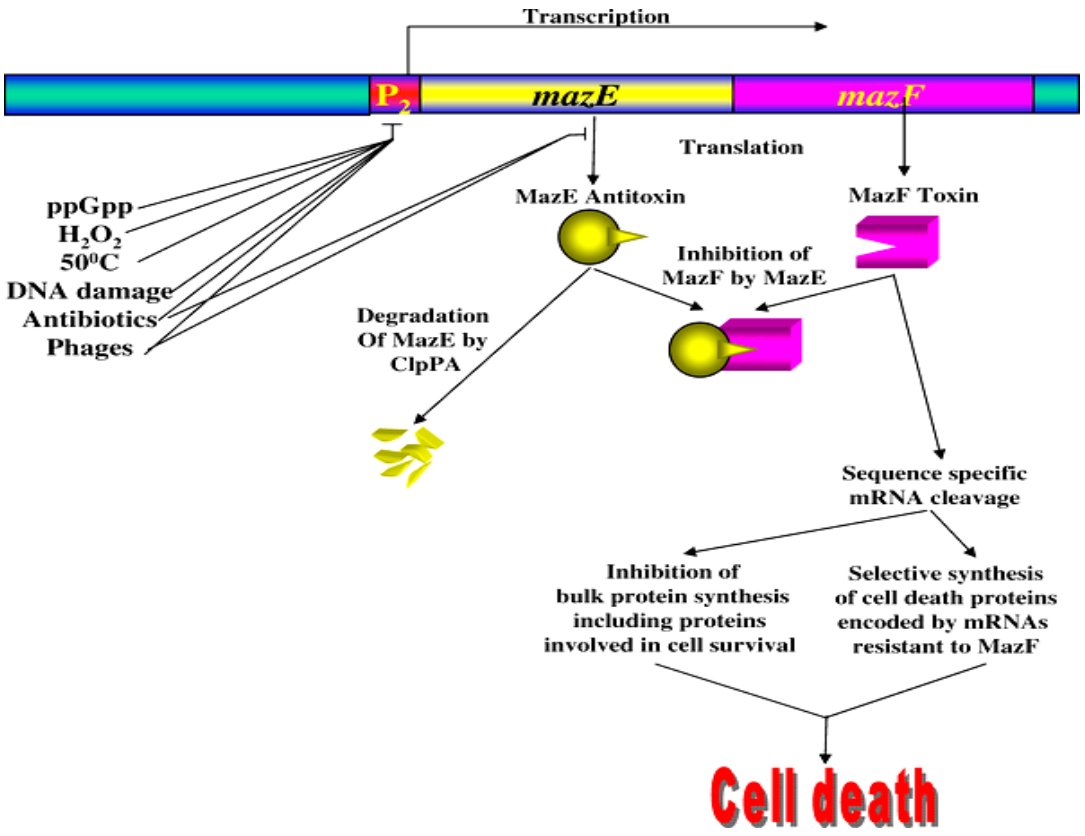

Reference: Engelberg-Kulka et al., 2006 [30]

Fig. 1.5: MazEF toxin antitoxin system in *E. coli*

Typically, transcription of the TA operon is autoregulated by binding of the antitoxin or by the toxin–antitoxin complex to the promoter. Depending on the stoichiometric ratio of the antitoxin to the toxin several types of complexes may be formed with distinct affinities to the promoter. For example, in an excess of RelB over RelE dimers of RelB (RelB2) and the 2:1 complex RelB2RelE are formed, both of which inhibit the *relB/relE* promoter (Fig. 1.6). The RelB2RelE has a stronger inhibitory effect on the *relB/relE* promoter than RelB2 and thus RelE acts as a transcriptional co-repressor [32]. On the contrary, in an excess of RelE the 2:2

complex (RelB2RelE2) is formed, which cannot bind the promoter and, consequently, transcription is activated. This mode of regulation is frequently called conditional cooperativity and is believed to be important for stabilization of the antitoxin level in rapidly growing cells to minimise random induction of relB/relE [32]. Also other TA systems including *phd-doc* from the *E.coli* bacteriophage P137 and *vapB/vapC* of *Salmonella enterica* are regulated by conditional cooperativity.

Figure 1.6

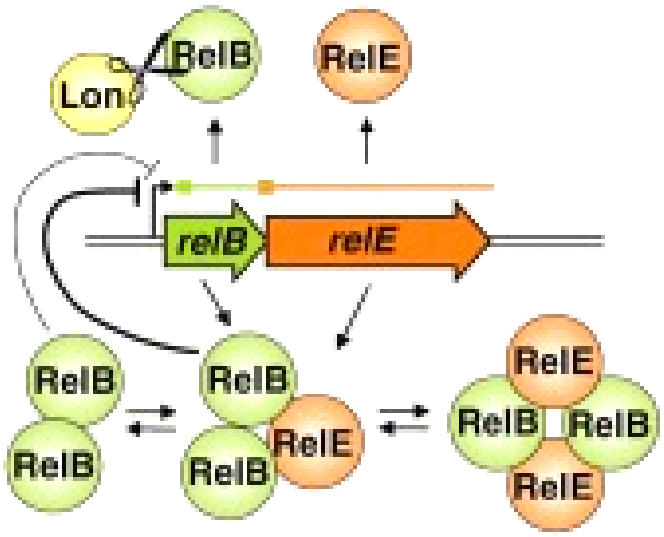

Reference: Unterholzner et al, 2013 [32].

Fig. 1.6: The *relB/E* TA module type II system from *E. coli.* The toxin and its encoding gene are shown in orange while the antitoxin and its encoding gene are shown in green.

(c) Type III

Similar to type I systems, the antitoxin of type III modules is RNA. Type III toxin-antitoxin systems encode protein toxins that are inhibited by pseudoknots of antitoxin RNA [40]. Type III TA loci were first isolated and defined as abortive infection (Abi) systems, protecting

bacterial populations from bacteriophage assault [41]. Within each Type III locus, a toxin gene is preceded by a short palindromic repeat, which is itself preceded by a tandem array of nucleotide repeats. The short palindromic repeat acts as a transcriptional terminator, regulating the relative levels of antitoxic RNA and toxin transcript [41]. The first reported Type III TA system, ToxIN, was encoded on plasmid pECA1039 of the Gram-negative phytopathogen, *Pectobacterium atrosepticum* [40,41]. This locus encodes a 19.7-kDa toxic protein, ToxN, and upstream of ToxN is a repetitive array containing 5.5 tandem repeats of a 36 nt sequence, collectively known as the ToxI antitoxin (Fig. 1.7). Through genetic studies, it was predicted that each 36 nt ToxI RNA repeat was able to inhibit the activity of ToxN [41]. The crystal structure of the ToxI/N complex revealed a heterohexameric triangular assembly of three ToxN proteins interspersed by three, 36 nt, ToxI RNA pseudoknots (Fig. 1.7). ToxN was demonstrated to be an endoribonuclease, related in structure to the endoribonucleases Kid and MazF [40].

Figure 1.7

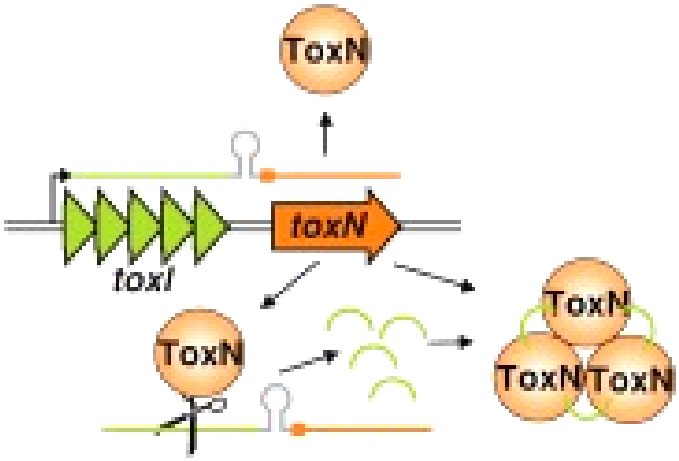

Reference: Unterholzner et al., 2013 [32].

Fig. 1.7: The *toxI/N* type III system from the *Erwinia carotovora* plasmid pECA1039. The toxin and its encoding gene are shown in orange while the antitoxin and its encoding gene are shown in green.

Recently, Samson and co-workers reported AbiQ system of *Lactococcus lactis* to behave as type III TA module [42,43]. AbiQ is a phage resistance mechanism found on a native plasmid pSRQ900 of *Lactococcus lactis* that abort virulent phage infections. The two components of the AbiQ system are *antiQ* repeats (antitoxin) and *abiQ* gene (encoding ABIQ endoribonuclease or toxin) [42]. The AbiQ system was found to be active against members of the common 936 and c2 phage groups as well as rare lactococcal phage groups [42,43]. It has also been demonstrated that the free toxin can cleave, through its endoribonuclease activity, the cognate antitoxins [42,43] as well as housekeeping bacterial RNA molecules [42,43] leading to cell death. During the phage infection process, this TA interaction is likely to be disrupted, leading to cell death and abortion of the phage infection.

(d) Type IV

A type IV TA system designation was proposed for the *yeeU/yeeV* (also named *cbtA/cbeA*) TA module of *E. coli* [44]. The functional analysis of this TA module revealed that the toxin YeeV interacts with cytoskeletal proteins MreB and FtsZ and thereby interferes with their polymerization (Fig. 1.8). The YeeU antitoxin protein counteracts YeeV by stabilizing MreB and FtsZ polymers (Fig. 1.8). A similar mode of action was also reported for cptA/cptB (ygfX/ygfY), another TA module of *E. coli* [45]. YgfX is the first membrane associating toxin in bacterial TA systems [45].While the toxin and antitoxin of all other TA classes interact either at the RNA or the protein level, the toxin and antitoxin of this TA class do not directly interact.

Figure 1.8

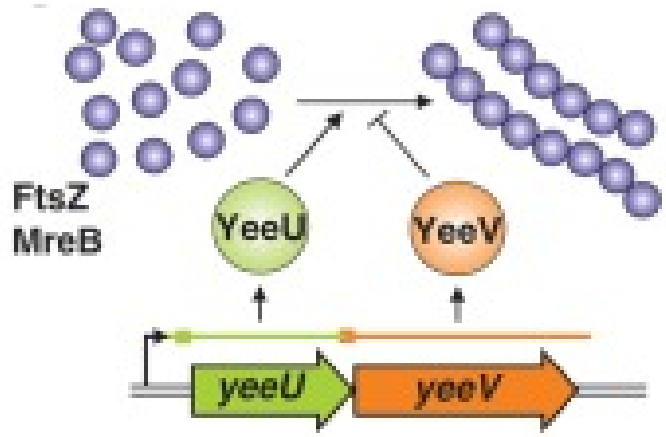

Reference: Unterholzner et al., 2013 [32]

Fig. 1.8: Type IV YeeU/V TA module of *E. coli*. The toxin and its encoding gene are shown in orange while the antitoxin and its encoding gene are shown in green.

(e) Type V

Recently, the *ghoS/ghoT* TA module of *E. coli* was designated as a type V TA system wherein the protein antitoxin (GhoS) inhibits the toxin by cleaving specifically its mRNA. (Fig. 1.9) [46]. GhoT (toxin) is a membrane lytic peptide that causes ghost cell formation (lysed cells with damaged membranes) and increases the population of persister cells (i.e. cells that are tolerant to antibiotics without undergoing genetic change) [46].The antitoxin protein GhoS has a sequence specific endoribonuclease activity for the cleavage of the GhoT toxin mRNA, and thereby prevents the translation of the toxin. The authors further revealed the NMR structure of GhoS indicating it to be related to the CRISPR-associated-2 RNase.

Figure 1.9

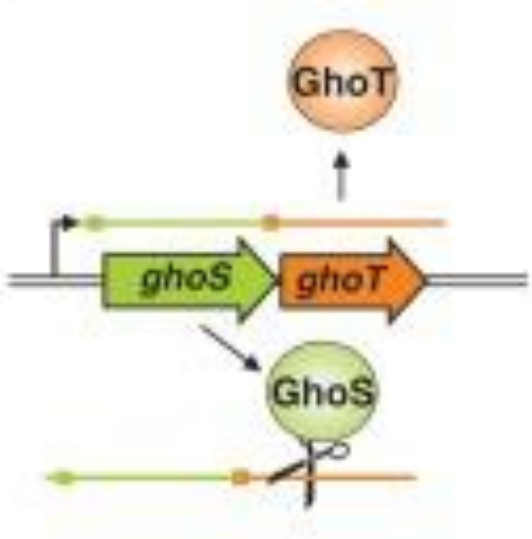

Reference: Unterholzner et al., 2013 [32].

Fig. 1.9: The type V GhoS/T TA module of *E. coli.* The toxin (GhoT) and its encoding gene are shown in orange while the antitoxin (GhoS) and its encoding gene are shown in green.

Toxin-antitoxin system has been implicated in the generation of "persisters," i.e. a subfraction of the population that is characterized by low growth and high resistance to antibiotics [47]. By adapting a mixed strategy in which some cells are specialized for growth while others are specialized for persistence, the culture can insure itself against a sudden loss [32].

1.8 Programmed Cell Death in *Streptococcus pneumoniae*: Fratricide

Streptococcus pneumoniae is a Gram positive pathogenic bacterium that causes pneumonia in humans. Although PCD in bacteria was initially thought to play an altruistic role wherein death of a few cells could benefit their kin, later, in certain bacterial populations undergoing cell death some cells in the population were reported to kill other sibling cells. One recently

identified example of this kind of cell death is the phenomenon of fratricide during competence development of *S. pneumoniae*. The ability of a population of *S. pneumoniae* cells to become competent is regulated by the ComDE two-component regulatory system (Fig 1.10 and 1.12) [48,49]. Induction of the competent state turns on the expression of proteinaceous toxins that lyse non-competent clones that are present in the same niche (Fig 1.10). The accumulation of a peptide pheromone called competence-stimulating peptide (CSP) (encoded by the comC gene), which is secreted by the growing *S. pneumoniae* culture, is sensed by ComD (a membrane-bound histidine kinase). When the extracellular concentration of CSP reaches a threshold level, it binds to ComD and triggers its autophosphorylation. The phosphoryl group is then transferred to the cognate response regulator ComE, which in turn upregulates the expression of the "early" com genes. One of these early com genes encodes sigma factor X (ComX), which subsequently regulates the expression of the "late" com genes, including the genes necessary for DNA binding, uptake, and recombination. Although this developmental process has been well studied for many decades, relatively little was known about how donor DNA was made available during competence development in the environment. A breakthrough in this field was made when it was shown, by measuring the release of either β-galactosidase or chromosomal DNA into the culture supernatant, that a lysing subpopulation of cells appeared during natural competence development in *S. pneumoniae* [50]. The emergence of this lysing subpopulation is dependent on the ComCDE regulatory system and results in the release of chromosomal DNA that could be used as a source of donor DNA for natural transformation [50] (Fig 1.10 and 1.12).

It was also shown by co-cultivation experiments using mutants deficient in various components of the ComCDE system that two populations of cells are present during competence development: one population of competent, non-lysing cells that lyse the second

population of noncompetent cells [51]. In other words, during competence development, donor DNA is provided by heterolysis/allolysis (lysis of one bacterial cell that is caused by another cell) as opposed to autolysis (lysis of self) [23,23,51]. The phenomenon of competence-induced cell lysis was subsequently named “pneumococcal fratricide,” defined as the intraspecies-specific killing of cells that occurs during the development of competence in *S. pneumoniae* [23].

Figure 1.10

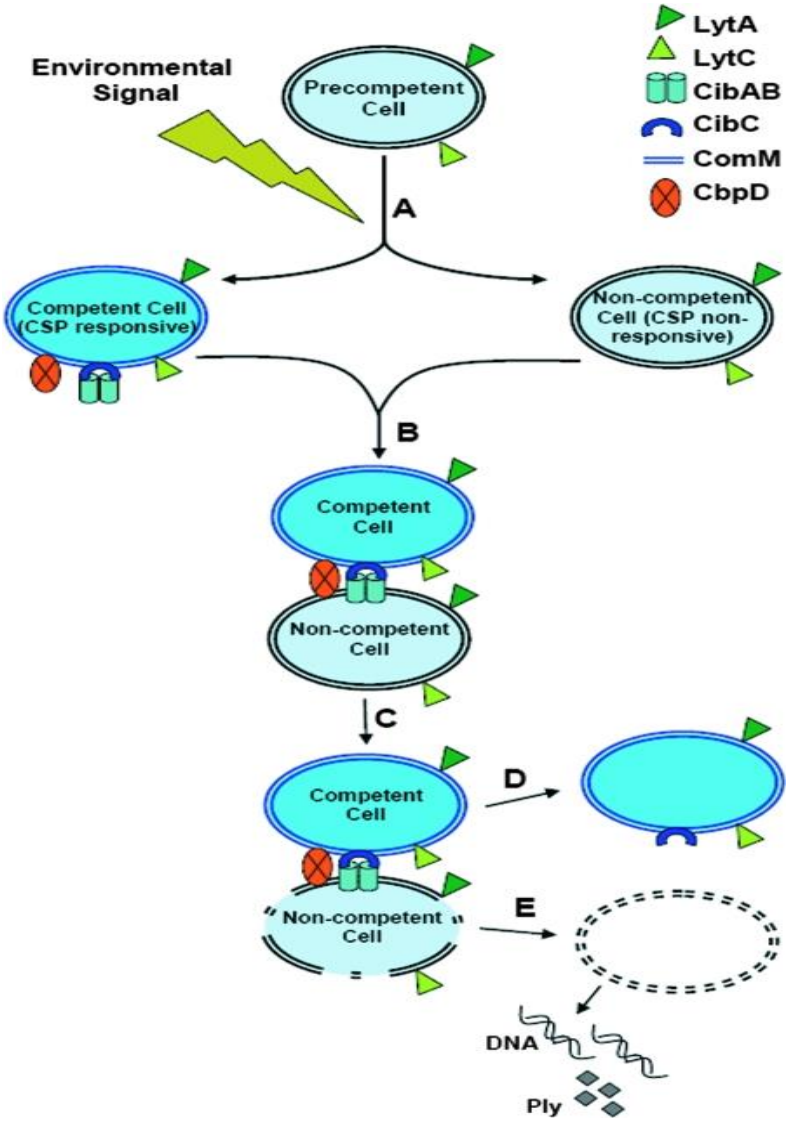

Reference: Rice and Bayles, 2008 [23]

Fig.1.10: Fratricide during competence development in *S. pneumoniae*. (A) An environmental signal(s) leads to the emergence of two subpopulations, competent cells (CSP responsive) and noncompetent cells (CSP nonresponsive), presumably via a bistable regulatory mechanism. Competent cells express the lytic factor CbpD, putative two-peptide bacteriocin CibAB, and immunity proteins ComM and CibC, whereas the murein hydrolases LytA and LytC are expressed by both competent and noncompetent cells. **(B)** Cell-to-cell

contacts between competent and noncompetent cells allow access of CibAB and CbpD to the noncompetent cells. **(C)** CibAB triggers the lytic action of CbpD, LytA, and LytC. **(D)** Competent cells are protected from the actions of these enzymes by the expression of immunity factors CibC and ComM. **(E)** Noncompetent cells lack these immunity proteins and undergo lysis, releasing DNA (used for genetic transformation of competent cells) and virulence factors (Ply) [23].

Interestingly, recent studies of the pyruvate oxidase (encoded by *spxB*) produced by *S. pneumoniae* have also revealed an important role for this enzyme in cell death during stationary phase of his organism [52]. Stationary phase cells harbouring a mutation in *spxB* gene were observed to have increased viability due to the absence of hydrogen peroxide (ROS), generated as a product of this enzyme's activity. Furthermore, the death process induced by hydrogen peroxide exhibited features similar to those of apoptosis in eukaryotic organisms, including alterations in membrane characteristics and increased degradation of DNA.

1.9 Programmed Cell Death in *Bacillus:* Cannibalism

Bacillus is a Gram positive soil bacterium. Cannibalism during *B. subtilis* sporulation is also an example of fratricidal cell killing within a population [23] (Fig. 1.11). Sporulation is a differentiation process whereby a dormant cell (the endospore) is produced which is able to survive harsh environmental conditions till the time growth conditions improve.

Figure 1.11

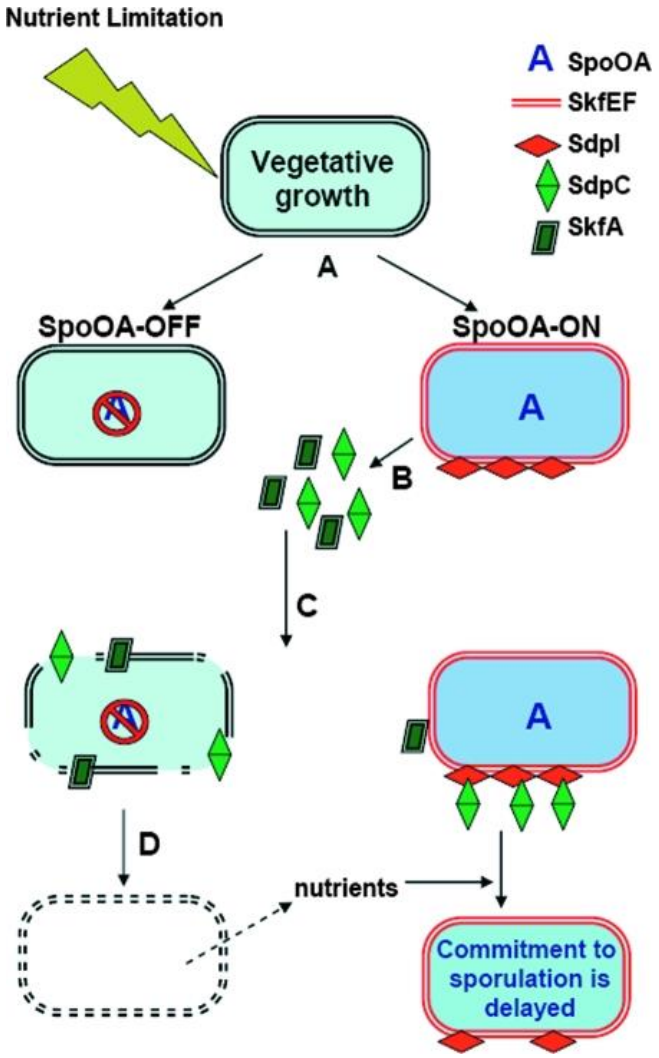

Reference: Rice and Bayles, 2008 [23].

Fig.1.11: Cannibalism during *B. subtilis* sporulation. (A) Nutrient limitation leads to the emergence of two subpopulations, SpoOA-ON (cells that have entered the sporulation pathway but have not yet passed the irreversible stages of sporulation) and SpoOA-OFF (nonsporulating cells), via a bistable regulatory switch. **(B)** SpoOA-ON cells express the killing factors SkfA (sporulating killing factor) and SdpC (sporulating delay protein) as well as their cognate immunity proteins SkfEF and SdpI. **(C)** SpoOA-OFF cells lack the immunity

proteins SkfEF and SdpI and therefore are susceptible to the lethal action of SkfA and SdpC; SpoOA-ON cells are protected from killing by the immunity proteins SkfEF and SdpI. **(D)** SpoOA-ON cells are able to delay their commitment to sporulation by feeding on the nutrients released from their dead siblings (SpoOA-OFF cells) [23].

In *B. subtilis*, sporulation normally occurs as a last-resort response to nutritional stress, but entry into sporulation is also regulated by other signals such as cell density and the cellular redox state [53]. The response regulator protein SpoOA (stage 0 sporulation) acts as master regulator that governs entry into sporulation. The various signals and inputs required for entry of sporulation feed into the SpoOA protein [53]. In a given population of genetically identical cells, only a subset actually initiates sporulation and this developmental process is irreversible once the asymmetrically positioned division septum (separating the prespore and mother cell) is formed [23]. The "decision" by an individual cell to enter into sporulation is regulated by a 'bistable switch' that controls the phosphorylated state of SpoOA and explains why some cells contain active Spo0A and others do not [23,54]. Since this developmental process is very energy consuming, cells need a means to delay spore formation for as long as possible in case the nutritional stress is only short-term. For example, if favourable growth conditions were to resume, cells that have irreversibly committed to sporulation would be at a growth disadvantage relative to vegetative cells that could rapidly reinitiate cell division [23]. A mechanism by which this is accomplished in *B. subtilis*, whereby cells that have entered the sporulation pathway (but not fully committed to sporulation and have not yet crossed the irreversible step of sporulation i.e. engulfment) are able to block sibling cells from sporulating and kill these cells in order to feed on their nutrients, thereby delaying commitment to sporulation, has been identified [55,56]. This mechanism was termed cannibalism and is similar to fratricide in that two groups with distinctive fates ("killer" cells

verses “victim” cells) arise from a genetically identical population of cells [23,48,55]. The operons *skf (*sporulating killing factor) and *sdp* (sporulating delay protein) have high affinity for Spo0A and encode killer proteins SkfA (has high sequence similarity to bacteriocin-like proteins) and SdpC respectively [48,55] (Fig 1.11). Sporulating cells express SkfA and SdpC as well as their cognate immunity proteins SkfEF and SdpI. The non-sporulating cells lack these immunity proteins, and are therefore, susceptible to the lethal action of SkfA and SdpC. The sporulating cells are able to delay their commitment to sporulation by feeding on the nutrients released from their dead siblings (SpoOA-OFF cells) (Fig 1.11 and 1.12). Although the most important stimulus for sporulation in *B. subtilis* is nutritional stress, additional physiological signals, such as high cell density and DNA damage, are also integrated through Spo0A [48].

Figure 1.12

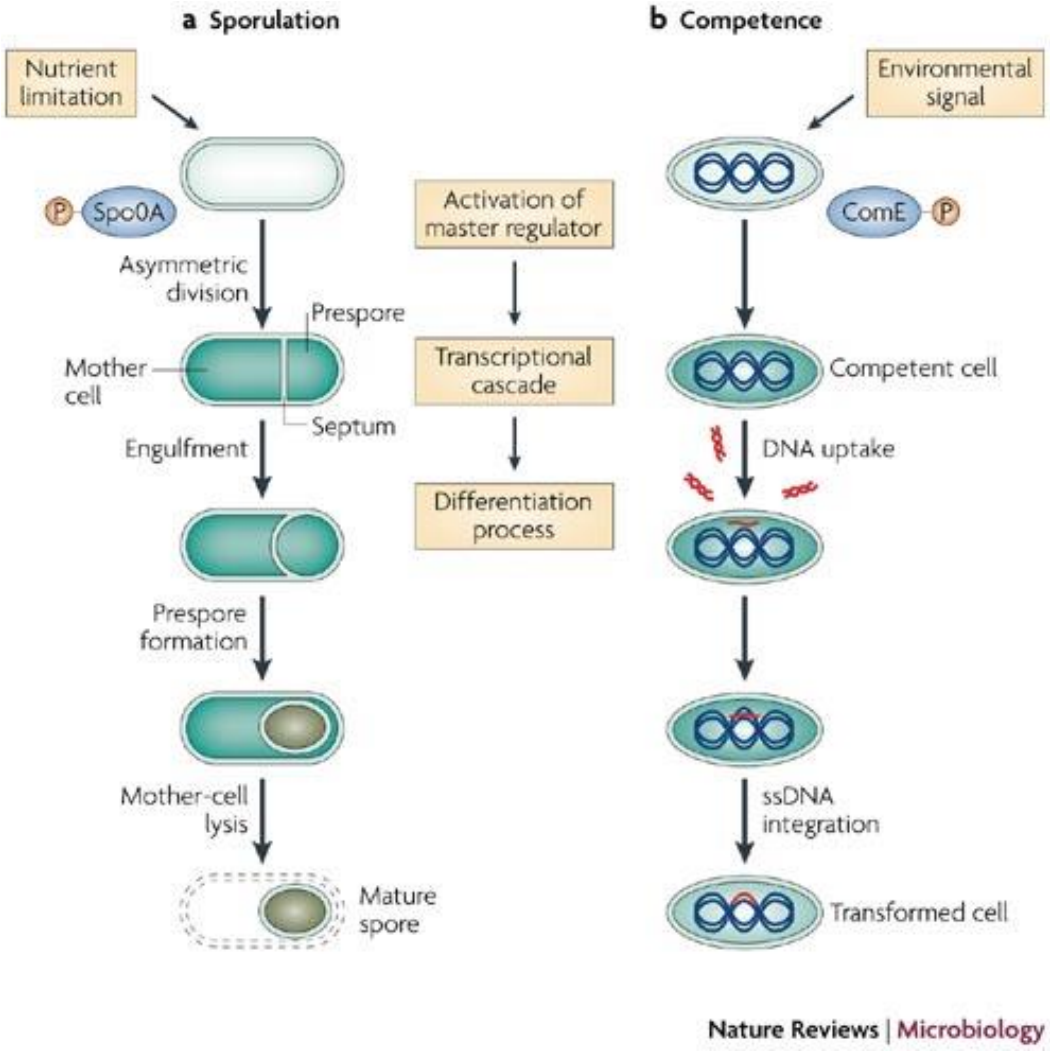

Reference: Claverys, and Havarstein, 2007 [48].

Fig.1.12: Sporulation and competence are multilevel controlled adaptive responses. In each case, initiation signals activate a master transcription regulator, Spo0A and ComE, respectively. Spo0A triggers the asymmetric sporulation division, which produces two distinct cells with different fates — the smaller prespore (also known as the forespore), which develops into the prespore through a process called engulfment, and the mother cell, which is necessary for spore formation and ultimately lyses to liberate the mature spore. ComE

triggers the expression of the com regulon, which includes genes encoding the DNA uptake and recombination machinery. Competent cells can therefore take up exogenous DNA in the form of single-stranded (ss) fragments. Homologous recombination proteins enable the formation of heteroduplex intermediates in genetic transformation if and when homologous DNA is internalized. Differentiating cells are shown in dark green [48].

1.10 Programmed cell death in *Caulobacter crescentus*

Caulobacter is a Gram negative bacterium and is commonly found in fresh water bodies [57]. Recently, Bos et al. screened for an SOS-induced factor that caused cell death and identified a previously uncharacterized protein, which they named bacterial apoptosis endonuclease (BapE) [58]. The authors reported that wild-type *Caulobacter crescentus* encodes this novel endonuclease that fragments the chromosome when the DNA is extensively damaged. Following DNA damage, bacterial cells typically induce the SOS response, which arrests the cell cycle and activates DNA repair pathways. To investigate the *C. crescentus* response to DNA damage, the authors used two different approaches to induce the SOS response: deletion of *lexA* (which encodes a repressor of the SOS response) and treatment of cells with the DNA crosslinker mitomycin C (MMC). A subpopulation of both lexA-null cells and MMC-treated cells were positive for DiBAC4 and TUNEL staining, which are markers for membrane depolarization and chromosomal fragmentation, respectively. This evidence indicated that DNA damage promotes apoptosis-like death in *C. crescentus* [58,59]. Deletion of the BapE encoding gene or a reduction in its cellular level had no phenotype in wild-type cells; however, the authors observed that DiBAC4 and TUNEL staining were significantly reduced in SOS-induced BapE-deficient cells, indicating that BapE is necessary for mediating cell death. Interestingly, purified BapE digested plasmid DNA in vitro in a sequence-

nonspecific manner. Furthermore, overexpression of BapE in vivo resulted in perturbed chromosome morphology and fragmentation [58].

To determine when and how *C. crescentus* makes the decision to switch from a DNA repair programme to a cell death programme following DNA damage, quantitative real-time PCR was used to measure the induction kinetics of SOS-responsive genes over time after MMC treatment. This analysis revealed that genes involved in cell division arrest and DNA repair were expressed early after MMC exposure and reached a plateau or declined at later time points. On the contrary, *bapE* induction was delayed, but its expression reached a high level at later time points. Additionally, the cell viability assays revealed that low levels of BapE resulted in reversible cell division arrest, whereas, high levels led to irreversible cell death. Thus, cell division arrest and repair pathways appear to be induced early; however, when DNA damage persists, the cell death programme is favoured owing to a rise in BapE levels and subsequent chromosome fragmentation [58].

1.11 Programmed cell death in *Xanthomonas*

Xanthomonas is a Gram negative, aerobic bacterium. Majority of its species are reported to be plant pathogens. A PCD dependent on a caspase-3 like protein has been demonstrated earlier in *Xanthomonas campestris* pv. *glycines* strain AM2 [1,5,60–62]. It was induced when this organism was grown in protein rich media like Luria bertani medium or nutrient broth with no other carbohydrate source added to the media. This phenomenon was not observed in cells grown in starch minimal medium. Addition of starch or glucose to LB medium was found to inhibit PCD [60,62]. A protein cross-reacting with anti-human caspase-3 antibody was also observed to be associated with PCD in this organism [62]. The *Xanthomonas* caspase 3-like protein appeared in cells at around 4 h of incubation and peaked at around 24 h

before finally diminishing at around 54 h of incubation. Interestingly, caspase enzyme activity was detected 12–13 h after incubation (in LB medium) which peaked at around 18 to 20 h. Addition of starch at the beginning or during the period of exponential growth in LB cultures of XcgAM2 terminated the synthesis of this protein indicating that starch acted as the repressor of biosynthesis of the *Xanthomonas* caspase, thereby preventing the organism from undergoing PCD. The cells undergoing PCD also displayed the other markers of eukaryotic apoptosis including PS externalization and the presence of nicked DNA in culture supernatant as evidenced by the TUNEL (terminal deoxynucleotidyl transferase dUTP nick-end labelling) assay. Moreover, caspase-negative mutants of *Xanthomonas* (XcgM42) obtained by N-methyl-N-nitro-N-nitrosoguanidine (MNNG) treatment did not display PCD [62].

1.12 Significance of PCD in bacteria

PCD is a genetically regulated process of cell suicide. Bacteria live as unicellular organisms and the idea of PCD in bacteria seems counterintuitive. This compels us to think about the possible evolutionary advantage to encode for a self-destruction program in bacteria. With the immense studies on biofilms bacteria are no longer looked upon as loners, rather they behave in a multicellular manner. PCD triggered in response to nutrient deprivation in a few cells of genetically identical clones benefits the entire population. This altruistic aspect is reflected in the PCD of the mother cell during sporulation in *Bacillus subtilis* and MazEF toxin-antitoxin dependent death in *E. coli* cells [63]. Secondly, a viral infection in a few cells acts as a trigger for self-destruction to save the genetically identical population [63]. Thirdly, PCD prevents the propagation of defective genome by eliminating damaged cells, thereby, acting as the guardian of the bacterial genome [63].

1.13 Apoptosis in unicellular eukaryotes

Many unicellular eukaryotes like *Leishmania, Blastocystis, Trypanosoma, Plasmodium* and *Dictyostelium discoideum* and *Saccharomyces cerevisiae* undergo PCD displaying its typical features [64–70]. *Leishmania* was first reported to undergo PCD when treated with certain anticancer drugs like amphotericin B and camptothecin [66,67]. Camptothecin was found to hyperpolarize mitochondria leading to oxidative stress in the cells. This was accompanied by the release of cytochrome c and activation of CED3/CPP32 group of proteases. Besides this, other markers of PCD like nuclear condensation, DNA fragmentation and cell shrinkage were also observed. *Blastocystis hominis* undergoes PCD when treated with metronidazole or surface-reactive cytotoxic monoclonal antibody [64,65]. It shows the characteristic features of PCD like chromosomal condensation, externalization of PS, although DNA laddering was not observed [65]. *Plasmodium falciparum* has been reported to undergo PCD in response to chloroquine treatment [70]. *Trypanosoma brucei rhodesiense* undergoes apoptosis when treated with concanavalin A [71].

1.14 Programmed cell death in yeast

Budding yeast, *Saccharomyces cerevisiae*, has been used as a model organism in several areas of cell biology. The functional advantage of yeast being a eukaryote coupled to the easy handling like that of bacteria made yeast a preferred research tool. Apoptosis was first discovered in yeast under oxidative stress in 1997 [72,73]. Since this discovery several yeast orthologs of mammalian apoptotic proteins like YCA1 (yeast caspase), AIF1 (apoptosis-inducing-factor-1) have been identified [69,72,73]. Both exogenous and endogenous triggers have been reported to induce apoptosis in yeast. Hydrogen peroxide, hypochlorous acid, acetic acid, high salt, heat stress, UV irradiation, heavy metals, certain drugs like aspirin,

paclitaxel have been reported to induce apoptosis in yeast [69]. Moreover, the heterologous expression of the human key apoptotic inducer Bax (pro-apoptotic factor) in yeast was also found to induce apoptotic cell death with the release of cytochrome c [74]. On the contrary, heterologous expression of Bcl-2 or Bcl-xL (anti-apoptotic factor) prevented the Bax-induced lethality and improved the resistance of yeast cells to H_2O_2 and acetic acid stress [74,75]. DNA damage (due to ROS generation), replication failure (e.g. during aging), defects in cellular processes like chromatid condensation and N-glycosylation, were also reported to induce apoptosis in yeast [76,77]. ROS have been identified as one of the small signalling molecules regulating yeast apoptosis. Probable cellular sources of ROS include the electron transport chain in mitochondria, the endoplasmic reticulum and the iron coupled Fenton and Haber-Weiss reactions.

1.15 Programmed cell death in higher eukaryotes

Apoptosis in higher eukaryotes is a well-studied phenomenon. It is essential for the maintenance of homeostasis and involves the interplay of several proteins. The most important role is played by caspases (cysteine-aspartic proteases) [2]. They cleave at a specific site in the target proteins. Till date 14 caspases have been identified in humans. They are highly conserved throughout the evolution. All known caspases possess a cysteine residue in the active site, and cleave substrates at Asp-Xxx bonds (i.e. after aspartic acid residues). Since they bring about the most visible changes in cell morphology characteristic of apoptosis, they are considered to be the main executioners of this process. Activation of caspases does not result in total degradation of cellular proteins; rather it selectively cleaves a restricted set of target proteins, usually at one or few positions in the primary sequence after an aspartate residue. Caspase-3 is known to cleave ICAD (inhibitor of caspase-activated

DNase) which leads to the activation of CAD (caspase-activated DNase) resulting in the characteristic DNA ladder pattern, the hallmark of apoptosis [2]. Caspases are mainly classified either as initiator or executioner based on their function. Caspase 1, 4, 8 and 9 belong to initiator caspases and aid in initiating the apoptotic cascade, whereas, caspases 3, 6 and 7 belong to executioner caspases as they cleave the downstream target proteins like ICAD, PARP and lamins.

1.16 Activation of Caspases

Caspases are synthesized as zymogens (enzymatically inert) [2]. In humans these are reported to be composed of three domains: an N-terminal prodomain, the p-20 and p-10 domains. The mature enzyme is a heterotetramer containing two p20/p10 heterodimers. There are following two pathways for activation of caspases:

a) Intrinsic pathway (mitochondrial pathway)

The intrinsic apoptotic pathway is characterized by permeabilisation of the mitochondria and release of cytochrome c into the cytoplasm [2]. Cytochrome c then forms a multi-protein complex known as the 'apoptosome' and initiates activation of the caspase cascade through caspase 9 which cleaves and activates caspase-3 and -7.

b) Extrinsic pathway (death receptor pathway)

Upon ligand binding the death receptors [(Fas Associated Death Domain (FADD) or Tumour associated Receptor death domain (TRADD)] aggregate to recruit procaspase-8 resulting in formation of a Death inducing signaling complex (DISC) [2]. This activates procaspase-8 which in turn activates other executioner caspases like caspase-3 or cleave BID (BH3-interacting domain death) eventually leading to the formation of apoptosome as described above.

1.17 Caspase-independent cell death

Dictyostelium discoideum is a protist which multiplies vegetatively as a unicellular organism in nutrient rich conditions (Fig 1.13). But under starvation conditions *Dictyostelium* cells aggregate due to periodic cAMP signals produced by a few cells which act as aggregation center (Fig 1.13) [1,78]. Individual cells chemotactically move towards the increasing cAMP level. *Dictyostelium* cells upon aggregation differentiate and morphogenize into a multicellular structure, called sorocarp, containing a mass of spores supported by a stalk [79]. The cells in the stalk undergo PCD which involves chromatin condensation but differs from apoptosis because it involves massive vacuolization, lacks DNA fragmentation and has been found to be independent of caspases.

Figure 1.13

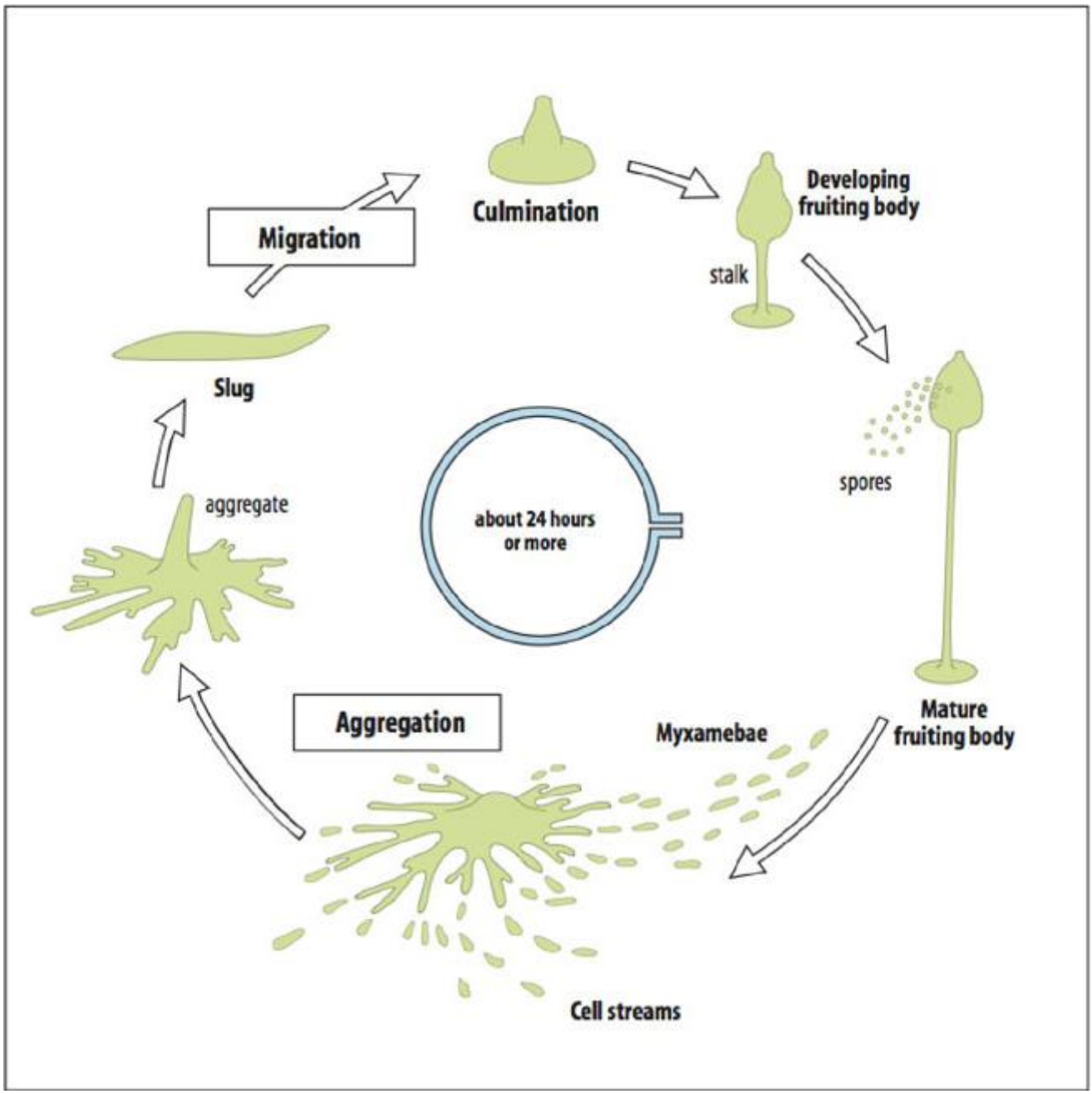

Reference: http://www.mun.ca/biology/desmid/brian/BIOL3530/DB_05/fig5_33.jpg

Fig. 1.13: Life cycle of *Dictyolstelium*

1.18 Necroptosis or Programmed Necrosis

Necroptosis is a form of programmed necrosis. Necroptotic stimuli (e.g. anticancer drugs, ionizing radiation and calcium overload) promote the interaction of the RIP1 (receptor-interacting protein 1) kinase and RIP3 (receptor-interacting protein 3) death domain containing kinase under conditions in which caspase-8 is not active [80–82]. This RIP1/RIP3 complex, known as complex IIb, mediates necroptosis. Caspases have no positive role in necroptosis. So far, an analogous class of executioner proteins has not been identified for necroptosis. Necroptosis is characterized by mitochondrial dysfunction, cell swelling (oncosis), organelle swelling membrane permeabilization and release of cytoplasmic content in the extracellular space [83,84]. Unlike apoptosis, DNA fragmentation does not occur during this process.

1.19 Autophagy

Autophagic vesicles are commonly observed in necroptotic cells. Autophagy has been proposed as a clean-up mechanism for necroptosis. Autophagy is a self-degradative process (self-eating) that is important for balancing sources of energy at critical times in development and in response to nutrient stress [85,86]. Autophagy also plays a housekeeping role in removing misfolded or aggregated proteins, clearing damaged organelles, such as mitochondria, endoplasmic reticulum and peroxisomes, as well as eliminating intracellular pathogens [85]. Currently, 32 different autophagy-related genes (Atg) have been identified by genetic screening in yeast. Significantly, many of these genes are conserved in mammals, plants, worms, flies, and slime mould, emphasizing the importance of the autophagic process in responses to starvation across phylogeny [85].

References

1. Gautam S., Sharma A (2005) Programmed cell death: an overview. Advances in biochemistry and biotechnology 122-157.

2. Elmore S (2007) Apoptosis: a review of programmed cell death. Toxicol Pathol 35: 495-516. 779478428 [pii];10.1080/01926230701320337 [doi].

3. Lewis K (2000) Programmed death in bacteria. Microbiol Mol Biol Rev 64: 503-514.

4. Ameisen JC (2002) On the origin, evolution, and nature of programmed cell death: a timeline of four billion years. Cell Death Differ 9: 367-393. 10.1038/sj/cdd/4400950 [doi].

5. Gautam S., Sharma A, Kobayashi I (2005) Programmed cell death in microorganisms. Survival and Death in Bacteria Research Sign Post Press, India .

6. Mousavi SA, Robson GD (2004) Oxidative and amphotericin B-mediated cell death in the opportunistic pathogen Aspergillus fumigatus is associated with an apoptotic-like phenotype. Microbiology 150: 1937-1945. 10.1099/mic.0.26830-0 [doi];150/6/1937 [pii].

7. Phillips AJ, Crowe JD, Ramsdale M (2006) Ras pathway signaling accelerates programmed cell death in the pathogenic fungus Candida albicans. Proc Natl

Acad Sci U S A 103: 726-731. 0506405103 [pii];10.1073/pnas.0506405103 [doi].

8. Rice KC, Bayles KW (2003) Death's toolbox: examining the molecular components of bacterial programmed cell death. Mol Microbiol 50: 729-738. 3720 [pii].

9. Ning SB, Guo HL, Wang L, Song YC (2002) Salt stress induces programmed cell death in prokaryotic organism Anabaena. J Appl Microbiol 93: 15-28. 1651 [pii].

10. Lindas AC, Bernander R (2013) The cell cycle of archaea. Nat Rev Microbiol 11: 627-638. nrmicro3077 [pii];10.1038/nrmicro3077 [doi].

11. Seth-Pasricha M, Bidle KA, Bidle KD (2013) Specificity of archaeal caspase activity in the extreme halophile Haloferax volcanii. Environ Microbiol Rep 5: 263-271. 10.1111/1758-2229.12010 [doi].

12. Bidle KD, Falkowski PG (2004) Cell death in planktonic, photosynthetic microorganisms. Nat Rev Microbiol 2: 643-655. 10.1038/nrmicro956 [doi];nrmicro956 [pii].

13. Bar-Zeev E, Avishay I, Bidle KD, Berman-Frank I (2013) Programmed cell death in the marine cyanobacterium Trichodesmium mediates carbon and nitrogen export. ISME J 7: 2340-2348. ismej2013121 [pii];10.1038/ismej.2013.121 [doi].

14. Berman-Frank I, Bidle K, Haramaty L, Falkowski P (2004) The demise of the marine cyanobacterium, Trichodesmium spp., via an autocatalyzed cell death pathway. Limnol Oceanogr 49: 997-1005.

15. Jiang Q, Qin S, Wu QY (2010) Genome-wide comparative analysis of metacaspases in unicellular and filamentous cyanobacteria. BMC Genomics 11: 198. 1471-2164-11-198 [pii];10.1186/1471-2164-11-198 [doi].

16. Yamaguchi Y, Park JH, Inouye M (2011) Toxin-antitoxin systems in bacteria and archaea. Annu Rev Genet 45: 61-79. 10.1146/annurev-genet-110410-132412 [doi].

17. Bayles KW (2014) Bacterial programmed cell death: making sense of a paradox. Nat Rev Microbiol 12: 63-69. nrmicro3136 [pii];10.1038/nrmicro3136 [doi].

18. Ranjit DK, Endres JL, Bayles KW (2011) Staphylococcus aureus CidA and LrgA proteins exhibit holin-like properties. J Bacteriol 193: 2468-2476. JB.01545-10 [pii];10.1128/JB.01545-10 [doi].

19. Rice KC, Mann EE, Endres JL, Weiss EC, Cassat JE, Smeltzer MS, Bayles KW (2007) The cidA murein hydrolase regulator contributes to DNA release and biofilm development in Staphylococcus aureus. Proc Natl Acad Sci U S A 104: 8113-8118. 0610226104 [pii];10.1073/pnas.0610226104 [doi].

20. Mann EE, Rice KC, Boles BR, Endres JL, Ranjit D, Chandramohan L, Tsang LH, Smeltzer MS, Horswill AR, Bayles KW (2009) Modulation of eDNA release and degradation affects Staphylococcus aureus biofilm maturation. PLoS One 4: e5822. 10.1371/journal.pone.0005822 [doi].

21. Sharma-Kuinkel BK, Mann EE, Ahn JS, Kuechenmeister LJ, Dunman PM, Bayles KW (2009) The Staphylococcus aureus LytSR two-component regulatory system affects biofilm formation. J Bacteriol 191: 4767-4775. JB.00348-09 [pii];10.1128/JB.00348-09 [doi].

22. Thomas VC, Sadykov MR, Chaudhari SS, Jones J, Endres JL, Widhelm TJ, Ahn JS, Jawa RS, Zimmerman MC, Bayles KW (2014) A central role for carbon-overflow pathways in the modulation of bacterial cell death. PLoS Pathog 10: e1004205. 10.1371/journal.ppat.1004205 [doi];PPATHOGENS-D-13-03034 [pii].

23. Rice KC, Bayles KW (2008) Molecular control of bacterial death and lysis. Microbiol Mol Biol Rev 72: 85-109, table. 72/1/85 [pii];10.1128/MMBR.00030-07 [doi].

24. Plas DR, Thompson CB (2002) Cell metabolism in the regulation of programmed cell death. Trends Endocrinol Metab 13: 75-78. S1043276001005288 [pii].

25. McFate T, Mohyeldin A, Lu H, Thakar J, Henriques J, Halim ND, Wu H, Schell MJ, Tsang TM, Teahan O, Zhou S, Califano JA, Jeoung NH, Harris RA, Verma A (2008) Pyruvate dehydrogenase complex activity controls metabolic and malignant phenotype in cancer cells. J Biol Chem 283: 22700-22708. M801765200 [pii];10.1074/jbc.M801765200 [doi].

26. Sutendra G, Michelakis ED (2013) Pyruvate dehydrogenase kinase as a novel therapeutic target in oncology. Front Oncol 3: 38. 10.3389/fonc.2013.00038 [doi].

27. Gatenby RA, Gillies RJ (2004) Why do cancers have high aerobic glycolysis? Nat Rev Cancer 4: 891-899. nrc1478 [pii];10.1038/nrc1478 [doi].

28. Gatenby RA, Gawlinski ET, Gmitro AF, Kaylor B, Gillies RJ (2006) Acid-mediated tumor invasion: a multidisciplinary study. Cancer Res 66: 5216-5223. 66/10/5216 [pii];10.1158/0008-5472.CAN-05-4193 [doi].

29. Yarmolinsky MB (1995) Programmed cell death in bacterial populations. Science 267: 836-837.

30. Engelberg-Kulka H, Amitai S, Kolodkin-Gal I, Hazan R (2006) Bacterial programmed cell death and multicellular behavior in bacteria. PLoS Genet 2: e135. 06-PLGE-RV-0068R3 [pii];10.1371/journal.pgen.0020135 [doi].

31. Gerdes K, Christensen SK, Lobner-Olesen A (2005) Prokaryotic toxin-antitoxin stress response loci. Nat Rev Microbiol 3: 371-382. nrmicro1147 [pii];10.1038/nrmicro1147 [doi].

32. Unterholzner SJ, Poppenberger B, Rozhon W (2013) Toxin-antitoxin systems: Biology, identification, and application. Mob Genet Elements 3: e26219. 10.4161/mge.26219 [doi];2013MGE0023R [pii].

33. Mruk I, Kobayashi I (2014) To be or not to be: regulation of restriction-modification systems and other toxin-antitoxin systems. Nucleic Acids Res 42: 70-86. gkt711 [pii];10.1093/nar/gkt711 [doi].

34. Agarwal S, Agarwal S, Bhatnagar R (2007) Identification and characterization of a novel toxin-antitoxin module from Bacillus anthracis. FEBS Lett 581: 1727-1734. S0014-5793(07)00323-7 [pii];10.1016/j.febslet.2007.03.051 [doi].

35. Chopra N, Saumitra, Pathak A, Bhatnagar R, Bhatnagar S (2013) Linkage, mobility, and selfishness in the MazF family of bacterial toxins: a snapshot of bacterial evolution. Genome Biol Evol 5: 2268-2284. evt175 [pii];10.1093/gbe/evt175 [doi].

36. Kolodkin-Gal I, Hazan R, Gaathon A, Carmeli S, Engelberg-Kulka H (2007) A linear pentapeptide is a quorum-sensing factor required for mazEF-mediated cell death in Escherichia coli. Science 318: 652-655. 318/5850/652 [pii];10.1126/science.1147248 [doi].

37. Kolodkin-Gal I, Engelberg-Kulka H (2008) The extracellular death factor: physiological and genetic factors influencing its production and response in Escherichia coli. J Bacteriol 190: 3169-3175. JB.01918-07 [pii];10.1128/JB.01918-07 [doi].

38. Kolodkin-Gal I, Sat B, Keshet A, Engelberg-Kulka H (2008) The communication factor EDF and the toxin-antitoxin module mazEF determine the mode of action of antibiotics. PLoS Biol 6: e319. 08-PLBI-RA-3169 [pii];10.1371/journal.pbio.0060319 [doi].

39. Belitsky M, Avshalom H, Erental A, Yelin I, Kumar S, London N, Sperber M, Schueler-Furman O, Engelberg-Kulka H (2011) The Escherichia coli extracellular death factor EDF induces the endoribonucleolytic activities of the

toxins MazF and ChpBK. Mol Cell 41: 625-635. S1097-2765(11)00165-1 [pii];10.1016/j.molcel.2011.02.023 [doi].

40. Blower TR, Short FL, Rao F, Mizuguchi K, Pei XY, Fineran PC, Luisi BF, Salmond GP (2012) Identification and classification of bacterial Type III toxin-antitoxin systems encoded in chromosomal and plasmid genomes. Nucleic Acids Res 40: 6158-6173. gks231 [pii];10.1093/nar/gks231 [doi].

41. Fineran PC, Blower TR, Foulds IJ, Humphreys DP, Lilley KS, Salmond GP (2009) The phage abortive infection system, ToxIN, functions as a protein-RNA toxin-antitoxin pair. Proc Natl Acad Sci U S A 106: 894-899. 0808832106 [pii];10.1073/pnas.0808832106 [doi].

42. Samson JE, Spinelli S, Cambillau C, Moineau S (2013) Structure and activity of AbiQ, a lactococcal endoribonuclease belonging to the type III toxin-antitoxin system. Mol Microbiol 87: 756-768. 10.1111/mmi.12129 [doi].

43. Samson JE, Belanger M, Moineau S (2013) Effect of the abortive infection mechanism and type III toxin/antitoxin system AbiQ on the lytic cycle of Lactococcus lactis phages. J Bacteriol 195: 3947-3956. JB.00296-13 [pii];10.1128/JB.00296-13 [doi].

44. Masuda H, Tan Q, Awano N, Wu KP, Inouye M (2012) YeeU enhances the bundling of cytoskeletal polymers of MreB and FtsZ, antagonizing the CbtA (YeeV) toxicity in Escherichia coli. Mol Microbiol 84: 979-989. 10.1111/j.1365-2958.2012.08068.x [doi].

45. Masuda H, Tan Q, Awano N, Yamaguchi Y, Inouye M (2012) A novel membrane-bound toxin for cell division, CptA (YgfX), inhibits polymerization of cytoskeleton proteins, FtsZ and MreB, in Escherichia coli. FEMS Microbiol Lett 328: 174-181. 10.1111/j.1574-6968.2012.02496.x [doi].

46. Wang X, Lord DM, Cheng HY, Osbourne DO, Hong SH, Sanchez-Torres V, Quiroga C, Zheng K, Herrmann T, Peti W, Benedik MJ, Page R, Wood TK (2012) A new type V toxin-antitoxin system where mRNA for toxin GhoT is cleaved by antitoxin GhoS. Nat Chem Biol 8: 855-861. nchembio.1062 [pii];10.1038/nchembio.1062 [doi].

47. Lewis K (2012) Persister cells: molecular mechanisms related to antibiotic tolerance. Handb Exp Pharmacol 121-133. 10.1007/978-3-642-28951-4_8 [doi].

48. Claverys JP, Havarstein LS (2007) Cannibalism and fratricide: mechanisms and raisons d'etre. Nat Rev Microbiol 5: 219-229. nrmicro1613 [pii];10.1038/nrmicro1613 [doi].

49. Claverys JP, Martin B, Havarstein LS (2007) Competence-induced fratricide in streptococci. Mol Microbiol 64: 1423-1433. MMI5757 [pii];10.1111/j.1365-2958.2007.05757.x [doi].

50. Steinmoen H, Knutsen E, Havarstein LS (2002) Induction of natural competence in Streptococcus pneumoniae triggers lysis and DNA release from a subfraction of the cell population. Proc Natl Acad Sci U S A 99: 7681-7686. 10.1073/pnas.112464599 [doi].

51. Steinmoen H, Teigen A, Havarstein LS (2003) Competence-induced cells of Streptococcus pneumoniae lyse competence-deficient cells of the same strain during cocultivation. J Bacteriol 185: 7176-7183.

52. Regev-Yochay G, Trzcinski K, Thompson CM, Lipsitch M, Malley R (2007) SpxB is a suicide gene of Streptococcus pneumoniae and confers a selective advantage in an in vivo competitive colonization model. J Bacteriol 189: 6532-6539. JB.00813-07 [pii];10.1128/JB.00813-07 [doi].

53. Piggot PJ, Hilbert DW (2004) Sporulation of Bacillus subtilis. Curr Opin Microbiol 7: 579-586. S1369-5274(04)00125-0 [pii];10.1016/j.mib.2004.10.001 [doi].

54. Dubnau D, Losick R (2006) Bistability in bacteria. Mol Microbiol 61: 564-572. MMI5249 [pii];10.1111/j.1365-2958.2006.05249.x [doi].

55. Gonzalez-Pastor JE (2011) Cannibalism: a social behavior in sporulating Bacillus subtilis. FEMS Microbiol Rev 35: 415-424. 10.1111/j.1574-6976.2010.00253.x [doi].

56. Higgins D, Dworkin J (2012) Recent progress in Bacillus subtilis sporulation. FEMS Microbiol Rev 36: 131-148. 10.1111/j.1574-6976.2011.00310.x [doi].

57. Curtis PD, Brun YV (2010) Getting in the loop: regulation of development in Caulobacter crescentus. Microbiol Mol Biol Rev 74: 13-41. 74/1/13 [pii];10.1128/MMBR.00040-09 [doi].

58. Bos J, Yakhnina AA, Gitai Z (2012) BapE DNA endonuclease induces an apoptotic-like response to DNA damage in Caulobacter. Proc Natl Acad Sci U S A 109: 18096-18101. 1213332109 [pii];10.1073/pnas.1213332109 [doi].

59. Kahrstrom CT (2012) Bacterial physiology: Caulobacter chooses to self-destruct. Nat Rev Microbiol 10: 802-803. nrmicro2913 [pii];10.1038/nrmicro2913 [doi].

60. Raju KK, Gautam S, Sharma A (2006) Molecules involved in the modulation of rapid cell death in Xanthomonas. J Bacteriol 188: 5408-5416. 188/15/5408 [pii];10.1128/JB.00056-06 [doi].

61. Gautam S, Sharma A (2002) Rapid cell death in Xanthomonas campestris pv. glycines. J Gen Appl Microbiol 48: 67-76.

62. Gautam S, Sharma A (2002) Involvement of caspase-3-like protein in rapid cell death of Xanthomonas. Mol Microbiol 44: 393-401. 2837 [pii].

63. Engelberg-Kulka H, Sat B, Reches M, Amitai S, Hazan R (2004) Bacterial programmed cell death systems as targets for antibiotics. Trends Microbiol 12: 66-71. 10.1016/j.tim.2003.12.008 [doi];S0966842X03003354 [pii].

64. Nasirudeen AM (2005) Cell death and human intestinal protozoa: a brief overview. Curr Issues Intest Microbiol 6: 77-82.

65. Nasirudeen AM, Hian YE, Singh M, Tan KS (2004) Metronidazole induces programmed cell death in the protozoan parasite Blastocystis hominis. Microbiology 150: 33-43.

66. Lee N, Bertholet S, Debrabant A, Muller J, Duncan R, Nakhasi HL (2002) Programmed cell death in the unicellular protozoan parasite Leishmania. Cell Death Differ 9: 53-64. 10.1038/sj.cdd.4400952 [doi].

67. Sen N, Das BB, Ganguly A, Mukherjee T, Tripathi G, Bandyopadhyay S, Rakshit S, Sen T, Majumder HK (2004) Camptothecin induced mitochondrial dysfunction leading to programmed cell death in unicellular hemoflagellate Leishmania donovani. Cell Death Differ 11: 924-936. 10.1038/sj.cdd.4401435 [doi];4401435 [pii].

68. Jimenez V, Paredes R, Sosa MA, Galanti N (2008) Natural programmed cell death in T. cruzi epimastigotes maintained in axenic cultures. J Cell Biochem 105: 688-698. 10.1002/jcb.21864 [doi].

69. Carmona-Gutierrez D, Eisenberg T, Buttner S, Meisinger C, Kroemer G, Madeo F (2010) Apoptosis in yeast: triggers, pathways, subroutines. Cell Death Differ 17: 763-773. cdd2009219 [pii];10.1038/cdd.2009.219 [doi].

70. Picot S, Burnod J, Bracchi V, Chumpitazi BF, Ambroise-Thomas P (1997) Apoptosis related to chloroquine sensitivity of the human malaria parasite Plasmodium falciparum. Trans R Soc Trop Med Hyg 91: 590-591.

71. Welburn SC, Lillico S, Murphy NB (1999) Programmed cell death in procyclic form Trypanosoma brucei rhodesiense --identification of differentially expressed genes during con A induced death. Mem Inst Oswaldo Cruz 94: 229-234.

72. Madeo F, Herker E, Maldener C, Wissing S, Lachelt S, Herlan M, Fehr M, Lauber K, Sigrist SJ, Wesselborg S, Frohlich KU (2002) A caspase-related protease regulates apoptosis in yeast. Mol Cell 9: 911-917. S1097276502005014 [pii].

73. Madeo F, Herker E, Wissing S, Jungwirth H, Eisenberg T, Frohlich KU (2004) Apoptosis in yeast. Curr Opin Microbiol 7: 655-660. S1369-5274(04)00136-5 [pii];10.1016/j.mib.2004.10.012 [doi].

74. Eisenberg T, Buttner S, Kroemer G, Madeo F (2007) The mitochondrial pathway in yeast apoptosis. Apoptosis 12: 1011-1023. 10.1007/s10495-007-0758-0 [doi].

75. Mazzoni C, Falcone C (2008) Caspase-dependent apoptosis in yeast. Biochim Biophys Acta 1783: 1320-1327. S0167-4889(08)00078-5 [pii];10.1016/j.bbamcr.2008.02.015 [doi].

76. Hauptmann P, Riel C, Kunz-Schughart LA, Frohlich KU, Madeo F, Lehle L (2006) Defects in N-glycosylation induce apoptosis in yeast. Mol Microbiol 59: 765-778. MMI4981 [pii];10.1111/j.1365-2958.2005.04981.x [doi].

77. Weinberger M, Ramachandran L, Feng L, Sharma K, Sun X, Marchetti M, Huberman JA, Burhans WC (2005) Apoptosis in budding yeast caused by defects in initiation of DNA replication. J Cell Sci 118: 3543-3553. 118/15/3543 [pii];10.1242/jcs.02477 [doi].

78. Olie RA, Durrieu F, Cornillon S, Loughran G, Gross J, Earnshaw WC, Golstein P (1998) Apparent caspase independence of programmed cell death in Dictyostelium. Curr Biol 8: 955-958. S0960-9822(98)70395-1 [pii].

79. Lam D, Golstein P (2005) [Genetic approaches to molecular mechanisms of programmed cell death in Dictyostelium]. J Soc Biol 199: 191-198.

80. Christofferson DE, Yuan J (2010) Necroptosis as an alternative form of programmed cell death. Curr Opin Cell Biol 22: 263-268. S0955-0674(09)00232-4 [pii];10.1016/j.ceb.2009.12.003 [doi].

81. Christofferson DE, Li Y, Yuan J (2014) Control of life-or-death decisions by RIP1 kinase. Annu Rev Physiol 76: 129-150. 10.1146/annurev-physiol-021113-170259 [doi].

82. Newton K, Dugger DL, Wickliffe KE, Kapoor N, de Almagro MC, Vucic D, Komuves L, Ferrando RE, French DM, Webster J, Roose-Girma M, Warming S, Dixit VM (2014) Activity of protein kinase RIPK3 determines whether cells die by necroptosis or apoptosis. Science 343: 1357-1360. science.1249361 [pii];10.1126/science.1249361 [doi].

83. Giampietri C, Starace D, Petrungaro S, Filippini A, Ziparo E (2014) Necroptosis: molecular signalling and translational implications. Int J Cell Biol 2014: 490275. 10.1155/2014/490275 [doi].

84. Kroemer G, Galluzzi L, Vandenabeele P, Abrams J, Alnemri ES, Baehrecke EH, Blagosklonny MV, El-Deiry WS, Golstein P, Green DR, Hengartner M, Knight RA, Kumar S, Lipton SA, Malorni W, Nunez G, Peter ME, Tschopp J, Yuan J, Piacentini M, Zhivotovsky B, Melino G (2009) Classification of cell death: recommendations of the Nomenclature Committee on Cell Death 2009. Cell Death Differ 16: 3-11. cdd2008150 [pii];10.1038/cdd.2008.150 [doi].

85. Glick D, Barth S, Macleod KF (2010) Autophagy: cellular and molecular mechanisms. J Pathol 221: 3-12. 10.1002/path.2697 [doi].

86. Marino G, Niso-Santano M, Baehrecke EH, Kroemer G (2014) Self-consumption: the interplay of autophagy and apoptosis. Nat Rev Mol Cell Biol 15: 81-94. nrm3735 [pii];10.1038/nrm3735 [doi].

Chapter 2: Metabolic Stress Induced and ROS Mediated PCD in *Xanthomonas*

2.1 Introduction

2.1.1 Metabolic stress response in bacteria

The term metabolism indicates the sum total of all the cellular chemical processes involving both catabolic and anabolic processes (Fig 2.1). These processes are very fine tuned in a healthy cell and any imbalance can lead to metabolic stress. Bacteria are metabolically much simpler but diverse organisms and therefore thrive in various harsh environments. Most bacteria are exposed to a constantly changing physical and chemical environment and respond to these changes through modifications in their metabolic activities and alterations in the levels of cellular constituents such as structural proteins, transport proteins, toxins and enzymes, which help them adapt to these changes. If required they conserve energy by genetic regulation and restricting gene expression depending upon their growth condition. For example, if simple metabolites such as amino acids and sugars are readily available in the environment then the enzymes involved in their biosynthesis are not expressed. Similarly, bacteria do not synthesize catabolic enzymes unless the respective substrate is present in the environment. Moreover, in case of lactose utilizing bacteria such as *E. coli* if glucose and lactose are both present then glucose is first utilized followed by lactose because catabolism of glucose (a monosaccharide) requires two less enzymes, β-galactoside permease and β-galactosidase than lactose catabolism. Similarly, the *trp* operon regulates the biosynthesis of the amino acid tryptophan such that if it is available in the environment, these genes are not transcribed.

Figure 2.1

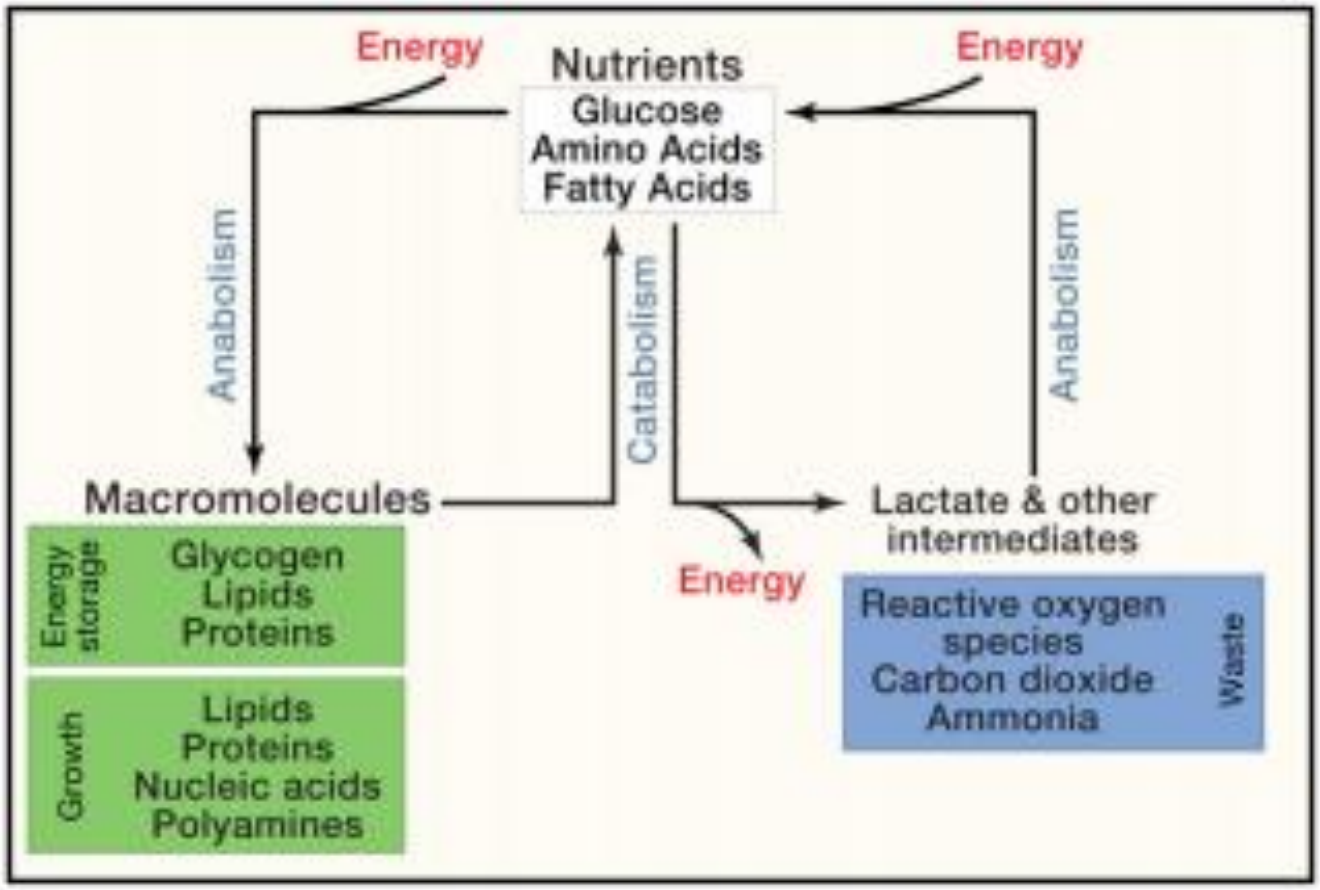

Reference: DeBerardinis and Thompson; 2012 [1]

Fig. 2.1: An overview of metabolism.

Bacterial stress response is an interesting field of study. A condition which is stressful for one bacterial species might not be so for others and their stress response can also vary to a certain extent. *Bacillus subtilis* undergo sporulation in response to nutritional stress [2]. These spores are sturdy and can survive in various environmental conditions and germinate once they encounter favourable environmental state. The mother cell undergoes programmed death during this process. Other bacteria like *E. coli,* exhibit a stress response termed as "stringent response" upon encountering stress like nutrient deprivation, heat shock and iron limitation.

This is mediated by an alarmone (p)ppGpp (GDP 3'-diphosphate or GTP 3'-diphosphate) which affects the central dogma in the cell [3].

2.1.2 Stress Response and Toxin-antitoxin (TA) modules in bacteria

The role of toxin-antitoxin module has been well established in bacterial PCD. The TA systems are not essential for cell growth but are considered to play important roles in survival under stress conditions [4]. This module comprises of a pair of closely linked genes that encode a toxin and an antitoxin. The toxin is always a protein, whereas, antitoxin can either be a protein or anti-sense RNA. These were first observed in *E. coli* on low copy number plasmids and were reported to be responsible for post-segregational killing. When the cells lose these plasmids, the cured cells are selectively killed by the toxin because the antitoxin is relatively less stable and is degraded faster [5–7]. Thus the cells are 'addicted' to the short-lived product called antitoxin, because its de novo synthesis is essential for cell survival and for maintaining the stability of extrachromosomal elements.

The toxin targets one of the following cellular processes: DNA replication, mRNA stability, protein synthesis, ATP synthesis or cell wall synthesis [4]. The toxin-antitoxin modules are classified into five types depending on the mechanism of their gene regulation and the nature of antitoxin [4]. The antitoxin can prevent the lethal action of toxin in various ways as elaborated in chapter 1.

2.1.3 Reactive Oxygen Species (ROS)

Reactive oxygen species (ROS) are highly reactive forms of oxygen and are formed by its incomplete reduction [8]. It includes O_2 derived radicals such as superoxide anion ($O_2^{\cdot-}$), hydroxyl ($OH^{\cdot}$), and alkoxyl ($RO^{\cdot}$) radicals, as well as O_2 derived non radical species such as

hydrogen peroxide (H_2O_2) [9] (Fig 2.2). ROS differ in their intrinsic chemical properties, lipid solubility and stability (half life) which govern its reactivity and preferred biological targets [8]. The chemical reactivity of ROS has a direct relationship with its stability i.e. longer the half life of a species greater the damaging effects produced by it. In *Escherichia coli*, the steady-state concentration of $O_2^{\cdot -}$ is very low (~10^{-11} M) mostly due to its instability and high reactivity. $O_2^{\cdot -}$ is unable to diffuse through membranes because of its negative charge [8]. Due to high chemical reactivity, $O_2^{\cdot -}$ oxidizes iron–sulphur ([Fe–S]) clusters at a rate that is almost diffusion-limited, and releases iron. The shorter half life (10^{-9} s) of $HO^{\bullet}$ limits its diffusion to sites of production. $HO^{\bullet}$ causes oxidation of lipids, proteins and DNA due to its indiscriminate reactivity resulting in damage to the cell. H_2O_2 is highly reactive towards thiols as well as cysteine residues and has a longer half life (~1 ms) than $O_2^{\cdot -}$. The selective reactivity and diffusibility of H_2O_2 through the membrane make it an ideal intercellular signaling molecule.

Figure 2.2

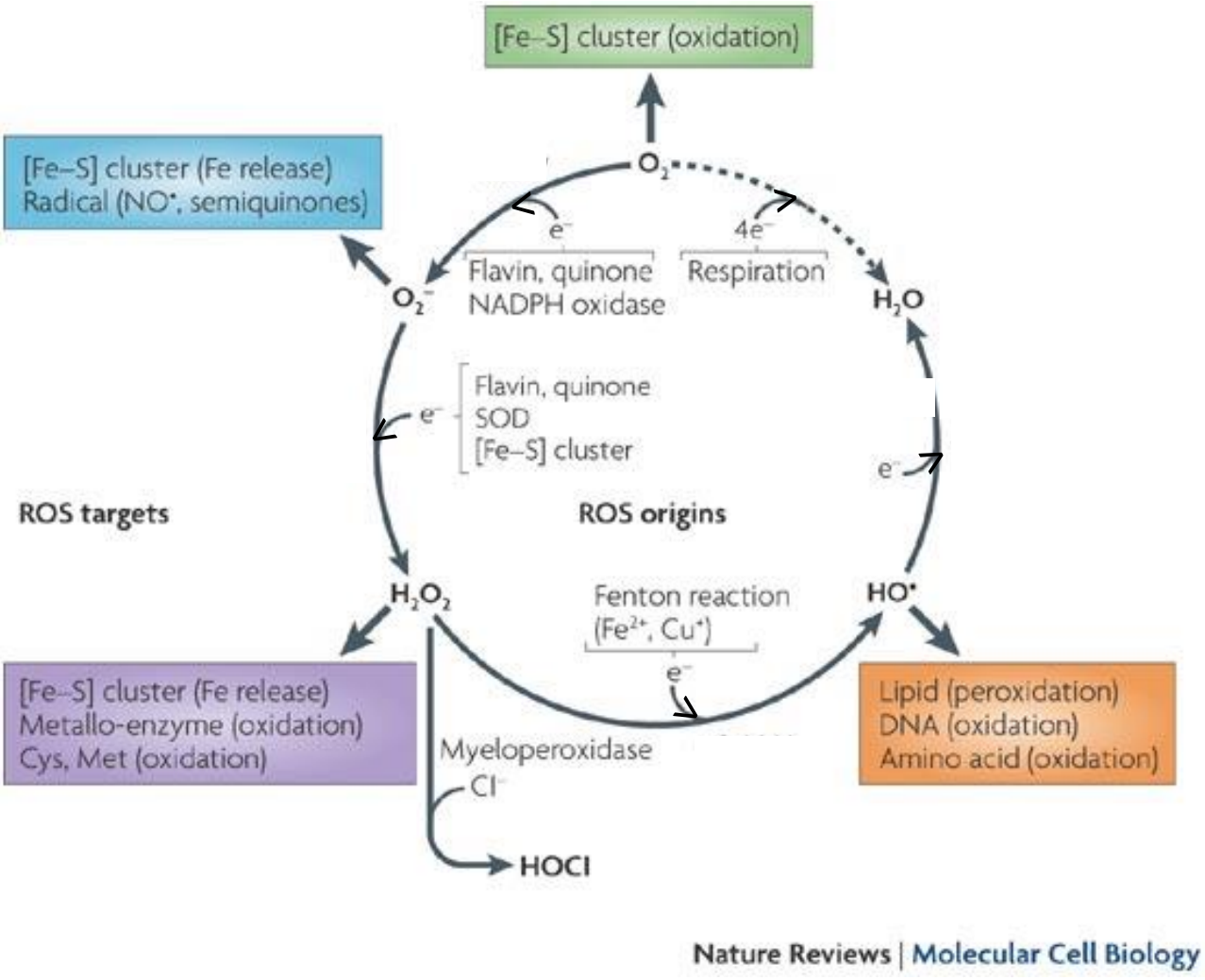

Reference: D'Autréaux and Toledano, 2007 [8]

Fig. 2.2 Origin of reactive oxygen species (ROS) and their cellular targets: ROS are generated from molecular O_2 by its subsequent reduction. The targets of ROS have been shown in colored boxes. Since they differ in their intrinsic properties, each ROS reacts with preferred biological targets. $O_2^{\bullet -}$ is a by-product of respiration and is produced by NADPH oxidases. $O_2^{\bullet -}$ oxidizes iron–sulphur ([Fe–S]) clusters at a rate that is almost diffusion-limited, and releases iron. O_2^- can react with thiols in vitro, but the slow reaction rates mean that this

cannot occur in vivo. In *Escherichia coli*, the steady-state concentration of $O_2^{\cdot -}$ is very low (approx10^{-11} M), which reflects its instability; this is not only due to its reaction with the [Fe–S] cluster, but also to spontaneous and superoxide-dismutase-mediated $O_2^{\cdot -}$ dismutation to H_2O_2. The instability of $O_2^{\cdot -}$ and its inability to diffuse through membranes because of its negative charge make this ROS a poor signalling molecule. H_2O_2 toxicity is essentially the consequence of its reduction to $HO^{\cdot}$ by metal-catalysed Fenton reaction. H_2O_2 is a poor oxidant and reacts mildly with [Fe–S] and loosely bound metals, and very slowly with glutathione and free cysteine and with methionine residues. By contrast, its reactivity towards cysteine residues can significantly increase depending on the protein environment. H_2O_2 is relatively stable (cellular half-life approx1 ms). Its selective reactivity and diffusibility makes H_2O_2 fit for signalling [8].

2.1.4 Electron Transport Chain (ETC)

The final stage of aerobic respiration occurs through a series of oxidation-reduction electron transfer reactions that yield the energy to drive oxidative phosphorylation; this in turn produces ATP. Oxidative phosphorylation is thus the culmination of energy yielding metabolism in aerobic organisms. All oxidative steps in the degradation of carbohydrates, fats, and amino acids converge at this final stage of cellular respiration, in which the energy of oxidation drives the synthesis of ATP. In eukaryotes the flow of electrons is:

NADH dehydrogenase (Complex I)→ ubiquinone → Cytochrome bc_1 complex (Complex III) → cytochrome → Cytochrome c oxidase (Complex IV) → O_2

The electron transport chain in bacteria is much more diverse than eukaryotes because it can use a number of electron donors, dehydrogenases, oxidases and reductases depending on its environment (Fig. 2.3 and 2.4). The enzymes involved in electron transport and oxidative

phosphorylation are located on the bacterial inner (cytoplasmic) membrane. This membrane is invaginated to form structures called respiratory vesicles, lamellar vesicles, or mesosomes, which function as the bacterial equivalent of the eukaryotic mitochondrial membrane.

Figure 2.3

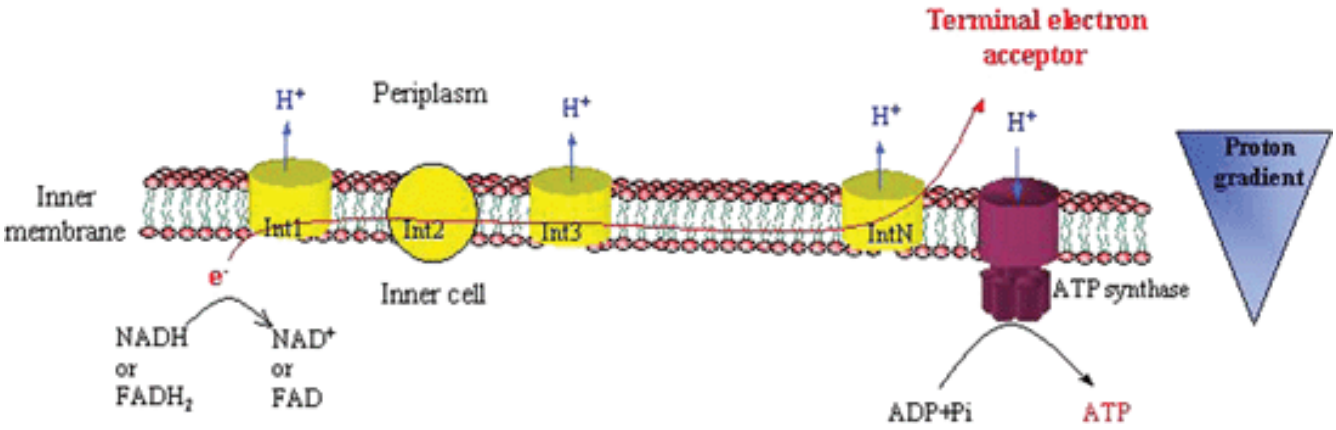

Reference: Schaetzle et al., 2008 [10]

Fig. 2.3: Schematic representation of electron transport chain (ETC) in bacterial membrane. The number of redox intermediaries i.e. Int 1, 2,twinkle#1 3….N) of the ETC varies with species.

Figure 2.4

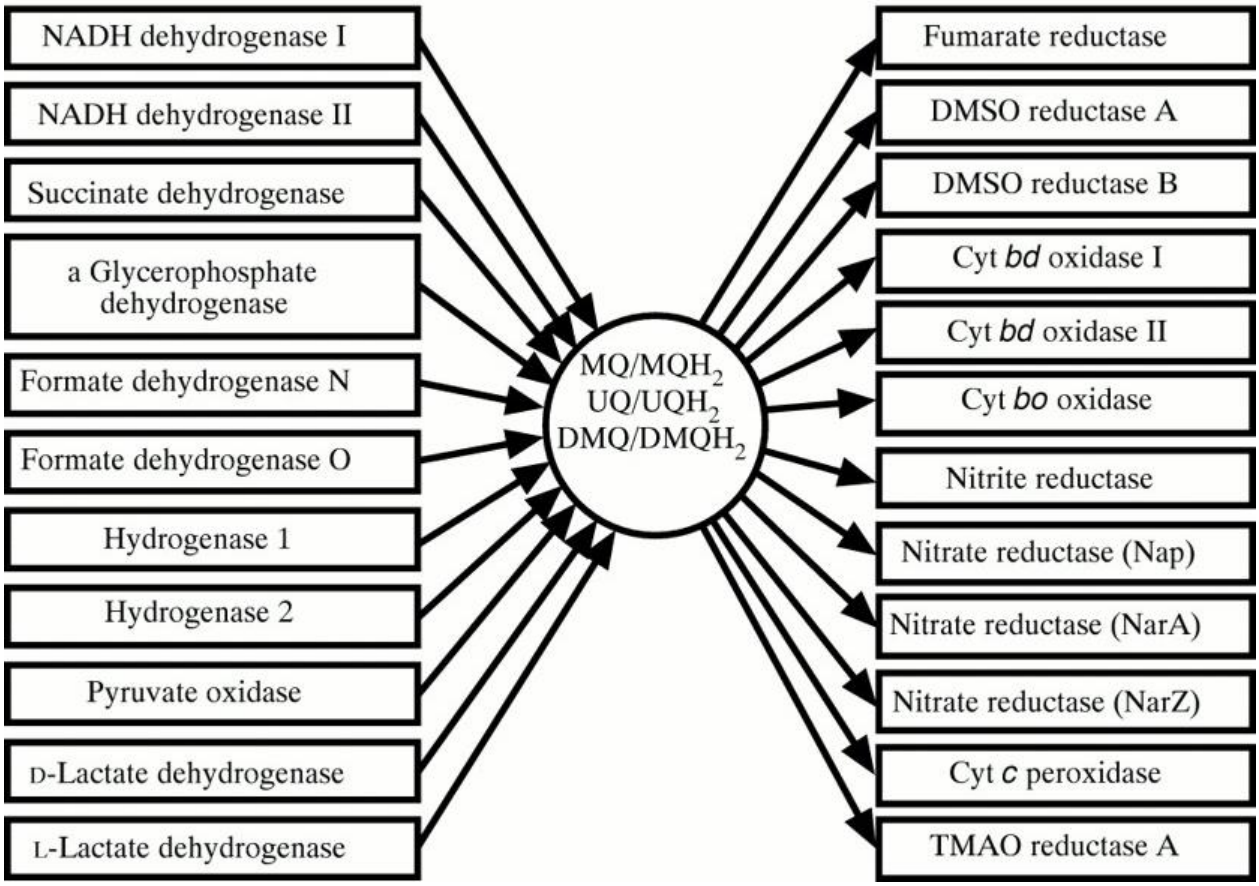

Reference: Richardson, 2000 [11]

Fig.2.4. Respiratory flexibility in *Escherichia coli.* MQ, menaquinone; UQ, ubiquinone; DMQ, demethylmenoquinone [11].

2.1.5 Electron Donors

Microbes can use either organic molecules like carbohydrates, proteins, or inorganic molecules like nitrate, sulphide, H_2S, ferrous ions, as electron donors. In the case where organic molecules mainly donate electrons, the organism is called an organotroph, whereas, if inorganic matter is used to derive energy, the organism is called chemolithotroph.

2.1.6 Dehydrogenases

Succinate dehydrogenase, NADH dehydrogenase and lactate dehydrogenase are a few dehydrogenases used by bacteria.

2.1.7 Terminal oxidase

In most bacteria, there is more than one terminal oxidase in the cytoplasmic membrane. Hence, the respiratory chain is branched both at the dehydrogenase and oxidase sites. There are two types of terminal oxidases. Class I or the cytochrome c oxidase receive electrons from ferrocytochrome c and reduce molecular O_2 to water. Class II or quinol oxidases are unique to bacteria and receive electrons from ubiquinols and/or menaquinols and transfer them to molecular O_2 [11].

2.1.8 Terminal electron acceptors

Unlike eukaryotes, where O_2 serves as the terminal electron acceptor, bacteria can use a diverse range of electron acceptors like, elemental sulphur and sulphur oxyanions, organic sulphoxides and sulphonates, nitrogen oxy-anions and nitrogen oxides, organic N-oxides, halogenated organics, metalloid oxy-anions such as selenate and arsenate, oxides of transition metals (such as iron and manganese) and radionuclides (such as uranium and technetium) [11]. This respiratory flexibility has enabled bacteria to thrive even in the harshest environments.

2.1.9 Uncouplers

Uncouplers are hydrophobic molecules that uncouple respiration (i.e. electron flow through ETC) from oxidative phosphorylation [12]. Some examples of uncouplers are: 2, 4

dinitrophenol (DNP), carbonyl cyanide-p-trifluorocarbonyl-cyanide methoxyphenyl hydrazone (FCCP), and Dicumarol. Being weak acids, these bind to protons on the acidic side of the membrane and carry them to the alkaline side thereby dissipating the proton gradient (Fig. 2.5). Uncouplers are known to reduce ROS generation through ETC by preventing one electron reduction of O_2. Leakage of electrons during ETC is considered as one of the important routes of free radical generation in obligate aerobic organisms [13,14]. At high proton motive force, respiration slows, so electron would accumulate on Q instead of passing down the ETC to oxygen. This would increase the steady-state concentration of semiquinone radical (QH·) which can directly transfer the electron to O_2 leading to increase in the rate of ROS production [12] (Fig. 2.5 and 2.6). DNP being a lipid soluble weak acid can cross the membrane barrier in both protonated or unprotonated state, and sets up a catalytic cycle that dissipates the protonmotive force leading to more oxidized ubiquinone (Q) and lesser semiquinone radical (QH·) (Fig.2.5). Uncouplers abolish link between oxidation and phosphorylation, allowing electron transport to proceed without coupled ATP synthesis [12]. Since the formation of superoxide radical depends on the level of QH·, the presence of an uncoupler results in the decrease in reactive oxygen species (ROS) generation from ETC [12].

Figure 2.5

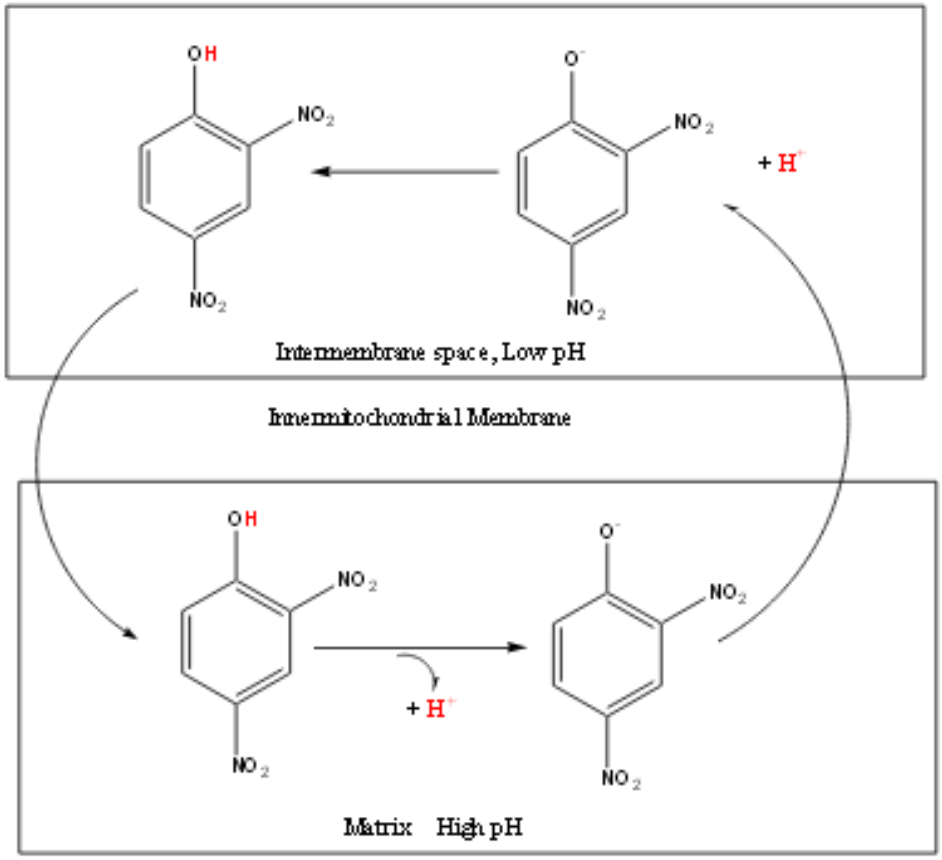

Fig 2.5: Mechanism of action of 2, 4 dinitrophenol (DNP)

Reference: https://www.tamu.edu/faculty/bmiles/lectures/uncoupler.pdf

Figure 2.6

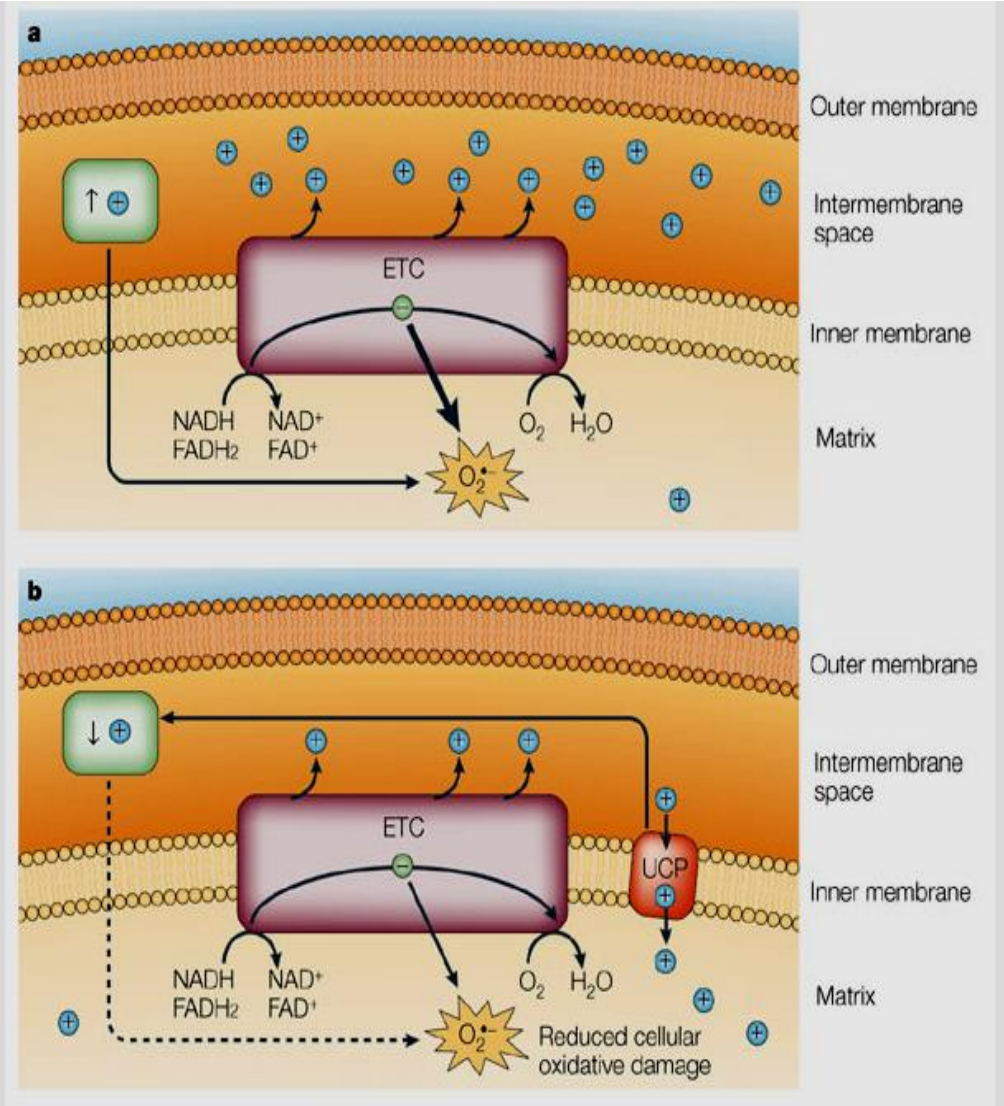

Reference: Andrews et.al, 2005 [15]

Fig. 2.6: ROS generation by electron leakage in electron transport chain (ETC) and mechanism of action of uncoupler (UCP).

2.1.10 Mechanism of intracellular ROS generation in bacteria

The leakage of electrons from the bacterial respiratory chain has been observed at the NADH dehydrogenase and ubiquinone sites, and was similar to that observed in eukaryotic mitochondria [14]. Almost 87% of H_2O_2 generation in the bacterial cell has been found to be

associated with electron leakage from ETC [14]. The second possible source of ROS in the bacterial cells is the auto-oxidation of flavoproteins [16]. A number of flavoproteins such as fumarate reductase, aspartate oxidase, glutathione reductase, lipoamide dehydrogenase and glutamate synthase produce ROS *in vitro*. The flavins of dehydrogenases were subsequently identified as the primary sources of the $O_2^{\cdot -}$ and H_2O_2. Flavoprotein autoxidation occurs when molecular oxygen adventitiously collides with the dihydroflavin of the reduced enzyme. Resultant electron transfer generates $O_2^{\cdot -}$ and a flavosemiquinone species. Sometimes the $O_2^{\cdot -}$ immediately diffuses away, but most of the time a second electron transfer occurs before $O_2^{\cdot -}$ escapes the active site eventually producing H_2O_2. Thus these enzymes are probably responsible for both $O_2^{\cdot -}$ and H_2O_2 generation. The autoxidation rates of flavoenzymes vary, depending upon the degree of flavin exposure, the flavin midpoint potential, and the residence time of electrons on it [16].

2.1.11 Metabolic rate, ROS generation and its implications

The "free radical theory of aging" was proposed by Harman more than fifty years ago [17] which suggested a correlation between metabolic rate and life span. According to this theory, a higher metabolic rate and energy turnover accelerates aging in organisms leading to early mortality [18]. This is due to the generation of free radicals or ROS which are the byproducts of metabolism in the cell. Several experiments on mice demonstrated that slowing down the metabolism by means of caloric restriction helps increase their longevity [19] [20]. In the case of fruit flies, their life span was reported to be increased by boosting the antioxidant defense mechanism like superoxide dismutase. This theory has been extended to unicellular eukaryotes like *Saccharomyces* and prokaryotes as well [21]. The rate of senescence in *E. coli* cells was reported to decrease significantly by reducing oxygen levels in the culture [22].

The levels of oxidized proteins were found to increase in the early stages of stasis in *E. coli* cultures thereby decreasing ribosome fidelity leading to mistranslation. The aberrant proteins synthesized were found to be susceptible to oxidative damage.

Rea et al (2003) [23] have proposed an 'Energy Switch' hypothesis to describe the longevity of mutants in *C.elegans*. They suggested that the relative balance between TCA-based mitochondrial dependent metabolism and alternative pathways (like glycolysis) that do not involve the entire ETC are independent of the mitochondria, may determine the overall redox homeostasis of the cell. In *C. elegans*, alternate energy pathways include malate dismutation. Such alternate pathways (like glycolysis in mammals) do not contribute much to the oxidative burden of the cell. On the contrary, metabolic pathways involving ETC tend to generate ROS leading to oxidative stress in the cell.

2.1.12 Role of Reactive oxygen species (ROS) in PCD

ROS are sensed by certain transcription factors in the bacterial cell [8]. Transcription factors SoxR and PerR sense superoxide and peroxide, respectively. These sensors help in keeping the levels of ROS from reaching toxic limits by inducing the expression of antioxidant and repair proteins. Additionally, the antioxidant enzymes (superoxide dismutase, peroxidase and catalase) play important roles in mitigating ROS. However, when ROS reach an unmanageable level, they can create havoc for the cell. These free radicals (mainly $OH^{\cdot}$) inflict significant damage on cellular macromolecules like lipids, proteins, and DNA. Cell death is imminent when the damage is irreparable. It has been demonstrated that certain antibiotics like kanamycin, tertracyclin execute their bactericidal action by generating ROS in the cells (the mechanism of which still remains unknown) [24]. However, two recent reports contradict these findings and indicate that ROS do not mediate antibiotic induced cell death

[25,26]. ROS seem to be associated with PCD. Its generation can either precede PCD process, leading to DNA damage and induction of PCD by different mechanism. On the other hand, PCD can also inflict ROS generation in neighboring cells leading to their death. Certain toxin-antitoxin modules in bacteria such as *mazEF* are known to cause ROS mediated cell death in bacteria [4,27].

Marchetti et al. (2006) [28] reported that replication stress leads to cell death due to ROS production in *Schizisacharromyces pombe* . In both budding and fission yeasts, conditional mutants of genes encoding replication initiation factors die with elevated levels of intracellular ROS at the non-permissive temperature. In *S. pombe*, there seems to be checkpoint-dependent and independent pathways leading to ROS generation and cell death.

Pyruvate oxidase in *Streptococcus pneumoniae* and *Staphylococcus aureus* plays an important role in cell death during stationary phase [29]. It was observed that *S. pneumoniae* cells containing a mutation in the *spxB* gene encoding this pyruvate oxidase exhibited increased viability in stationary phase due to the absence of the reactive oxygen species (ROS), generated as a product of this enzyme's activity [29].

2.1.13 ROS scavengers

ROS scavengers or antioxidants eliminate ROS by converting them to non toxic or less toxic molecules. They can be classified into two categories:

(a) **Enzymes as ROS scavengers**: They form the main framework of antioxidant defense system of the cell. Some of them include catalase, peroxidase and superoxide dismutase. Catalase is commonly found in all organisms. It converts hydrogen peroxide to water through the following reaction:

$$2\ H_2O_2 \rightarrow 2\ H_2O + O_2$$

On the other hand, peroxidases act on hydrogen peroxide as well as other organic peroxides (e.g. lipid peroxides) and catalyzes the following reaction;

$$ROOR' + \text{electron donor } (2\ e^-) + 2H^+ \rightarrow ROH + R'OH$$

Majority of the H_2O_2 in the cell is a byproduct of the activity of a metalloenzyme, superoxide dismutase (SOD) which converts superoxide radical to H_2O_2 in the following way:

$$2O_2^- + 2H^+ \rightarrow O_2 + H_2O_2$$

Depending on the type of co-factor present in the enzyme, SOD can be classified into three types:-

(i) Cooper (Cu) /Zinc (Zn): These SODs bind both copper and zinc and are most commonly found in the cytosol of eukaryotes.

(ii) Iron (Fe)/Manganese (Mn): These SODs bind either Fe or Mn and are mostly found in prokaryotes, mitochondria and peroxisomes.

(iii) Nickel (Ni): This SOD is commonly found in prokaryotes.

(b) **Non-enzymatic ROS scavengers**: These are small molecules which eliminate ROS by reacting with them to generate a non-toxic product and thus prevent the oxidation of other cellular components. Some of these include glutathione (GSH), dimethylsulfoxide (DMSO), ascorbic acid (vitamin C) and tocopherol (vitamin E). GSH undergoes oxidation to convert into GSSG which can be recycled back to GSH in the cell by the enzyme GSSG reductase (Fig. 2.7).

Figure 2.7

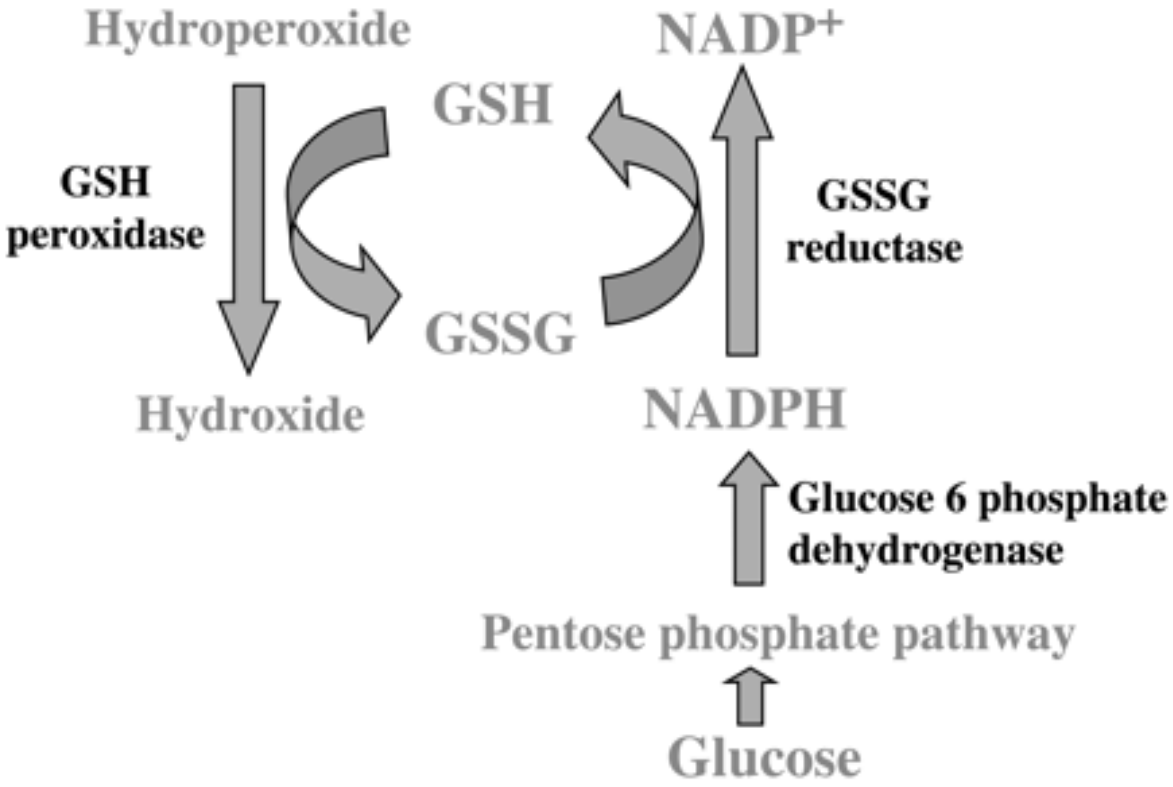

Reference: Tak Yee Aw, 2003 [30]

Fig. 2.7: Maintenance of cellular reduced GSH status during oxidative challenge. During peroxide elimination, the regeneration of GSH from GSSG is maintained by the GSH peroxidase and GSSG reductase system, the GSH redox cycle. The continued function of the redox cycle activity is dependent on the availability of NADPH, of which the pentose phosphate pathway is a major source. The cellular rate of NADPH supply is regulated by glucose flux in the pathway and the activity of glucose-6-phosphate dehydrogenase [30].

This chapter addresses the question whether nutrionally regulated PCD in *Xanthomonas* is an outcome of metabolic stress generated due to varied nutritional condition. To investigate this hypothesis, the status of intracellular molecules like NADH, ATP, and reactive oxygen species (ROS) under PCD inducing and non-inducing conditions was examined. Further,

impact of ROS scavengers on caspase-3 biosynthesis as well as activity, and PCD profile of Xcg was investigated.

2.2 Materials and Methods

2.2.1 Bacterial culture and growth conditions

Xanthomonas campestris pv. *glycines* cells were grown at 26 ± 2 °C in a rotary shaker at 150 rpm in Luria-Bertani (LB) broth {PCD inducing medium (PIM)}, or raw starch broth (RSB) {PCD non-inducing medium (PNIM); 1% starch, 0.3% $K_2HPO_4.3H_2O$, 0.15% KH_2PO_4, 0.2% ammonium sulphate, 0.05% L-methionine, 0.025% nicotinic acid, and 0.025% L-glutamate, pH 6.8±0.2}. The cell number was enumerated using the standard plate count method by serially diluting the cells in sterile saline (0.85%) and spreading an aliquot (100 µl) of the appropriate dilution on Luria Agar (LA) plates. The plates were incubated at 26 ± 2 °C for 48 h for the colonies to appear for counting [31].

2.2.2 Quantification of intracellular NADH

Alkaline extraction of NADH was carried out using protocol of Caruso *et al*. 2004, with some modifications [32]. Briefly, an aliquot (20 ml) from 18 h LB or RSB grown Xcg culture was centrifuged at 12500g for 10 min at 4°C. The cell pellet was washed once with 20 ml PBS (10 mM, pH 7.5) and suspended in 2 ml of chilled KOH (0.5 M). To this alkaline suspension, 2 volumes of cold milliQ water was added and vortexed for 2 min. The mixture was centrifuged at 12500g for 40 min at 4°C. The supernatant was collected and neutralized by adding 10% volume of KH_2PO_4 (1 M, pH 6.5). The sample was filtered through 0.22 µm filter (Millipore, USA) and analyzed using HPLC (Waters, USA). C18 column (dimension 150 mm x 4 mm) was used for analysis. Sample was loaded into a vial of the autosampler.

The mobile phase consisted of buffers A and B [A: 0.1 M KH_2PO_4, pH 6.0; and B: 0.1 M KH_2PO_4, (pH 6.0) having 10% (v/v) methanol)]. Buffers were filtered through 0.22 μm filter (Millipore, USA) and degassed. Before beginning the analysis of samples, the HPLC system was equilibrated with 50% buffer A / 50% buffer B for 30 min. The flow rate was adjusted to 1 ml min^{-1}. The analysis of each sample was performed using the binary gradient [32](Caruso *et al*., 2004): 100% buffer A for 2 min followed by sample injection, 100% buffer A for 5 min, 0-25% buffer B for 6 min, 25-60% buffer B for 2.5 min, 60 - 100% buffer B for 5 min, 100% buffer B for 7.5 min, and lastly 100% buffer A for 2 min to equilibrate the system for the next analysis. Detection was performed by measuring the absorbance at 254 nm (Waters 996 Photodiode array detector).

2.2.3 Quantification of intracellular ATP and ADP

Acid extraction of ATP and ADP was carried out based on the method described previously [33]. Briefly, an aliquot (20 ml) from 18 h grown LB or RSB grown Xcg cultures was centrifuged at 12, 500 x g for 10 min at 4°C. The cells were washed once with 20 ml PBS (10mM, pH 7.5) and the pellet suspended in 4 ml chilled perchloric acid (PCA) (0.5 M). The cell suspension was sonicated for 3 min and further incubated for 45 min with vigorous shaking at 10 min interval. The acid extract was neutralized by 0.8 x of 0.5 M KOH and 0.2x of 1 M KH_2PO_4 (pH 7.5) and kept on ice for 15 min. The potassium perchlorate precipitate was finally removed by centrifugation (12500g for 30 min at 4°C). The supernatant was filtered through 0.22 μm filter (Millipore, USA) and was subjected to HPLC analysis (Waters, USA) using C18 column (dimension 150 mm x 4 mm). Samples were loaded into a vial of the autosampler. The mobile phase consisted of buffers A (0.1 M KH_2PO_4, pH 6.0; and 8 mM tetrabutlylammonium hydrogen sulphate (TBA)) and B (0.1 M KH_2PO_4, pH 6.0; 8

mM TBA, and 30% (v/v) acetonitrile). The buffers were filtered through 0.22 μm filter (Millipore, USA) and degassed. Before starting the analysis, HPLC system was equilibrated with 50% buffer A / 50% buffer B for 30 min. The flow rate was adjusted to 1ml min^{-1}. The analysis of each sample was performed by the following binary gradient (13): 100% buffer A for 2 min followed by sample injection, 100% buffer A for 2.5 min, 0 - 10% buffer B for 1.5 min, 10% buffer B for 2 min, 10 - 20% buffer B for 1 min, 20 - 40% buffer B for 5 min, 40 - 100% buffer B for 3 min, 100% buffer B for 5 min, 100 - 0% buffer B for 1 min, and 100% buffer A for 9 min to equilibrate the system for the next analysis. Absorbance at 254 nm was measured for detection using a Waters 996 Photodiode array detector.

2.2.4 Dichlorohydrofluorescein staining

Xcg cells were grown at 26 ± 2 °C in a rotary shaker at 150 rpm in culture media (LB or RSB) for 16 h. A 2 ml culture (10^8cfu/ml) was withdrawn and centrifuged at 12500 x g for 2 min and the pellet was resuspended in 1ml saline (0.85%). It was then incubated with 2 μl H_2DCFDA (5 mM, prepared in absolute ethyl alcohol) at 37ºC for 30 min. An aliquot was smeared on a glass slide, air dried, and examined under a fluorescent microscope (Carl Zeiss, Germany) using oil immersion objective (1000x) and filter set 15 (Carl Zeiss, Germany; Excitation: 546 nm; emission: 590 nm).

2.2.5 Electron spin resonance (ESR) spectroscopy

Hydroxyl radical ($OH^{\cdot}$) formation inside the cells during the course of PCD was detected with an ESR based spin trapping system, which contained 50 mM α-(4-pyridyl-1-oxide)-N-tert-butyl-nitrone (POBN) and 250 mM DMSO. A 2 ml aliquot of 20 h grown culture containing around 10^8cells/ml was mixed with POBN. Analysis was then performed using ESR

spectrometer (Bruker, Germany). The spin trapping spectra are the result of four signal averaged scans and were obtained at ambient temperature (26 ± 2ºC). Instrument settings were as follows: Power, 15.94 mW; receiver gain, 7.96 x 10^4; modulation frequency, 100 kHz; modulation amplitude, 0.920 G; sweep width, 100G; and sweep time, 83.886 sec.

2.2.6 Scopoletin assay

Intracellular H_2O_2 level was measured by scopoletin assay. An aliquot of Xcg culture was withdrawn and centrifuged at 12500 x g for 5 min. In a fresh tube, one ml supernatant was mixed with fluorogenic substrate scopoletin (2.5 µM) and horseradish peroxidase (5 U/ml), and incubated for 5 min at ambient temperature (26 ± 2ºC). The fluorescence intensity was measured (Excitation: 360 nm, emission: 465 nm) using spectrofluorometer (FP-6500, Jasco, Japan)

2.2.7 Assay of caspase-3-like activity

Caspase-3-like activity was assayed according to the manufacturer's guidelines (caspase-3 assay kit, BD Pharmingen, USA). Briefly, a 1 ml aliquot of 24 h grown culture was washed twice with phosphate buffered saline (PBS) (10 mM, pH 7.5) and resuspended in saline (0.85%). The cell suspension was centrifuged at 12,500 x g for 10 min. The pellet was resuspended in 100 µl of sodium phosphate buffer (10 mM, pH 7.5), mixed with 1 ml cell lysis buffer {Tris-HCl (10 mM), sodium phosphate buffer (10 mM, pH 7.5), NaCl (130 mM), triton X-100 (1%) and sodium pyrophosphate (10 mM)} and kept at 4ºC for 4 h for lysis. The cell lysate was then centrifuged at 12,500 x g for 15 min and an aliquot (50 µl) of the above supernatant was used for caspase-3 assay using synthetic fluorogenic substrate Ac-DEVD-AMC (BD Pharmingen, USA). In the control set the reaction was inhibited by 10 µl (0.1mg

ml^{-1}) of the synthetic inhibitor of caspase-3 (Ac-DEVD-CHO) per reaction. After incubation the fluorescence intensity was measured using a spectroflourophotometer (Ex 380 nm, Em 440 nm, and bandwidth 10 nm).

2.2.8 Analysis of caspase-3-like protein biosynthesis by SDS PAGE and immunoblotting

Level of biosynthesis of caspase-3 was analysed using SDS-PAGE and Western hybridization using affinity-purified, biotin-conjugated, polyclonal rabbit anti-active human caspase-3 antibody. The cells were grown for 24 h and harvested by centrifuging at 10, 000 x g for 10 min. The pellet was washed twice with PBS (10mM, pH 7.5) and suspended in sterile Milli-Q water.

The washed cell suspension was mixed with an equal volume of 2X gel loading buffer (100 mM Tris-HCl, pH 6.8; 4% SDS; 20% glycerol; 0.002% bromophenol blue, and 200mM b-mercaptoethanol). The mixture was heated at 95°C for 10 min and centrifuged at 12 000 x g for 10 min. A 50 µl aliquot of the supernatant was loaded on a 12% (w/v) SDS-polyacrylamide gel, which was run vertically at 25 mA constant current on a PAGE system (Techno Source). Electroblotting was performed after the completion of the electrophoresis, using a Hybond–P membrane (Amersham-Pharmacia) in a chilled transfer buffer [25 mM Tris, 192 mM glycine (pH 8.3), 20% methanol] using 50 mA constant current at 4°C overnight. The blotted membrane was wetted with methanol and then equilibrated with Tris-buffered saline (TBS) (20 mM Tris, pH 7.6; 500 mM NaCl) for 30 min. This was followed by incubation with the blocking reagent (TBS containing 0.05% Tween-20 and 3% gelatin) for 1 h. The blot was washed twice with TBS–Tween-20 (0.05%) for 5 min and incubated with 10 ml (0.5 mg ml^{-1}) of affinity-purified biotin-conjugated, polyclonal rabbit anti-active human caspase-3 antibody (BD Pharmingen, USA) in 100 ml antibody buffer (TBS containing

0.05% Tween-20 and 1% gelatin) for 20 h. After incubation, the blot was washed twice with TBS–Tween-20 (0.05%) for 10 min followed by incubation in the antibody buffer containing streptavidin–horseradish peroxidase conjugate (BD Pharmingen, USA) for 1.5 h. The blot was washed once with TBS–Tween-20 (0.05%) and once with TBS for 5 min. Finally, the blot was dipped in the colour reagent solution [4-chloro-1-naphthol (Sigma)/H_2O_2] and kept static for 5–10 min or until the colour appeared. The band intensity (optical density /mm) of caspase-3-like protein from the blot was determined using a TLsee 2.0 software (demo version).

2.2.9 TUNEL (Terminal deoxynucleotidyl transferase dUTP nick end labeling) assay

TUNEL assay was performed according to the manufacturer's guidelines (APO-Direct Kit, BD Pharmingen). Briefly, 1 ml aliquot of 24 h grown culture containing ~10^6 cfu/ml was washed twice with PBS and resuspended in saline (0.85%). The cell suspension was mixed with 50 µl DNA labelling solution [reaction buffer (10 µl), Terminal deoxynucleotidyl transferase **(**TdT) enzyme (0.75 µl), FITC-dUTP (8 µl) and distilled water (32.25 µl)] and incubated for 60 min at 37 ºC in dark. After that 1ml rinse buffer was added and the suspension was centrifuged at 12,500 x g for 10 min. This rinsing step was repeated once more. PI/RNase staining buffer (500 µl) was added to the samples which were further incubated in dark for 30 min followed by FACS (10^5 cells for each sample) using flow cytometry system (Partec CyFlow space, Germany) and analyzed using FCS Express V4 software (demo version).

2.2.10 Statistical analysis

The experiments were repeated in three independent sets, each set comprising of three replicates. The mean and standard deviations (SD) were calculated taking all the data points in consideration. The mean values were further compared using one-way ANOVA (analysis of variance) test for establishing the significance of variation among the means ($p < 0.05$). With respect to flow cytometry analysis and microscopic examinations, a representative data is presented.

2.3 Results and Discussion

2.3.1 Increased accumulation of NADH and ATP

The levels of NADH, ATP, and ADP were quantified using high performance liquid chromatography (HPLC) in Xcg cells growing in PCD inducing (LB) and non-inducing (RSB) media as shown in Fig. 2.8. Henceforth, PCD inducing medium and PCD non-inducing medium have been abbreviated as PIM, and PNIM, respectively. NADH level was found to be around 40 times higher in PIM grown cells than those grown in PNIM. This indicated a hyper active TCA cycle and metabolism in these cells since NADH is the by-product of the TCA cycle. A protein rich medium contains many freely available amino acids. Some of these amino acids readily convert to tricarboxylic acid cycle (TCA) intermediates through transamination reaction [34].

ATP levels in PIM grown cells were found to be around 1.6 times higher than the cells grown in PNIM at similar cell density. This increase was found to be statistically significant ($p<0.05$). Conversely, ADP levels were found to be lower in PIM and higher in PNIM. ATP/ADP ratio in PIM growing cells was found to be as high as 14 as compared to 1.2 in

PNIM grown cells. This indicated faster conversion of NADH to ATP through electron transport chain (ETC) in PIM growing cells. However, ATP level did not increase in proportion to NADH level noticed during PCD probably due to simultaneous electron leakage.

Figure 2.8

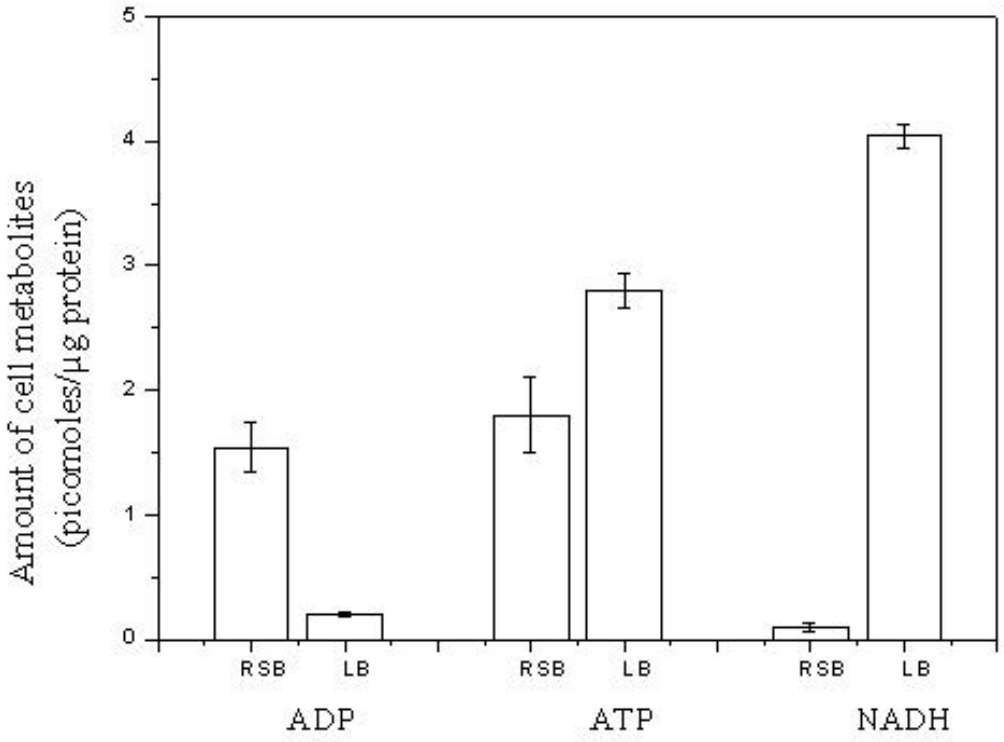

Fig.2.8: Increase in NADH and ATP level in Xcg cells undergoing PCD.

2.3.2 Estimation of free radical status in Xcg cells undergoing PCD

NADH is known to act as a pro-oxidant in bacteria as well as eukaryotic cells [35–39]. NADH is oxidized by complex I (NADH dehydrogenase) and the electrons (e-) are subsequently transferred to other respiratory complexes to eventually reduce O_2 to H_2O [38]. The proton motive force created by the movement of electrons is harnessed to produce ATP by ATP synthase. Although this process is universal among all aerobic organisms, it is inherently dangerous due to its ability to create a highly oxidative intracellular environment. The inefficient transfer of e- via the respiratory complexes results in the one electron reduction of oxygen leading to toxic ROS formation [35,38]. The status of ROS was checked

by 2', 7'- dichlorofluorescein diacetate (H_2DCFDA) staining and electron spin resonance (ESR) spectroscopy. H_2DCFDA is a unique fluorescence precursor that rapidly diffuses inside the cells where cellular esterases cleave the acetate moiety, allowing accumulation of the membrane impermeable form H_2DCF [40]. Further, H_2DCF is usually oxidized by peroxides (e.g. H_2O_2) in the presence of peroxidase, cytochrome c, or Fe^{2+} to form 2', 7', dichlorofluorescein (DCF) which can then be visualized using a fluorescent microscope. The assay provides a semi-quantitative measure of general intracellular reactive oxygen species (ROS) activity. The intensity of fluorescence is proportional to the levels of ROS generated within the cell. Cells from PIM culture when stained with H_2DCFDA fluoresced brightly under the fluorescence microscope (Fig.2.9A), whereas, negligible number of fluorescent cells was found in PNIM culture (Fig.2.9B).

Figure 2.9

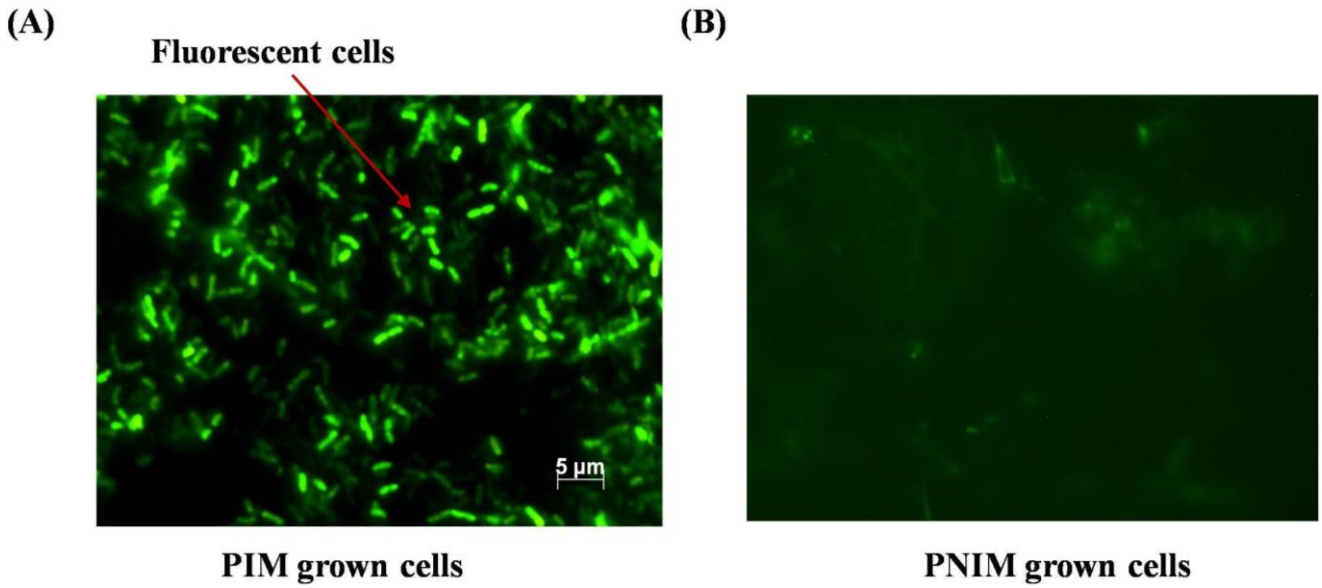

Fig. 2.9: Evaluation of ROS generation in Xcg cells: H_2DCFDA stained- **(A)** PIM grown cells, **(B)** PNIM grown cells. An aliquot was smeared on a glass slide, air dried, and examined under a fluorescent microscope (Carl Zeiss, Germany) using oil immersion

objective (1000x) and filter set 15 (Carl Zeiss, Germany; Excitation: 546 nm; emission: 590 nm).

The presence of free radicals was further investigated by electron spin resonance (ESR) spectroscopy using a spin trap system containing α-(4-pyridyl 1-oxide)-N-tert-butylnitrone (POBN) and DMSO, which showed the presence of hydroxyl radical ($OH^{\cdot}$). In the spin trap system employed here, dimethyl sulfoxide (DMSO) reacted with $OH^{\cdot}$ and converted it into methyl radical ($^{\cdot}CH_3$). In addition, $^{\cdot}CH_3$ is converted to methoxy radical ($^{\cdot}OCH_3$) in the presence of O_2. The $^{\cdot}CH_3$ and $^{\cdot}OCH_3$ then reacted with POBN to form adducts [41]. These POBN adducts were detected using ESR spectroscopy. ESR studies of PCD exhibiting Xcg cells confirmed the presence of hydroxyl radical (Fig.2.10A). The triplet of POBN adducts was observed in Xcg cells undergoing PCD, but was found to be absent in PCD inhibiting condition (Fig.2.10A and B). Source of hydroxyl radical ($OH^{\cdot}$) in PCD exhibiting Xcg cells could be intracellularly generated hydrogen peroxide. The most important mechanism of $OH^{\cdot}$ generation from H_2O_2 inside cells is via Fenton reaction [H_2O_2 + Fe(II) or Cu(I)→ $OH^{\cdot}$ + $OH^{\cdot}$ + Fe(III) or Cu(II)] [42].

Figure 2.10

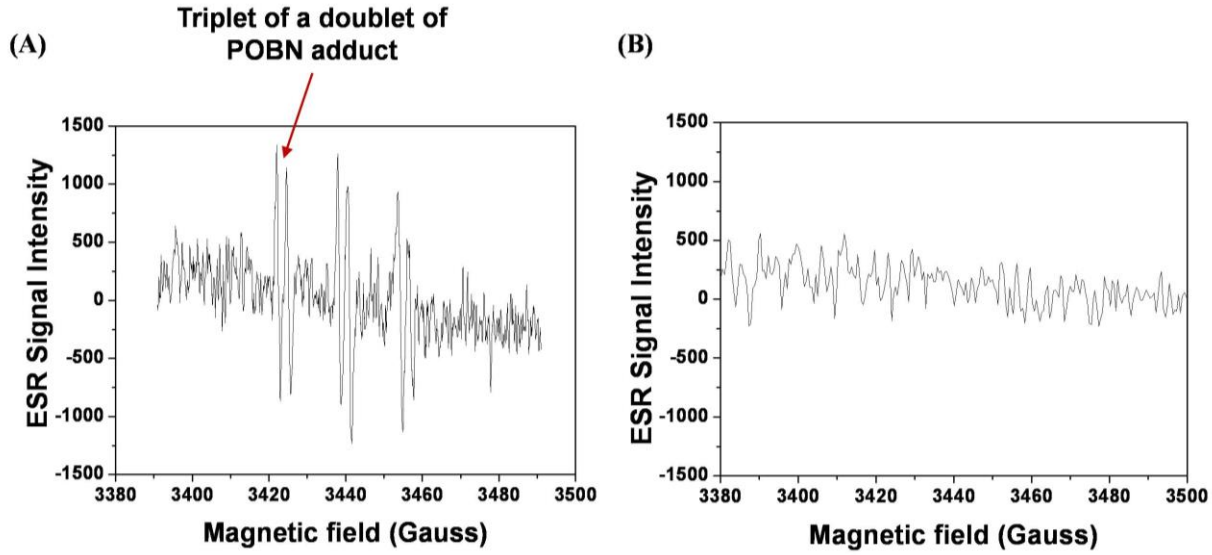

Fig. 2.10: ESR profile of POBN adducts in- (A) PIM grown cells, **(B)** PNIM grown cells

2.3.3 Effect of ETC uncoupler 2, 4-dinitrophenol

It has been reported that ~87% ROS in the *E. coli* cells origins from ETC [14]. In the bacterial and mitochondrial electron transport chain (ETC), there are two sites of electron leakage which lead to ROS formation [14,40]: site 1 on complex I (NADH-Q oxidoreductase) and site 2 at the interface between mobile lipid-soluble carrier, ubiquinone (Q) and complex III (Q-cytochrome c oxidoreductase). To explore the possibility of ETC as a source of ROS in the cells, 2, 4- dinitrophenol (DNP), an uncoupler was used in this study. Uncouplers are known to reduce ROS generation through ETC by preventing one electron reduction of O_2 as explained earlier (Fig.2.5). When Xcg cells were grown in PIM with DNP, the cell survival was found to be increased by one log cycle (Fig. 2.11A). Hydrogen peroxide levels were significantly lower in Xcg cells grown in PIM in the presence of 500 µM DNP as detected by scopoletin assay (Fig.2.11B)

Figure 2.11

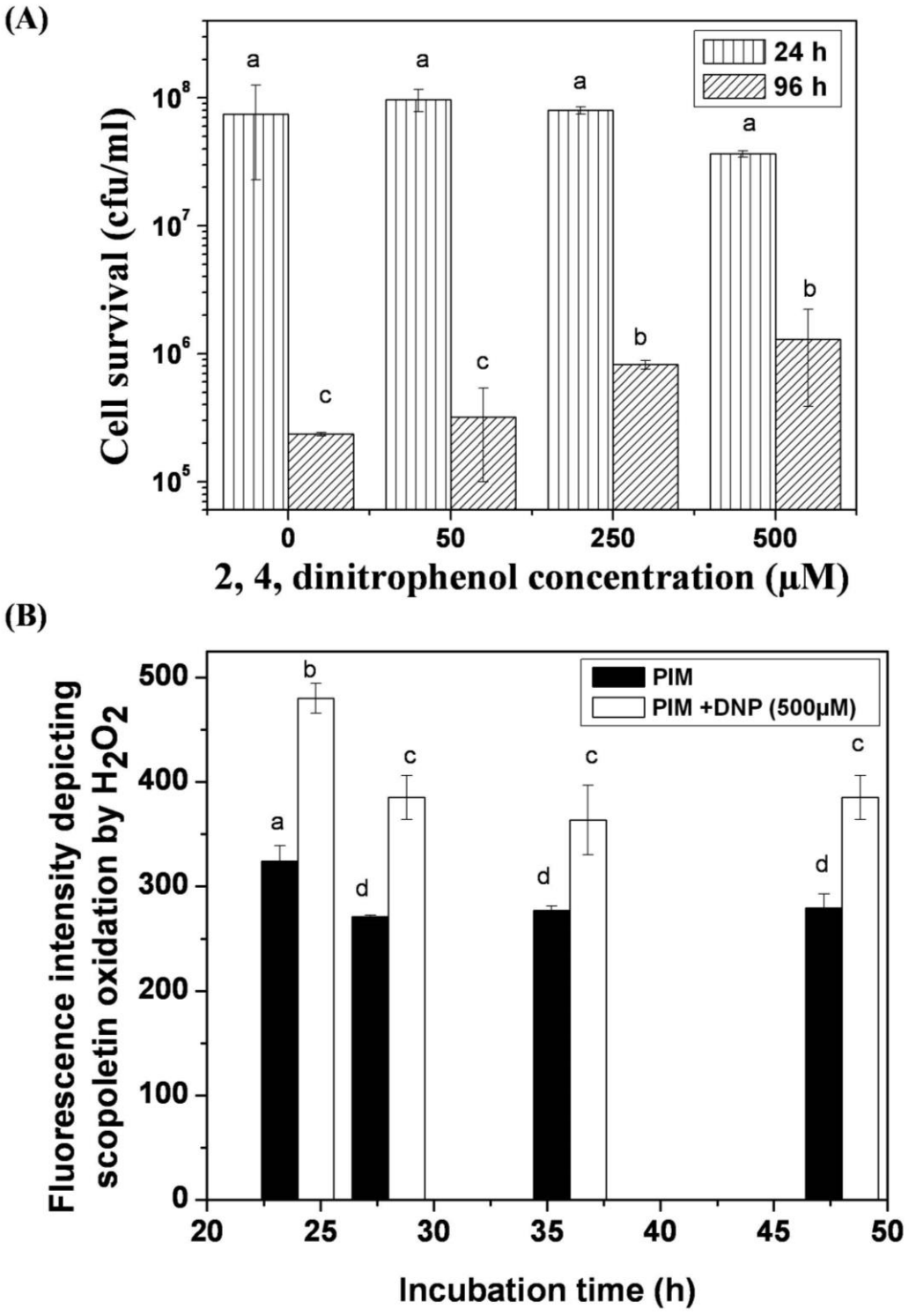

Fig. 2.11: Effect of ETC uncoupler 2, 4 dinitrophenol (DNP): (A) Xcg was grown in PIM in the presence of varying concentrations of DNP. Inhibition of PCD by DNP was observed

in PIM growing Xcg cells in a concentration dependent manner; **(B)** Inhibition of intracellular H_2O_2 generation (Scopoletin assay) in PIM growing Xcg cells in the presence of DNP. Scopoletin is a fluorescent dye. Its oxidation by hydrogen peroxide (H_2O_2) leads to a decrease in fluorescence which is proportional to the levels of H_2O_2 in the medium. The different letter on bars indicates that the means are significantly different at $p<0.05$.

2.3.4 Effect of ROS scavengers on PCD profile of *Xanthomonas*

Although above studies ascertained the formation of free radicals during PCD in Xcg, it was not clear if these radicals are the cause or the effect of PCD. To answer this question, ROS scavengers dimethysulfoxide (DMSO), glutathione (GSH), n-propyl gallate (nPG), and catalase were tested for their effect on PCD. The cell survival almost doubled in the presence of DMSO (0.25 – 0.5%) compared to control at the end of 96 h incubation period and the increase was found to be statistically significant ($p<0.05$) (Fig.2.12A). However, the increase observed in survival was not found to be significantly affected by increase in DMSO concentration ($p\leq 0.05$). When GSH was added to PIM, a concentration dependent increase in cell survival was observed when assayed at 96 h of incubation and PCD was completely inhibited with 10 mM GSH (Fig.2.12B). Similar to GSH, PCD was significantly abolished with 100 µM nPG (Fig.2.12C), and 500 U/ml of catalase (Fig.2.12D). No growth was observed at higher concentrations of GSH or nPG and both were found to be more effective than DMSO in inhibiting the PCD. Caspase-3 biosynthesis was also found to be lower in cells grown in the presence of these ROS scavengers (Fig 2.13A). In comparison to PIM grown Xcg cells, the caspase-3 band intensity was 14, 25, 53, and 57% in cells grown in PIM in the presence of GSH (10 mM), DMSO (0.5%), nPG (100 µM), and catalase (500 U/ml), respectively. The inhibition of caspase-3 expression by DMSO (0.5%), or GSH (10 mM) was

quite prominent compared to npG, or catalase. This effect could be possibly due to difference in the mechanism of action of different ROS scavengers. Caspase-3 activity decreased by 15, 10, and 20% in Xcg cells grown in PIM in the presence of GSH (10 mM), nPG (100 μM), and catalase (100 U/ml), respectively as compared to Xcg cells grown in PIM alone (Fig. 2.13B). Caspase-3 activity in Xcg cells grown in PIM in the presence of DMSO (0.5%) was negligible (data not shown).

Figure 2.12

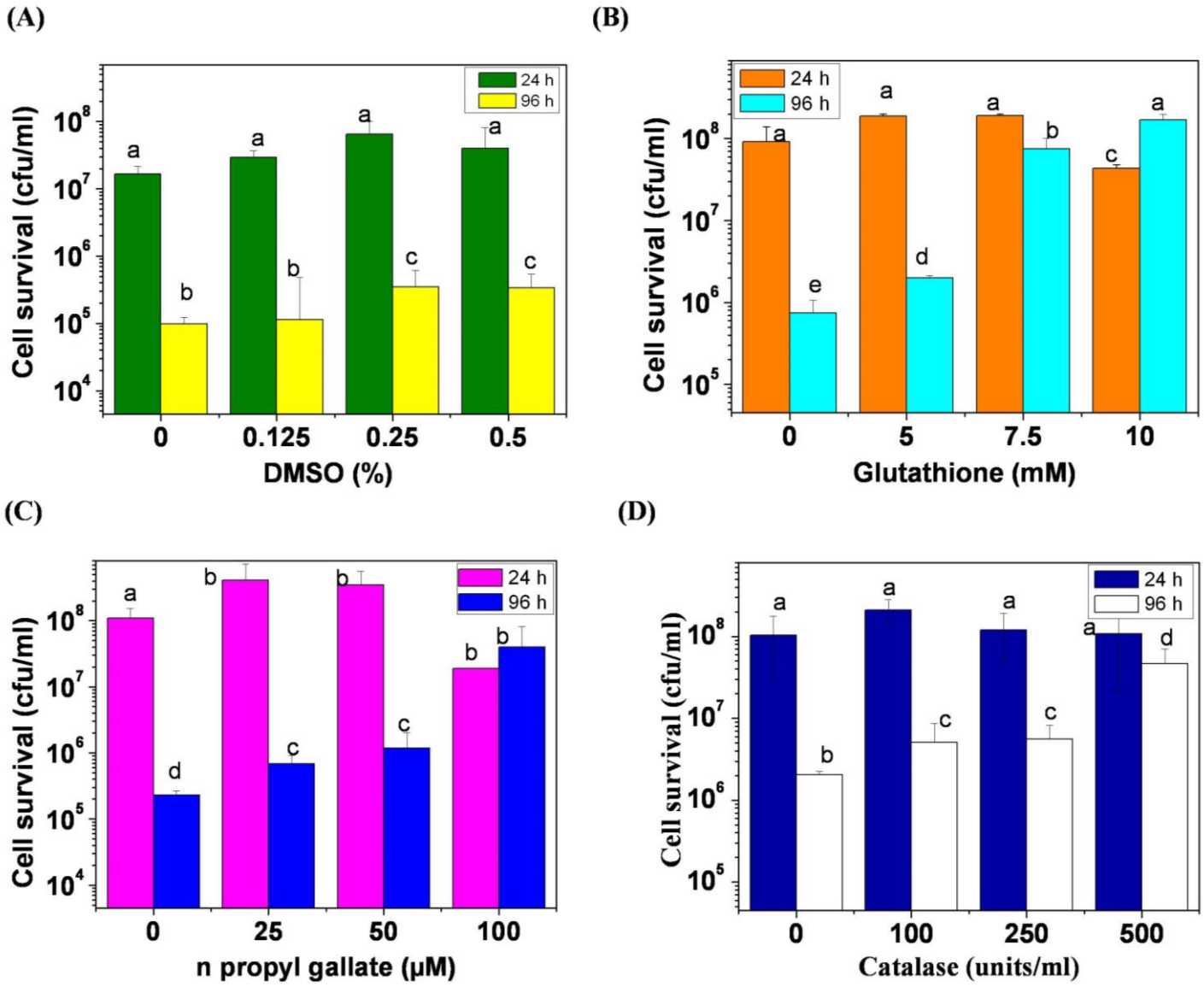

Fig. 2.12: Inhibition of PCD by ROS scavengers. PCD inhibition by: **(A)** DMSO, **(B)** GSH, **(C)** nPG, and **(D)** catalase. The different letter on bars indicates that the means are significantly different at $p<0.05$.

Figure 2.13

(A)

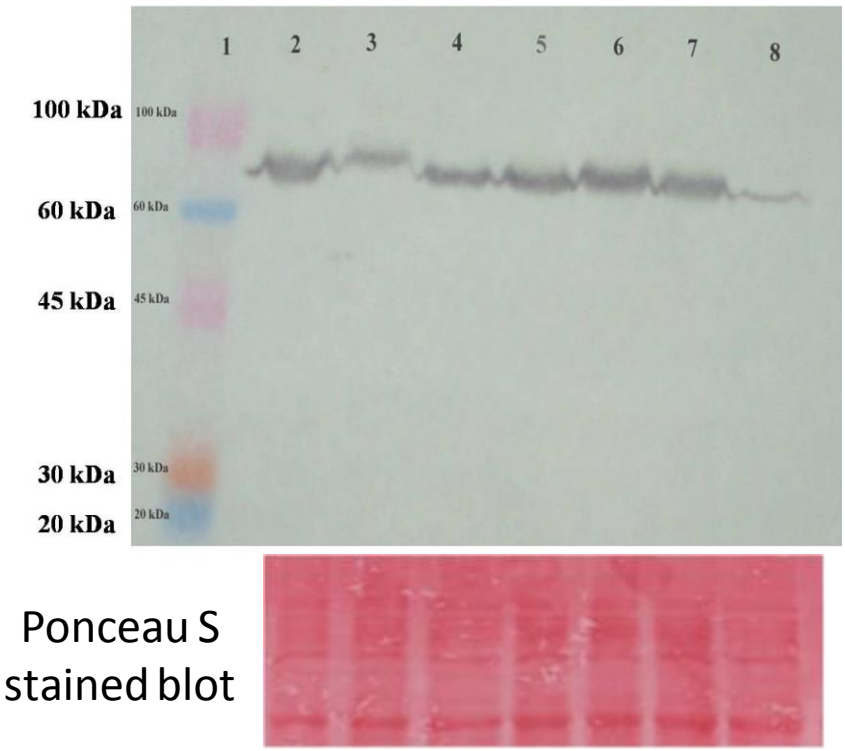

(B)

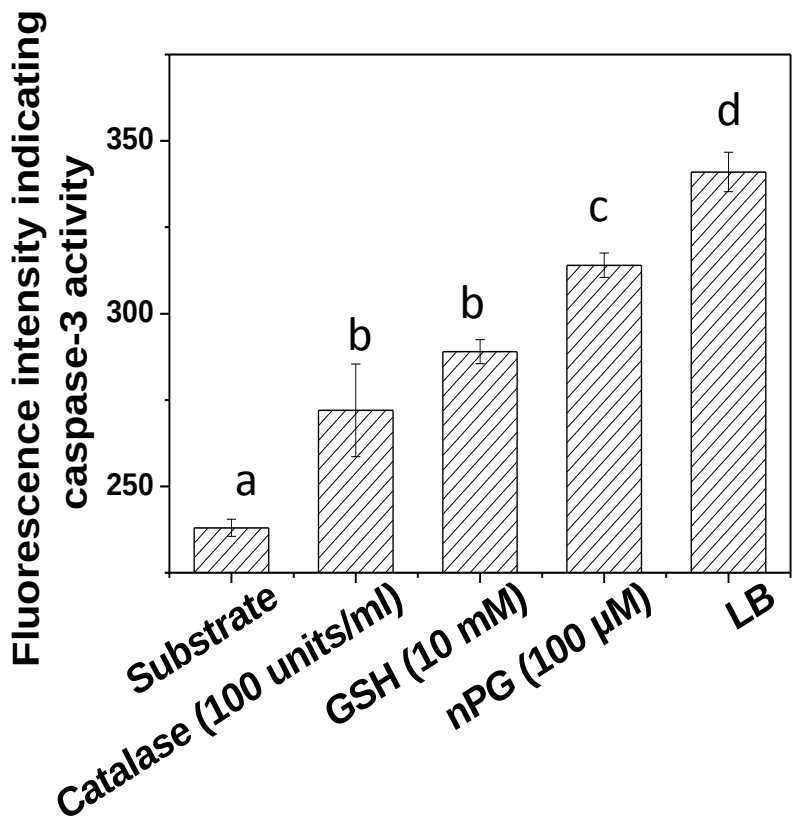

Fig. 2.13: Inhibition caspase-3 biosynthesis and activity in PIM growing Xcg cells by ROS scavengers: (A) Caspase biosynthesis inhibition (western blot): lane1: Coloured molecular weight marker, lane 2: PIM grown cells, lanes 3 - 8: PIM grown cells in presence of different ROS scavengers; 3- DMSO, 4- nPG (50 µM), 5- nPG (100µM), 6- catalase (500 units/ml), 7- GSH (5 mM), 8- GSH (10 mM)}. Ponceau S staining was carried out to check protein transfer and confirm equal protein amount in each lane.; **(B)** Inhibition of caspase-3 activity. The different letter on bars indicates that the means are significantly different at $p<0.05$.

To monitor the level of DNA damage, TUNEL assay was performed in the presence of above ROS scavengers. The population of TUNEL positive cells increased to 23% in PIM. It decreased significantly to 2, 4, and 6% in cultures grown independently in the presence of ROS scavengers, n-propyl gallate, catalase, and glutathione respectively (Fig 2.14).

Figure 2.14

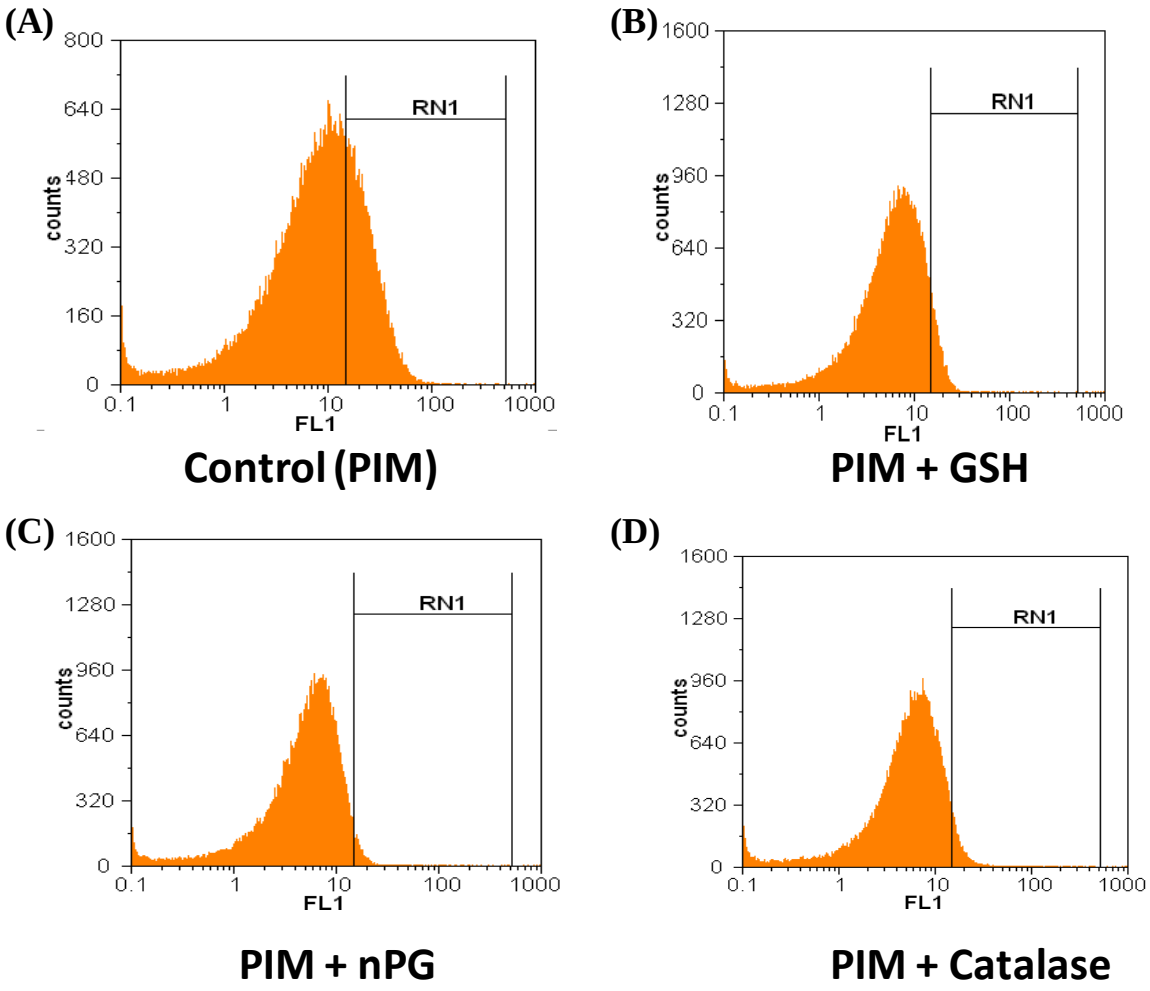

Fig. 2.14: Inhibition of DNA damage in Xcg cells grown in PIM in the presence of ROS scavengers as assessed by TUNEL assay: (A) Xcg cells grown in PIM; (B) Xcg cells grown in the presence of GSH (10 mM); (C) Xcg cells grown in the presence of nPG (100 µM); (D) Xcg cells grown in the presence of catalase (500 units/ml).

2.3.5 Effect of catalase on survival of Xcg

Addition of catalase in PIM increased the Xcg cell survival by two log cycles (Fig 2.15 A). On the contrary, addition of Proteinase K to the same didn't prevent PCD, hence ruling out

the possibility of protein or peptide to act as signaling molecule which has been reported earlier in many cases to have this role. This indicated that H_2O_2 plays an important role in accelerating PCD in Xcg (Fig 2.15 A and B).

The cell survival improved significantly in the presence of ROS scavengers DMSO, GSH, n-propyl gallate (nPG), and catalase. DMSO scavenges OH^-, whereas, npG scavenges superoxide radical. GSH and catalase can degrade hydrogen peroxide. Maximum protection was seen in the presence of GSH, indicating a significant role of H_2O_2 during PCD in Xcg. Catalase increased the cell survival by two log cycles indicating a possible role of H_2O_2 in cell-cell signaling during PCD in Xcg, as catalase being a large molecule (250 kDa) cannot enter the cell.

Among the various types of ROS produced in a cell, due to chemical stability, and membrane permeability, H_2O_2 is considered to be one of the good candidates for involvement in intercellular signaling during the process of PCD [43–45]. H_2O_2 produced by lysine oxidase has been reported to help in biofilm differentiation and dispersal in several Gram negative bacteria [46]. Besides microbes, ROS was found to play a vital role in eukaryotic (both in plants and animals) apoptosis where it has been reported to act as a long distance cell messenger [45–47]. In animals H_2O_2 could mediate induction of apoptosis during self-elimination of organs in ontogenesis such as the disappearance of the tadpole tail [45]. Similarly, H_2O_2 production was found to be enhanced in human cervical carcinoma (HeLa) cells undergoing apoptosis [43,45].

Figure 2.15

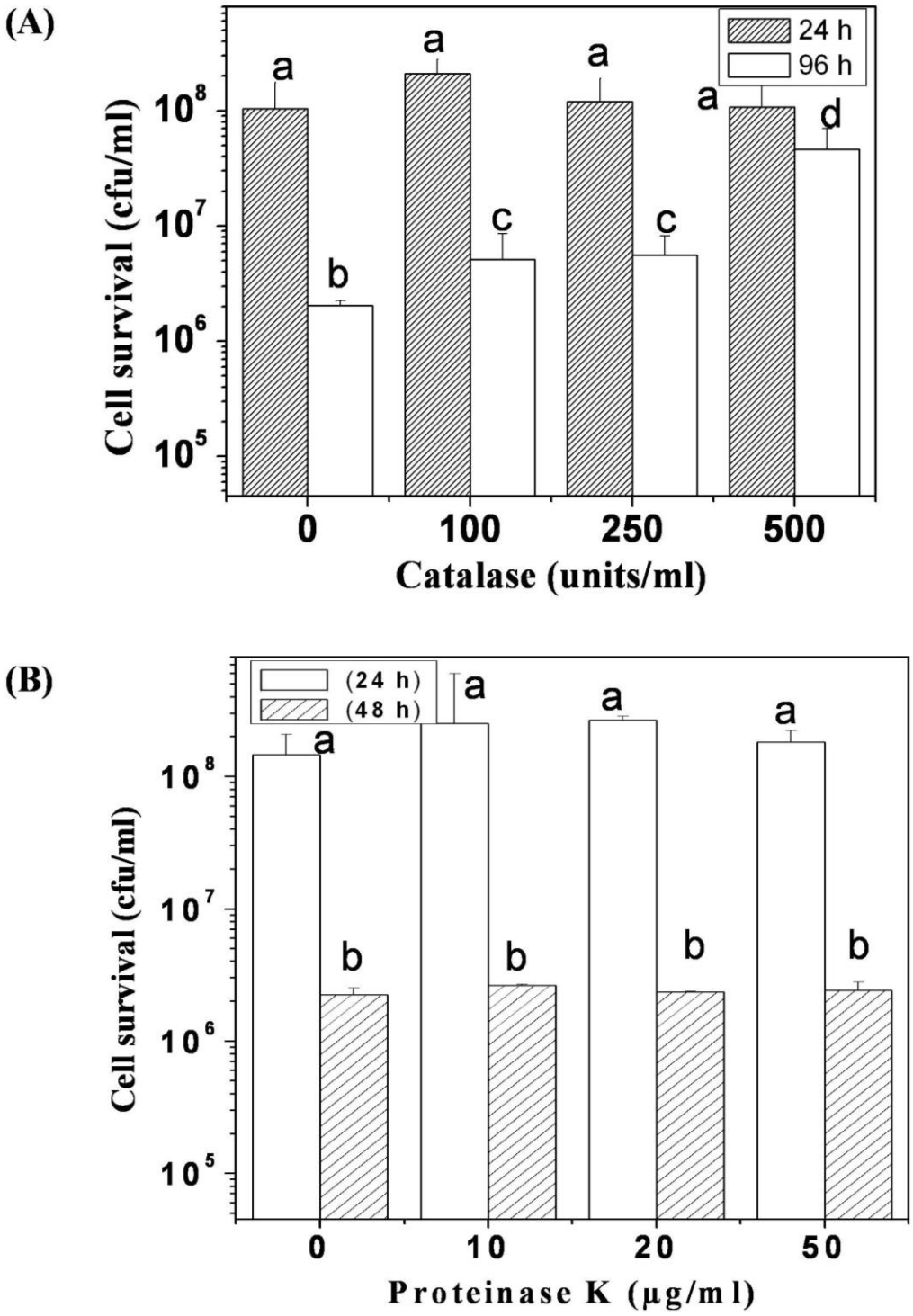

Fig. 2.15: Growth profile of Xcg in the presence of catalase or proteinase K: (A) Inhibition of PCD in PIM growing Xcg cells by catalase; **(B)** Xcg growth profile in the

presence of proteinaseK. The different letter on bars indicates that the means are significantly different at $p<0.05$.

2.3.6 H_2O_2 accumulation

Intracellular concentration of H_2O_2 was compared using scopoletin assay [48]. The amount of H_2O_2 was measured by horseradish peroxidase catalyzed oxidation of the fluorescent dye scopoletin (7-hydroxy-6-methoxycoumarin). The fluorescence intensity was proportional to the amount of H_2O_2 present in the cell. In PNIM culture, H_2O_2 was below detectable level. H_2O_2 concentration in PIM growing cells steadily increased till 24 h and further remained stable till 48 h of incubation (Fig 2.16A). As reported earlier [31,49], PCD started at this time point only.

2.3.7 *In vitro* activation of Xcg caspase by H_2O_2

When PNIM grown Xcg cell lysate was exposed to H_2O_2, the level of caspase activity increased in a concentration dependent manner as evidenced by the observed increase in the fluorescence intensity (Fig 2.16B). Together these findings indicate that hydrogen peroxide is involved in induction of PCD signal in Xcg. Recently it has been shown that oxidative modification of Cys-403 of caspase-9 facilitates its activation via disulfide mediated interaction with Apaf-1 [50].

Caspase has been reported to be activated by direct oxidative modification of its cysteine residue in higher organisms [50]. H_2O_2, a mild oxidant, can oxidize specific protein sulfhydryl groups, producing proteins with cysteine sulfinic acid (CysS-OH) or disulfide residues, both of which can be reduced back to Cys-SH by various cellular reductants. Very few proteins are expected to have a Cys-SH that is susceptible to oxidation by H_2O_2 in cells because this

oxidation requires that the target Cys-SH have a pKa below 7.0, whereas, the pKa values of most protein Cys-SH residues are higher than 8.0. Proteins like cysteine proteases (e.g. caspases) are known to contain an essential Cys-SH with a low pKa at their active sites [51], and is thus a potential candidate for reversible oxidation by intracellularly generated H_2O_2 [52]. Interestingly, H_2O_2 exposure activated Xcg caspase-3 activity *in vitro*.

Figure 2.16

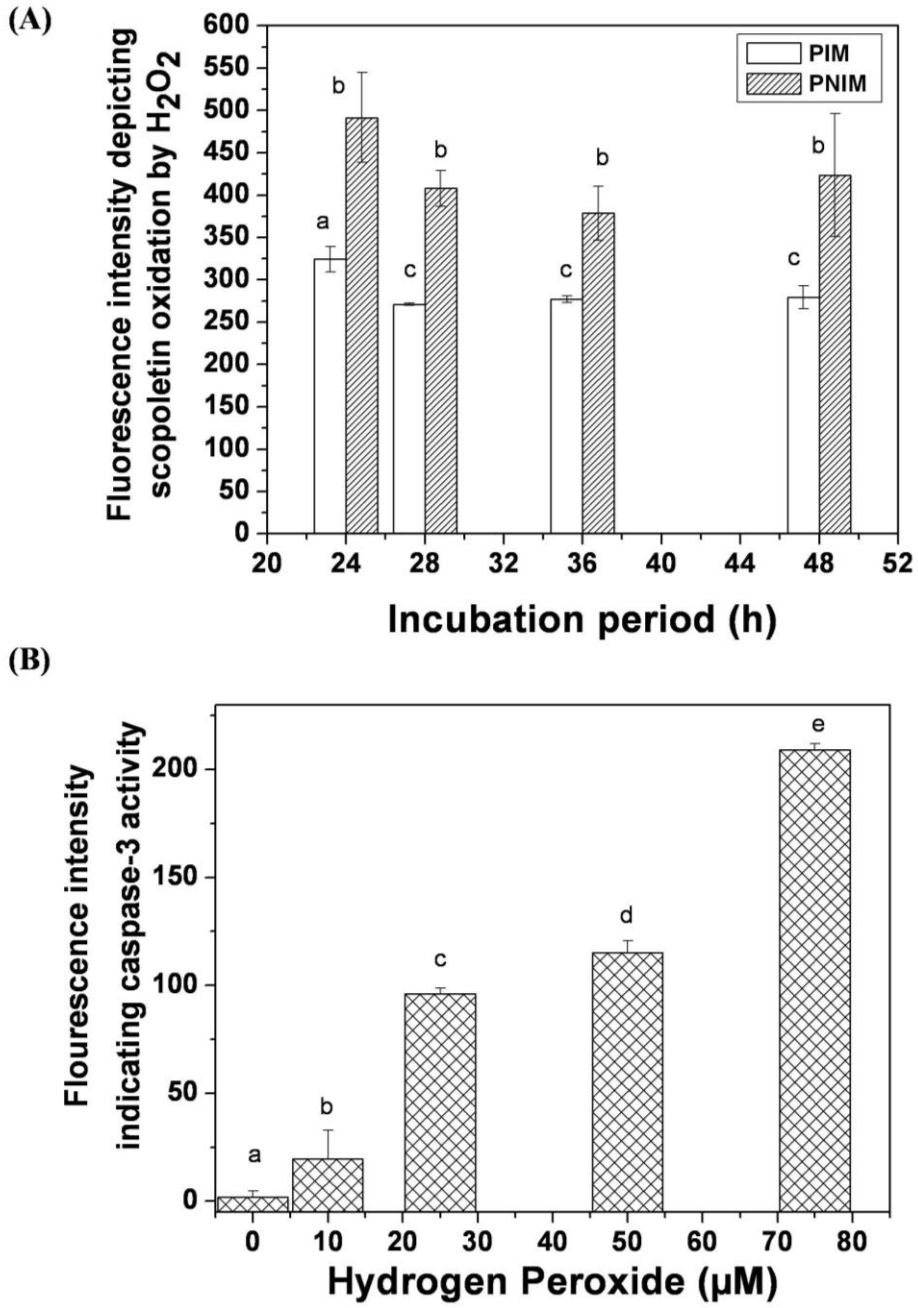

Fig. 2.16: Level of H_2O_2 in Xcg cultures and in vitro activation of Xcg caspase by H_2O_2

(A) H_2O_2 level measured in PIM and PNIM Xcg cultures by scopoletin assay; **(B)** *In vitro* activation of Xcg caspase-3 by hydrogen peroxide. The different letter on bars indicates that the means are significantly different at $p<0.05$.

References

1. DeBerardinis RJ, Thompson CB (2012) Cellular metabolism and disease: what do metabolic outliers teach us? Cell 148: 1132-1144. S0092-8674(12)00232-2 [pii];10.1016/j.cell.2012.02.032 [doi].

2. Higgins D, Dworkin J (2012) Recent progress in Bacillus subtilis sporulation. FEMS Microbiol Rev 36: 131-148. 10.1111/j.1574-6976.2011.00310.x [doi].

3. Boutte CC, Crosson S (2013) Bacterial lifestyle shapes stringent response activation. Trends Microbiol 21: 174-180. S0966-842X(13)00013-9 [pii];10.1016/j.tim.2013.01.002 [doi].

4. Yamaguchi Y, Park JH, Inouye M (2011) Toxin-antitoxin systems in bacteria and archaea. Annu Rev Genet 45: 61-79. 10.1146/annurev-genet-110410-132412 [doi].

5. Engelberg-Kulka H, Hazan R, Amitai S (2005) mazEF: a chromosomal toxin-antitoxin module that triggers programmed cell death in bacteria. J Cell Sci 118: 4327-4332. 118/19/4327 [pii];10.1242/jcs.02619 [doi].

6. Yarmolinsky MB (1995) Programmed cell death in bacterial populations. Science 267: 836-837.

7. Gerdes K, Christensen SK, Lobner-Olesen A (2005) Prokaryotic toxin-antitoxin stress response loci. Nat Rev Microbiol 3: 371-382. nrmicro1147 [pii];10.1038/nrmicro1147 [doi].

8. D'Autreaux B, Toledano MB (2007) ROS as signalling molecules: mechanisms that generate specificity in ROS homeostasis. Nat Rev Mol Cell Biol 8: 813-824. nrm2256 [pii];10.1038/nrm2256 [doi].

9. Circu ML, Aw TY (2010) Reactive oxygen species, cellular redox systems, and apoptosis. Free Radic Biol Med 48: 749-762. S0891-5849(09)00793-X [pii];10.1016/j.freeradbiomed.2009.12.022 [doi].

10. Schaetzle O, Barrière F, Baronianb K (2008) Bacteria and yeasts as catalysts in microbial fuel cells: electron transfer from micro-organisms to electrodes for green electricity. Energy Environ Sci 1: 607-620.

11. Richardson DJ (2000) Bacterial respiration: a flexible process for a changing environment. Microbiology 146 (Pt 3): 551-571.

12. Brand MD (2000) Uncoupling to survive? The role of mitochondrial inefficiency in ageing. Exp Gerontol 35: 811-820. S0531-5565(00)00135-2 [pii].

13. Gonzalez-Flecha B, Demple B (1995) Metabolic sources of hydrogen peroxide in aerobically growing Escherichia coli. J Biol Chem 270: 13681-13687.

14. Cabiscol E, Tamarit J, Ros J (2000) Oxidative stress in bacteria and protein damage by reactive oxygen species. Int Microbiol 3: 3-8.

15. Andrews ZB, Diano S, Horvath TL (2005) Mitochondrial uncoupling proteins in the CNS: in support of function and survival. Nat Rev Neurosci 6: 829-840. nrn1767 [pii];10.1038/nrn1767 [doi].

16. Imlay JA (2013) The molecular mechanisms and physiological consequences of oxidative stress: lessons from a model bacterium. Nat Rev Microbiol 11: 443-454. nrmicro3032 [pii];10.1038/nrmicro3032 [doi].

17. Harman D (1981) The aging process. Proc Natl Acad Sci U S A 78: 7124-7128.

18. Jumpertz R, Hanson RL, Sievers ML, Bennett PH, Nelson RG, Krakoff J (2011) Higher energy expenditure in humans predicts natural mortality. J Clin Endocrinol Metab 96: E972-E976. jc.2010-2944 [pii];10.1210/jc.2010-2944 [doi].

19. Weindruch R, Walford RL, Fligiel S, Guthrie D (1986) The retardation of aging in mice by dietary restriction: longevity, cancer, immunity and lifetime energy intake. J Nutr 116: 641-654.

20. Masoro EJ (2005) Overview of caloric restriction and ageing. Mech Ageing Dev 126: 913-922. S0047-6374(05)00078-3 [pii];10.1016/j.mad.2005.03.012 [doi].

21. Nystrom T (2003) The free-radical hypothesis of aging goes prokaryotic. Cell Mol Life Sci 60: 1333-1341. 10.1007/s00018-003-2310-X [doi].

22. Nystrom T (2003) Conditional senescence in bacteria: death of the immortals. Mol Microbiol 48: 17-23. 3385 [pii].

23. Rea S, Johnson TE (2003) A metabolic model for life span determination in Caenorhabditis elegans. Dev Cell 5: 197-203. S1534580703002429 [pii].

24. Kohanski MA, Dwyer DJ, Hayete B, Lawrence CA, Collins JJ (2007) A common mechanism of cellular death induced by bactericidal antibiotics. Cell 130: 797-810. S0092-8674(07)00899-9 [pii];10.1016/j.cell.2007.06.049 [doi].

25. Liu Y, Imlay JA (2013) Cell death from antibiotics without the involvement of reactive oxygen species. Science 339: 1210-1213. 339/6124/1210 [pii];10.1126/science.1232751 [doi].

26. Keren I, Wu Y, Inocencio J, Mulcahy LR, Lewis K (2013) Killing by bactericidal antibiotics does not depend on reactive oxygen species. Science 339: 1213-1216. 339/6124/1213 [pii];10.1126/science.1232688 [doi].

27. Wu X, Wang X, Drlica K, Zhao X (2011) A toxin-antitoxin module in Bacillus subtilis can both mitigate and amplify effects of lethal stress. PLoS One 6: e23909. 10.1371/journal.pone.0023909 [doi];PONE-D-10-06048 [pii].

28. Marchetti MA, Weinberger M, Murakami Y, Burhans WC, Huberman JA (2006) Production of reactive oxygen species in response to replication stress and inappropriate mitosis in fission yeast. J Cell Sci 119: 124-131. 119/1/124 [pii];10.1242/jcs.02703 [doi].

29. Thomas VC, Sadykov MR, Chaudhari SS, Jones J, Endres JL, Widhelm TJ, Ahn JS, Jawa RS, Zimmerman MC, Bayles KW (2014) A central role for carbon-overflow pathways in the modulation of bacterial cell death. PLoS Pathog 10: e1004205. 10.1371/journal.ppat.1004205 [doi];PPATHOGENS-D-13-03034 [pii].

30. Aw TY (2003) Cellular redox: a modulator of intestinal epithelial cell proliferation. News Physiol Sci 18: 201-204.

31. Gautam S, Sharma A (2002) Involvement of caspase-3-like protein in rapid cell death of Xanthomonas. Mol Microbiol 44: 393-401. 2837 [pii].

32. Caruso R, Campolo J, Dellanoce C, Mariele R, Parodi O, Accinni R (2004) Critical study of preanalytical and analytical phases of adenine and pyridine nucleotide assay in human whole blood. Anal Biochem 330: 43-51. 10.1016/j.ab.2004.03.063 [doi];S0003269704003215 [pii].

33. Giannattasio S, Gagliardi S, Samaja M, Marra E (2003) Simultaneous determination of purine nucleotides, their metabolites and beta-nicotinamide adenine dinucleotide in cerebellar granule cells by ion-pair high performance liquid chromatography. Brain Res Brain Res Protoc 10: 168-174. S1385299X02002155 [pii].

34. Raju KK, Gautam S, Sharma A (2006) Molecules involved in the modulation of rapid cell death in Xanthomonas. J Bacteriol 188: 5408-5416. 188/15/5408 [pii];10.1128/JB.00056-06 [doi].

35. Thorenoor N, Lee JH, Lee SK, Cho SW, Kim YH, Kim KS, Lee C (2010) Localization of the death effector domain of Fas-associated death domain protein into the membrane of Escherichia coli induces reactive oxygen species-involved cell death. Biochemistry 49: 1435-1447. 10.1021/bi901783s [doi].

36. Kohanski MA, Dwyer DJ, Collins JJ (2010) How antibiotics kill bacteria: from targets to networks. Nat Rev Microbiol 8: 423-435. nrmicro2333 [pii];10.1038/nrmicro2333 [doi].

37. Knuuti J, Belevich G, Sharma V, Bloch DA, Verkhovskaya M (2013) A single amino acid residue controls ROS production in the respiratory Complex I from Escherichia coli. Mol Microbiol 90: 1190-1200. 10.1111/mmi.12424 [doi].

38. Mailloux RJ, Beriault R, Lemire J, Singh R, Chenier DR, Hamel RD, Appanna VD (2007) The tricarboxylic acid cycle, an ancient metabolic network with a novel twist. PLoS One 2: e690. 10.1371/journal.pone.0000690 [doi].

39. Tretter L, Adam-Vizi V (2004) Generation of reactive oxygen species in the reaction catalyzed by alpha-ketoglutarate dehydrogenase. J Neurosci 24: 7771-7778. 10.1523/JNEUROSCI.1842-04.2004 [doi];24/36/7771 [pii].

40. Blackstone NW, Bivins MJ, Cherry KS, Fletcher RE, Geddes GC (2005) Redox signaling in colonial hydroids: many pathways for peroxide. J Exp Biol 208: 383-390. 208/2/383 [pii];10.1242/jeb.01394 [doi].

41. Nakai K, Kadiiska MB, Jiang JJ, Stadler K, Mason RP (2006) Free radical production requires both inducible nitric oxide synthase and xanthine oxidase in LPS-treated skin. Proc Natl Acad Sci U S A 103: 4616-4621. 0510352103 [pii];10.1073/pnas.0510352103 [doi].

42. Stadtman ER, Berlett BS (1998) Reactive oxygen-mediated protein oxidation in aging and disease. Drug Metab Rev 30: 225-243. 10.3109/03602539808996310 [doi].

43. Pletjushkina OY, Fetisova EK, Lyamzaev KG, Ivanova OY, Domnina LV, Vyssokikh MY, Pustovidko AV, Alexeevski AV, Alexeevski DA, Vasiliev JM, Murphy MP, Chernyak BV, Skulachev VP (2006) Hydrogen peroxide produced inside mitochondria takes part in cell-to-cell transmission of apoptotic signal. Biochemistry (Mosc) 71: 60-67. BCM71010075 [pii].

44. Corcoran A, Cotter TG (2013) Redox regulation of protein kinases. FEBS J 280: 1944-1965. 10.1111/febs.12224 [doi].

45. Pletjushkina OY, Fetisova EK, Lyamzaev KG, Ivanova OY, Domnina LV, Vyssokikh MY, Pustovidko AV, Vasiliev JM, Murphy MP, Chernyak BV, Skulachev VP (2005) Long-distance apoptotic killing of cells is mediated by hydrogen peroxide in a mitochondrial ROS-dependent fashion. Cell Death Differ 12: 1442-1444. 4401685 [pii];10.1038/sj.cdd.4401685 [doi].

46. Veal E, Day A (2011) Hydrogen peroxide as a signaling molecule. Antioxid Redox Signal 15: 147-151. 10.1089/ars.2011.3968 [doi].

47. Lam E, Kato N, Lawton M (2001) Programmed cell death, mitochondria and the plant hypersensitive response. Nature 411: 848-853. 10.1038/35081184 [doi].

48. Waddell TK, Fialkow L, Chan CK, Kishimoto TK, Downey GP (1994) Potentiation of the oxidative burst of human neutrophils. A signaling role for L-selectin. J Biol Chem 269: 18485-18491.

49. Gautam S, Sharma A (2002) Rapid cell death in Xanthomonas campestris pv. glycines. J Gen Appl Microbiol 48: 67-76.

50. Zuo Y, Xiang B, Yang J, Sun X, Wang Y, Cang H, Yi J (2009) Oxidative modification of caspase-9 facilitates its activation via disulfide-mediated interaction with Apaf-1. Cell Res 19: 449-457. cr200919 [pii];10.1038/cr.2009.19 [doi].

51. Ischiropoulos H (1998) Living and dying with reactive species. Focus on "peroxynitrite induces apoptosis of HL-60 cells by activation of a caspase-3 family protease". Am J Physiol 274: C853-C854.

52. Rhee SG (1999) Redox signaling: hydrogen peroxide as intracellular messenger. Exp Mol Med 31: 53-59. 10.1038/emm.1999.9 [doi].

Chapter 3: Accumulation of Proline and Associated Proline Oxidase (PutA) Activity during Metabolic Stress Induced PCD in *Xanthomonas*

3.1 Introduction

3.1.1 Proline metabolism

Besides serving as important building blocks for proteins, amino acids can also serve as sole source of carbon, nitrogen, sulphur and energy [1]. Proline metabolism is distinct from that of primary amino acids and plays a regulatory role in certain physiological conditions [2]. Proline catabolism has been observed to be an important source of energy in some Gram negative bacteria such as *Helicobacter pylori*, *Bradyrhizobium japonicum*, *Sinorhizobium meliloti*, and *Mycobacterium smegmatis* during stress [3–7]. PutA is significantly upregulated in *Mycobacterium smegmatis* and is preferentially used as an electron donor to the respiratory chain during energy limiting conditions [6]. Proline is a non-essential, secondary amino acid having cyclic structure due to bonding between amine group and the two alkyl groups (Fig 3.1).

Figure 3.1

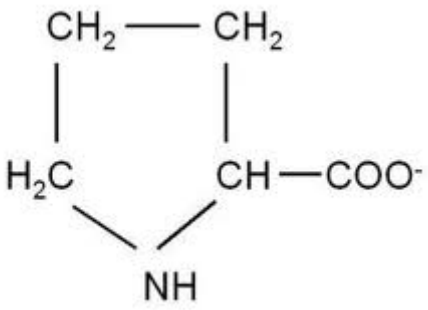

Reference: http://brc.se.fju.edu.tw/protein/character/kinds.htm

Fig. 3.1: Structure of amino acid proline

Proline is converted to glutamate via a four electron oxidation process (Fig 3.2). Proline dehydrogenase (PRODH or POX) performs the first oxidative step, resulting in the intermediate pyrroline-5-carboxylate (P5C). P5C is subsequently hydrolyzed to glutamic semialdehyde (GSA), which is then further oxidized by P5C dehydrogenase (P5CDH) to generate glutamate. Glutamate can be converted to α-ketoglutarate through deamination, which may be incorporated into the tricarboxylic acid (TCA) cycle. In Gram-negative bacteria, PRODH and P5CDH are fused together in a bifunctional enzyme called proline utilization A (PutA). The $FADH_2$ generated during this process directly transfers the electrons to ubiquinone of electron transport chain (ETC) [8](Fig. 3.2).

Proline anabolism begins with phosphorylation of glutamate by gamma-glutamyl kinase (GK) to generate gamma-glutamyl phosphate (gamma-GP). This is subject to feedback inhibition by proline (even at very low concentrations) in bacteria [9,10]. Gamma-GP is reduced by gamma-glutamyl phosphate reductase (GPR) to GSA, which cyclizes to form P5C. P5C is then reduced to proline via pyrroline-5-carboxylate reductase (P5CR). In higher eukaryotes such as plants and animals, GPR and GK are fused together in the bifunctional enzyme pyrroline-5-carboxylate synthase (P5CS) [11]. In bacteria (such as *Escherichia coli*) the three enzymes; gamma-glutamyl kinase (GK), glutamate-5-semialdehyde dehydrogenase or glutamyl phosphate reductase (GPR), and pyrroline-5-carboxylate reductase (P5CR), are encoded by genes *proB*, *proA* and *proC*, respectively [12].

Figure 3.2

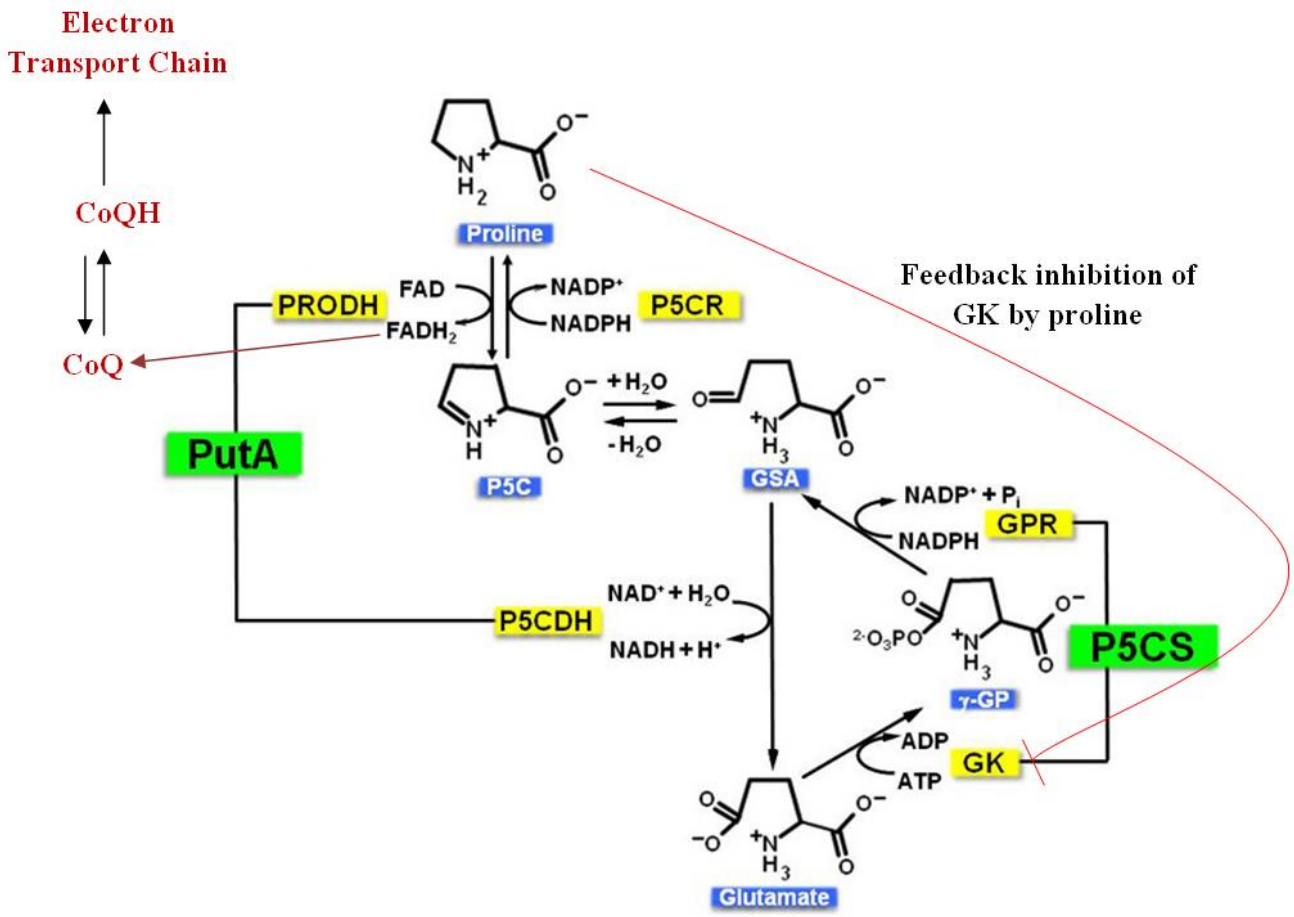

Reference: Arentson et al, 2012 [11] (Adapted and modified)

Fig.3.2: Metabolic pathways of proline. PRODH – Proline dehydrogenase; P5CDH – P5C dehydrogenase; P5CR – P5C reductase; GK- gamma glutamyl kinase; GPR - gamma-glutamyl phosphate reductase; P5CS - pyrroline-5-carboxylate synthase; GSA - glutamate-5-semialdehyde; P5C - pyrroline-5-carboxylate; γ-GP - gamma-glutamyl phosphate; CoQ – ubiquinone [11].

POX and P5CDH are encoded by two different genes in eukaryotes, whereas, in bacteria it is encoded by a single gene, *putA* [13]. PutA is located in the bacterial membrane or inner mitochondrial membrane in higher organisms. In bacteria, it typically consists of 1000-1300 amino acid residues. In some bacteria, like *Escherichia coli* and *Salmonella typhimurium,* it also contains a DNA binding domain that auto-regulates its transcription [13].

3.1.2 Proline transport in bacteria

Proline porter I and PutA regulate the catabolism of proline in *E.coli* [14]. They are induced when proline is provided as a carbon or nitrogen source in the environment. *E.coli* PutA regulates the transcription of *putA* and *putP* (Na^+/proline symporter) genes, and it switches its intracellular location and function by sensing the environmental proline levels. When the intracellular proline levels are low, it binds to DNA and represses the transcription of *put* genes. Conversely, when proline is available to the cell, PutA binds to the inner membrane and catalyzes the oxidation of proline to glutamate [15]. However, in *Salmonella, Klebsiella* and *Vibrio* the *putA* gene expression is regulated by c-AMP receptor protein [16–18]. *Xanthomonas* PutA has not been studied yet and the regulation of proline metabolism in this bacterium is not fully understood.

3.1.3 Proline metabolism and stress tolerance

Paradoxically, proline has been reported to act as an osmoprotectant in certain bacteria growing under osmotic stress [19,20]. Proline and glutamine were found to accumulate in *Staphylococcus aurues* grown in medium containing 5 and 10% NaCl [19]. This accumulation of proline was attributed to its preferential transport into the cell [19]. Proline pool was also found to increase in several other non halophilic bacteria as well like *E. coli,*

Salmonella, *Bacillus*, *Lactobacillus and Clostridium* when exposed to osmotic stress [21]. Proline has been reported to stimulate growth and respiration in some bacteria [6,21]. It has also been reported to protect *E. coli* from cold and heat stress [22]. Besides bacteria, proline has been shown to protect fungi, plants, and mammalian cells against oxidative stress [23]. Proline accumulation has also been reported in plants during conditions of drought, salinity, intense light, UV irradiation, heavy metals, oxidative stress, and biotic stresses [24,25].

3.1.4 Proline utilization protein A (PutA)

As mentioned above, PutA (or proline oxidase/dehydrogenase) oxidizes proline to glutamate. PutA is a flavoenzyme and requires $FADH_2$ as a cofactor to perform the first step of proline oxidation i.e. conversion of proline to P5C. Based on the functional domains present in the polypeptide, PutA can be classified into three types (Fig 3.3):

a) Monofunctional PutA

Monofunctional enzymes are functionally similar to eukaryotic POX as they only have PRODH domain and convert proline to P5C (Fig 3.3). Monofunctional PRODHs are typically 200–540 amino acid residues in length [11]. The best studied example of this group is the PRODH of *Thermus thermophilus.*

Figure 3.3

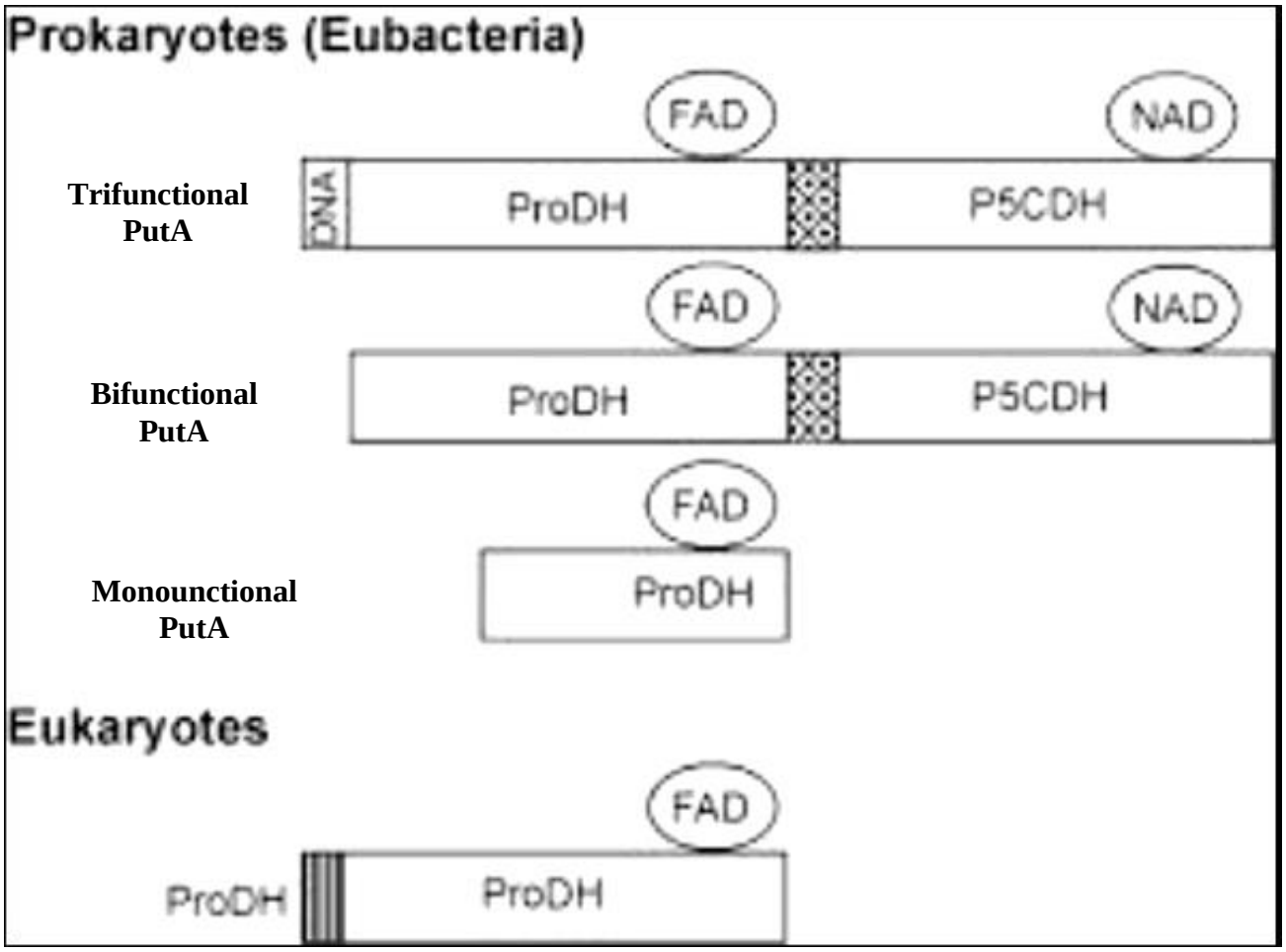

Reference: Servet et al., 2012 [26].

Fig.3.3: Structural organization of proline dehydrogenase. DNA indicates the DNA-binding domain of PutA. Vertical hatching indicates the mitochondrial transit peptide. Cross-hatching shows the linker that connects the two enzymatic activities. FAD: flavin adenine dinucleotide, NAD: nicotinamide adenine dinucleotide, P5CDH: P5C dehydrogenase, P5CR: P5C reductase, ProDH: proline dehydrogenase, PutA: proline utilization A [26].

b) Bifunctional PutA

Bifunctional PutA have both PRODH and P5CDH domains in a single polypeptide which is usually around 1100 amino acids long (Fig 3.3). These PutA also have a C-terminal domain (known as CTD) of unknown function. This fusion of enzymes PRODH and P5CDH catalyzing sequential steps of proline catabolism provides a kinetic advantage, because the intermediate (P5C/GSA) can be channeled between active sites without equilibrating into the bulk solvent [27]. Recently, Singh et al. provided kinetic data supporting substrate channeling for *Geobacter sulfurreducens* PutA [11,27]. This group reported the existence of a 75 Aº long tunnel that links the two active sites. Such substrate channeling has been reported for *Bradyrhizobium japonicum* PutA and *Salmonella typhimurium* PutA as well [11]. Such fused proteins like PutA, are termed as 'Rosetta Stone proteins', because they decipher interactions between protein pairs [28]. Thus, the 'Rosetta Stone hypothesis' of protein evolution predicts that eukaryotic PRODH and P5CDH form physical and functional interactions. The best characterized PutA of this group is of *Bradyrhizobium japonicum*.

c) Trifunctional PutA

The trifunctional PutA have a DNA binding domain along with PRODH and P5CDH domains at the N-terminal end of the polypeptide (Fig 3.3). The length of this type of PutA is usually around 1320 amino acid residues. The protein is present in enterobacteria. The trifunctional PutA has an additional function of autoregulating transcription. It exists both as a transcriptional repressor and as a membrane-associated proline dehydrogenase (Fig 3.3; 3.4). The *E. coli* PutA has been well characterized and it is reported to repress transcription of *put* regulon (comprising of the *putA* and *putP* genes coding for PutA and a proline transporter, respectively) by binding to the control region of the *put* intergenic DNA [29]. The

enzymatically active, membrane-bound form of PutA is unable to bind DNA and to repress transcription [29]. Studies led to the identification of the two factors that contribute to induction of *put* regulon: availability of FAD and proline. The shuttle of PutA from the DNA to the membrane is accompanied by a conformational change in the protein that is triggered by the availability of proline and FAD [30]. The proline-dependent reduction of the cofactor FAD directs PutA to the membrane and subsequently causes loss of DNA-binding activity, indicating that the two locations and the two biochemical activities of the protein are mutually exclusive [13]. It has been reported that a single proline binding site is involved both in enzymatic activity and induction of the *put* genes. This indicated that enzymatic activity was essential for the release of PutA from DNA and for *put* gene induction [31].

Figure 3.4

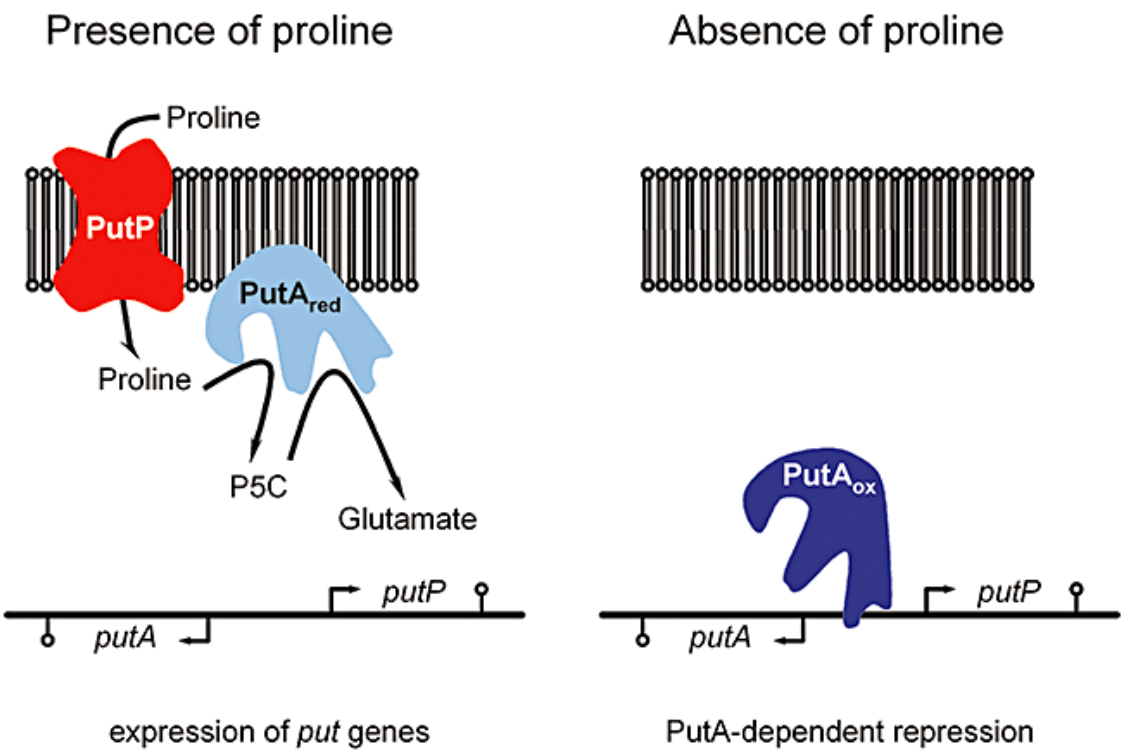

Reference: Commichau and Stülke, 2008 [29].

Fig.3.4: Localization of PutA determines its role in proline metabolism. In the presence of proline, the bifunctional enzyme PutA catalyses the two-step reaction from proline to glutamate. The reduced form of PutA ($PutA_{red}$) is localized in the membrane. The putP and putA genes, encoding the proline transporter PutP and the enzyme PutA, respectively, are expressed in the presence of proline. In the absence of proline, the oxidized PutA protein ($PutA_{ox}$) binds to the intergenic region of the putA and putP genes and represses their transcription. P5C, Δ1-pyrroline-5-carboxylate [29].

3.1.5 Proline oxidase and reactive oxygen species (ROS)

During the oxidation of proline to glutamate, $FADH_2$ and NADH are generated (Fig 3.2). These enter the electron transport chain and can eventually lead to enhanced production of ROS. Hence, PutA activity is essential for maintaining the redox homeostasis in the cell. In eukaryotes, impairment of P5C dehydrogenase activity results in P5C-proline cycling [32]. Recently, it has been shown that proline dehydrogenase of *Arabidopsis* is involved in ROS generation during the hypersensitive response [25,33]. Similarly, human POX has been reported to contribute to apoptosis by generation of ROS (mainly superoxide) either directly by interacting with oxygen at the enzyme active site or indirectly by increasing the electron flux in the electron transport chain [34]. Interestingly, the recently discovered P5C–proline cycle explains the delivery of electrons to mitochondrial electron transport without producing glutamate and, under certain conditions, this can lead to enhanced ROS generation [24,35]. Proline catabolism is, therefore, an important regulator of cellular ROS balance and can influence numerous additional regulatory pathways. Proline metabolism has also been reported to influence cellular ATP and NADPH/NADP+ ratio during oxidative and nutrient stress in animal cell lines [36].

Similarly, structural biology studies in bacteria have revealed that proline dehydrogenase of the bacterium *Thermus thermophilus* directly interacts with oxygen to produce superoxide radical [37]. *Helicobacter* PutA has also been reported to have high reactivity with molecular oxygen leading to the formation of ROS [38]. Flavin adenine dinucleotide (FAD), the cofactor of this enzyme is accessible to dissolved oxygen allowing the direct reduction of O_2 to superoxide. Hence, the electrons from proline are channelized to generate ROS.

In the current study discussed in this chapter, *putA* gene was knocked out from one of the pathogenic strains of *Xanthomonas*, namely *X*. *campestris* pv. *campestris* strain 8004 (Xcc 8004) to understand the role of proline metabolism in PCD of *Xanthomonas.* The wild type (wt) and mutant strains were examined under similar growth conditions for viability, as well as PCD specific markers such as activity of caspase-3-like protease, level of phosphatidylserine (PS) externalization and the extent of DNA damage. For further understanding, the intracellular reactive oxygen species (ROS) level as well as the change in membrane potential were also analyzed. Additionally, the *putA* gene was cloned in an *E.coli* - *Xanthomonas* shuttle vector, and Xcc 8004 Δ*putA* was complemented for PutA activity by transforming it with the recombinant plasmid, and the above mentioned biochemical and molecular markers were examined.

3.2 Materials and Methods

3.2.1 Bacterial strains and growth conditions

Xanthomonas strains were grown at 26 ± 2° C in a rotary shaker at 150 rpm in Luria-Bertani (LB) broth {PCD inducing medium (PIM)}, or starch broth (SB) {PCD non-inducing medium (PNIM); 1% starch, 0.3% $K_2HPO4.3H_2O$, 0.15% KH_2PO4, 0.2% ammonium sulphate, 0.05% L-methionine, 0.025% nicotinic acid, and 0.025% L-glutamate, pH 6.8±0.2}. All *E.coli* strains were grown in LB medium on a rotary shaker (150 rpm) at 37± 2^{o}C. The cell number was enumerated by the standard plate count method [39].

3.2.2 Determination of intracellular level of proline in *Xanthomonas* cells

Intracellular proline levels were determined in Xcc cells as mentioned before [40]. Briefly, an aliquot of overnight grown culture was washed twice with equal volume of PBS (Phosphate

buffer saline) (10 mM, pH 7.5) and resuspended in 3% sulphosalicylic acid. The cells were sonicated for 2 min (60% power) followed by heating at 95°C for 10 min. The culture was centrifuged at 12,000 x g for 10 min. To this clear supernatant 1 ml glacial acetic acid and 1ml acidic ninhydrin (prepared by warming 1.25 g ninhydrin in 30 ml glacial acetic acid and 20 ml 6M phosphoric acid) was added. This reaction mixture was kept at 100°C for 1h after which the reaction was terminated on ice bath for 20 min. The reaction mixture was extracted with 2 ml toluene and the absorbance was read at 520 nm using UV–visible spectrophotometer (UV4, Unicam, Cambridge, UK).

3.2.3 Estimation of intracellular cysteine levels

The intracellular cysteine levels were estimated as described earlier [41]. Briefly, overnight grown cells were washed twice with PBS (10 mM, pH 7.5) and resuspended in 5% perchloric acid. Samples were boiled for 10 min followed by centrifugation at 12,000 x g for 10 minutes. The clear supernatant (100 µl) was mixed with 100 µl acetic acid and 100 µl acidic ninhydrin reagent (prepared by mixing 250 mg ninhydrin in 6ml acetic acid and 4ml concentrated HCl and kept at 100°C for 15 min). The reaction mixture was cooled on ice and diluted to 1 ml with 95% ethanol. The absorbance was read at 560 nm using UV–visible spectrophotometer.

3.2.4 Measurement of PutA activity in terms of proline oxidase activity

The proline oxidase activity was assayed according to Dendinger and Brill (1970) [42]. Briefly, an aliquot of 24 h culture was washed twice with PBS (10 mM, pH 7.5) and resuspended in 100 mM Tris-HCl (pH 7.4). Wherever required, inhibitors were added to the cell suspension and incubated at room temperature for 30 min. For permeabilization, 5 µl

toluene was added to the cell suspension. After 10 min, 1ml L-proline (1M) and 200 µl o-aminobenzaldehyde (50 mM in 20% ethanol) was added. The reaction mixture was kept for shaking at 26 ± 2 °C for an hour and was terminated by adding 200 µl trichloroacetic acid (20%). The cell debris was removed by centrifugation at 12,500 x g for 15 min. The absorbance of the clear supernatant was measured at 443 nm using UV - visible spectrophotometer. The millimolar extinction coefficient of the P5C (pyrroline-5-carboxylate) - o-aminobenzaldehyde complex is 2.71 [42]. PutA activity was expressed as micromoles of P5C formed min^{-1} mg^{-1} protein. The protein content was estimated by Lowry's method [43].

3.2.5 Construction of *putA* knockout in *Xanthomonas*

To further verify the role of PutA in metabolic stress induced PCD of *Xanthomonas*, a *putA* knockout of *Xanthomonas campestris* pv. *campestris* strain 8004 (Xcc 8004) was constructed by insertional mutagenesis using pKNOCK-Km suicide plasmid (2 kbp) vector which has R6Kγ origin of replication [44]. Hence, the plasmid can only replicate in only those *E. coli* strains which can provide the replication initiator pi protein [45]. Xcc was used for this study because its genome sequence is known and it also shows post exponential cell death in LB medium similar to Xcg (Fig.3.5). An internal 600 bp region of *putA* gene (complete size around 3.2 kbp) was amplified using FP1 and RP1 primers (Table 3.1). Hind III restriction enzyme site was introduced at each end. The derivative pKNOCK plasmid carrying the 600 bp *putA* gene fragment is henceforth termed as pKNOCK-putA. This pKNOCK-putA plasmid was then used to transform competent *E. coli* PIR1 cells (prepared using $CaCl_2$ method) by heat shock and transformants were selected on LB-kanamycin (25 µg ml^{-1}) - agar plate. Competent Xcc cells (prepared by washing thrice with 10% ice-chilled glycerol) were

transformed using electroporation [46]. pKNOCK plasmid disrupts the target gene by insertional mutagenesis (Fig 3.6). This is achieved by homologous recombination between the target gene and the complimentary gene fragment cloned in the pKNOCK plasmid. The integration of pKNOCK-putA into the *putA* gene was confirmed by PCR amplification of full length *putA* gene from the transformed Xcc colony.

Figure 3.5

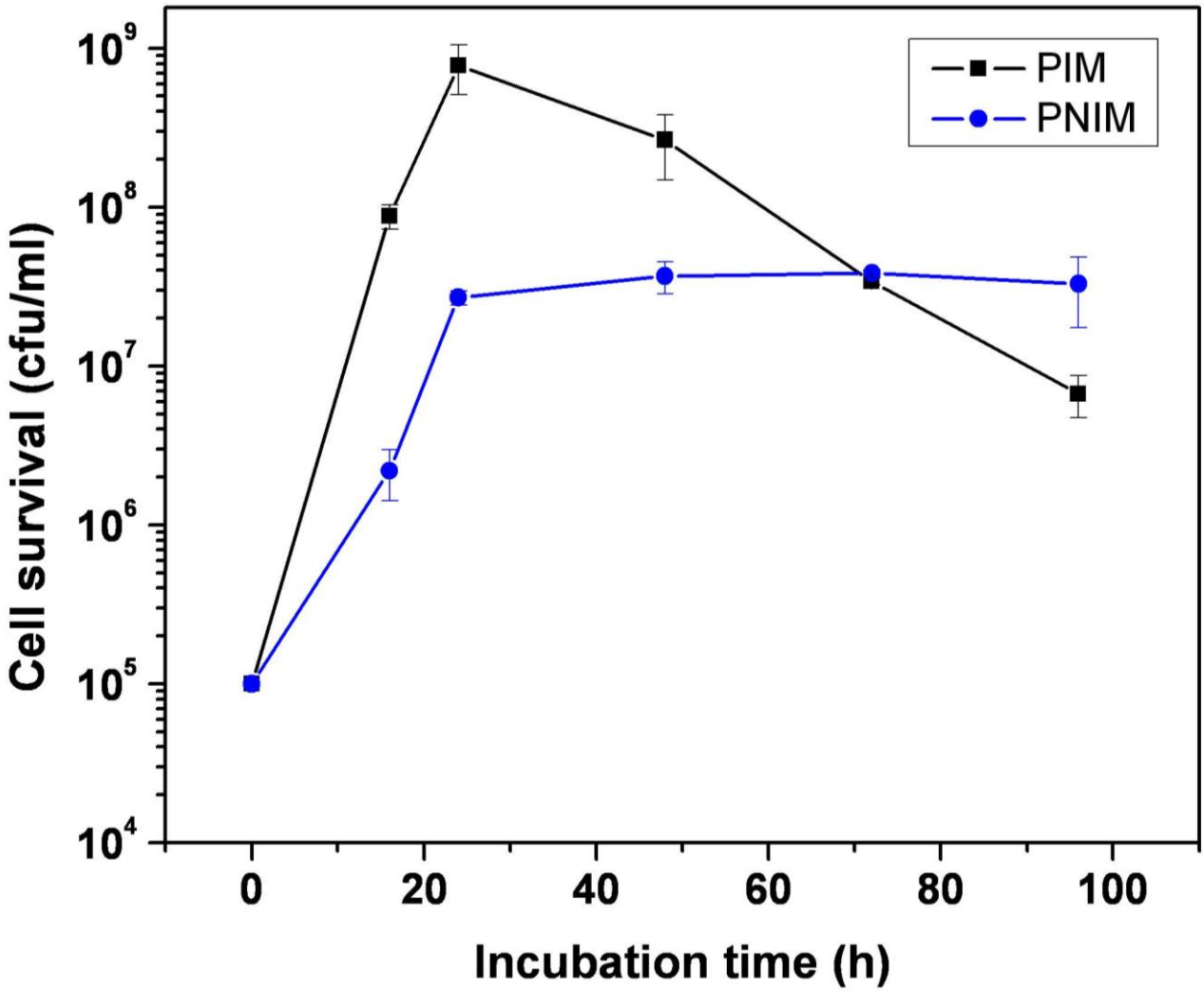

Fig.3.5: Growth curve of *Xanthomonas campestris* pv. *campestris* strain 8004 in PCD inducing medium (PIM) and PCD non-inducing medium (PNIM).

Figure 3.6

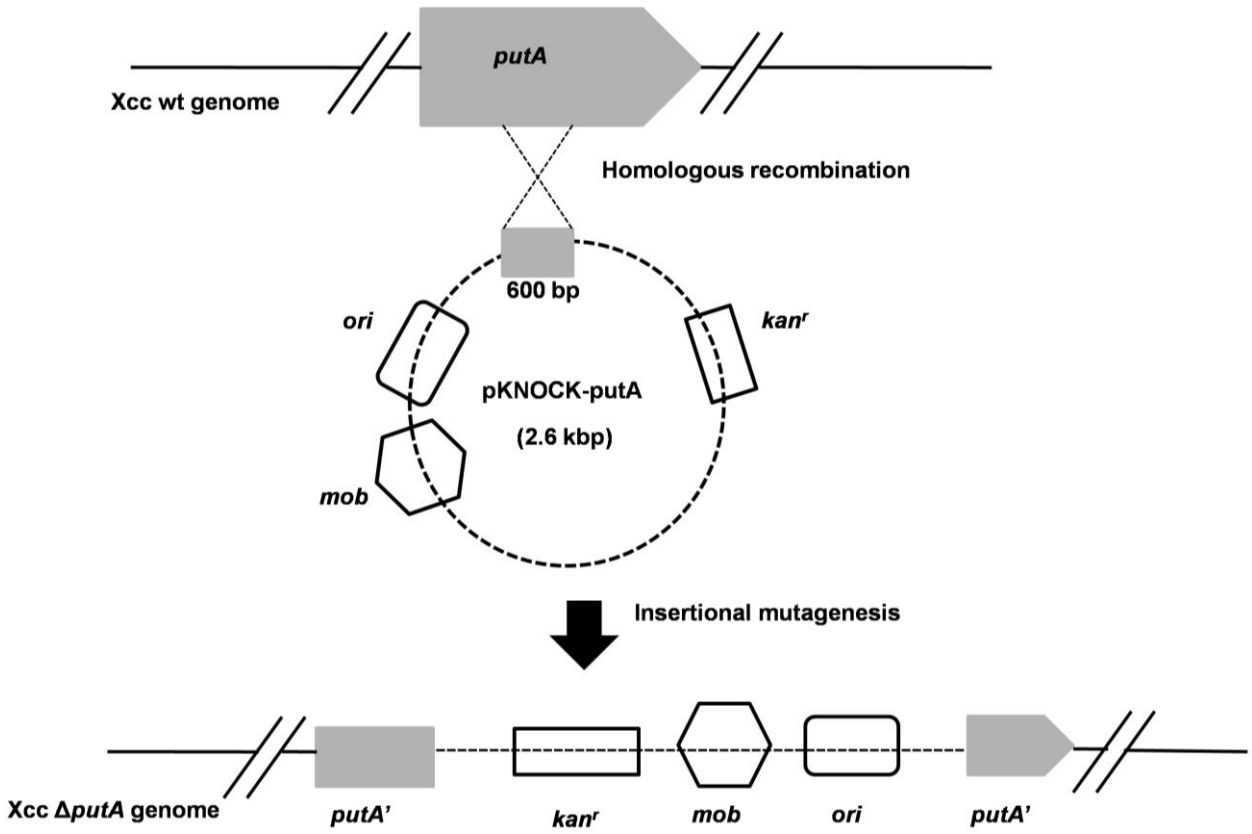

Footnote: pKNOCK-putA - pKNOCK-Km* (2 kbp) with cloned 600 bp internal fragment of *putA; kan*r – kanamycin resistance; ori – R6K γ origin of replication; mob – RP4 plasmid oriT region; *putA'* – disrupted *putA*. *Source: Alexeyev, 1999.

Fig.3.6: Schematic representation of insertional mutagenesis of Xcc8004 *putA* using pKNOCK vector.

Table 3.1: Bacterial strains, plasmids and primers used in this study

Strain/ plasmid/ primer	Relevant characteristic	Source
Xanthomonas		
Xanthomonas campestris campestris str. 8004 (Xcc)	Wild type; Rif^r	[47]
Xcc Δ*putA*	*putA* deletion mutant of Xcc 8004; Rif^r Kan^r	This work
Xcc Δ*putA*/pPutA	Xcc Δ*putA* harboring pBBR1MCS5 containing the entire *putA* gene; ; Rif^r Kan^r Gm^r	This work
E. coli		
E. coli pir1	{F- Δlac169 rpoS(Am) robA1 creC510 hsdR514 endA recA1 uidA(ΔMluI)::pir-116}	Invitrogen
E. coli pir1/ pKNOCK-putA	*E. coli* pir1harboring suicide plasmid pKNOCK-putA; Kan^r	This work
E. coli DH5α	F– Φ80*lac*ZΔM15 Δ(*lac*ZYA-*arg*F) U169 *rec*A1 *end*A1 *hsd*R17 (rK–, mK+) *pho*A *sup*E44 λ– *thi*-1 *gyr*A96 *rel*A1	Invitrogen
E. coli DH5α/pPutA	*E. coli* DH5α harboring pBBR1MCS5 containing the entire *putA* gene; Gm^r	This work
Plasmids		
pKNOCK-Km	Suicide vector in *Xanthomonas;* Kan^r	[44]
pKNOCK-putA	pKNOCK-Km with an internal gene fragment of *putA*	This work
pBBR1MCS-5	Broad host range cloning vector; Gm^r	[48]
pPutA	pBBR1MCS5 containing the entire *putA* gene; Gm^r	This work
Primers		
FP1	5’ CCGAAGCTTATGTGCGTGGCCGAAGCCTTGC 3’	This work
RP1	5’ CCGAAGCTTCTTGGCCAGTTGTGCCAGCTCC 3’	This work
FP2	5’ CCCAAGCTTGTCCCAACCCCTTCGGACA 3’	This work
RP2	5’ CGCGGATCCTCAGTCACCCAAGGTCAG 3’	This work

3.2.6 Cloning of Xcc *putA* in a broad host range (bhr) shuttle vector and complementation of Xcc Δ*putA* strain

The *putA* gene in Xcc 8004 is present in single copy. It is flanked upstream by a gene for hypothetical protein (XC_3906; location: 4,610,064 - 4,610,495) and downstream by IS1478 transposase gene (XC_3908; location: 4,614,266 – 4,615,633) (Fig 3.7A). The full length *putA* gene excluding the promoter region in Xcc 8004 is 3.2 kb in size (XC_3907; location: 4,610,819 – 4,614,019). For complementing Xcc Δ*putA* strain with functional PutA, the 319 bp non-coding region present between XC_3906 gene and *putA* was amplified along with the *putA* gene (Fig 3.7B) using Pfu polymerase, FP2 and RP2 primers (Table 3.1) by colony PCR technique. This non-coding 319 bp sequence contains the *putA* promoter region which has not been characterized yet. In this study, BPROM software was used to identify the possible promoter region of *putA* and the findings have been shown in Fig S2B. The PCR product (3.52 kb in size) was cloned into a broad host range (bhr) vector pBBR1MCS5 (Fig 3.8). This vector was originally derived from pBR322 by subsequent modifications to have several advantages such as relatively smaller size (4.7 kb), extended multiple cloning site (MCS), possibility of direct selection of recombinant plasmid in *E.coli* via disruption of the LacZα peptide, mobilizable when the RK2 transfer functions are provided in *trans,* and compatible with IncP, IncQ and IncW group plasmids, as well as with ColE1- and P15a-based replicons [48]. The recombinant plasmid carrying *putA* gene is henceforth termed as pPutA and was used to transform *E.coli* DH5α cells. The transformants were selected on LB-gentamycin plate (10 µg ml^{-1}). Xcc Δ*putA* strain was further transformed with pPutA by electroporation as described above. The transformants were confirmed by PCR amplification using *putA* specific primers (Table 3.1).

Figure 3.7

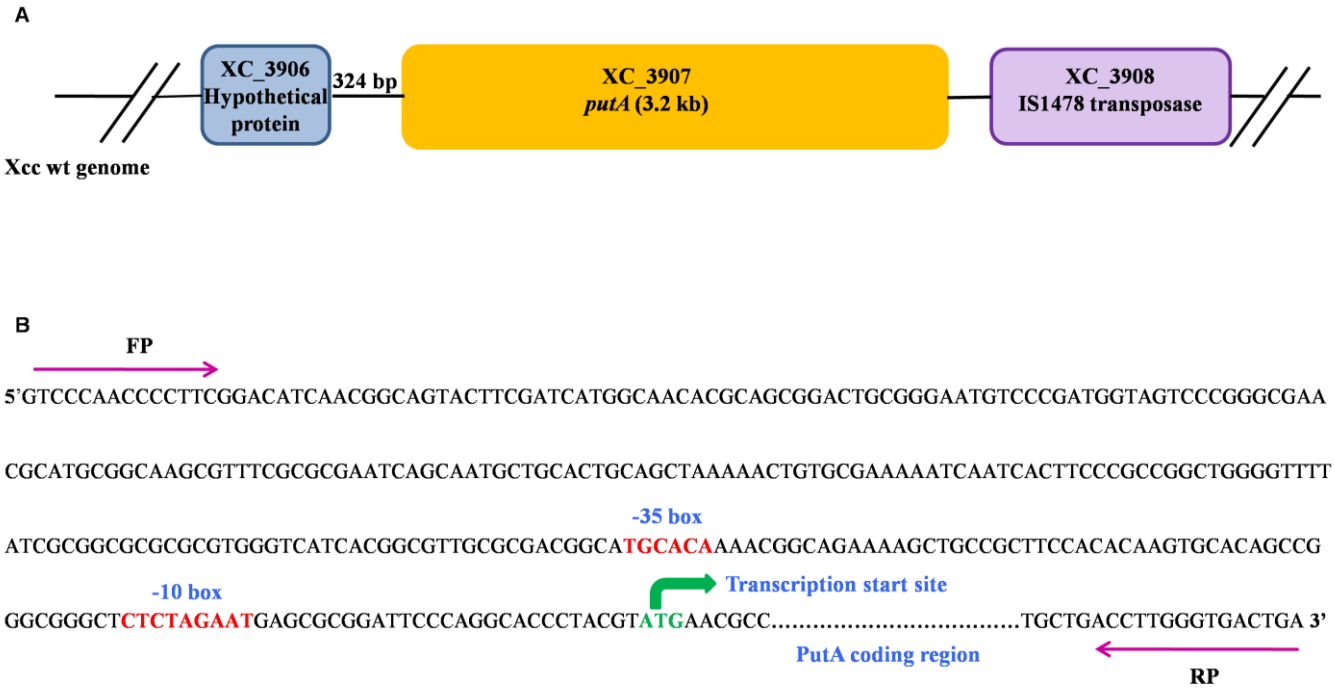

Fig.3.7: Organization and sequence of Xcc *putA* gene (A) Organization of *putA* (NCBI gene ID: 3379526) in Xcc genome, **(B)** The sequence of upstream non coding promoter containing region (319 bp; source: NCBI database) of Xcc *putA* included in *putA* complementation construct. BPROM software was used for promoter prediction (-10 and -35 box). FP and RP indicate the sites for forward and reverse primers respectively, used for PCR amplification of *putA* along with its promoter.

Figure 3.8

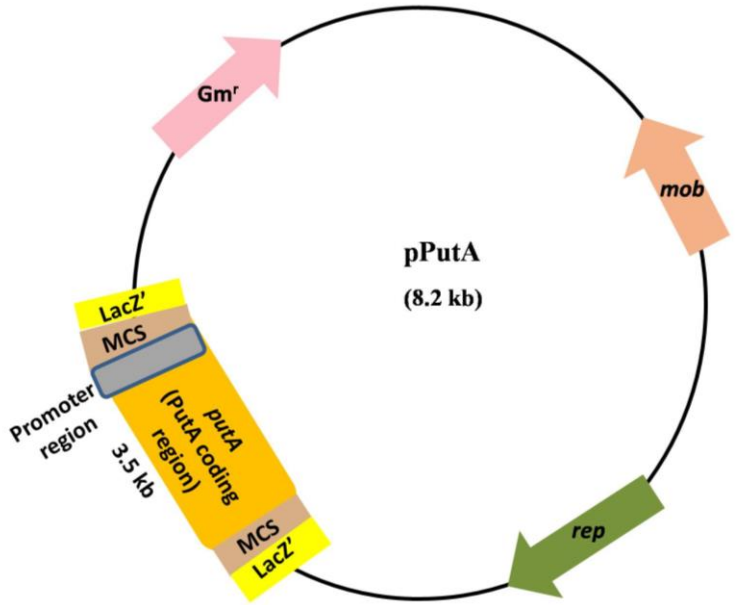

Footnote: pPutA - pBBR1MCS5-Gm* (4.7 kb) with cloned *putA; Gm^r* – Gentamycin resistance; MCS – multiple cloning site; rep – gene required for plasmid replication; mob – gene required for plasmid mobilization. *Source: Kovach et al., 1995.

Fig.3.8: pBBR1MCS5 vector map depicting cloned *putA* (full length) along with its promoter region.

3.2.7 Screening of recombinants

Screening of *E. coli* DH5α recombinants with pPutA was carried out by blue white screening method as mentioned earlier [46]. Briefly, to a premade LB agar plate containing the appropriate antibiotic, 40 µl X-gal (20 mg/ml in DMSO) and 4 µl of IPTG solution (200 mg/ml) were spread. These components were allowed to absorb for at least 30 min or until the plate surface appeared dry at 37°C prior to plating cells.

3.2.8 Assay of caspase-3-like activity and immunoblotting

Caspase-3-like activity was assayed according to the manufacturer's guidelines (caspase-3 assay kit, BD Pharmingen, USA). Briefly, a 1 ml aliquot of 24 h grown culture was washed twice with phosphate buffered saline (PBS) (10 mM, pH 7.5) and resuspended in saline (0.85%). The cell suspension was centrifuged at 12,500 x g for 10 min. The pellet was resuspended in 100 µl of sodium phosphate buffer (10 mM, pH 7.5), mixed with 1 ml cell lysis buffer {Tris-HCl (10 mM), sodium phosphate buffer (10 mM, pH 7.5), NaCl (130 mM), triton X-100 (1%) and sodium pyrophosphate (10 mM)} and kept at 4ºC for 4 h for lysis. The cell lysate was then centrifuged at 12,500 x g for 15 min and an aliquot (50 µl) of the above supernatant was used for caspase-3 assay using synthetic fluorogenic substrate Ac-DEVD-AMC (BD Pharmingen, USA) as described earlier [39].

Level of biosynthesis of caspase-3-like protein was analyzed using SDS-PAGE and Western hybridization as described earlier in chapter 2 [39] using affinity-purified, biotin-conjugated, polyclonal rabbit anti-active human caspase-3 antibody.

3.2.9 Analysis of active caspase-3-like protein *in situ* by FITC-DEVD-FMK staining

The assay was carried out using caspase-3 detection kit (Catalog no. QIA91, Calbiochem). An aliquot (250 µl) of 24 h grown cell culture containing ~10^6 cfu ml^{-1} was washed twice with PBS (10 mM, pH 7.5). The cell pellet was resuspended in 300 µl PBS. To this cell suspension 1 µl of FITC-DEVD-FMK was added and incubated at room temperature for 30 min in dark. After that, the cells were centrifuged at 12,500 x g for 5 min and supernatant was discarded. The cells were washed twice with wash buffer and resuspended in 200 µl of the same. An aliquot (10 µl) was smeared on a glass slide, air dried and examined under a

fluorescent microscope (Carl Zeiss, Germany) using oil immersion objective (100x) and filter set 9 (Carl Zeiss, Germany; Excitation: 450 nm; emission: 515 nm).

3.2.10 Observation of cell filamentation

An aliquot (1 ml) of cells grown in PIM (24 h) or PNIM (72 h) was washed twice with PBS (10 mM, pH 7.5), resuspended in saline (0.85%). An aliquot (10 µl) was smeared on a glass slide, air dried, heat fixed, stained with crystal violet and examined under a microscope (Carl Zeiss, Germany) using oil immersion objective (100X) for observation of cell filaments.

3.2.11 Quantification of DNA damage by TUNEL (Terminal deoxynucleotidyl transferase dUTP nick end labeling) assay

TUNEL assay was performed using the APO-Direct kit, BD Pharmingen as described earlier in chapter 2. Briefly, an aliquot (1 ml) of 24 h grown cell culture containing ~10^6 cfu ml^{-1} was washed twice with PBS (10 mM, pH 7.5). The cell pellet was resuspended in 50 µl DNA labeling solution [reaction buffer (10 µl), Terminal deoxynucleotidyl transferase (TdT) enzyme (0.75 µl), FITC-dUTP (8 µl) and distilled water (32.25 µl)] and incubated for 60 min at 37 ºC in dark. After that, 1 ml rinse buffer was added and cell suspension was centrifuged at 12,000 x g for 10 min. This rinsing step was repeated once more. PI/RNase staining buffer (500 µl) was added to the samples which were further incubated in dark for 30 min, and analyzed by Fluorescence Activated Cell Sorter (FACS) (10^5 cells for each sample) using flow cytometry system (Partec CyFlow space, Germany).

3.2.12 Quantification of phosphatidylserine (PS) externalization using annexin-V labeling

The assay was performed using annexinV-FITC apoptosis detection Kit (catalog no. 556547, B D Pharmingen). Briefly, an aliquot (1 ml) of 24 h cell culture containing ~10^6cfu ml^{-1} was washed twice with PBS (10 mM, pH 7.5) and the pellet was resuspended in 250 µl of the same buffer. An aliquot (650 µl) of annexinV binding buffer (10 mM HEPES, pH 7.4; 140 mM NaCl and 2.5 mM $CaCl_2$) and annexinV (5 µl) were added to the cell suspension and incubated in dark for 15 min. Propidium iodide (5 µl, 50 µg ml^{-1}) was then added into the cell suspension and incubated at ambient temperature in dark for 15 min. For each analysis, 10^5 cells were analyzed by flow cytometry (Partec CyFlow space, Germany). Data was analyzed using FCS Express V4 software (demo version).

3.2.13 Analysis of reactive oxygen species (ROS) generation by dichlorohydrofluorescein staining

Dichlorohydrofluorescein (H_2DCFDA) staining was carried out as mentioned previously in chapter 2. Briefly, *Xanthomonas* cells were grown at 26 ± 2 °C in a rotary shaker at 150 rpm in culture medium (LB) for 18 h. A 2 ml aliquot was withdrawn and centrifuged at 12,500 x g for 2 min and the pellet was resuspended in 1 ml saline (0.85%). It was then incubated with 2 µl H_2DCFDA (5 mM, prepared in absolute ethyl alcohol) at room temperature for 30 min. An aliquot was smeared on a glass slide, air dried and examined under a fluorescent microscope (Carl Zeiss, Germany) using oil immersion objective (100x) and filter set 15 (Carl Zeiss, Germany; excitation: 546 nm; emission: 590 nm).

3.2.14 Determination of membrane potential

It was carried out using BacLight bacterial membrane potential assay kit (Molecular Probes, catalog no. B34950) as per the manufacturer's guidelines. Briefly, an aliquot (1 ml) of 24 h grown cell culture containing ~10^6cfu ml^{-1} was washed twice with PBS (10 mM, pH 7.5) and the pellet was resuspended in 1 ml of the same buffer. For preparing the depolarized control sample, 10 µl of an uncoupler CCCP (carbonyl cyanide 3-chlorophenylhydrazone) (50 mM) was added to 1 ml of cell suspension (~10^6 cfu ml^{-1}) and incubated at room temperature for 30 min. CCCP is a proton ionophore which dissipates membrane potential by eliminating the proton gradient. Thereafter, cells were stained with 5 µl (50 nM final concentration) of $DiOC_2(3)$ (3,3′-diethyloxacarbocyanine iodide), and 10^5 cells were analyzed by flow cytometry (Partec CyFlow space, Germany, and Express V4 software, demo version).

3.3 Results and Discussion

3.3.1 Effect of addition of amino acids on PCD profile of *Xanthomonas campestris* pv. *campestris* (Xcc)

The preceding chapter provided evidence of stress experienced by the cells grown in PIM. Since the PCD process in this bacterium was observed to be induced under conditions where the protein content of the medium was higher than the carbohydrate content, a fine balance of these two major nutrients was thought to be an essential factor governing survival of this microorganism. The designed conditions of growth of this organism in laboratory are quite distinct from its natural habitat on soybean leaf. Therefore in this study, starch minimal medium was used as PCD non-inducing medium (PNIM). The PNIM is composed of 1% starch, 0.3% $K_2HPO4.3H_2O$, 0.15% KH_2PO4, 0.2% ammonium sulphate, 0.05% L-

methionine, 0.025% nicotinic acid, and 0.025% L-glutamate. Being rich in starch, this medium is quite similar to the *ex situ* conditions encountered by *Xanthomonas,* a plant pathogen. On the other hand, a protein rich medium like Luria Bertani (LB) broth was used as PCD –inducing medium (PIM). This medium is predominantly composed of tryptic and casein digests which provide very high levels of glutamate (15%) and proline (6%) [49,50]. Hence, the effect of addition of these two amino acids, either individually or in combination in PCD non-inducing medium (PNIM), on the PCD process in *Xanthomonas campestris* pv. *campestris* (Xcc) was examined. Xcc was used in this study instead of Xcg because its genome sequence is known and it also shows post exponential cell death in LB medium similar to Xcg (Fig. 3.5).

A concentration dependent decrease in viability was observed when *Xanthomonas* was grown in PNIM in the presence of varying concentrations of proline (5 - 100 mM) and the viability at 96h was lowest at 100 mM. When *Xanthomonas* cells were grown in PNIM supplemented with proline (5-100 mM), the cell count peaked at 24 h of incubation followed by a sharp decline in viable cell number during further post-exponential incubation under similar growth conditions (150 rpm, 26ºC). The viable cell count was found to be 2.1 x 10^8 and 5.3 x 10^8 for 5 mM and 50 mM respectively at 24 h followed by a decline during the course of incubation. The viable count decreased by 48% and 72% at 5 mM and 50 mM proline respectively at the end of 96 h. However, at the end of 96 h of incubation, one log cycle decrease in viable cell count was observed in case of culture where 100mM proline was added (Fig. 3.9).

Interestingly, the cell number was found to be more in the cultures supplemented with glutamate with respect to control cells (without glutamate) and it remained almost unchanged (at ~10^8 cfu/ml) at the end of 96 h of incubation (Fig. 3.9). Glutamate and glutamine are

important amino acids for bacterial metabolism [51]. Glutamate participates in both catabolism and anabolism. It can be deaminated to form α-ketoglutarate, a TCA intermediate. Glutamate accounts for ~88% of cellular nitrogen and is required for the biosynthesis of purines, pyrimidines and amino sugars [51]. Hence, when starch minimal medium (PCD non–inducing medium or PNIM) was supplemented with excess glutamate, it provided a ready source of nitrogen favoring anabolic events as it was observed to accelerate Xcc growth.

Moreover, the growth profile upon addition of both proline and glutamate together in the culture medium (PNIM) behaved similar to proline addition and the loss of viability by around one log cycle was noticed at 96 h. The observations thus indicated a regulatory role for proline in the death of *Xanthomonas* cells under unfavorable nutritional condition.

Figure 3.9

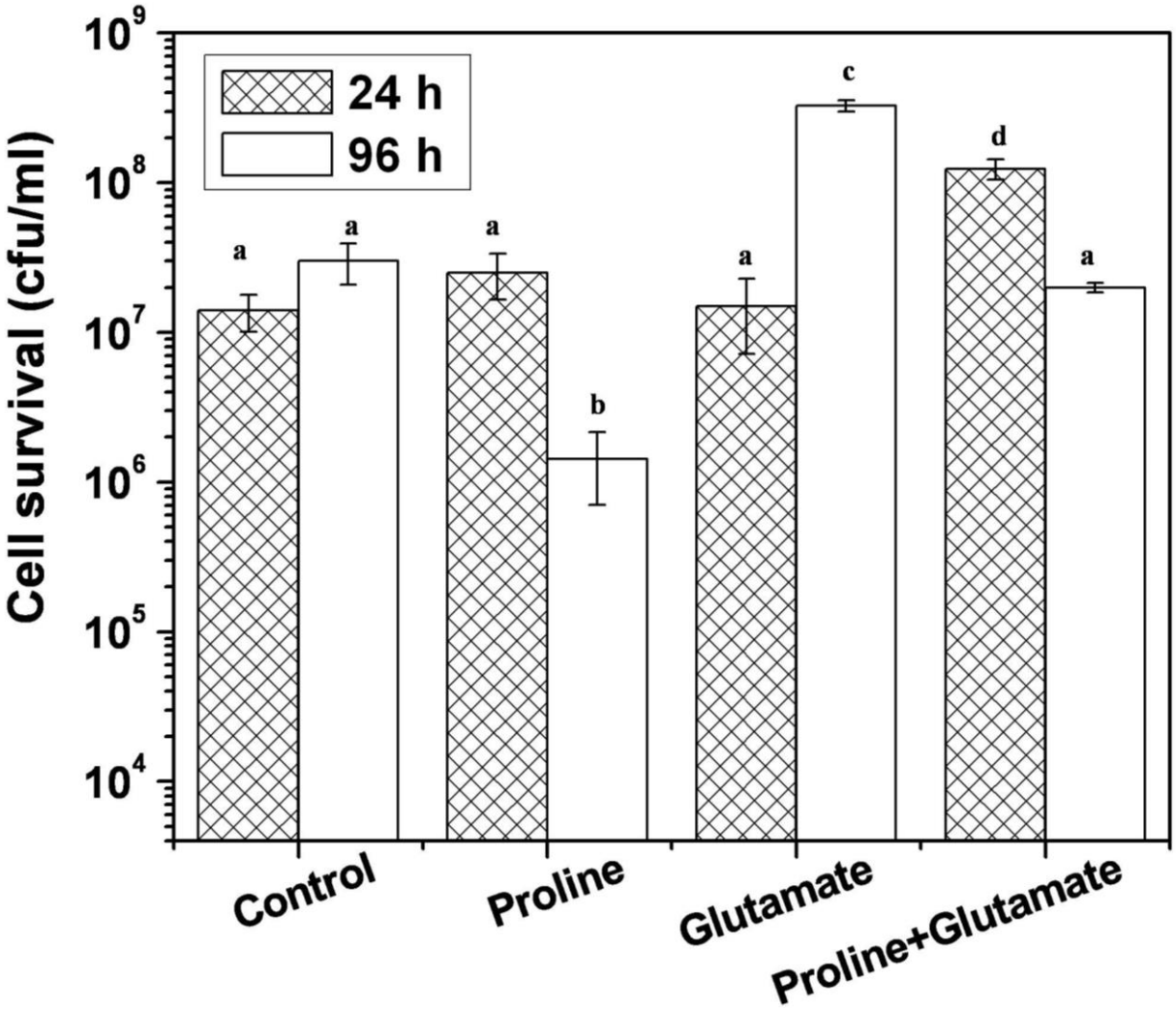

Fig.3.9: The effect of proline and glutamate supplementation on the survival of *Xanthomonas campestris* pv. *campestris* in PNIM. The different letter on the bar indicates that the means are significantly different at $p<0.05$.

3.3.2 PutA activity in Xcc cultures grown in PIM and PNIM

The above observations indicated the role of proline in induction of PCD in this bacterium. The growth medium favoring PCD during this study namely LB medium also contains higher concentration of proline compared to other amino acids [49,50]. Its concentration in casein

tryptic digest is close to 6%, next to glutamic acid (around 15%), which can also get converted to proline enzymatically inside the cell. As expected, intracellular proline level in PNIM was found to be quite low (2.4 µM mg^{-1} protein) in Xcc which increased to around 35 fold (83 µM mg^{-1} protein) in PIM growing cells (Fig 3.10A). The proline levels were even higher in Xcc Δ*putA* cells (151 µM mg^{-1} protein) (Fig 3.10A). Supplementing PNIM with glutamate increased the intracellular proline levels slightly (~ 5 µM mg^{-1} protein), indicating that probably only a small amount of glutamate is being converted to proline inside the cells. This is probably because the first enzyme of proline biosynthesis pathway, gamma glutamyl kinase (GK) is subject to feedback inhibition by proline (even at very low concentrations) in bacteria [9,10] thereby limiting the conversion of glutamate to proline. Intracellular proline levels were found to be around fourteen fold higher (~34.5 µM mg^{-1} protein) in Xcc cells grown in PNIM fortified with either proline or proline along with glutamate. LB medium is predominantly composed of amino acids and peptides. As a result, the microorganism has to use them both as carbon and nitrogen source. During such growth conditions certain metabolic pathways can be preferentially upregulated over others. High intracellular levels of proline in Xcc cells can be attributed to abundant free proline and peptides present in PIM.

Figure 3.10

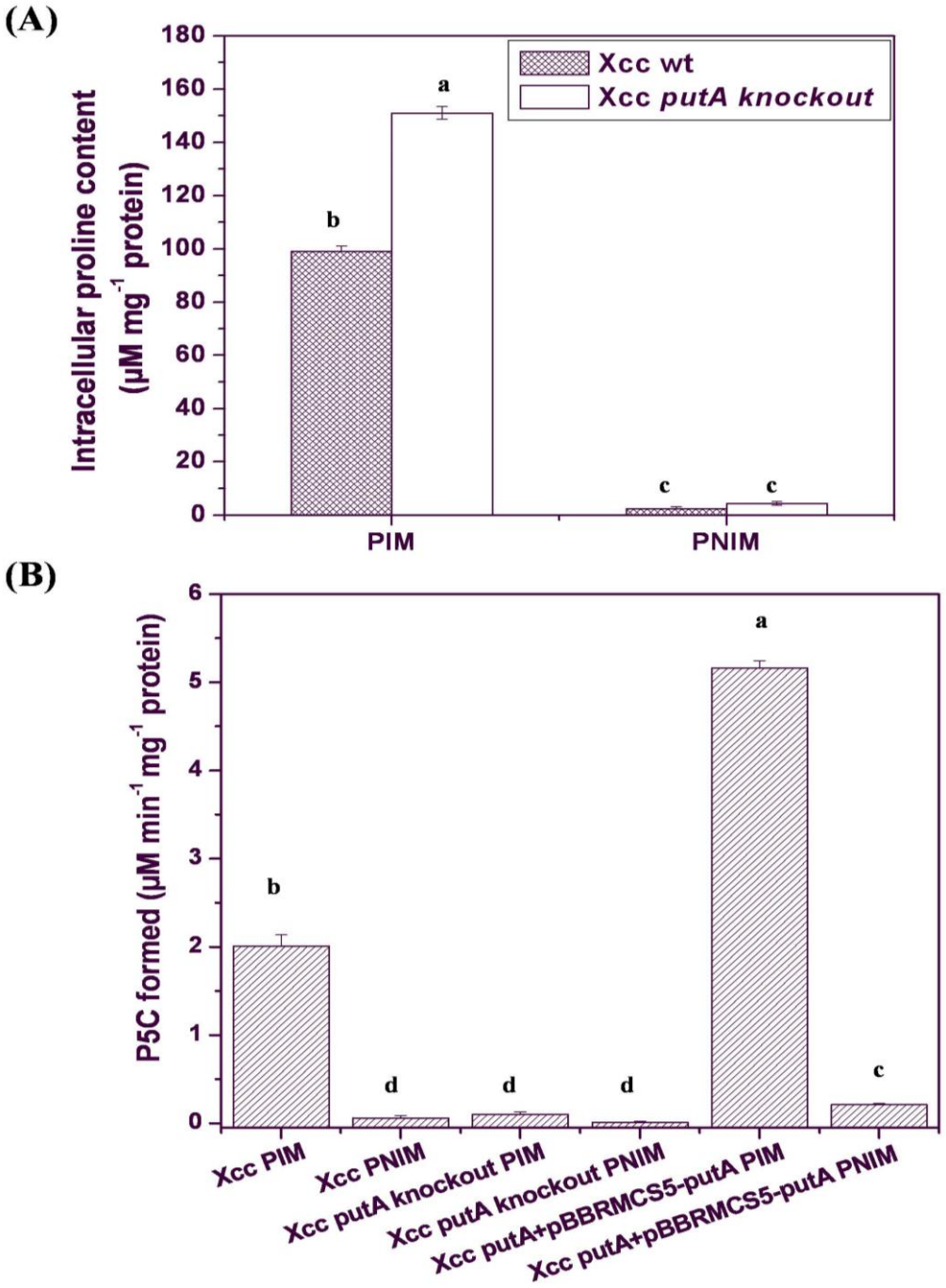

Footnote: PIM – programmed cell death (PCD) inducing medium; PNIM- PCD non-inducing medium

Fig.3.10: Intracellular proline level and PutA activity in Xcc 8004. **(A)** Intracellular proline level, and **(B)** PutA activity in Xcc 8004, Xcc Δ*putA* and Xcc Δ*putA*-pPutA cells in

PIM and PNIM. The different letter on bars indicates that the means are significantly different at $p<0.05$.

Increased substrate concentration can affect the activity of the enzymes involved in its utilization. Hence, examining the status of proline oxidase (PutA) which is involved in metabolism of proline becomes important to further understand the regulation of PCD in these cells. It has been reported that L-proline is preferentially used as a carbon source by *E.coli* growing in LB medium and this amino acid gets depleted quite early during its growth [49]. Unlike eukaryotes, bacterial PutA has dual activity, where first proline oxidase (or dehydrogenase) activity oxidizes proline to P5C (pyrroline-5-carboxylate), which spontaneously converts to γ-glutamate semialdehyde [8,13]. This γ-glutamate semialdehyde is then eventually oxidized to glutamate by P5C dehydrogenase activity of PutA [13]. In this study the PutA activity was measured as its proline oxidase (POX) activity. PutA activity was monitored in Xcc cell lysates by measuring the adduct formed between P5C and o-aminobenzaldehyde because the formation of P5C is very specific to this pathway. PutA activity was found to be 0.06 µM min^{-1} mg^{-1} protein in PNIM in Xcc wt cells which increased by around 34 fold to 2.01 µM min^{-1} mg^{-1} protein in PIM (Fig 3.10B). This observation can be attributed to the higher intracellular proline found in Xcc cells cultured in PIM. High proline levels have been reported to induce PutA activity as well [53]. A good correlation was found between intracellular proline levels and PutA activity in Xcc wt cells cultured in PIM (Fig 3.10A, B). These results also indicated that it is not excess proline but its increased oxidation by PutA that caused cell death.

Intracellular level of cysteine was also checked as a control. Basal level of cysteine was found to be comparatively high (50 µM mg^{-1} protein) even in PNIM indicating its constitutive

requirement for cellular metabolism. However, in PIM growing Xcc cells, cysteine level merely increased to around six fold to 301 µM mg^{-1} protein. It is worth mentioning here that the level of cysteine in LB medium is quite lower than that of proline [49]. The findings thus indicated comparatively preferential regulation of proline metabolism in stressed Xcc cells undergoing PCD.

The above observations suggested a role of proline metabolism in PCD of this organism which was further revalidated by studying the effect of addition of tetrahydro-2-furoic acid (THFA, ≤5 mM), a competitive inhibitor of PutA (a proline analog) in PIM. Interestingly, the inhibition of PCD was observed in Xcc culture when this PutA inhibitor was added in the medium prior to inoculation, and the extent of PCD inhibition was found to be inhibitor concentration dependent (Fig.3.11). Almost two log cycle increase in the cell viability was observed at 96 h of incubation in the presence of THFA (5 mM). These findings thus confirmed the involvement of PutA activity during PCD of *Xanthomonas* cells in PIM.

Figure 3.11

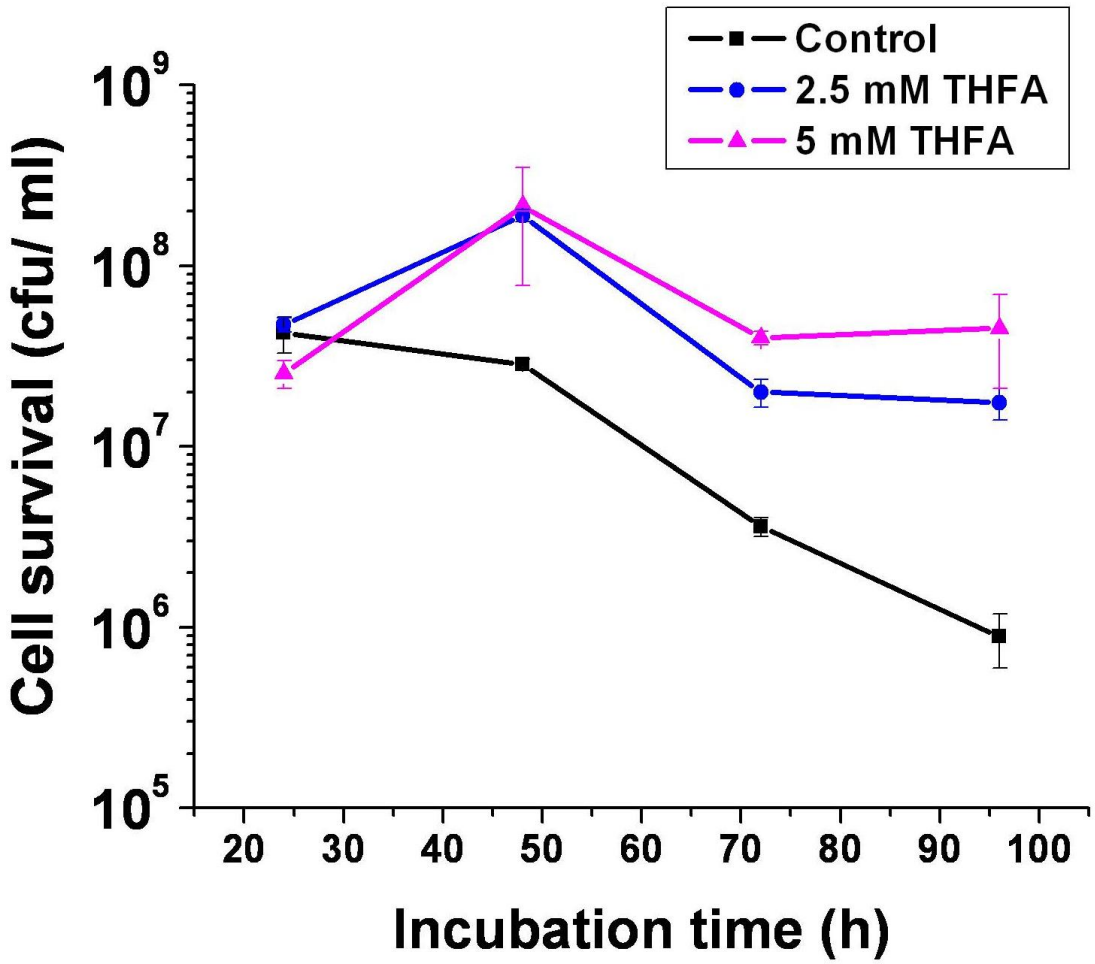

Fig.3.11: Effect of PutA inhibitor, tetrahydro-2-furoic acid (THFA) on PCD process in Xcc 8004 cells grown in PIM

3.3.3 Effect of knocking out Xcc *putA* gene and its complementation

Xcc genome has been sequenced and *putA* gene was found to be present in single copy (NCBI accession number: XC_3907). Knocking out of *putA* resulted in Xcc Δ*putA* strain (Fig. 3.12, 3.13), which showed an increase in the cell survival in PIM by more than one log cycle (viable plate count 6.3 x10^7 cfu ml^{-1}) at 96 h of incubation as compared to the wild type

(wt) counterpart (2.5 x10^6 cfu ml^{-1}) (Fig 3.16A). The viability in Xcc Δ*putA* strain in PNIM was very close to that of wt Xcc cells growing in the same medium (Fig 3.16B) and remained unaltered even when PNIM was supplemented with proline (100 mM) unlike that observed for the wt strain (Fig 3.16B and 3.9 respectively). An increase in cell number was observed when Xcc Δ*putA* strain was grown in PNIM supplemented with glutamate (100 mM) (Fig 3.16B). This observation was similar to that found in the case of Xcc wt strain (Fig 3.9). The increase in growth of Xcc Δ*putA* cells in the presence of glutamate could be attributed to the fact that since 88% of the nitrogen in the cell is derived from glutamate, it provided a ready source of nitrogen favoring anabolic events [51].

The findings thus indicated of inhibition PCD upon abolition of PutA activity in Xcc Δ*putA* strain which could be attributed to the loss of PutA activity (Fig 3.10B). As expected, this activity was found to be completely abolished in Xcc Δ*putA* strain indicating that it is precisely regulated by the *putA* gene, which is present in single copy in the Xcc genome. Moreover, the intracellular proline levels were almost double (151 µM mg^{-1} protein) in Xcc Δ*putA* strain compared to Xcc wt grown in PIM (Fig 3.16A). Thus, these observations confirmed that high levels of proline alone do not cause death, rather its enhanced oxidation by PutA plays a role in inducing PCD (Fig 3.16).

Figure 3.12

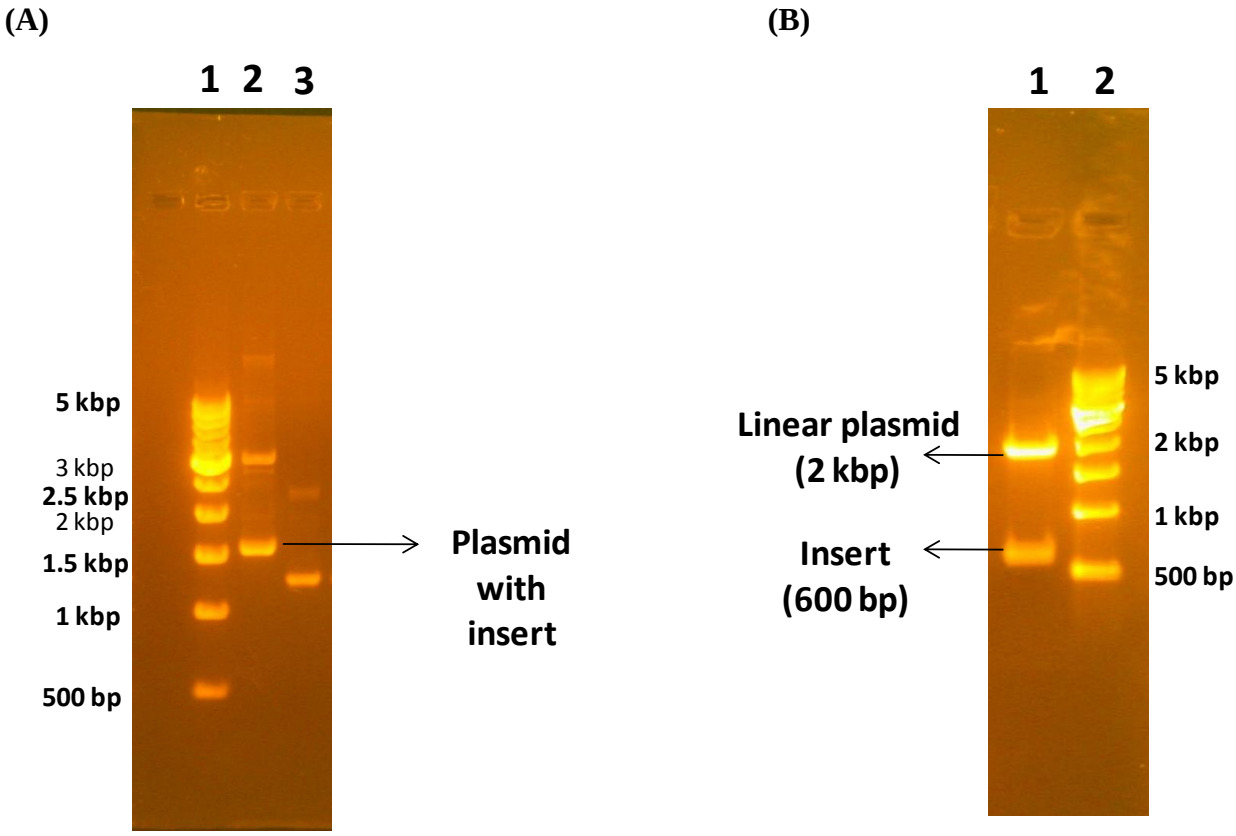

Fig.3.12: Construction of XccΔ*put*Astrain (A) Screening of recombinant plasmid (pKNOCK-Km; 2kbp) carrying the desired insert: lane 1- 500 bp DNA ladder, lane 2- recombinant plasmid with insert, lane 3 – native plasmid ; **(B)** Confirmation of recombination by restriction digestion of the plasmid: lane 1- restriction digestion profile of recombinant plasmid, lane 2 - 500 bp DNA ladder.

Figure 3.13

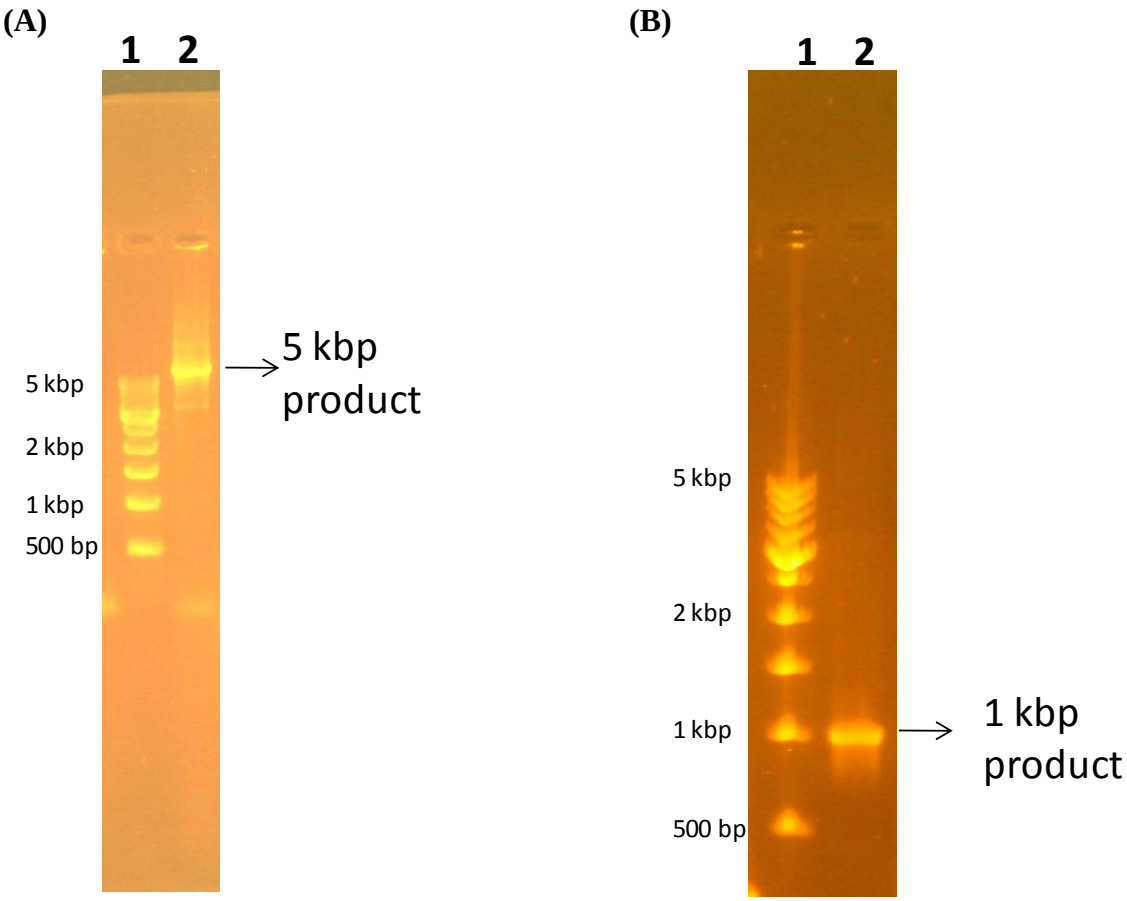

Fig.3.13: Confirmation of Xcc Δ*putA* strain (A) PCR amplification of disrupted full length *putA* (with pPutA inserted) increasing its size from 3 kbp to 5 kbp: lane 1 - 500 bp DNA ladder; lane 2 - 5kbp PCR product; **(B)** PCR amplification of *putA* gene using internal primers: lane 1 - 500 bp DNA ladder, lane 2 – 1 kbp PCR product.

Further, Xcc Δ*putA* strain was complemented with *putA* gene cloned in a plasmid shuttle vector pBBR1MCS-5 (Fig 3.14 and 3.15) and its viability was monitored in PIM. The PCD phenotype was found to be restored upon complementation with functional PutA. The cell death was 15 fold higher in Xcc Δ*putA* strain carrying pPutA vector (2.75 x 10^6 cfu ml^{-1}) at

96 h of incubation in PIM compared to the strain carrying the vector without *putA* (4.14 x 10^7 cfu ml^{-1}) (Fig 3.16A). PutA activity was also found to be restored in Xcc Δ*putA* strain upon complementation with functional Xcc PutA and was around three fold higher than the Xcc wt strain growing in PIM (Fig 3.10B and 3.15C). However, negligible enzyme activity was detected when this strain was cultured in PNIM (Fig 3.10B and 3.15C).

Figure 3.14

(A) **(B)**

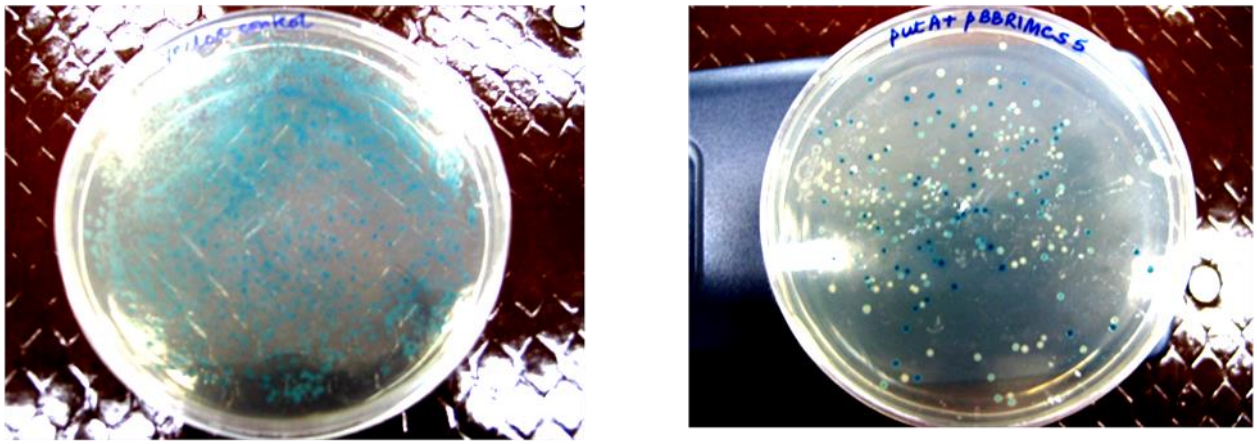

Fig.3.14: Screening of recombinants by blue white screening method: (A) *E .coli* harboring native pBBR1MCS5 plasmid spread on IPTG-X-gal plate; **(B)** *E. coli* transformants spread on IPTG-X-gal plate

Figure 3.15

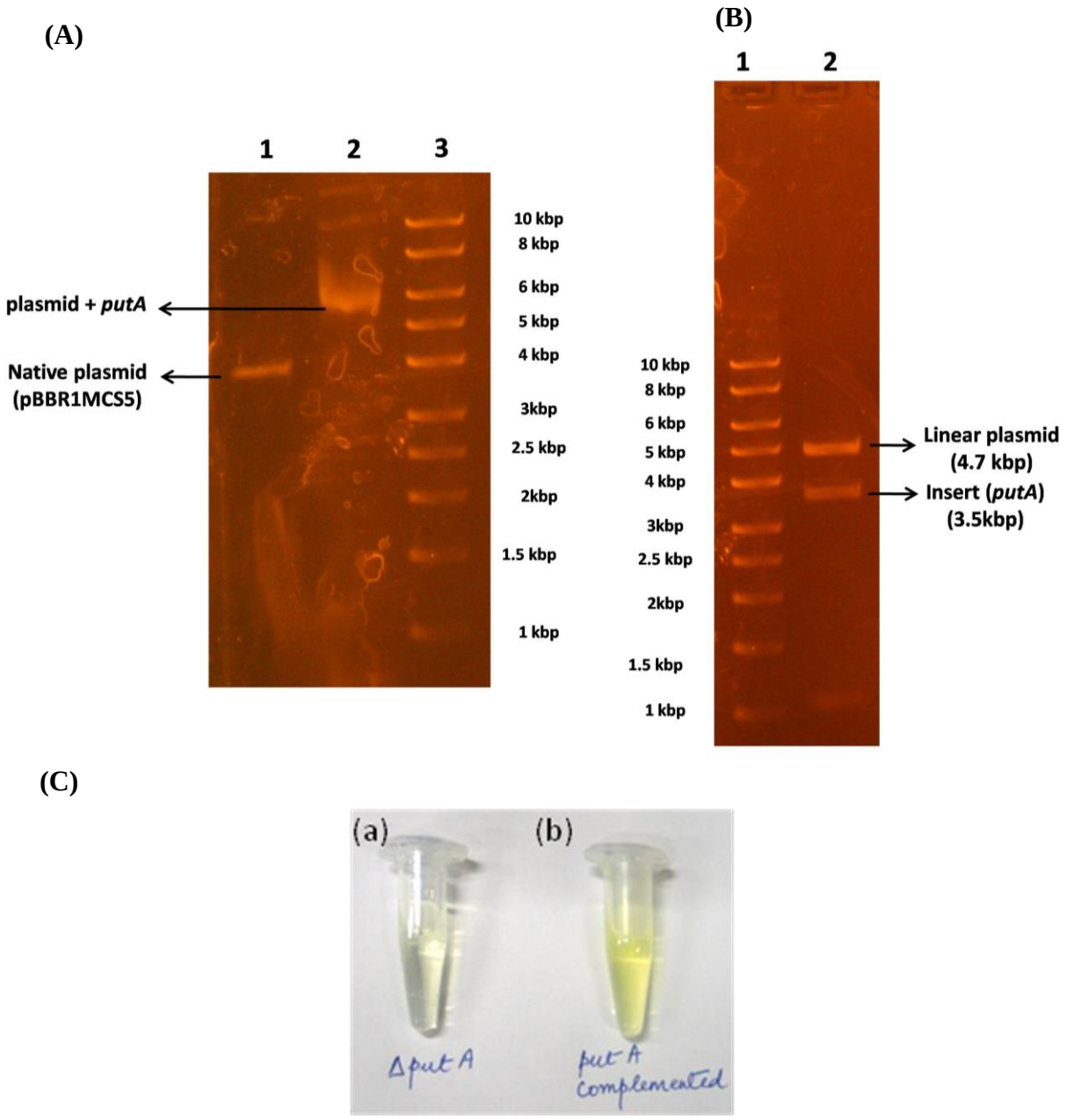

Fig.3.15: Construction of Xcc Δ*putA*-pPutA strain: (A) Screening of recombinant plasmid: lane 1 – native plasmid DNA, lane 2 – recombinant plasmid with *putA* gene, lane 3 – 1 kbp DNA ladder; **(B)** Confirmation of recombination by restriction digestion of the plasmid: lane 1 - 1 kbp DNA ladder, lane 2 - restriction digestion profile of recombinant plasmid; **(C)** PutA activity analysis to confirm the complementation of XccΔ*putA*strain. The yellow colored OBA-P5C adduct measured at 520 nm in (a) Xcc Δ*putA* and (b) Xcc Δ*putA*-pPutA strain.

Figure 3.16

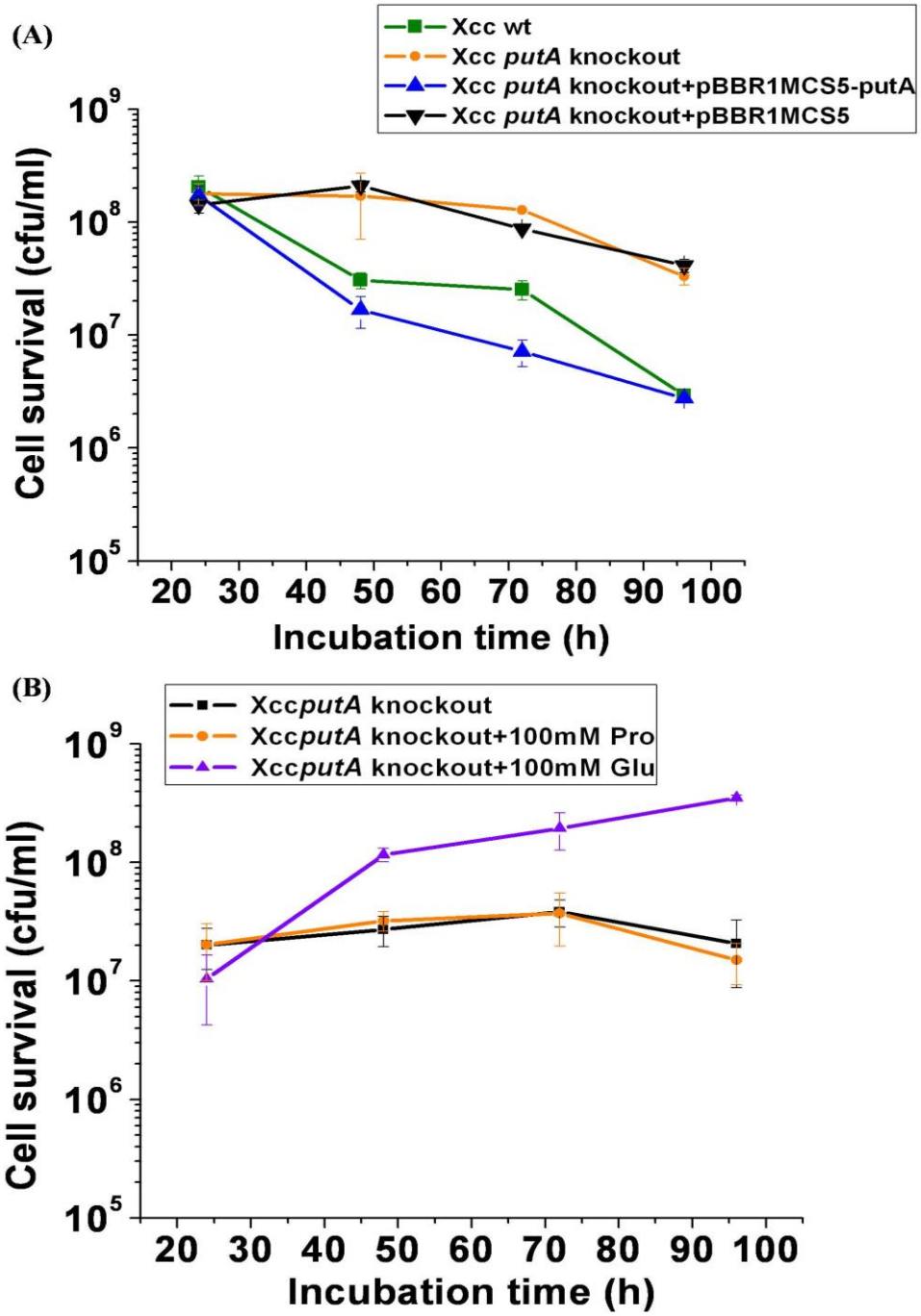

Fig.3.16: PCD in *Xanthomonas* cells: (A) Effect of knocking out of *putA* and its complementation on the PCD profile of Xcc 8004 strains grown in PIM; **(B)** Effect of supplementation of proline and glutamate in PNIM on the growth of Xcc Δ*putA* cells.

3.3.4 Status of PCD specific markers in Xcc (wild type), Xcc Δ*putA* and Xcc Δ*putA*-pPutA strains

In our earlier studies *Xanthomonas* cells were found to undergo PCD in PIM and displayed certain PCD specific markers such as activation of caspase-3-like protease activity (analyzed by enzyme assay as well as Western blot using polyclonal human caspase-3 antibody), externalization of membrane phosphatidylserine (PS) (assayed using annexinV-FITC labeling), and DNA damage (determined by TUNEL- Terminal deoxynucleotidyl transferase dUTP nick end labeling assay) [39,54–57]. The status of these PCD markers was also examined in this study in wild type Xcc, Xcc Δ*putA* and Xcc Δ*putA*- pPutA strains.

3.3.5 Caspase-3-like protease activity

Caspase-3-like activity which was quantified in terms of fluorescence level of AMC (amino methyl coumarin) released from a synthetic tetrapeptide substrate (Ac-DEVD-AMC) due to protease activity of caspase-3 [58]. Caspase-3-like activity in Xcc Δ*putA* strain while growing in PIM was found to be around 40% less than Xcc wt strain at 24 h of growth in PIM (Fig 3.17A), however no change in its levels were detected by western blotting in Xcc Δ*putA* strain (Fig 3.17B). FITC-DEVD-FMK, a fluorescent dye tagged with an irreversible caspase-3 inhibitor (DEVD-FMK) was also used for *in situ* labeling of *Xanthomonas* cells having active caspase-3-like enzyme. Interestingly, Xcc wt and XccΔ*putA*-pPutA cells grown in PIM fluoresced brightly when treated with this dye (Fig 3.17 C and E). A negligible number of Xcc Δ*putA* cells fluoresced when treated with FITC-DEVD-FMK (Fig 3.17D). Notably, cells showing caspase activity were mostly found to be filamented. Cell filamentation was also observed in PIM growing cells by monochrome (crystal violet) staining. Some hypochromic cell filaments were also observed indicating loss of membrane integrity (Fig 3.17G). On the

contrary, *Xanthomonas* cells grown in PNIM did not display any significant morphological change even after 72 h of incubation (Fig 3.17F). Among different possible explanations for cell filamentation, one could be due to ROS mediated DNA damage leading to upregulation of error prone repair pathway like SOS response in different bacteria. The induction of SOS response depends upon the extent and nature of DNA damage.

Figure 3.17

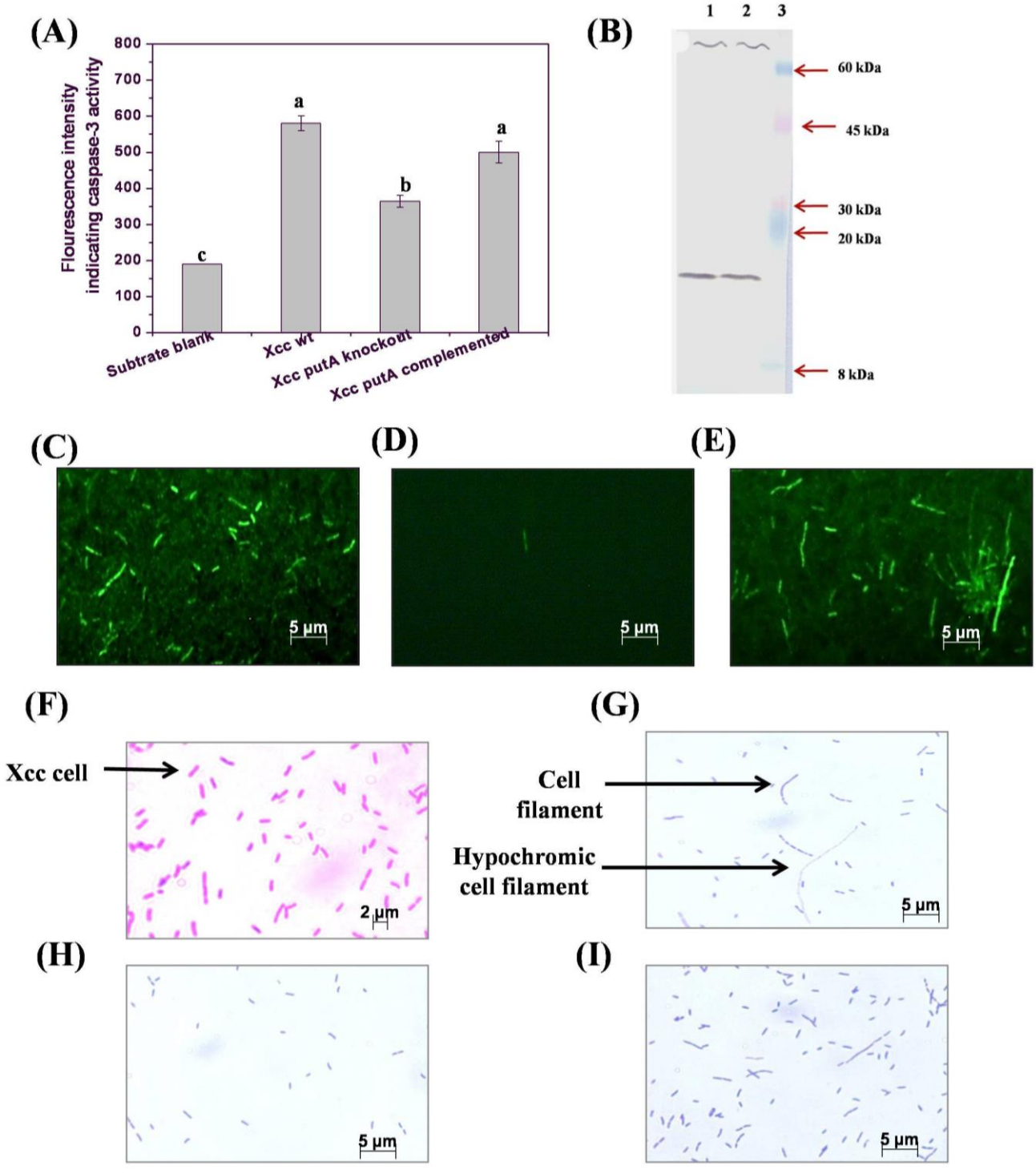

Fig.3.17: Caspase-3-like protein activity and cell morphology of Xcc strains grown in PIM (A) Caspase-3-like activity in Xcc wt, Xcc Δ*putA*, and Xcc *ΔputA*-pPutA cells in PIM.

The different letter on bars indicates that the means are significantly different at $p<0.05$. **(B)** Western blot indicating the status of caspase-3-like protein: lane 1: Xcc wt cells, lane 2: Xcc Δ*putA* cells, lane 3: ccoloured protein molecular weight marker. *In situ* labeling with FITC-DEVD-FMK indicating active caspase-3-like protein in **(C)** Xcc wt, **(D)** Xcc Δ*putA* and, **(E)** Xcc Δ*putA*-pPutA cells grown in PIM. Cell morphology of: **(F)** Xcc wt cells in PNIM, **(G)** Xcc wt cells in PIM, **(H)** Xcc Δ*putA* and, **(I)** Xcc Δ*putA*-pPutA cells in PIM.

3.3.6 Extent of DNA fragmentation in Xcc strains in PIM as monitored by TUNEL assay

Activation of caspase-3 enzyme has been reported to activate CAD (caspase activated DNase) resulting in DNA fragmentation prior to cell death [59]. With this analogy in this study too, DNA fragmentation was measured in Xcc strains growing in PIM by TUNEL assay. DNA breaks are labeled *in situ* with dUTPs tagged with a fluorophore, fluorescein isothiocyanate (FITC) with the help of an enzyme, terminal deoxynucleotidyl transferase (TdT) and the extent of labeling which obviously depends upon the extent of DNA fragmentation, is monitored by flow cytometry. This assay has also been used earlier to detect DNA fragmentation in bacteria [60]. Only 4% Xcc Δ*putA* cells were found to be TUNEL positive compared to 24% of Xcc wt and 19% in Xcc Δ*putA* complemented with PutA (Fig 3.18).

Figure 3.18

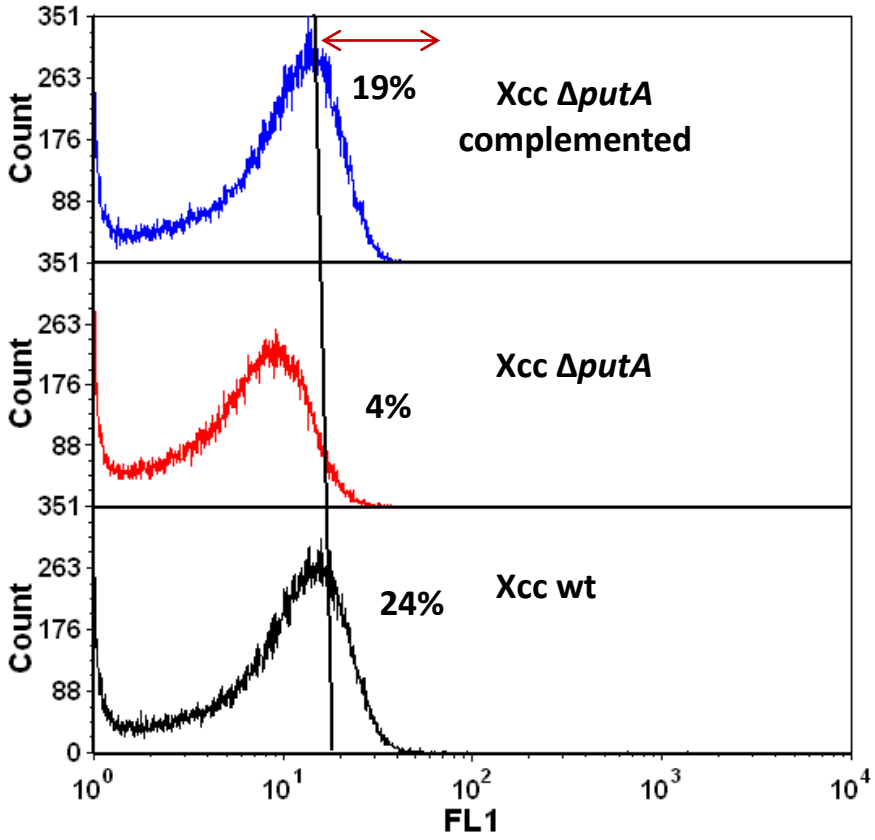

Fig.3.18: Status of DNA fragmentation in Xcc 8004, Xcc Δ*putA* and Xcc *ΔputA*-pPutA cells in PIM as detected by TUNEL assay. The gated region (represented by the arrow) depicts the area under the histogram and indicates the percentage of cells labeled by FITC-dUTP which implies DNA damage

3.3.7 Level of phosphatidylserine externalization in Xcc strains in PIM

Phosphatidylserine (PS) externalization has been reported as an important marker of PCD in various organisms, however, its exact implication remains to be elucidated, particularly in the case of microorganisms [61]. It has been reported as the hallmark of PCD in various systems including *E.coli*, *Saccharomyces* and *Aspergillus* [61–63]. PS externalization is detected by

flow cytometry using AnnexinV-FITC fluorophore. AnnexinV is a 36 kDa Ca^{2+} dependent phospholipid binding protein having high affinity for PS. Only 7% Xcc Δ*putA* cells were found to be AnnexinV-FITC positive as compared to 50% of Xcc wt cells growing in PIM (Fig.3.19).

Figure 3.19

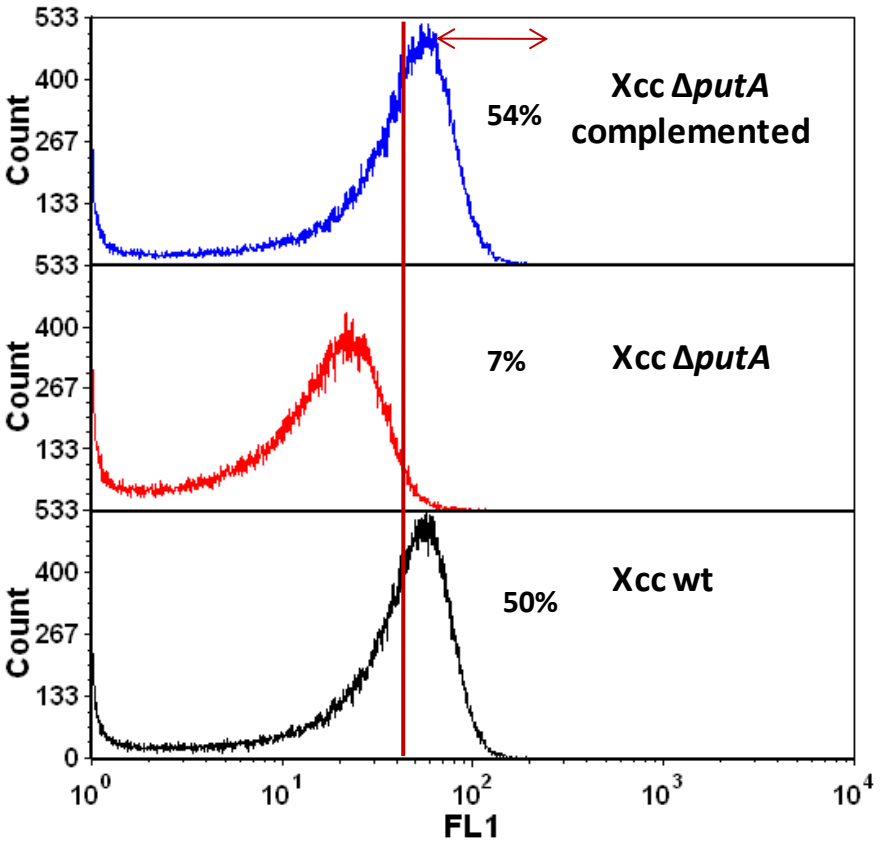

Fig.3.19: Status of PS externalization in Xcc 8004, Xcc Δ*putA* and Xcc *ΔputA*-pPutA cells in PIM as detected by AnnexinV-FITC assay. The gated region (represented by the arrow) depicts the area under the histogram and indicates the percentage of cells labeled by AnnexinV-FITC.

3.3.8 Status of membrane depolarization in *Xanthomonas* strains grown in PIM

Recently, membrane depolarization has also been used to monitor PCD in *E.coli* [60]. Membrane depolarization can be monitored by using the membrane potential sensitive carbocyanine dye, $DiOC_2(3)$ (3, 3'- diethyloxa-carbocyanine iodide). The proportion of depolarized cells was found to be greater in Xcc wt culture (29%) compared to Xcc Δ*putA* (5%) (Fig.3.20). In eukaryotes too, mitochondrial membrane depolarization leading to cytochrome c release has been reported as one of the early events occurring during apoptosis [64].

Figure 3.20

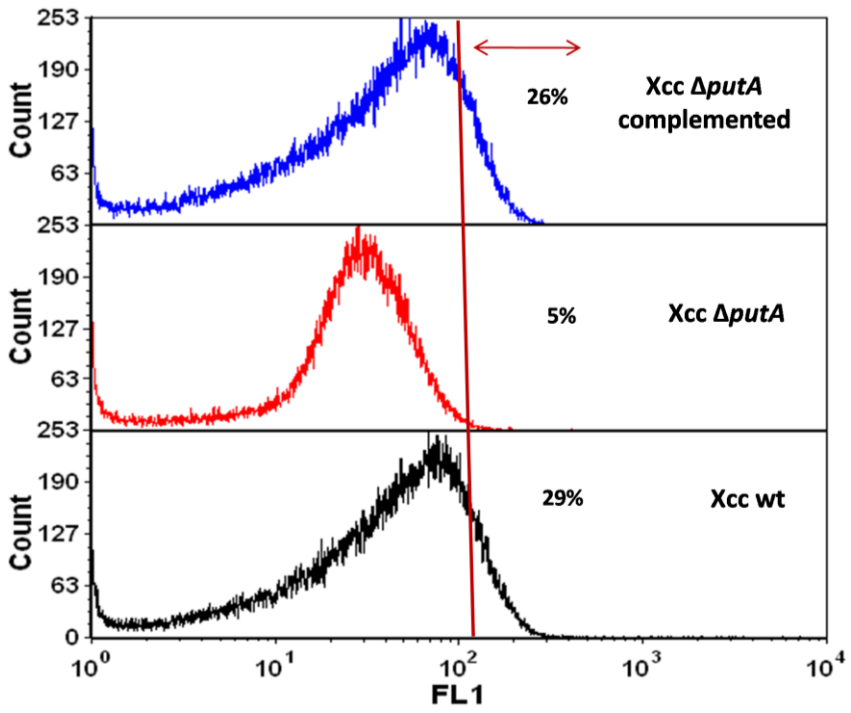

Fig.3.20: Membrane depolarization in *Xanthomonas* strains in PIM analyzed by flow cytometry. The gated region (represented by the arrow) indicates the percentage of depolarized cells.

3.3.9 Inhibition of PutA activity by electron transport chain (ETC) inhibitors

Involvement of proline metabolism in ETC was confirmed by using ETC inhibitors like rotenone and antimycin. Both these inhibitors were found to inhibit the activity of Xcc PutA by 65% (Fig.3.21A). Rotenone inhibits the electron flow from the Fe-S centres of complex I to ubiquinone, whereas, antimycin A inhibits the transfer of electrons from cytochrome b to c_1 (complex III). Similar inhibitor of complex I (amytal) has been reported as a non-competitive inhibitor of PutA in *E.coli* [65]. *Xanthomonas* PutA activity was found to be linked to ETC (Fig.3.21A) suggesting that PutA is also involved in regulating the redox homeostasis of the cell.

3.3.10 Status of ROS in Xcc strains

Proline oxidase (POX) in higher organisms, which is functionally similar to PutA in prokaryotes, has been reported to be an inner mitochondrial membrane protein that generates electrons during oxidation of proline to glutamate, and subsequent coupled reduction of FAD to $FADH_2$. This $FADH_2$ transfers electron to ubiquinone (UQ), an electron carrier in ETC. Thus proline can eventually get oxidized to generate ATP as well as superoxide. Though bacteria lack mitochondria, a similar process of electron transfer exists in membrane. The possibility of increased ROS generation upon activation of PutA was examined by monitoring the level of ROS in the Xcc wt, Xcc Δ*putA* and Xcc Δ*putA*-pPutA strains using H_2DCFDA staining (Fig.3.21B, C and D). The ROS level in *putA* knockout strain was 30% lower than the wt Xcc strain. This observation indicated that PutA was partly involved in generating ROS in *Xanthomonas* cells growing in PIM.

Since the extent of DNA damage and the level of ROS were found to be lower in Xcc Δ*putA* compared to the wt strain, it indicated that PutA is possibly involved in ROS generation

leading to DNA damage and eventually cell death (Fig.3.18, 3.21B and C). There are previous reports regarding the role of this enzyme in ROS generation in other organisms including *Helicobacter* and *Thermus thermophilus.* It has been demonstrated recently that proline dehydrogenase of *Arabidopsis* is involved in ROS formation during the hypersensitive response [25,33]. Similarly, human POX also contributes to generation of ROS (mainly superoxide) either directly by interacting with oxygen at the enzyme active site or indirectly by increasing the electron flux in the electron transport chain eventually leading to apoptosis [24,34]. Interestingly, the recently discovered P5C–proline cycle can deliver electrons to mitochondrial electron transport without producing glutamate and, under certain conditions, can generate more ROS in the mitochondria [24,35]. Proline catabolism is, therefore, an important regulator of cellular ROS balance and can influence numerous additional regulatory pathways.

Figure 3.21

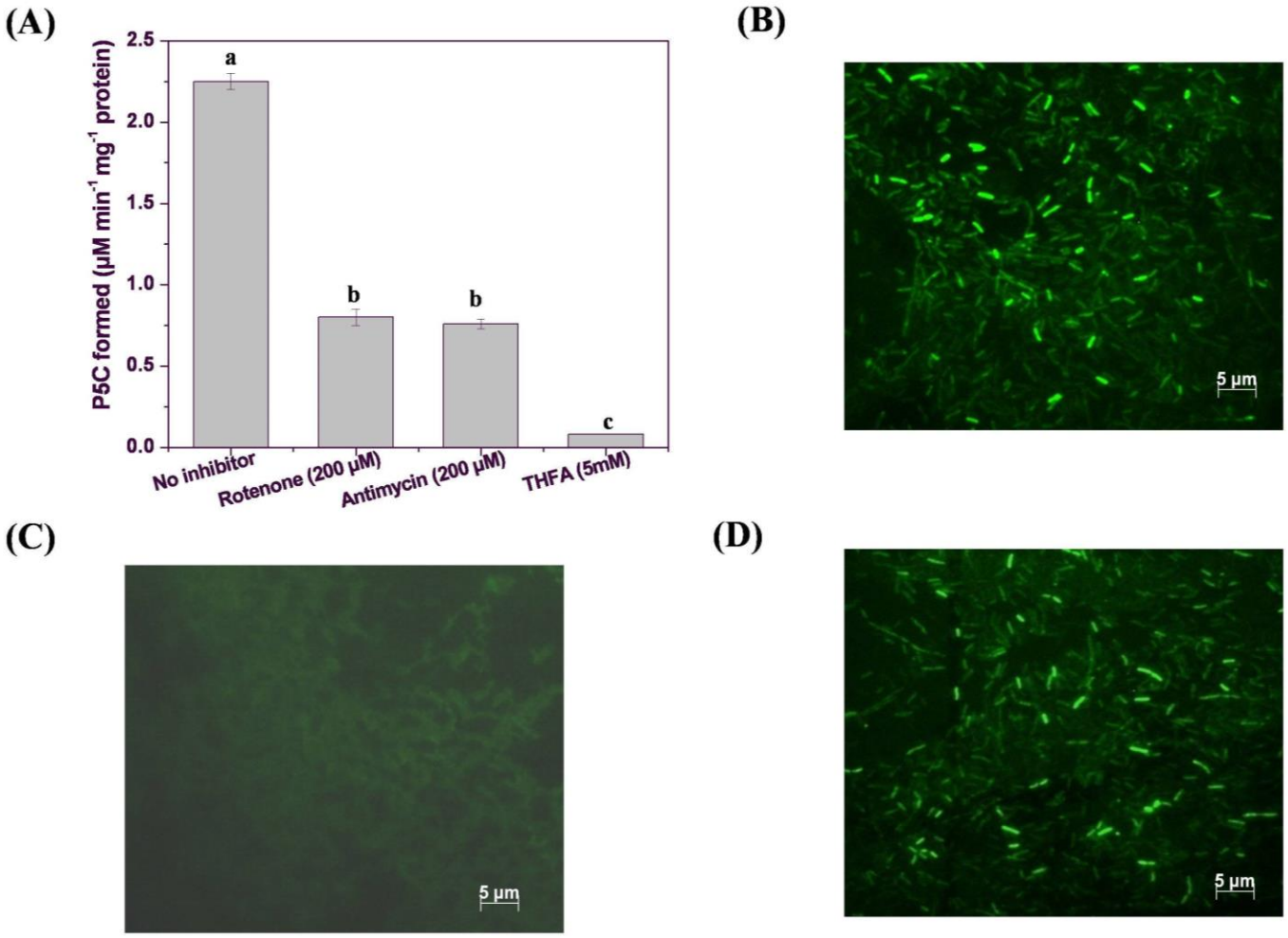

Fig.3.21: PutA activity and status of ROS in Xcc cells (A) PutA activity in Xcc 8004 cells in the presence of different inhibitors. The different letter on bars indicates that the means are significantly different at $p<0.05$. **(B-D)** Reactive oxygen species (ROS) generation observed by 2', 7'-dichlorohydrofluorescein-diaceate (H_2DCFDA) stain in **(B)** Xcc wt, **(C)** Xcc Δ*putA* and, **(D)** Xcc Δ*putA*-pPutA cells in PIM.

POX is reported to play an important role in cancer, apoptosis and schizophrenia in humans [66]. It has been found to be one of the 14 genes to be induced more than 10 fold by p53 and

has been termed as p53-induced gene 6 (PIG6) [53]. POX is regarded as a tumor suppressor protein and any anomaly in its functioning results in cancer [67]. POX activation in higher systems has been reported to induce both intrinsic and extrinsic pathways of apoptosis by regulating the redox homeostasis of the cell and has been observed to activate caspase-3, 8 and 9 [68]. Overexpression of POX leads to apoptotic cell death in several cancer cell types [68–70]. Its role has been established in eukaryotic apoptosis and is considered as an important protein for preventing initiation of cancer.

This study provides evidence of involvement of proline oxidase (PutA) in the observed PCD of *Xanthomonas.* This could be due to proline oxidase linked leakage of electrons from electron transport chain causing ROS generation and the resultant activation of caspase-3-like protein leading to cell death (Fig. 3.22). The findings are quite similar to the events observed in higher organisms indicating an evolutionarily conserved role of this protein in PCD.

Figure 3.22

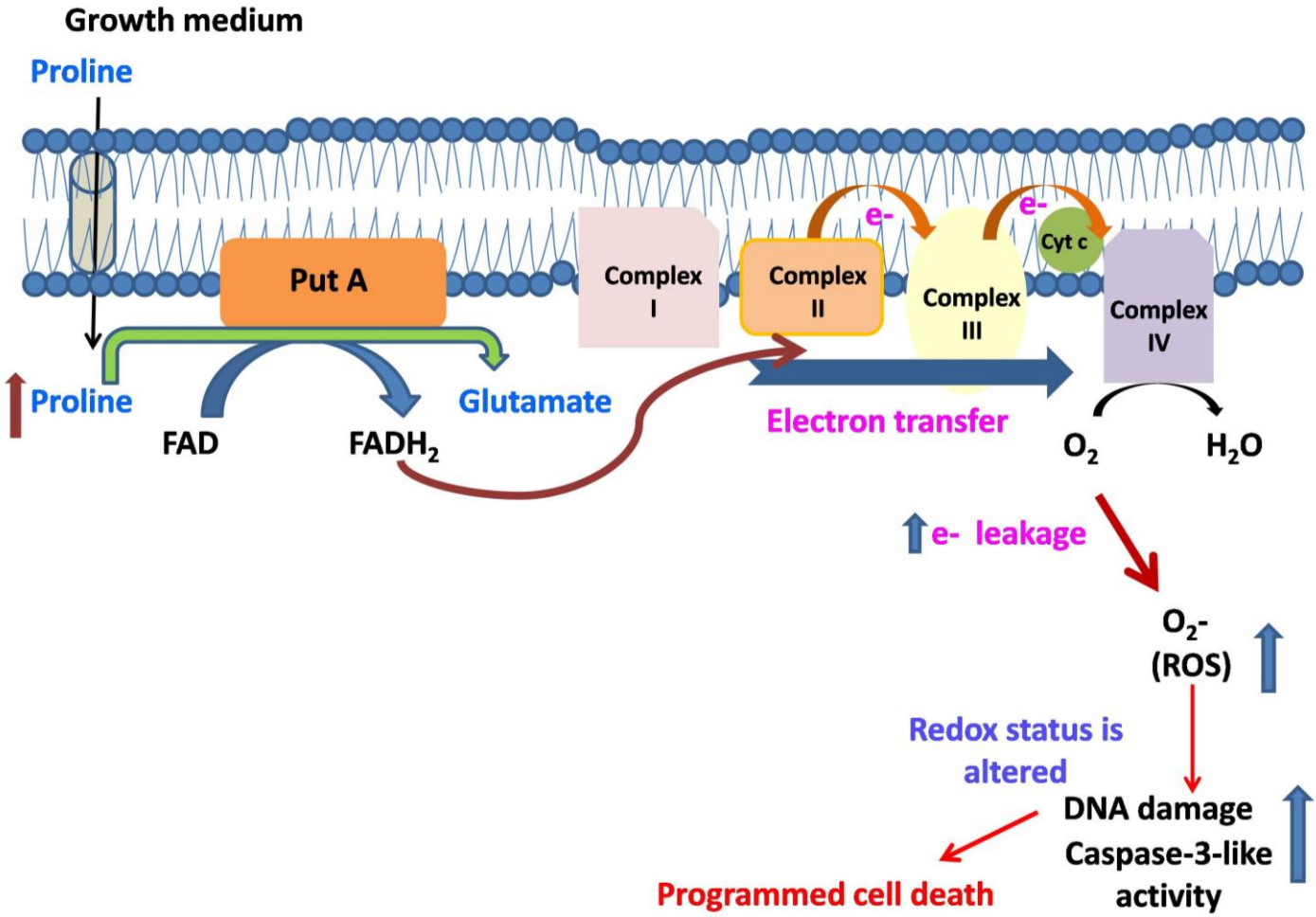

Fig. 3.22: Proposed mechanism of PCD in *Xanthomonas* due to enhanced PutA activity

References

1. Moses S, Sinner T, Zaprasis A, Stoveken N, Hoffmann T, Belitsky BR, Sonenshein AL, Bremer E (2012) Proline utilization by Bacillus subtilis: uptake and catabolism. J Bacteriol 194: 745-758. JB.06380-11 [pii];10.1128/JB.06380-11 [doi].
2. Phang JM, Donald SP, Pandhare J, Liu Y (2008) The metabolism of proline, a stress substrate, modulates carcinogenic pathways. Amino Acids 35: 681-690. 10.1007/s00726-008-0063-4 [doi].
3. van DP, Soto MJ, Villadas PJ, Toro N (2001) Construction and environmental release of a Sinorhizobium meliloti strain genetically modified to be more competitive for alfalfa nodulation. Appl Environ Microbiol 67: 3860-3865.
4. Nagata K, Nagata Y, Sato T, Fujino MA, Nakajima K, Tamura T (2003) L-Serine, D- and L-proline and alanine as respiratory substrates of Helicobacter pylori: correlation between in vitro and in vivo amino acid levels. Microbiology 149: 2023-2030.
5. Curtis J, Shearer G, Kohl DH (2004) Bacteroid proline catabolism affects N(2) fixation rate of drought-stressed soybeans. Plant Physiol 136: 3313-3318. 10.1104/pp.104.044024 [doi];pp.104.044024 [pii].
6. Berney M, Cook GM (2010) Unique flexibility in energy metabolism allows mycobacteria to combat starvation and hypoxia. PLoS One 5: e8614. 10.1371/journal.pone.0008614 [doi].
7. Kohl DH, Straub PF, Shearer G (1994) Does proline play a special role in bacteroid metabolism? Plant Cell Environ 17: 1257-1262.

8. Liu W, Phang JM (2012) Proline dehydrogenase (oxidase) in cancer. Biofactors 38: 398-406. 10.1002/biof.1036 [doi].
9. Smith CJ, Deutch AH, Rushlow KE (1984) Purification and characteristics of a gamma-glutamyl kinase involved in Escherichia coli proline biosynthesis. J Bacteriol 157: 545-551.
10. Omori K, Suzuki S, Imai Y, Komatsubara S (1991) Analysis of the Serratia marcescens proBA operon and feedback control of proline biosynthesis. J Gen Microbiol 137: 509-517.
11. Arentson BW, Sanyal N, Becker DF (2012) Substrate channeling in proline metabolism. Front Biosci (Landmark Ed) 17: 375-388. 3932 [pii].
12. Veeravalli K, Boyd D, Iverson BL, Beckwith J, Georgiou G (2011) Laboratory evolution of glutathione biosynthesis reveals natural compensatory pathways. Nat Chem Biol 7: 101-105. nchembio.499 [pii];10.1038/nchembio.499 [doi].
13. Zhang M, White TA, Schuermann JP, Baban BA, Becker DF, Tanner JJ (2004) Structures of the Escherichia coli PutA proline dehydrogenase domain in complex with competitive inhibitors. Biochemistry 43: 12539-12548. 10.1021/bi048737e [doi].
14. Milner JL, McClellan DJ, Wood JM (1987) Factors reducing and promoting the effectiveness of proline as an osmoprotectant in Escherichia coli K12. J Gen Microbiol 133: 1851-1860.
15. Zhou Y, Zhu W, Bellur PS, Rewinkel D, Becker DF (2008) Direct linking of metabolism and gene expression in the proline utilization A protein from Escherichia coli. Amino Acids 35: 711-718. 10.1007/s00726-008-0053-6 [doi].

16. Hahn DR, Maloy SR (1986) Regulation of the put operon in Salmonella typhimurium: characterization of promoter and operator mutations. Genetics 114: 687-703.
17. Chen LM, Maloy S (1991) Regulation of proline utilization in enteric bacteria: cloning and characterization of the Klebsiella put control region. J Bacteriol 173: 783-790.
18. Lee JH, Park NY, Lee MH, Choi SH (2003) Characterization of the Vibrio vulnificus putAP operon, encoding proline dehydrogenase and proline permease, and its differential expression in response to osmotic stress. J Bacteriol 185: 3842-3852.
19. Anderson CB, Witter LD (1982) Glutamine and proline accumulation by Staphylococcus aureus with reduction in water activity. Appl Environ Microbiol 43: 1501-1503.
20. Wood JM, Bremer E, Csonka LN, Kraemer R, Poolman B, van der Heide T, Smith LT (2001) Osmosensing and osmoregulatory compatible solute accumulation by bacteria. Comp Biochem Physiol A Mol Integr Physiol 130: 437-460. S1095-6433(01)00442-1 [pii].
21. Measures JC (1975) Role of amino acids in osmoregulation of non-halophilic bacteria. Nature 257: 398-400.
22. Shahjee HM, Banerjee K, Ahmad F (2002) Comparative analysis of naturally occurring L-amino acid osmolytes and their D-isomers on protection of Escherichia coli against environmental stresses. J Biosci 27: 515-520.
23. Krishnan N, Dickman MB, Becker DF (2008) Proline modulates the intracellular redox environment and protects mammalian cells against oxidative stress. Free

Radic Biol Med 44: 671-681. S0891-5849(07)00756-3 [pii];10.1016/j.freeradbiomed.2007.10.054 [doi].

24. Szabados L, Savoure A (2010) Proline: a multifunctional amino acid. Trends Plant Sci 15: 89-97. S1360-1385(09)00298-2 [pii];10.1016/j.tplants.2009.11.009 [doi].
25. Cecchini NM, Monteoliva MI, Alvarez ME (2011) Proline dehydrogenase contributes to pathogen defense in Arabidopsis. Plant Physiol 155: 1947-1959. pp.110.167163 [pii];10.1104/pp.110.167163 [doi].
26. Servet C, Ghelis T, Richard L, Zilberstein A, Savoure A (2012) Proline dehydrogenase: a key enzyme in controlling cellular homeostasis. Front Biosci (Landmark Ed) 17: 607-620. 3947 [pii].
27. Singh H, Arentson BW, Becker DF, Tanner JJ (2014) Structures of the PutA peripheral membrane flavoenzyme reveal a dynamic substrate-channeling tunnel and the quinone-binding site. Proc Natl Acad Sci U S A 111: 3389-3394. 1321621111 [pii];10.1073/pnas.1321621111 [doi].
28. Marcotte EM, Pellegrini M, Ng HL, Rice DW, Yeates TO, Eisenberg D (1999) Detecting protein function and protein-protein interactions from genome sequences. Science 285: 751-753. 7711 [pii].
29. Commichau FM, Stulke J (2008) Trigger enzymes: bifunctional proteins active in metabolism and in controlling gene expression. Mol Microbiol 67: 692-702. MMI6071 [pii];10.1111/j.1365-2958.2007.06071.x [doi].
30. Zhu W, Becker DF (2003) Flavin redox state triggers conformational changes in the PutA protein from Escherichia coli. Biochemistry 42: 5469-5477. 10.1021/bi0272196 [doi].

31. Muro-Pastor AM, Maloy S (1995) Proline dehydrogenase activity of the transcriptional repressor PutA is required for induction of the put operon by proline. J Biol Chem 270: 9819-9827.

32. Lee IR, Lui EY, Chow EW, Arras SD, Morrow CA, Fraser JA (2013) Reactive oxygen species homeostasis and virulence of the fungal pathogen Cryptococcus neoformans requires an intact proline catabolism pathway. Genetics 194: 421-433. genetics.113.150326 [pii];10.1534/genetics.113.150326 [doi].

33. Cecchini NM, Monteoliva MI, Alvarez ME (2011) Proline dehydrogenase is a positive regulator of cell death in different kingdoms. Plant Signal Behav 6: 1195-1197. 15791 [pii];10.4161/psb.6.8.15791 [doi].

34. Wanduragala S, Sanyal N, Liang X, Becker DF (2010) Purification and characterization of Put1p from Saccharomyces cerevisiae. Arch Biochem Biophys 498: 136-142. S0003-9861(10)00162-1 [pii];10.1016/j.abb.2010.04.020 [doi].

35. Miller G, Honig A, Stein H, Suzuki N, Mittler R, Zilberstein A (2009) Unraveling delta1-pyrroline-5-carboxylate-proline cycle in plants by uncoupled expression of proline oxidation enzymes. J Biol Chem 284: 26482-26492. M109.009340 [pii];10.1074/jbc.M109.009340 [doi].

36. Natarajan SK, Becker DF (2012) Role of apoptosis-inducing factor, proline dehydrogenase, and NADPH oxidase in apoptosis and oxidative stress. Cell Health Cytoskelet 2012: 11-27. 10.2147/CHC.S4955 [doi].

37. White TA, Krishnan N, Becker DF, Tanner JJ (2007) Structure and kinetics of monofunctional proline dehydrogenase from Thermus thermophilus. J Biol Chem 282: 14316-14327. M700912200 [pii];10.1074/jbc.M700912200 [doi].

38. Krishnan N, Becker DF (2006) Oxygen reactivity of PutA from Helicobacter species and proline-linked oxidative stress. J Bacteriol 188: 1227-1235. 188/4/1227 [pii];10.1128/JB.188.4.1227-1235.2006 [doi].

39. Gautam S, Sharma A (2002) Involvement of caspase-3-like protein in rapid cell death of Xanthomonas. Mol Microbiol 44: 393-401. 2837 [pii].

40. Bates LS, Waldren RP, Teare ID (1973) Rapid determination of free proline for water-stress studies. Plant Soil 39: 205-207.

41. Gaitonde MK (1967) A spectrophotometric method for the direct determination of cysteine in the presence of other naturally occurring amino acids. Biochem J 104: 627-633.

42. Dendinger S, Brill WJ (1970) Regulation of proline degradation in Salmonella typhimurium. J Bacteriol 103: 144-152.

43. LOWRY OH, ROSEBROUGH NJ, FARR AL, RANDALL RJ (1951) Protein measurement with the Folin phenol reagent. J Biol Chem 193: 265-275.

44. Alexeyev MF (1999) The pKNOCK series of broad-host-range mobilizable suicide vectors for gene knockout and targeted DNA insertion into the chromosome of gram-negative bacteria. Biotechniques 26: 824-6, 828.

45. Ratnakar PV, Mohanty BK, Lobert M, Bastia D (1996) The replication initiator protein pi of the plasmid R6K specifically interacts with the host-encoded helicase DnaB. Proc Natl Acad Sci U S A 93: 5522-5526.

46. Sambrook J, Fritsch EF, Maniatis T (1989) Molecular Cloning. Cold Spring Harbor Laboratory Press 1.75.

47. Daniels MJ, Barber CE, Turner PC, Sawczyc MK, Byrde RJ, Fielding AH (1984) Cloning of genes involved in pathogenicity of Xanthomonas campestris pv. campestris using the broad host range cosmid pLAFR1. EMBO J 3: 3323-3328.

48. Kovach ME, Elzer PH, Hill DS, Robertson GT, Farris MA, Roop RM, Peterson KM (1995) Four new derivatives of the broad-host-range cloning vector pBBR1MCS, carrying different antibiotic-resistance cassettes. Gene 166: 175-176. 0378111995005841 [pii].

49. Sezonov G, Joseleau-Petit D, D'Ari R (2007) Escherichia coli physiology in Luria-Bertani broth. J Bacteriol 189: 8746-8749. JB.01368-07 [pii];10.1128/JB.01368-07 [doi].

50. Becton, Dickinson, and Company, USA (2006) BD Bionutrients technical manual . 53.

51. Yan D (2007) Protection of the glutamate pool concentration in enteric bacteria. Proc Natl Acad Sci U S A 104: 9475-9480. 0703360104 [pii];10.1073/pnas.0703360104 [doi].

52. Liu W, Phang JM (2012) Proline dehydrogenase (oxidase) in cancer. Biofactors 38: 398-406. 10.1002/biof.1036 [doi].

53. Donald SP, Sun XY, Hu CA, Yu J, Mei JM, Valle D, Phang JM (2001) Proline oxidase, encoded by p53-induced gene-6, catalyzes the generation of proline-dependent reactive oxygen species. Cancer Res 61: 1810-1815.

54. Gautam S, Sharma A (2002) Rapid cell death in Xanthomonas campestris pv. glycines. J Gen Appl Microbiol 48: 67-76.

55. Raju KK, Gautam S, Sharma A (2006) Molecules involved in the modulation of rapid cell death in Xanthomonas. J Bacteriol 188: 5408-5416. 188/15/5408 [pii];10.1128/JB.00056-06 [doi].

56. Bayles KW (2014) Bacterial programmed cell death: making sense of a paradox. Nat Rev Microbiol 12: 63-69. nrmicro3136 [pii];10.1038/nrmicro3136 [doi].

57. Rice KC, Bayles KW (2003) Death's toolbox: examining the molecular components of bacterial programmed cell death. Mol Microbiol 50: 729-738. 3720 [pii].

58. Elmore S (2007) Apoptosis: a review of programmed cell death. Toxicol Pathol 35: 495-516. 779478428 [pii];10.1080/01926230701320337 [doi].

59. Earnshaw WC, Martins LM, Kaufmann SH (1999) Mammalian caspases: structure, activation, substrates, and functions during apoptosis. Annu Rev Biochem 68: 383-424. 10.1146/annurev.biochem.68.1.383 [doi].

60. Erental A, Sharon I, Engelberg-Kulka H (2012) Two programmed cell death systems in Escherichia coli: an apoptotic-like death is inhibited by the mazEF-mediated death pathway. PLoS Biol 10: e1001281. 10.1371/journal.pbio.1001281 [doi];PBIOLOGY-D-11-02298 [pii].

61. Dwyer DJ, Camacho DM, Kohanski MA, Callura JM, Collins JJ (2012) Antibiotic-induced bacterial cell death exhibits physiological and biochemical hallmarks of apoptosis. Mol Cell 46: 561-572. S1097-2765(12)00349-8 [pii];10.1016/j.molcel.2012.04.027 [doi].

62. Ludovico P, Rodrigues F, Almeida A, Silva MT, Barrientos A, Corte-Real M (2002) Cytochrome c release and mitochondria involvement in programmed cell

death induced by acetic acid in Saccharomyces cerevisiae. Mol Biol Cell 13: 2598-2606. 10.1091/mbc.E01-12-0161 [doi].

63. Mousavi SA, Robson GD (2004) Oxidative and amphotericin B-mediated cell death in the opportunistic pathogen Aspergillus fumigatus is associated with an apoptotic-like phenotype. Microbiology 150: 1937-1945. 10.1099/mic.0.26830-0 [doi];150/6/1937 [pii].

64. Gottlieb E, Armour SM, Harris MH, Thompson CB (2003) Mitochondrial membrane potential regulates matrix configuration and cytochrome c release during apoptosis. Cell Death Differ 10: 709-717. 10.1038/sj.cdd.4401231 [doi];4401231 [pii].

65. Abrahamson JL, Baker LG, Stephenson JT, Wood JM (1983) Proline dehydrogenase from Escherichia coli K12. Properties of the membrane-associated enzyme. Eur J Biochem 134: 77-82.

66. Luo M, Arentson BW, Srivastava D, Becker DF, Tanner JJ (2012) Crystal structures and kinetics of monofunctional proline dehydrogenase provide insight into substrate recognition and conformational changes associated with flavin reduction and product release. Biochemistry 51: 10099-10108. 10.1021/bi301312f [doi].

67. Liu Y, Borchert GL, Donald SP, Diwan BA, Anver M, Phang JM (2009) Proline oxidase functions as a mitochondrial tumor suppressor in human cancers. Cancer Res 69: 6414-6422. 0008-5472.CAN-09-1223 [pii];10.1158/0008-5472.CAN-09-1223 [doi].

68. Liu Y, Borchert GL, Surazynski A, Hu CA, Phang JM (2006) Proline oxidase activates both intrinsic and extrinsic pathways for apoptosis: the role of

ROS/superoxides, NFAT and MEK/ERK signaling. Oncogene 25: 5640-5647. 1209564 [pii];10.1038/sj.onc.1209564 [doi].

69. Liu Y, Borchert GL, Donald SP, Diwan BA, Anver M, Phang JM (2009) Proline oxidase functions as a mitochondrial tumor suppressor in human cancers. Cancer Res 69: 6414-6422. 0008-5472.CAN-09-1223 [pii];10.1158/0008-5472.CAN-09-1223 [doi].

70. Maxwell SA, Rivera A (2003) Proline oxidase induces apoptosis in tumor cells, and its expression is frequently absent or reduced in renal carcinomas. J Biol Chem 278: 9784-9789. 10.1074/jbc.M210012200 [doi];M210012200 [pii].

Chapter 4: Occurrence of Caspase Dependent PCD in Different Bacterial Genera upon Oxidative Stress

4.1 Introduction

In the preceding chapters, oxidative stress due to enhanced metabolism was found to be the main driving force for PCD in *Xanthomonas.* To evaluate the conserved existence of PCD-like process in other bacteria besides *Xanthomonas,* the study was performed in *Bacillus subtilis, Bordetella bronchiseptica, Escherichia coli* and *Salmonella enterica* sv. Typhimurium. Here gamma radiation was used to generate ROS and to study its effect on survival of these bacteria and also to understand the underlying mechanism of cell death.

4.1.1 Oxidative stress

The term 'oxidative stress' was coined by Fridovich in 1978 [1]. It was defined as a disturbance in the cell or organism that causes the prooxidant-antioxidant balance to shift in favour of the former [2]. Many external genotoxic stresses, such as hyperbaric oxygen, γ-radiation, near-UV radiation, trioxygen (ozone), peroxides and redox-cycling drugs have also been found to have toxic consequences for both prokaryotic and eukaryotic cells [1]. The main targets for ROS in the cell are DNA, lipids and proteins. Majority of the damage is caused by hydroxyl radical ($OH^{\cdot}$) formed from H_2O_2 which is formed in the presence of metal ions by Fenton reaction. The toxic effects of reactive oxygen species (ROS) were first described by Harman in 1956 in the 'free radical theory of aging' [1]. This theory further gained ground by the subsequent discovery of the antioxidant enzyme superoxide dismutase (SOD) [3].

4.1.2 Oxidative Stress Caused by Radiation

Electromagnetic radiation can be divided into high and low energy waves based on their wavelength. Low energy spectrum includes visible light, microwaves, infrared and radio

waves. X-rays and gamma rays fall into the high energy category. These radiations ionize the medium and hence are termed as ionizing radiations (IR). Their effect has been well studied in several animal models and cell lines [4]. Ionizing radiation can damage cell or its macromolecules, including DNA, either directly or indirectly through free radicals generated by radiolysis of water. The harmful effects of ionizing radiations are primarily due to radiolysis of water which leads to generation of different harmful radicals including hydroxyl radical ($OH^{\cdot}$) (Fig.4.1). It reacts indiscriminately and is hence the most harmful radical.

Figure 4.1

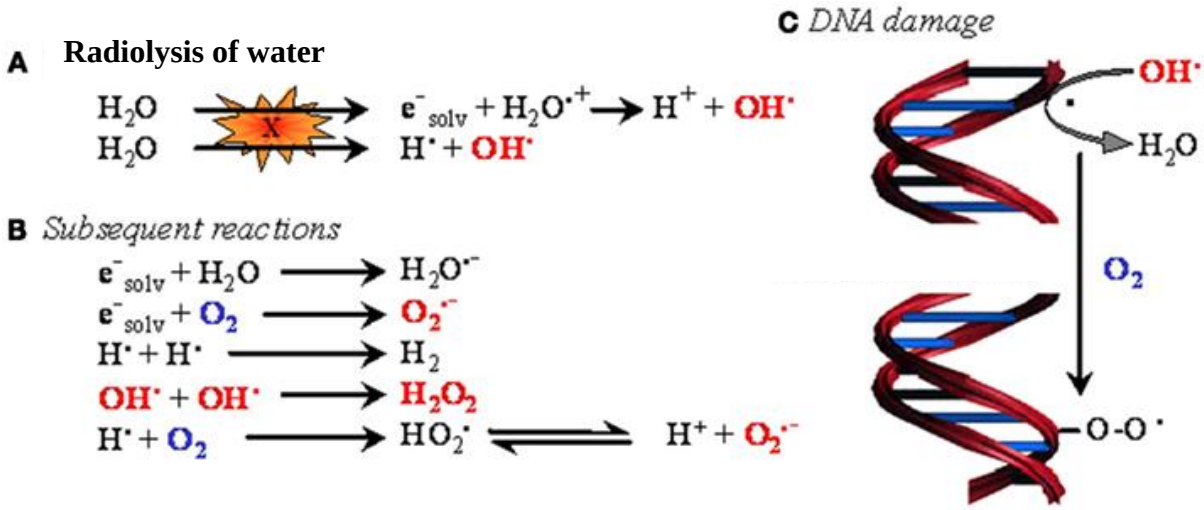

Reference: Jordan and Sonveaux, 2012 [5]

Fig.4.1: **Radiolysis of water (A)** In biological tissues, irradiation primarily induces ionization of water, leading to the formation of reactive radical species; **(B)** These species then react with neighboring molecules to yield reactive oxygen species (ROS) among which the hydroxyl radical is believed to be the most cytotoxic. **(C)** When generated in the proximity of DNA, hydroxyl radicals attack it [5].

4.1.3 Effect of radiation on different biomolecules

4.1.3.1 DNA damage

ROS can cause DNA modifications by oxidizing the bases (purine and pyrimidines) and sugar moities. The highly reactive hydroxyl radical ($OH^{\bullet}$) reacts with DNA by addition to double bonds of DNA bases and by abstraction of an H atom from the methyl group of thymine and C-H bonds of 2′-deoxyribose [6]. Reactions of pyrimidines and purines result in multiple products in DNA, as depicted in Fig.4.2. Guanine, adenine and cytosine can be oxidized to 8-hydroxyguanine, 8-hydroxyadenine and 5-hydroxycytosine, respectively [6]. The base radicals can undergo addition reaction with aromatic amino acids of proteins or combine with amino acid radical, leading to DNA–protein cross-linking. Reactions of $OH^{\bullet}$ with the sugar moiety of DNA by H abstraction give rise to sugar modifications and strand breaks, and the latter is quite fatal for the cell [6].

Figure 4.2

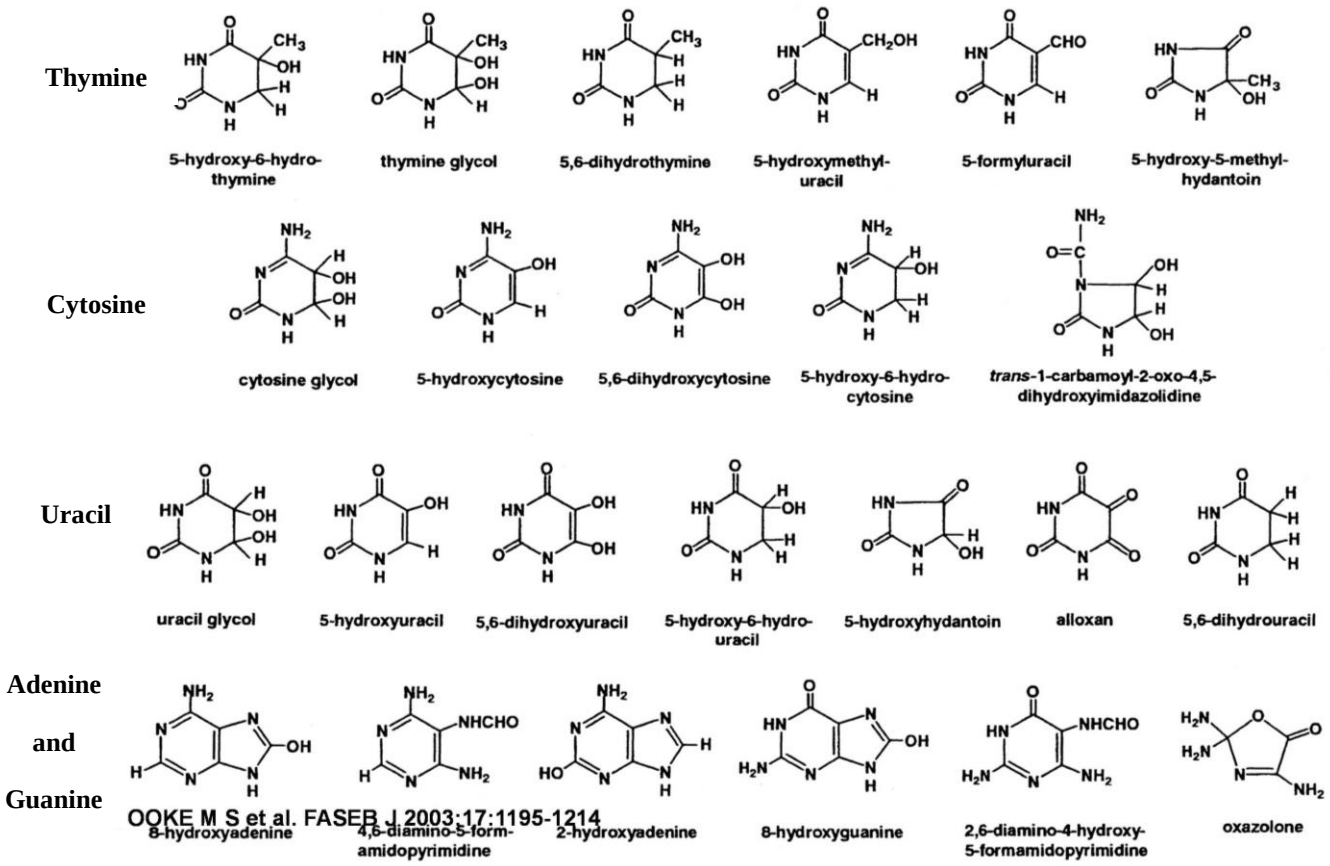

Reference: Cooke et al, 2003 [6].

Fig.4.2: DNA base products after reaction with reactive oxygen species (ROS).

4.1.3.2 Lipid peroxides

Lipids are major targets during oxidative stress. Free radicals can directly attack polyunsaturated fatty acids in membranes and initiate lipid peroxidation (termed ‘initiation’) (Fig. 4.3). A primary effect of lipid peroxidation is a decrease in membrane fluidity, which alters membrane properties and can disrupt membrane bound proteins significantly. This effect sets in a chain reaction leading to more radical formation (termed as ‘propagation’) and polyunsaturated fatty acids are degraded to a variety of products (Fig 4.3). Some of them,

such as aldehydes, are very reactive and can damage proteins as well [7]. Unlike reactive free radicals, aldehydes are rather long lived and can therefore diffuse from the site of their origin and reach and attack targets which are distant from the initial free-radical generating events, acting as “second toxic messengers” of the complex chain reactions initiated. Among the many different aldehydes which can form during lipid peroxidation, the most intensively studied are malonaldehyde (MDA) and 4-hydroxyalkenals, in particular 4-hydroxynonenal (HNE) [7].

Figure 4.3

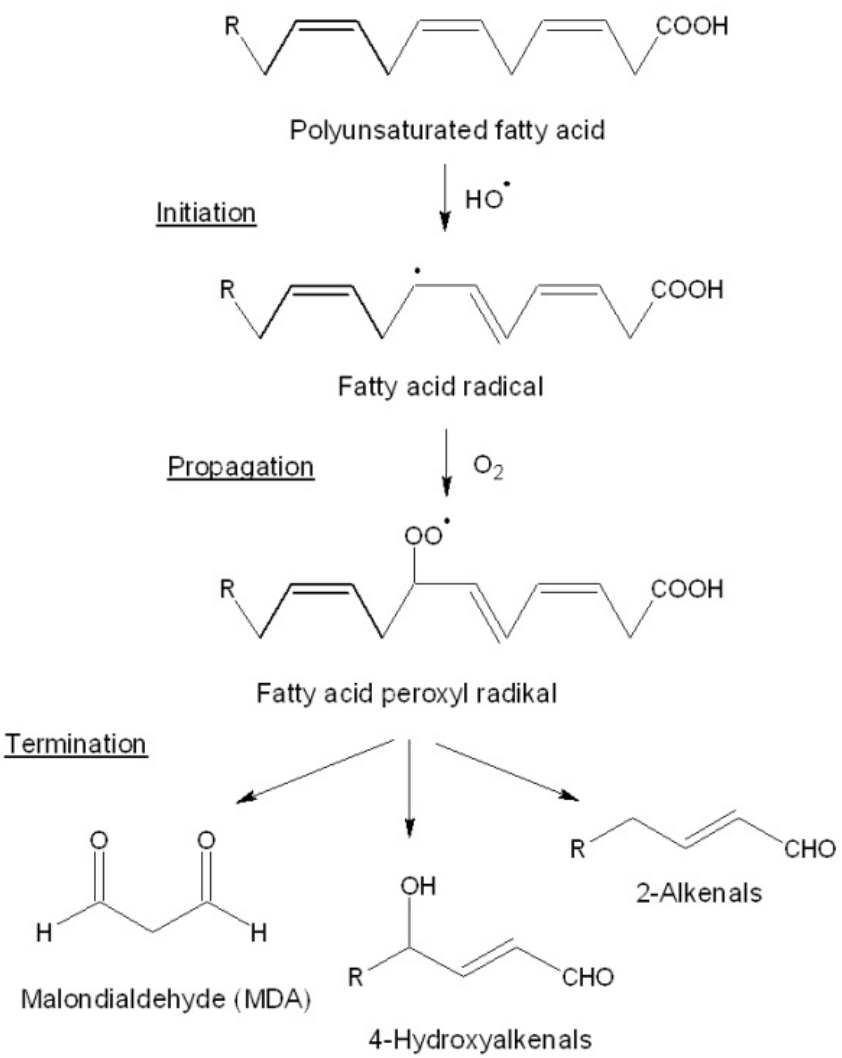

Reference: Mimica-Dukić et al, 2012 [8].

Fig.4.3: Lipid peroxidation reactions.

4.1.3.3 Protein oxidation

Proteins are the functional work horses of a cell. The oxidization of amino acids due to ROS can lead to altered protein structure, folding and activity, creating an imbalance in cellular homeostasis. In higher organisms, several disease conditions like diabetes, atherosclerosis,

neurodegenerative diseases and aging are accompanied by the damaging actions of oxidized proteins. The major protein modifications include: amino acid modifications (Fig. 4.4), carbonyl group formation, decrease in thermal stability, fragmentation, formation of protein-protein cross-links, formation of S–S bridges, increased susceptibility to proteolysis and loss of catalytic activity [7].

Figure 4.4

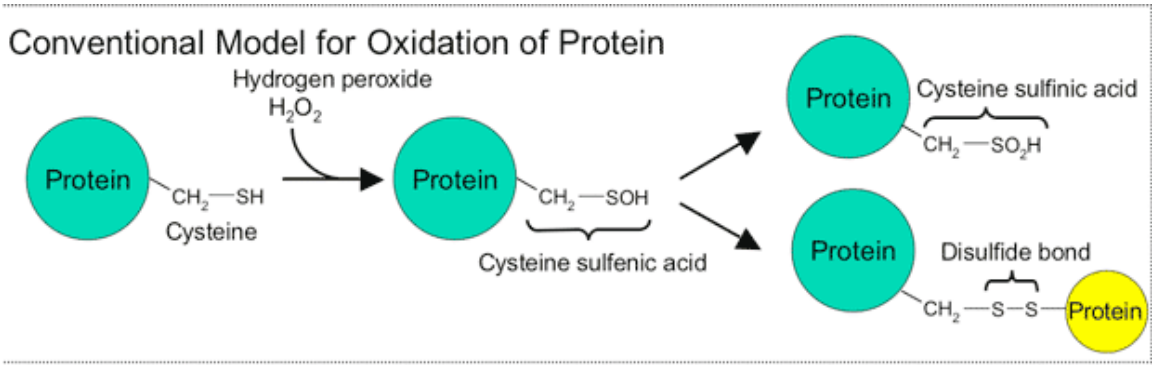

Reference: http://www.aist.go.jp/aist_e/latest_research/2008/20080521/20080521.html

Fig.4.4: Reaction mechanism of oxidation of cysteine side chains of proteins

4.1.4 Effect of radiation on bacteria

Although the mechanism of post irradiation recovery has been well studied in *Deinococcus radiodurans,* which is the most radioresistant bacterium reported so far [9], the effect of radiation on survival and cell death has not been well addressed in other bacteria. Hence the bacteria like *E. coli, Salmonella, Bordetella, Bacillus* and *Xanthomonas* were investigated to understand the mechanism of cell death upon gamma radiation exposure.

4.1.4.1 *Escherichia coli*

It is a Gram negative, facultative anaerobic bacterium which is commonly found in the intestinal tract of mammals. Most *E. coli* strains are harmless, but some serotypes can cause serious food poisoning in their hosts, and are occasionally responsible for product recalls due to food contamination. The harmless strains are part of the normal flora of the gut, and can benefit their hosts by producing vitamin K2 and preventing colonization of the intestine with pathogenic bacteria. The various mechanisms by which *E. coli* cells respond to stresses have been reported. One such mechanism is expression of toxin-antitoxin module which has been explained in chapter 1. Apart from this, different sensors (transcription factors) like OxyR, SoxR and PerR sense the oxidative stress and induce the synthesis of around 30 different proteins including catalase, superoxide dismutase, endonuclease IV, RecA, and glutathione reductase [10].

4.1.4.2 *Salmonella enterica* sv. Typhimurium

Salmonella is a Gram negative bacterium and comprises many pathogenic strains. It is a food borne pathogen and more than 99% human infections by *Salmonella* are caused by subspecies *enterica*. The stress response of *Salmonella* is quite similar to that of *E. coli* [10]. Due to its efficient stress response system, it is proposed that *Salmonella* is difficult to eradicate from the food chain [11]. The sigma factor RpoS (RNA polymerase S) has been reported to play vital role in the stress response and pathogenicity of this organism. It has been shown to regulate the expression of around 50 proteins during nutrient deprivation, pH and temperature stress [11].

4.1.4.3 *Bacillus subtilis*

Bacillus subtilis is a Gram positive bacterium commonly found in the soil and has been frequently used as model organism. It is a prominent food spoiler, causing ropiness in bread and other foods. The other strain of *Bacillus, B. anthracis* causes anthrax in cattle and humans. *Bacillus* species produce spores which are quite sturdy and can survive even the extreme environment. PerR and OhrR proteins play important roles in *Bacillus* stress response. The general stress response factor, RNA polymerase σ^B subunit and the thiol-based sensor Spx, provide protective response to the cells against oxidants under multiple stress conditions [12,13].

4.1.4.4 *Bordetella bronchiseptica*

Bordetella bronchiseptica is a Gram negative bacterium. It is not pathogenic to humans but infects the respiratory tract of smaller mammals like rabbit, cat and dog. It is closely related to *B. pertussis*, which causes pertussis or whopping cough in humans. Some two component regulatory systems (like RisA-RisS) have been reported to play an important part in imparting resistance to *Bordetella* against oxidative stress [14].

4.1.5 Markers of Programmed Cell Death (PCD) reported in different bacteria

PCD implies that the cell death is governed by certain internal factors/ molecules as opposed to accidental death or necrosis wherein the cell dies in an uncontrolled manner. PCD displays specific biochemical and morphological markers [4]. These markers include activation of caspases (or caspase-like protein in bacteria and metacaspase in fungi/ lower eukaryotes), DNA damage, membrane depolarization and phosphatidylserine (PS) externalization [4,15,16]

Phosphatidylserine (PS) externalization which occurs during the later stages of apoptosis has been reported in fungi and bacteria including *Saccharomyces, Aspergillus* and *E. coli* [16–18]. The exact significance of PS externalization has not been clearly understood in unicellular eukaryotes and bacteria. Externalization of PS during apoptosis in eukaryotes helps in the recognition and uptake of these cells by phagocytes [19]. This helps in containment of the cellular contents and thus minimizes the damage to the neighbouring cells. Phosphatidylserine belongs to a class of acidic phospholipids. Although it is distributed widely among animals, plants and microorganisms, it is usually less than 10% of the total phospholipids. The outer membrane of Gram negative bacteria has an asymmetric lipid distribution with lipopolysaccharides in the outer leaflet and phospholipids in the inner leaflet. In other unicellular eukaryotes like *Blastocystis hominis, Leishmania* and *Trypanosoma cruzi* this phenomenon has been well established in cells undergoing apoptosis where the probable significance of PS externalization has been proposed to promote phagocytosis by the host leading to their internalization and eventual suppression of inflammatory response [19,20].

4.1.6 Cleavage of poly (ADP-ribose) polymerase (PARP)

Poly (ADP-ribose) polymerase (PARP) is an enzyme which is constitutively expressed in the cell. When DNA of the cell gets damaged due to certain external or internal agents, PARP binds to the damaged site of DNA and allows the DNA excision repair machinery to repair the damaged site [21]. However, if the extent of damage is more and cell decides to undergo suicidal programmed cell death or apoptosis, caspase-3 cleave the PARP molecule and the damaged DNA is chewed up by nucleases (caspase activated DNAses) leading to cell death. PARP catalyzes the cleavage of NAD^+ into ADP and ADP-ribose and attaches several

molecules of the latter to the target protein in a process called poly ADP-ribosylation. PARP is activated by DNA breaks, and can deplete NAD^+ and ATP of a cell in an attempt to repair the damaged DNA. However, severe ATP depletion in a cell can lead to its lysis and death. As PARP acts as a DNA damage-sensor molecule, it has also been considered as a 'guardian of the genome' and described as a 'multi-talented molecule' [22]. In fact, PARP plays a double role, PARP-1 normally acts as a pro-survival factor, essentially because of its role in promoting DNA repair; under massive DNA damage/stress conditions, it turns on the darker side and causes cell death [23]. Hence, PARP inhibitors rescue cells undergoing either apoptosis or necrosis. Most of the PARP inhibitors mimic the nicotinamide moiety of NAD^+ [24]. The benzamides inhibit PARP by interfering with the binding of NAD^+ to the enzyme's active site [24].

4.1.7 Cellular defense mechanism against DNA breaks: SOS response

Radiation is also known to induce SOS response, an error prone DNA repair pathway in many bacteria including *E. coli*. This DNA repair system was first described by Miroslav Radman around 40 years ago [25]. SOS repair system has been well studied in *E. coli* and is often considered as the DNA damage check point in bacteria [26]. Damaging agents like UV and gamma radiation cause DNA lesions leading to stalled replication fork [27,28]. In *E. coli* such a condition activates RecA protein which induces autocatalytic cleavage of LexA repressor (Fig. 4.5). RecA is a conserved protein and is ubiquitously present in all organisms from bacteria to human beings [29]. The cleavage of LexA derepresses the LexA regulated genes leading to induction of around 40 different genes resulting in SOS response in an attempt to restore the capacity of DNA to replicate (Fig. 4.5). These genes are induced in an orderly manner. The first few genes to be induced are *uvrA, uvrB* and *uvrD.* These proteins

along with endonuclease UvrC, catalyze nucleotide excision repair (NER) in which the damaged nucleotides are excised from dsDNA. Additionally, the expression of *recA* increases by 10-50 folds. RecA along with RecB and RuvC participates in homologous recombination wherein the lesions on dsDNA are repaired. RecB is a part of RecBCD enzyme complex which serves as an exonuclease that participates in double strand break repair of DNA. RuvA is a 22 kDa protein and is one of the first proteins to be expressed during SOS induction. Together with RuvBC it forms RuvABC complex which is involved in resolving the Holliday junction formed during homologous recombination. Eventually, around 40 minutes after DNA damage if the damage is not fully repaired by NER and homologous recombination, then genes *sulA* and *umuDC* are induced. *umuDC* encode polymerase V ($UmuD_2'C$) which carries out translesion DNA synthesis, a compromised recovery mechanism. SulA inhibits cell division by preventing the polymerization of FtsZ protein, thereby giving time for cell recovery.

Figure 4.5

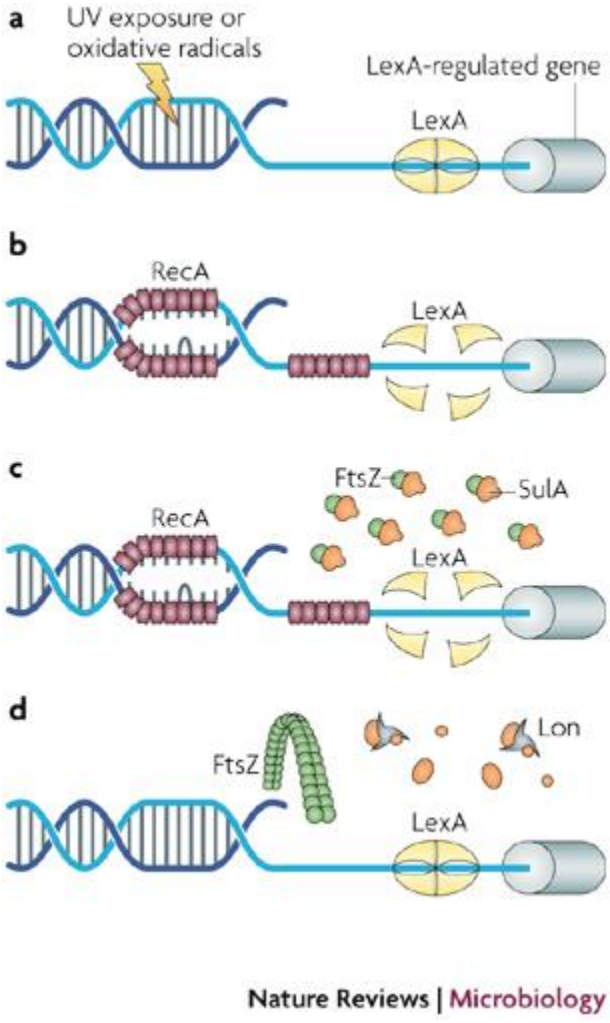

Reference: Justice et al; 2008 [30]

Fig.4.5: Induction of SOS response. a: Exposure to ultraviolet (UV) radiation or oxidative radicals can damage chromosomal DNA, thereby leading to the induction of the DNA-damage response system (the SOS response). The transcription of over 40 unlinked genes is coordinately activated, which facilitates the repair of damaged DNA without transmission to daughter cells; **b:** On a molecular level, mismatched base pairs produce regions of single-stranded DNA that serve as a polymerization platform for RecA, the major bacterial recombinase. Polymerized RecA is activated in the presence of free nucleotide triphosphates

and stimulates the autoproteolysis of the SOS transcriptional repressor LexA. Most of the genes that are transcriptionally activated are DNA-repair enzymes; **c:** The LexA regulon also includes a cell-division inhibitor, SulA, to prevent the transmission of mutant DNA to new daughter cells. SulA specifically inhibits polymerization of the division protein FtsZ by binding to the FtsZ monomer. This blocks FtsZ ring formation at mid-cell, which results in the formation of non-septate bacterial filaments; **d:** Once DNA repair is complete, LexA repression of the SOS genes is restored. In addition, the general cytoplasmic protease Lon degrades SulA, thereby restoring cell-division capacity [30].

4.1.8 Assay employed to test SOS induction: Selectable *in vivo* expression technology (SIVET) assay

Many bacteria harbour prophage in their genome. The repressed prophage is integrated in the bacterial chromosome and replicates as a part of the host genome (termed as the lysogenic phase). The transition from lysogenic to lytic phase (also known as induction) can happen in different conditions including damage to host DNA. Selectable in vivo expression technology (SIVET) has been developed as a reporter system used to quantify cells in which the SOS response has been induced leading to a scorable permanent selectable change in the cell [31,32]. The SIVET system consists of two components (a) a gene encoding the TnpR resolvase inserted downstream of a defective H-19B prophage. (b) The second component is a chloramphenicol transacetylation gene (*cat*) disrupted by an inserted tetracycline (*tet*) gene (Fig. 4.6). This *tet* gene is flanked by altered resolvase target sequences (*resC*). When cells are exposed to DNA damage leading to SOS induction, the prophage promoter is derepressed and the resulting activity of resolvase excises the *tet* gene and one *resC* site. Excision results in a sequence bearing functional *cat* gene converting the cell from Tet^R Cm^S phenotype to a

Tet^S Cm^R phenotype. Thus, the frequency of Cm^R cells within a SIVET strain culture (*E. coli* SG104) is a measure of prophage induction, which in turn reflects SOS induction.

Figure 4.6

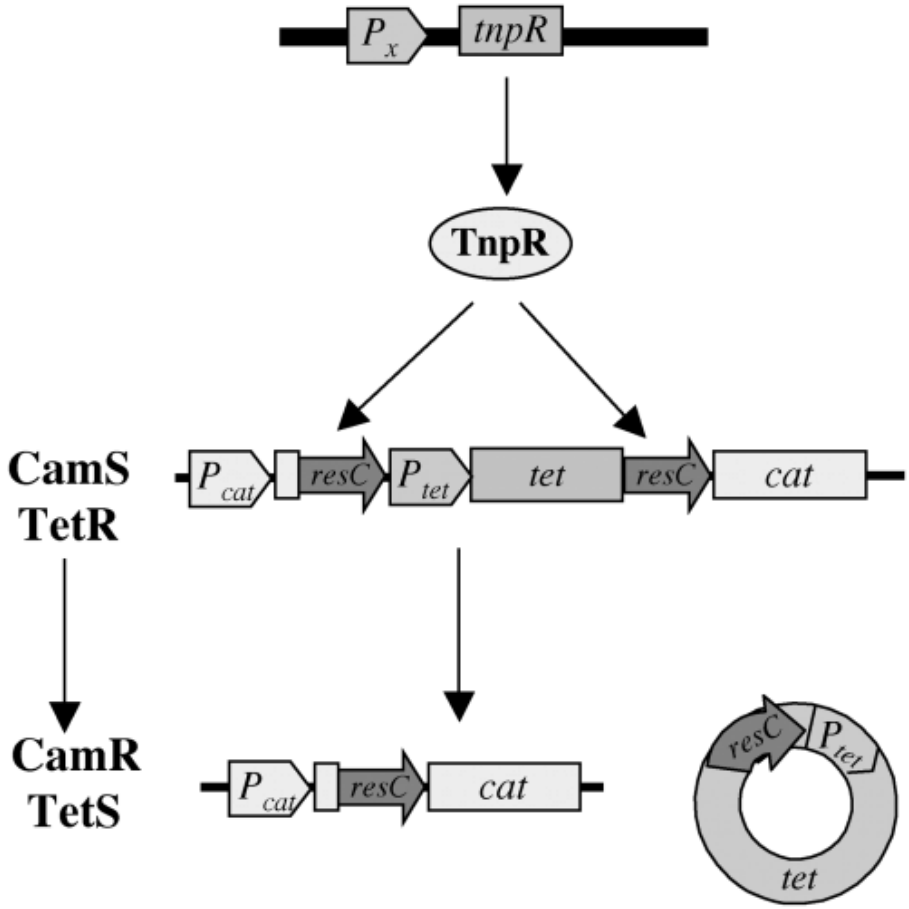

Reference: Linvy and Friedman,2004 [33]

Fig.4.6: General scheme of the selectable in vivo expression technology (SIVET). Expression of TnpR following activation of transcription from a promoter of interest results in excision and circularization of the *tet* gene and one modified resolvase excision site (*resC*). The excised DNA does not replicate and thus is lost by segregation. Excision of *tet* creates a functional *resC-cat* ORF. TnpR does not catalyse the reinsertion of *tet*, which is lost through segregation. Thus cells in which TnpR has been expressed undergo a genetic conversion

which renders them and their progeny resistant to chloramphenicol and sensitive to tetracycline [33].

Chapters 2 and 3 demonstrate metabolic stress induced PCD, dependent on a caspase-3 like protein, in *Xanthomonas campestris* [34–38]. In a recent study it was shown that *Streptococcus pneumoniae* and *Haemophilus influenzae* undergo apoptosis-like death and displayed its characteristic morphological as well as biochemical features when treated with a human milk complex of alpha-lactalbumin and oleic acid (termed HAMLET) [39]. *E. coli* has been reported to exhibit characteristic markers of apoptosis including DNA fragmentation and phosphatidylserine exposure when subjected to cell death triggering stress like antibiotic treatment [16]. Interestingly, *E. coli* RecA was shown to bind a peptide sequence that serves as substrate for eukaryotic caspases [16]. The effect of gamma radiation stress has been well studied in a radioresistant bacterium *Deinococcus radiodurans* [9]. Many studies have been carried out on repair of DNA damage caused by gamma radiation in *E. coli* [27]. The study discussed in this chapter focuses on biochemical and physiological events occurring in the bacterial cells undergoing gamma radiation induced death. Since eukaryotes are known to undergo radiation induced PCD involving caspase activation [4], it was interesting to investigate whether radiation induced cell death (RICD) in bacteria was programmed or not. To ascertain this, specific markers of PCD like caspase-3 activation, PARP activation and PS externalization which have been well established in bacteria were analyzed during the course of the study.

4.2 Materials and Methods

4.2.1 Bacterial strains and growth conditions

Xanthomonas campestris pv. *glycines* (Xcg) wild type (wt) cells and its PCD and caspase negative mutant, XcgM42 were grown in starch medium at 26 ± 2°C for 18 h (log phase) as described earlier [36]. *Bacillus subtilis* (ATCC6633), *Bordetella bronchiseptica* (NCIM 2267) and *Salmonella enterica* sv. Typhimurium were grown in Luria Broth (LB) medium on a rotary shaker (150 rpm) at 37± 2 ºC for 3-5 h. Inoculums used for growing these bacteria were taken from their active cultures.

4.2.2 Viable plate count determination

An aliquot (1 ml) of log phase grown bacterial culture was withdrawn and serially diluted using saline (0.85%) to achieve the cell density of ~10^6 cfu/ml. The cell suspension was irradiated at doses ranging from 0 to 1000 Gy in a Gamma Chamber (Co^{60} source, dose rate 5 Gy/min). The viable plate count was determined immediately after irradiation. In the studies involving caspase-3 inhibitor (Ac-DEVD-CMK, 40 µM), and PARP inhibitor (3-Aminobezamide, 500 µM) the culture was incubated with the inhibitor for 30 min before subjecting to irradiation.

4.2.3 Analysis of caspase-3-like activity

Caspase-3-like activity was assayed using a caspase-3 assay kit (BD Pharmingen, USA) as per the method described earlier in chapters 2 and 3 [36].

4.2.4 Western blotting

Level of biosynthesis of caspase-3-like protein was analyzed using SDS-PAGE and Western hybridization as described earlier in chapter 2 [36] using affinity-purified, biotin-conjugated, polyclonal rabbit anti-active human caspase-3 antibody.

Control (non-irradiated) as well as radiation exposed cell suspensions were incubated at 37°C for 1 h for caspase-3 analysis, 20 min for LexA analysis, later subjected to lysis by adding gel loading buffer (50 mM Tris-HCl, 100 mM DTT, 2% SDS, 0.1% bromophenol blue and 10% glycerol) and incubating at 95ºC for 10 min. Protein equivalent to 100 µg/ml was loaded in each lane and subjected to SDS-PAGE followed by Western blotting as described earlier [36]. Bacterial alkaline phosphatase was detected as a positive control using its antibody (Abcam, catalog no. ab7321) on a separate blot. The band intensity was measured using TLSee 2.0 (Demo version) software. Protein content was estimated by modified Lowry's method [40].

4.2.5 AnnexinV-FITC labelling

An aliquot (1 ml) of log phase cells containing ~10^6cfu/ml was washed twice with PBS (10 mM, pH 7.5) and resuspended in saline (0.85%). The cells were then irradiated at their respective D_{10} dose. Cell suspension was centrifuged at 12,500 x g for 2 min and the pellet was resuspended in 250 µl PBS (10 mM, pH 7.5) and later kept at ambient temperature (26 ± 2º C) for 60 min. AnnexinV-FITC staining was carried out using the AnnexinV-FITC apoptosis detection kit (B D Pharmingen). For each analysis ~ 10^5 cells were analyzed by flow cytometry system (Partec CyFlow space, Germany).

4.2.6 TUNEL (Terminal deoxynucleotidyl transferase dUTP nick end labelling) assay

TUNEL assay was performed according to the manufacturer's guidelines (APO-Direct Kit, BD Pharmingen). Briefly, 1 ml aliquot of log phase cells containing ~10^6 cfu/ml were washed twice with PBS and resuspended in saline (0.85%). The cells were then irradiated at respective D_{10} doses. Later the samples were centrifuged at 12,500 x g for 10 min, the cell pellet was resuspended in 50 µl DNA labeling solution [reaction buffer (10 µl), Terminal deoxynucleotidyl transferase **(**TdT) enzyme (0.75 µl), FITC-dUTP (8 µl) and distilled water (32.25 µl)] and incubated for 60 min at 37 ºC in dark. After that 1ml rinse buffer was added and cell suspension was centrifuged at 12,500 x g for 10 min. This rinsing step was repeated once more. PI/RNase staining solution (500 µl) was added and the samples were further incubated in dark for 30 min. For each analysis, 10^5 cells were analyzed by flow cytometry (Partec CyFlow space, Germany). Data was analyzed using FCS Express V4 software (demo version).

4.2.7 Cell filamentation assay

LB grown log phase *E. coli* cells (OD_{600nm} 0.5-0.6) were washed with PBS (10 mM, pH 7.5), resuspended in saline (0.85%) and exposed to radiation (90 Gy gamma or 12 sec UV exposure). The cells were centrifuged (12,500 x g, 10 min), added to fresh LB broth (20 ml) and incubated on a rotary shaker (150 rpm) at 37 ± 2ºC for 2 h. An aliquot (1ml) of culture (cell density~10^6 cfu/ml) was withdrawn and centrifuged at 12,500 x g for 10 min. The pellet was washed with 1ml saline (0.85%) and resuspended in 100 µl of the same. An aliquot was smeared on a glass slide, air dried, heat fixed, stained with crystal violet and examined under a microscope (Carl Zeiss, Germany) using oil immersion objective (100X).

4.2.8 Analysis of active caspase-3-like protein *in situ* by FITC-DEVD-FMK staining

The assay was carried out using caspase-3 detection kit (Catalog no. QIA91, Calbiochem) as described earlier in chapter 3. Briefly, *E. coli* cells were processed as mentioned above for cell filamentation assay. At the end of the 1h incubation on rotary shaker, an aliquot (1ml) of culture (cell density ~10^6 cfu/ml) was withdrawn and centrifuged at 12,500 x g for 10 min. The pellet was washed with 1ml saline (0.85%) and resuspended in 300 µl PBS. To this cell suspension 1 µl of FITC-DEVD-FMK was added and incubated at room temperature for 30 min in dark. After that, the cells were centrifuged at 12,500 x g for 5 min and supernatant was discarded. The cells were washed twice with wash buffer and resuspended in 200 µl of the same. An aliquot (10 µl) was smeared on a glass slide, air dried and examined under a fluorescent microscope (Carl Zeiss, Germany) using oil immersion objective (100x) and filter set 9 (Carl Zeiss, Germany; Excitation: 450 nm; emission: 515 nm).

4.2.9 SIVET (Selectable In Vivo Expression Technology) assay

SIVET assay was performed as mentioned earlier [31]. Briefly, an aliquot (50 µl) of log phase *E. coli* strain SG104 was exposed to UV for 12 sec in dark. This cell suspension was inoculated in LB and grown on a rotary shaker (150 rpm) at 37± 2 ºC for 16 h. An aliquot of this overnight culture was withdrawn and total plate count was determined on LA containing kanamycin (20 µg/ml) and ampicillin (30 µg/ml) and SIVET induced cells were determined on LA plates containing kanamycin (20 µg/ml), ampicillin (30 µg/ml) and chroramphenicol (10 µg/ml). The SIVET induction frequency was calculated as the ratio of SIVET induced cells (Kan^r Amp^r Cm^r) to total viable cells (Kan^r Amp^r).

4.2.10 rpoB/rif^r assay forward mutation assay

This assay was performed as mentioned earlier [41]. Briefly, an aliquot (50 µl) of log phase *E. coli* MG1655 culture was exposed to either UV (for 12 sec in dark) or gamma radiation (90 Gy). This cell suspension was inoculated in LB and grown on a rotary shaker (150 rpm) at 37± 2 ºC for 16 h in dark. An aliquot of this overnight culture was withdrawn and standard plate count was determined using LA with or without rifampicin (100 µg/ml). Cell count on rifampicin plates indicated the mutants whereas that on LA plates indicated total viable count. The mutation frequency was calculated as the ratio of number of mutant/100 million cells.

4.2.11 Bioinformatic Analysis

Multiple sequence alignment of proteins containing caspase-like domain was performed using ClustalW2 - multiple sequence alignment tool of EMBL (European Molecular Biology Laboratory). The protein sequences for this purpose were taken from NCBI (National Center for Biotechnology Information) protein database.

4.3 Results and Discussion

4.3.1 Section I

4.3.1.1 Effect of gamma radiation on bacteria

A radiation dose dependent effect on cell killing was observed in the bacteria investigated in this study i.e. *Xanthomonas campestris* pv. *glycines* (Xcg), *Escherichia coli*, *Salmonella enterica* sv. Typhimurium, *Bordetella bronchiseptica* and *Bacillus subtilis*. Decimal reduction dose or the D_{10} value, (the dose required to kill 90% of the cell population) for these bacteria was determined by irradiating cells at different doses between 0 - 1 kGy [42].

The D_{10} in the given experimental set up was found to be as follows: 330 Gy for *B. subtilis*, 318 Gy for *B. bronchiseptica*, 180 Gy for *E.coli*, 148 Gy for *S. enterica* sv. Typhimurium, and 66 Gy for Xcg (Fig. 4.7). The comparatively lower D_{10} of Xcg indicated that it is more radiation sensitive than other bacteria investigated in the current study (Fig. 4.7). The D_{10} for XcgM42, a caspase and PCD negative mutant of *X. campestris* pv. *glycines* (Fig. 4.8) was found to be 77 Gy which was 17% higher than its wild type counterpart. An increase in D_{10} or in other words radio-resistance in XcgM42 indicated that probably caspase mediated PCD plays a significant role in radiation induced cell death (RICD) in this organism. Although possible existence of caspase/metacaspase like protein has been reported from different bacterial species by many authors, still the exact sequence of gene and protein has not been resolved [43–46].

Figure 4.7

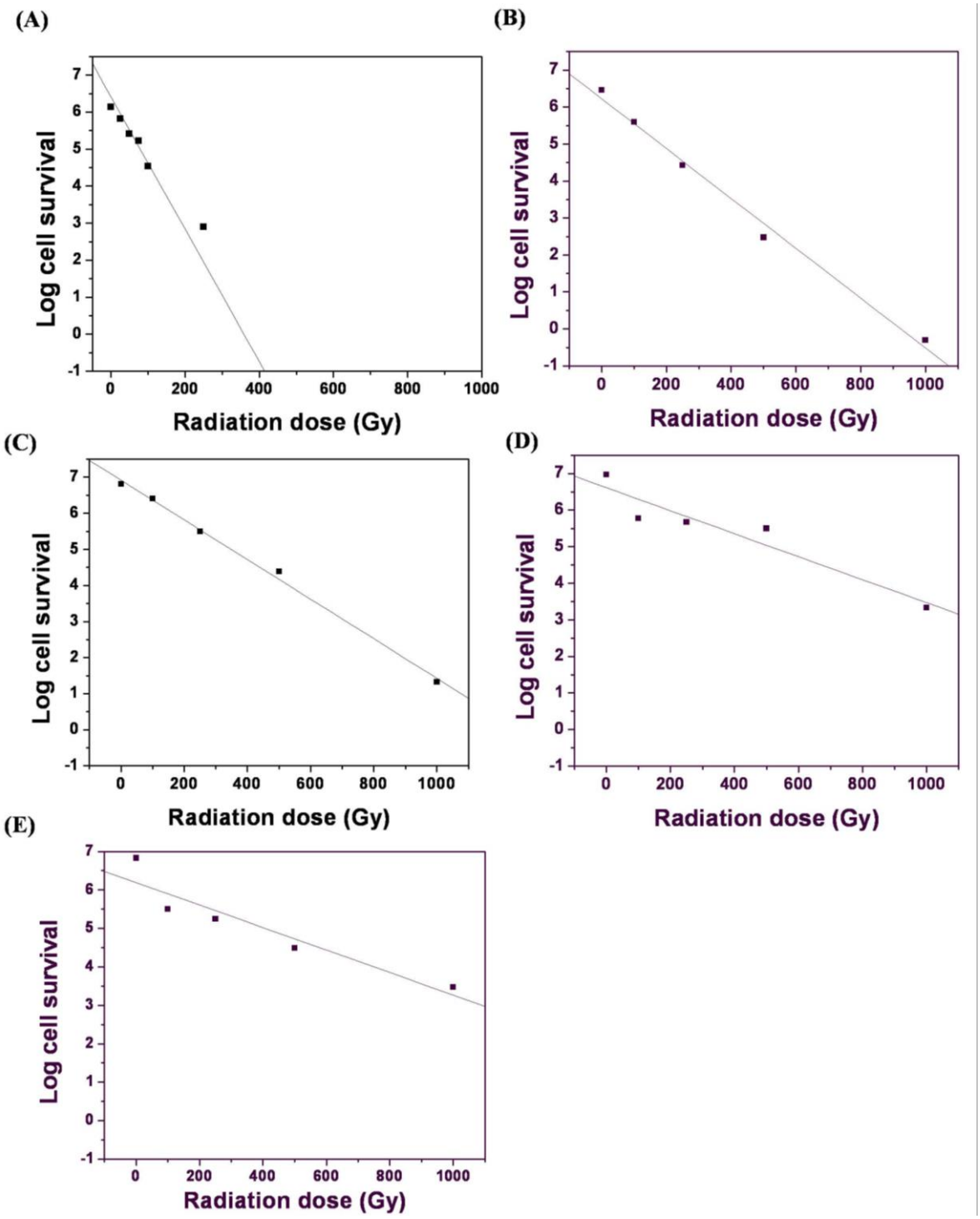

Fig.4.7: Effect of radiation treatment (0-1000 Gy) on the survival of bacteria (A) *Xanthomonas campestris* pv. *glycines* (Xcg wild type); **(B)** *Salmonella enterica* sv. Typhimurium; **(C)** *E. coli;* **(D)** *Bordetella bronchiseptica*; **(E)** *Bacillus subtilis.*

Figure 4.8

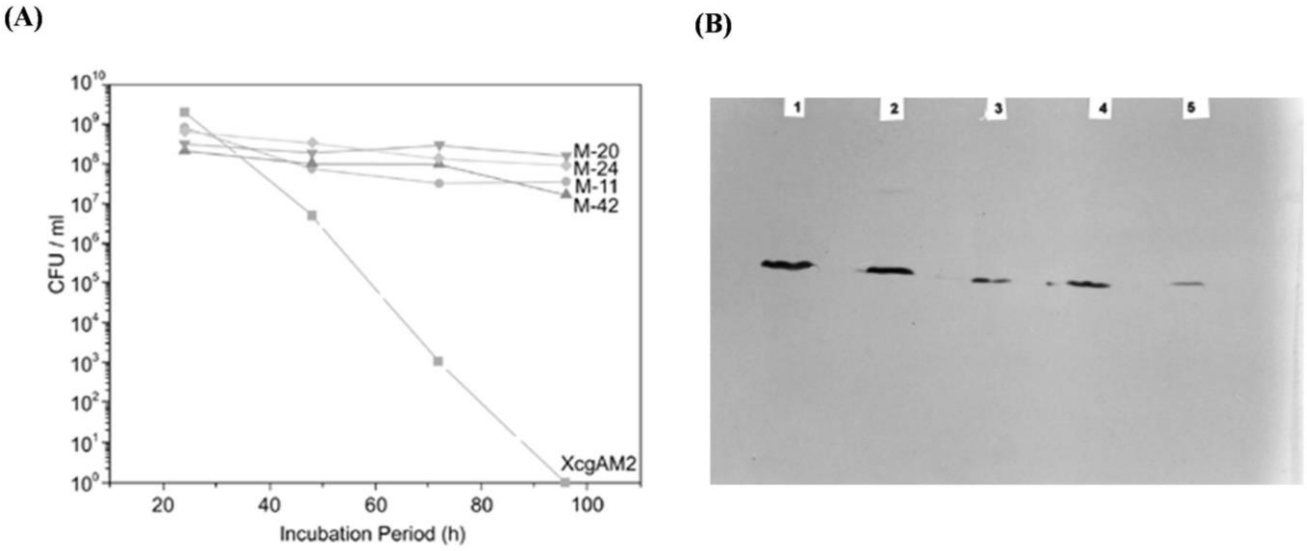

Reference: Gautam and Sharma, 2002 [36]

Fig.4.8: Growth profile and status of caspase-3-like protein in XcgAM2 (wt) and its mutants: (A) Viable cell number of XcgAM2 and its mutants (M11, M20, M24 and M42) in post-exponential phase when the organisms were grown in LB medium; **(B)** Western blot hybridization showing the presence of caspase-3-like protein in LB-grown XcgAM2 cells (lane 1) and mutants M11 (lane 2), M42 (lane 3), M20 (lane 4) and M24 (lane 5). The cells were harvested after 22 h of growth and the cell number from all the cultures was normalized to about 10^8 cells ml^{-1} to obtain similar protein concentrations. The band intensity of caspase protein in different lanes was: lane1, 786; lane 2, 674; lane 3, 480; lane 4, 577; and lane 5, 473. The band intensity (optical density × mm) of caspase-3-like protein from a Western blot was determined using a gel documentation system [36].

4.3.1.2 Radiation exposure resulted in activation of caspase-3-like protein in bacteria

Activation of caspase-3 enzyme is an important marker of PCD [4]. Radiation exposure was found to significantly induce caspase-3-like activity (CLA) in these bacteria (Fig.4.9A). CLA was negligible in all the non-irradiated control samples. However, it was found to increase by around four fold in irradiated *E. coli*, *S. enterica* sv. Typhimurium cells, 2.7 fold in *B. subtilis* and *B. bronchiseptica* and 2.3 fold in *X. campestris.* The current study is the first report indicating the presence of CLA in *S. enterica* sv. Typhimurium and *B. bronchiseptica*. Moreover, the CLA dropped significantly in the cells pre-incubated with a cell permeable caspase-3 inhibitor, Ac-DEVD-CMK which is a water soluble chloromethylketone derivative. This strongly correlated with the increase in cell survival found in these bacteria when exposed to radiation in the presence of caspase-3 inhibitor (Fig.4.10). This clearly implies that RICD in bacteria was caspase dependent. Similarly, induction of CLA has also been reported in *Bacillus subtilis* cells under shear stress eventually resulting in cell death [44]. However, no earlier report exists suggesting induction of caspase-like protein in radiation exposed bacterial cells.

On the other hand, no significant increase in caspase-3-like protein biosynthesis was observed in these bacteria after gamma radiation exposure, as analyzed by immunoblotting using polyclonal anti-caspase-3 antibody (Fig.4.9B). The molecular weight of bacterial caspase-3-like protein (BCLP) which was detected by the caspase-3 antibody varied in different bacterial strains as indicated by immunoblotting. BCLP was found to be smaller in molecular weight (~ 15 kDa) in *S. enterica* sv. Typhimurium and *E.coli* (Fig 4.9B, lanes 8-11). The molecular weight was significantly higher (~ 150 kDa) in *B. subtilis* and *B. bronchiseptica* (Fig 4.9B, lanes 2-5) and moderate (~ 90 kDa) in *X. campestris* (Fig 4.9B,

lanes 6 and 7). The presence of caspase-3-like protein in a bacterial system was reported for the first time from this laboratory in different *X. campestris* strains [36] (Fig 4.8) and later in *B. subtilis* by other authors [44]. In the case of mammalian system caspase-3 zymogen (32 kDa) has been found to cleave into 17 and 12 kDa subunits upon activation that can be detected in a western blot [47]. As bacterial caspase gene has not been characterized yet, the enzyme activity was used as a measure of its induction.

Figure 4.9

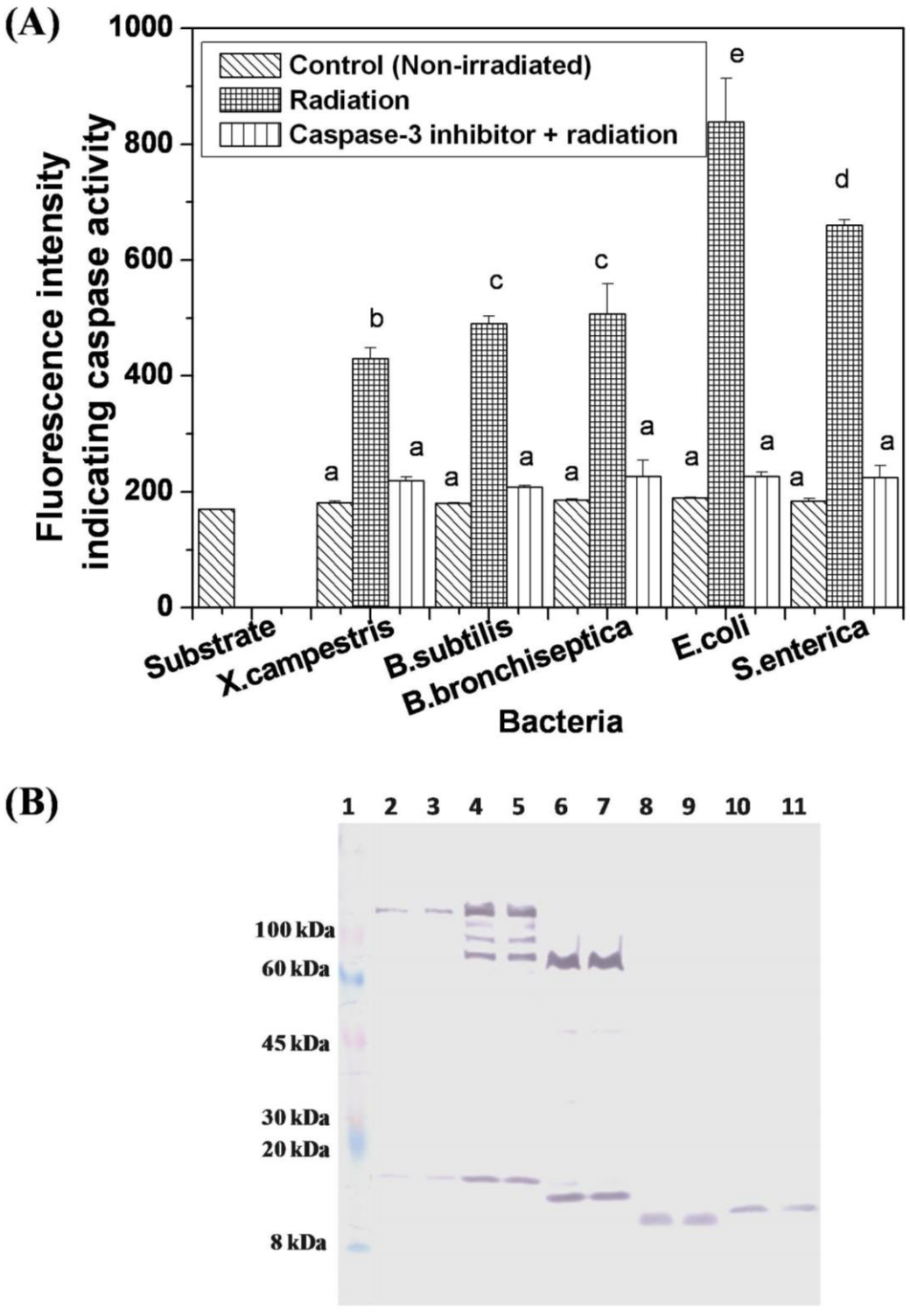

Fig.4.9. Status of caspase-3-like enzyme in radiation exposed bacterial cells (A) Caspase-3-like enzyme activity in radiation treated (at respective D_{10}) bacterial cells in the presence

and absence of caspase-3 inhibitor. The different letter on bars indicates that the means are significantly different at $p<0.05$; **(B)** Western blot hybridization indicating caspase-3-like protein status in different bacteria (lane 1: colour protein molecular weight marker; lane 2: *B. bronchiseptica* cells – non-irradiated; lane 3: *B. bronchiseptica* cells – irradiated at one D_{10}; lane 4: *B. subtilis* – non-irradiated; lane 5: *B. subtilis* – irradiated; lane 6: *X. campestris* – non-irradiated; lane 7: *X. campestris* – irradiated; lane 8: *S.* Typhimurium – non-irradiated; lane 9: *S.* Typhimurium – irradiated, lane 10: *E. coli* - non-irradiated; lane 11: *E. coli*- irradiated. All the samples have been irradiated at one D_{10} dose).

4.3.1.3 Inhibition of radiation induced cell death (RICD) by caspase-3 inhibitor

Several small peptide inhibitors mimicking the recognition sequence of caspases irreversibly alkylate the cysteine residue in the active site of caspase and irreversibly inactivate it [48]. Hence, the effect of an irreversible caspase-3 inhibitor on the survival of radiation exposed bacterial population was investigated. Interestingly, the cell survival in all these bacteria was found to improve remarkably when cells were incubated for 30 min before radiation exposure (at their respective D_{10} values) with the caspase-3 inhibitor (Fig. 4.10). This resulted in two fold increase in survival in *S. enterica* sv. Typhimurium and *B. subtilis* cells and a threefold increase in *B. bronchiseptica* and *X. campestris.* Unlike its wild type counterpart, no increase in cell survival of radiation exposed XcgM42 cultures was observed even after pre-incubation with caspase-3 inhibitor. There are similar reports of reversal of PCD induced by radiation or other stress in eukaryotic cells and thymocytes in the presence of peptide based caspase inhibitors [49]. Caspase has also been reported to be activated upon radiation exposure in other systems like neural cell precursors and HeLa cells [50,51]. Probably, a fraction of the dying population undergoes caspase dependent cell death and the rest die by some other

mechanism like necrosis due to acute cellular damage as in none of the cases complete inhibition of radiation induced bacterial cell death was observed in the presence of caspase-3 inhibitor.

Figure 4.10

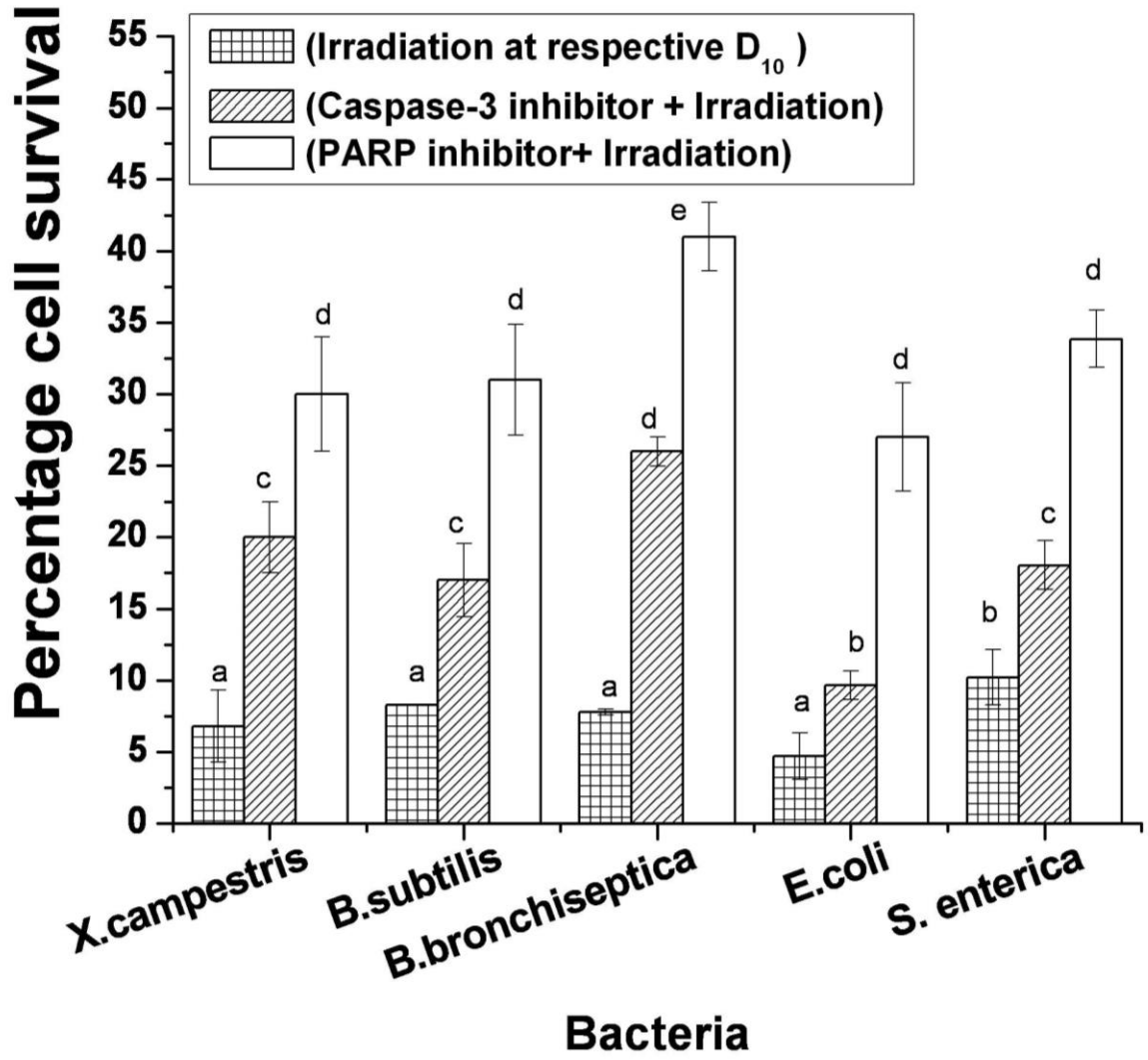

Fig.4.10: Rescue of bacterial cells from radiation induced death by inhibitors of caspase-3 and PARP. The different letter on bars indicates that the means are significantly different at $p<0.05$.

4.3.1.4 Inhibition of PARP-like protein by its cell permeable inhibitor protects bacteria from radiation induced death

Poly (ADP-ribose) polymerase (PARP) is reported to be involved in DNA repair and PCD [21]. It catalyzes the cleavage of NAD^+ into ADP and ADP-ribose and attaches several molecules of the latter to the target protein in a process called poly ADP-ribosylation. PARP is activated by DNA breaks, and can deplete NAD^+ and ATP of a cell in an attempt to repair the damaged DNA. ATP depletion in a cell could lead to necrosis. Presence of PARP inhibitor, 3-Aminobenzamide (3-ABA), was found to offer varying degrees of protection against RICD in these bacteria (Fig.4.10). Cell survival increased by three fold in *S. enterica* sv. Typhimurium, four fold in *B. subtilis* and *X. campestris*, five fold in *B. bronchiseptica* cells as well as by two fold in XcgM42 when these cells were pre-incubated with PARP inhibitor for 30 min and later irradiated in its presence. Increased cell survival in the presence of PARP inhibitor in caspase and PCD negative mutant, XcgM42, indicate that the observed cell death is not due to specific inhibition of PCD, else it could be due to some other some other reason such as restoration of energy pool (NADP is conserved if PARP is inhibited).

4.3.1.5 Phosphatidylserine externalization in radiation treated cells

Phosphatidylserine (PS) belongs to a class of acidic phospholipids normally found on the internal leaflet of lipid bilayer [52]. PS externalization serves as a marker of apoptosis and is a downstream event of caspase activation. PS externalization was observed by annexin V labeling and FACS analysis in radiation exposed bacterial cultures. The extent of PS externalization increased by around 1.5-2.5 fold in radiation exposed cultures of *S. enterica* sv. Typhimurium, *B. bronchiseptica*, *B. subtilis* and *X. campestris* (Fig 4.11 A-E middle panels). PS externalization dropped significantly in the presence of caspase-3 inhibitor (Fig.

4.11 A-E top panels) which was added 30 min prior to radiation exposure and was similar to that found in control non-irradiated cells (Fig. 4.11 A-E bottom panels).

Figure 4.11

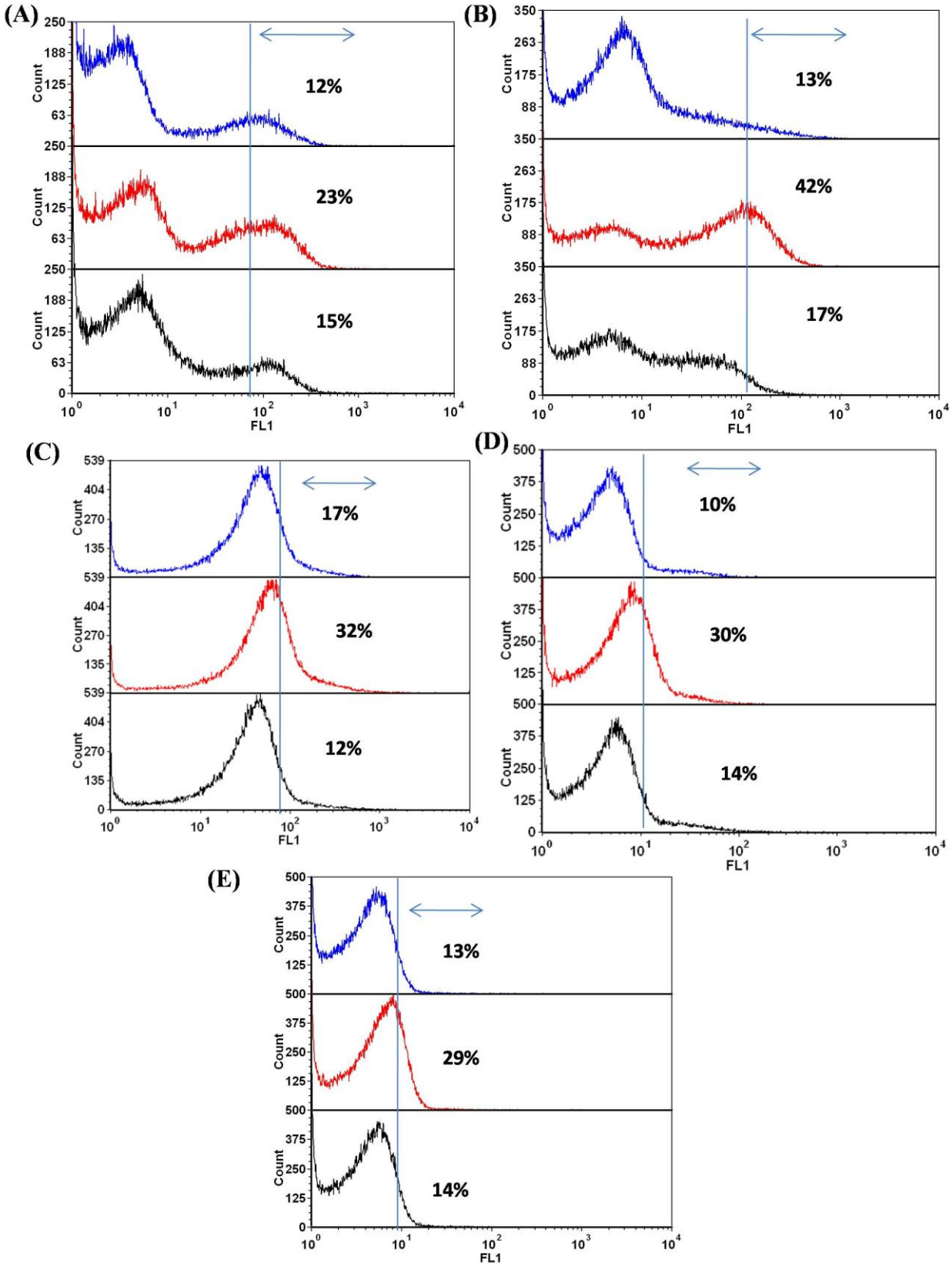

Fig.4.11: PS externalization detected by Annexin V staining in: (A) *Bacillus*; **(B)**

Bordetella; **(C)** *E. coli*; **(D)** *Salmonella*; **(E)** Xcg. Black curve: cells without radiation exposure; red curve – cells exposed to radiation at respective D_{10}, blue curve – cells exposed to radiation in the presence of caspase-3 inhibitor

4.3.1.6 2, 7' dichlorohydrofluorescein (H_2DCFDA) staining of bacterial cells

An increase in ROS level was observed when bacterial cells (*Xanthomonas campestris, Bacillus subtilis, Bordetella bronchiseptica* and *Salmonella enterica* sv. Typhimurium) were exposed to radiation (at half D_{10} dose) and stained by H_2DCFDA (2, 7' dichlorohydrofluorescein) (Fig. 4.12). This increase in intracellular level of ROS in radiation exposed bacterial cells was found to be least in the case of Xcg (~1.5 fold), around four fold in *S. enterica sv.* Typhimurium and *E. coli*, and highest in *B. bronchiseptica* (27 fold) followed by *B. subtilis* (25 fold). The observation indicates that Xcg is comparatively more sensitive to oxidative stress. This observation also explains the difference in D_{10} values of these bacteria. Unlike *B. subtilis* and *B. bronchiseptica* which have higher D_{10}, Xcg succumbs to death even at lower ROS level making it comparatively more radiosensitive.

Figure 4.12

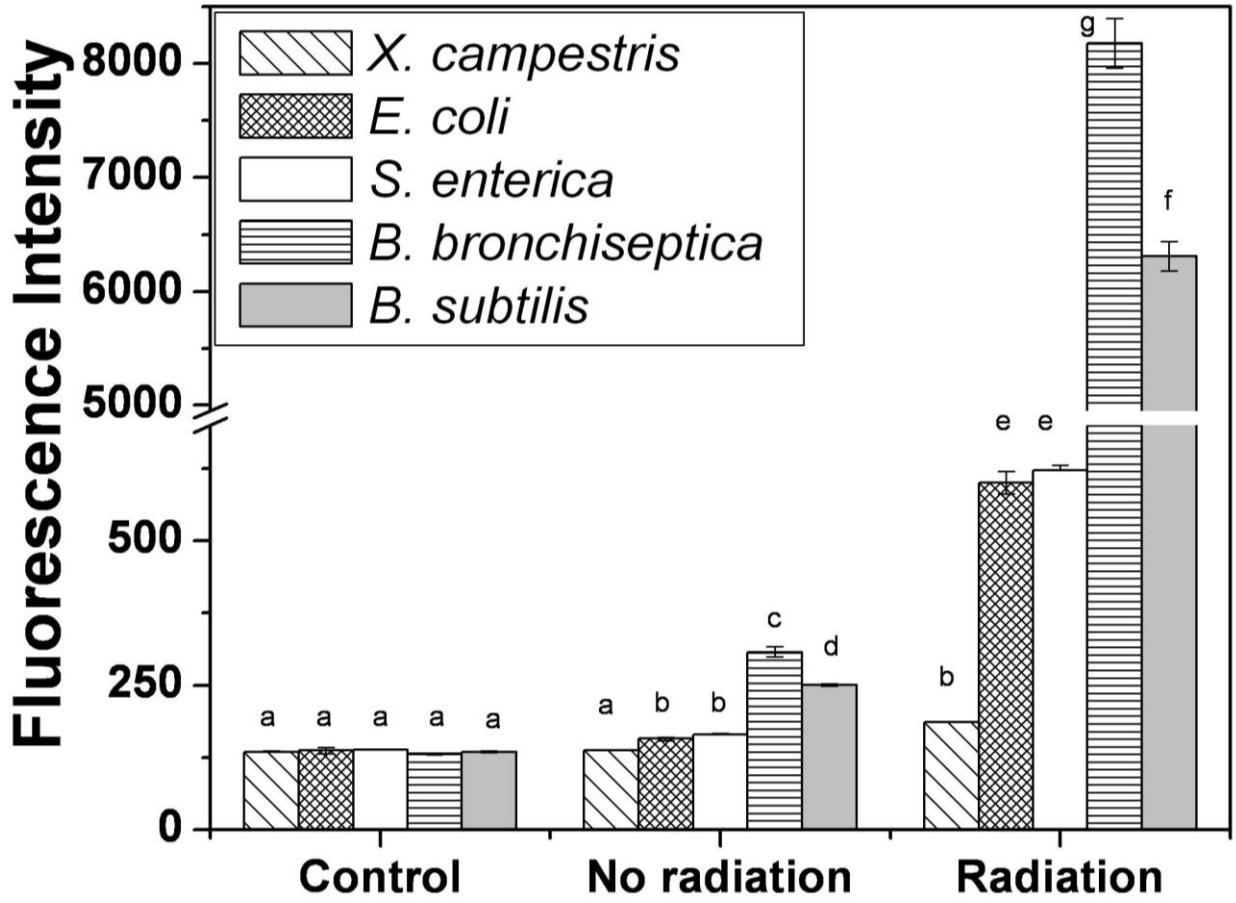

Fig 4.12: Status of reactive oxygen species (ROS) in different bacterial cells upon gamma radiation treatment. The different letter on bars indicates that the means are significantly different at $p<0.05$.

4.3.2 Section II

4.3.2.1 Inhibition of radiation induced SOS response by caspase-3 inhibitor

Radiation is also known to induce SOS response, an error prone DNA repair pathway, in many bacteria including *E. coli*. SOS repair system has been well studied in *E. coli* and is often considered as the DNA damage check point in bacteria [26]. In order to decipher the mechanism of caspase-3 inhibitor mediated cell rescue, its effect on SOS response was also

investigated. Since cell survival at D_{10} dose was rather low (~10%), the studies pertaining to SOS response were carried out at 1/2 D_{10} dose of *E. coli* (90 Gy). Radiation (90 Gy) exposed *E. coli* cells were found to display SOS specific phenotypic markers. These cells were found to undergo extensive cell filamentation due to induction of SOS regulon [53] (Table 4.1; Fig.4.13A and B). Interestingly, the presence of caspase-3 significantly reduced this cell filamentation (Table 4.1 and Fig. 4.13C).

Table 4.1: Extent of cell filamentation in radiation exposed cells and the effect of caspase-3 inhibitor

Treatment condition	Percentage cells with specified filament length (± standard deviation)			
	Non-filamented cells (< 2 µM)	**2-5 µM**	**6-15 µM**	**>15 µM**
Control (non-irradiated)	100	Nil	Nil	Nil
90 Gy	16 ± 4	46 ± 6.8	21 ± 2.6	17 ± 3.7
90 Gy + caspase-3 inhibitor	80 ± 7	17 ± 7	3 ± 0.9	Nil
UV (12 s)	3 ± 0.2	8 ± 0.5	45 ± 3.6	44 ± 2.9
UV (12 s) + caspase-3 inhibitor	13 ± 3	54 ± 2	29 ± 2	3.6 ± 0.4

The level of LexA, a constitutive repressor of SOS regulon, was found to decrease transiently in radiation exposed culture (Fig.4.13E, lane 2), but its level was found to be significantly restored in the presence of caspase-3 inhibitor. The LexA band intensity compared to control (non-irradiated culture) was 9 and 41%, respectively, in the absence and presence of the

caspase-3 inhibitor (Fig.4.13E, lanes 2 and 3 respectively). These findings suggested the existence of interplay between caspase dependent cell death and SOS pathway in bacteria.

Besides caspase-3 inhibitor, an endonuclease inhibitor, aurintricarboxylic acid (ATA), was also found to decrease both the filamentation frequency as well as the length of filaments in irradiated (90 Gy) *E. coli* culture (Fig.4.13D). The presence of ATA was found to improve the survival in radiation exposed *E. coli* cells. The findings suggested that these inhibitors decrease the DNA damage caused by some unknown cellular factor(s) after radiation exposure as confirmed by TUNEL assay (Fig.4.13F). It has been reported earlier in eukaryotes that during PCD, activated caspase-3 degrade ICAD (inhibitor of caspase activated DNAses) leading to the activation of CAD (caspase activated DNAses) which causes DNA fragmentation [4]. In view of the current findings, it is suggested that a similar signalling cascade is perhaps involved during PCD in bacteria. Inhibition of cell death as well as SOS response in radiation exposed *E. coli* culture by inhibitors of the two enzymes-caspase and endonuclease imply the existence of a mechanism analogous to eukaryotes.

SOS repair is induced in response to DNA damage and since caspase-3 inhibitor was observed to decrease SOS induction, the extent of DNA damage in cells irradiated in its presence was monitored by Fluorescence Activated Cell Sorter (FACS) based TUNEL (Terminal deoxynucleotidyl transferase dUTP nick end labeling) assay. This assay has been long used to detect DNA fragmentation occurring during apoptosis [54]. It is based on the extension of DNA nicks by the enzyme terminal deoxynucleotidyl transferase. In doing so this enzyme adds dUTPs tagged with a fluorophore, fluorescein isothiocyanate (FITC). The proportion of dUTP-FITC labelled cells after irradiating at 90 Gy increased from 12 to 36% as compared to non-irradiated control cells (Fig. 4.13F). However, a 46% decrease in DNA

fragmentation was observed in the cells irradiated in the presence of caspase-3 inhibitor as compared to those irradiated in its absence (Fig. 4.13F).

Figure 4.13

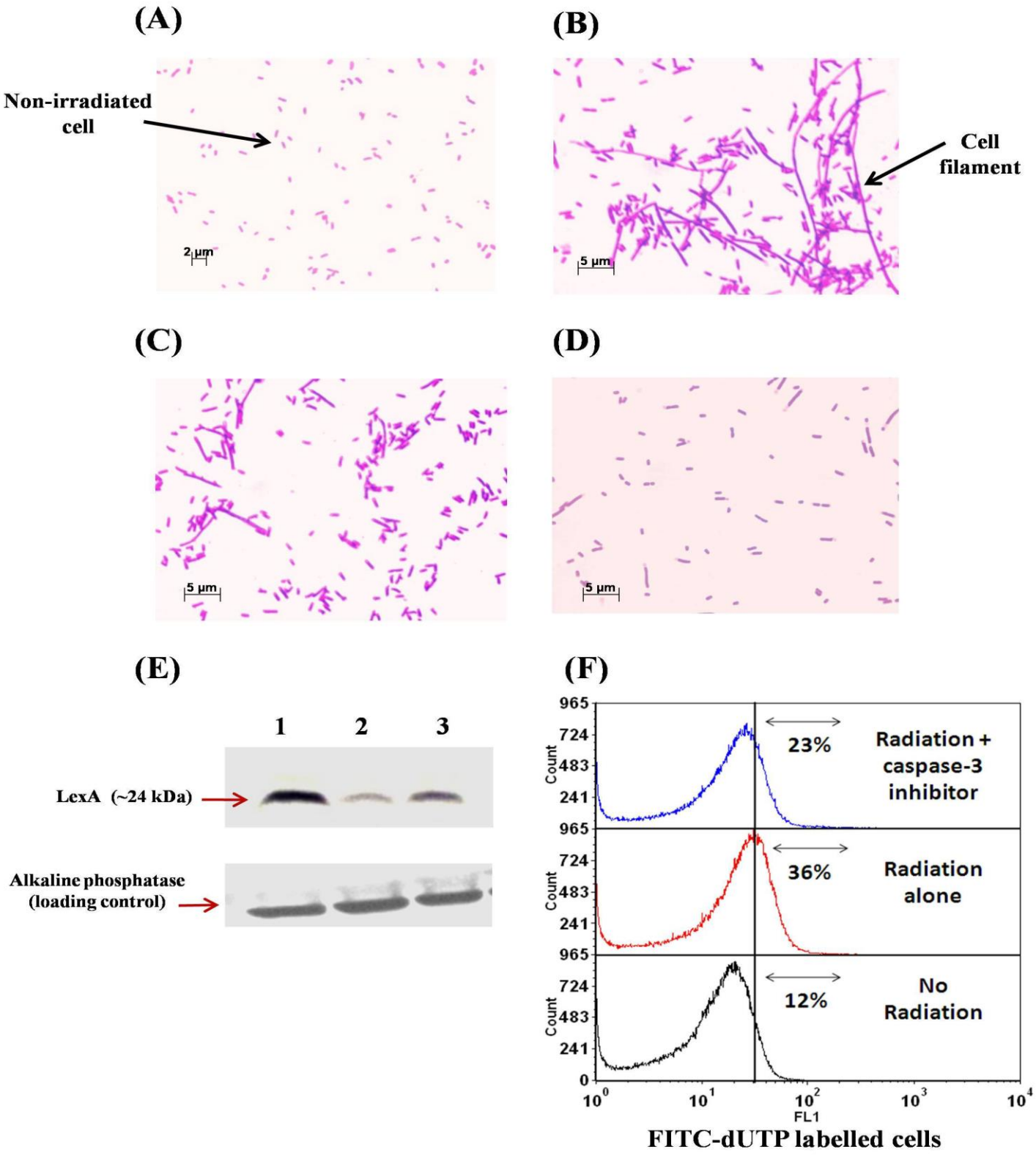
(A)
Non-irradiated cell
2 µm
(B)
Cell filament
5 µm
(C)
5 µm
(D)
5 µm
(E)
1
2
3
LexA (~24 kDa)
Alkaline phosphatase (loading control)
(F)
Count
965
724
483
241
0
23%
Radiation + caspase-3 inhibitor
36%
Radiation alone
12%
No Radiation
10^0
10^1
10^2
10^3
10^4
FL1
FITC-dUTP labelled cells

Fig. 4.13: Status of SOS induction in radiation exposed *E. coli* cells: Cell filamentation in **(A)** Non- irradiated cells; **(B)** cells irradiated at 90 Gy; **(C)** cells irradiated in presence of caspase-3 inhibitor (40 µM); **(D)** cells irradiated in the presence of endonuclease inhibitor (aurintricarboxylic acid, 30 µM); **(E)** Immunoblot using anti-LexA antibody indicating inhibition of LexA degradation in radiation exposed (90 Gy) culture in the presence of caspase-3 inhibitor (40 µM) {lane 1: non irradiated cells; lane 2: irradiated cells (90 Gy); lane 3: cells irradiated in the presence of caspase-3 inhibitor (40 µM)}. Alkaline phosphatase served as loading control and was detected using anti-bacterial alkaline phosphatase antibody. **(F)** TUNEL assay indicating DNA fragmentation. The gated region (represented by the arrow) depicts the area under the histogram and indicates the percentage of cells labeled by FITC-dUTP which implies DNA damage.

4.3.2.2 Effect of UV exposure on *E. coli* cells

4.3.2.2.1 Phenotypic changes: Cell filamentation

UV exposed (6-12 sec) *E. coli* cells exhibited filamentation which was found to be inhibited by the caspase-3 inhibitor (Fig.4.14 and Table 4.1). UV exposure of *E. coli* was found to induce caspase-3-like activity as well. Similar observations were also noticed when the cells were exposed to gamma radiation (90 Gy) (Fig.4.13). Cell filamentation has been reported to be a phenotypic marker of SOS [53,55].

Figure 4.14

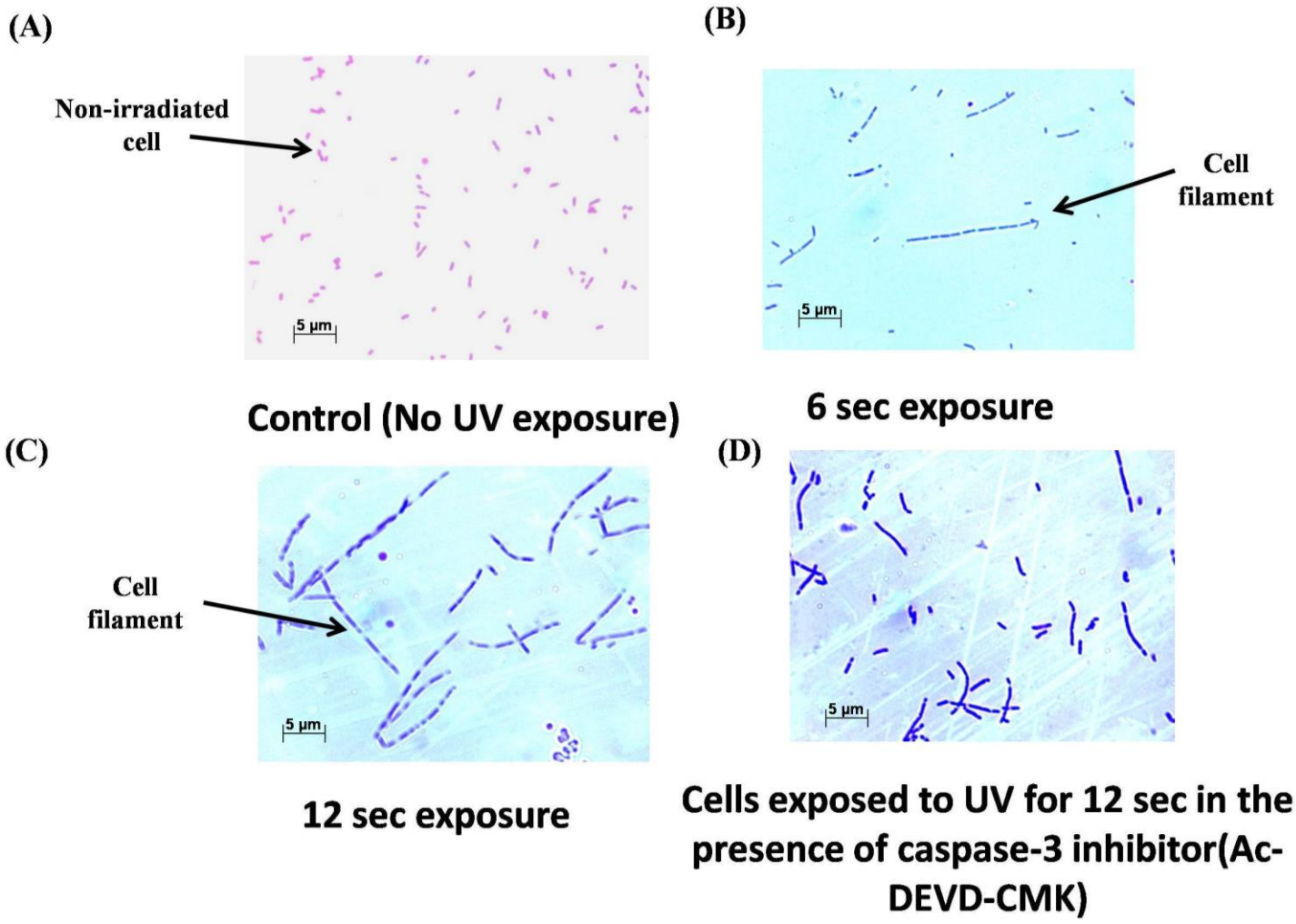

Fig.4.14: Cell filamentation in UV radiation exposed cells: status of cell filamentation in **(A)** Non- irradiated cells; **(B)** cells irradiated for 6 sec; **(C)** cells irradiated for 12 sec; **(D)** cells irradiated in presence of caspase-3 inhibitor (40 µM) for 12 sec.

4.3.2.2.2 SIVET Assay

The SIVET induction frequency (calculated as the ratio of SIVET induced cells to total viable cells) increased around tenfold in UV exposed (12 sec) cultures (Fig.4.15). The induction frequency was found to decrease significantly in the cells pre-incubated with caspase-3

inhibitor (it dropped to 51% from 80% in the presence of caspase-3 inhibitor) (Fig. 4.15). The results indicated a possible linkage of cell death with activation of caspase-3-like protein in *E. coli*.

Figure 4.15

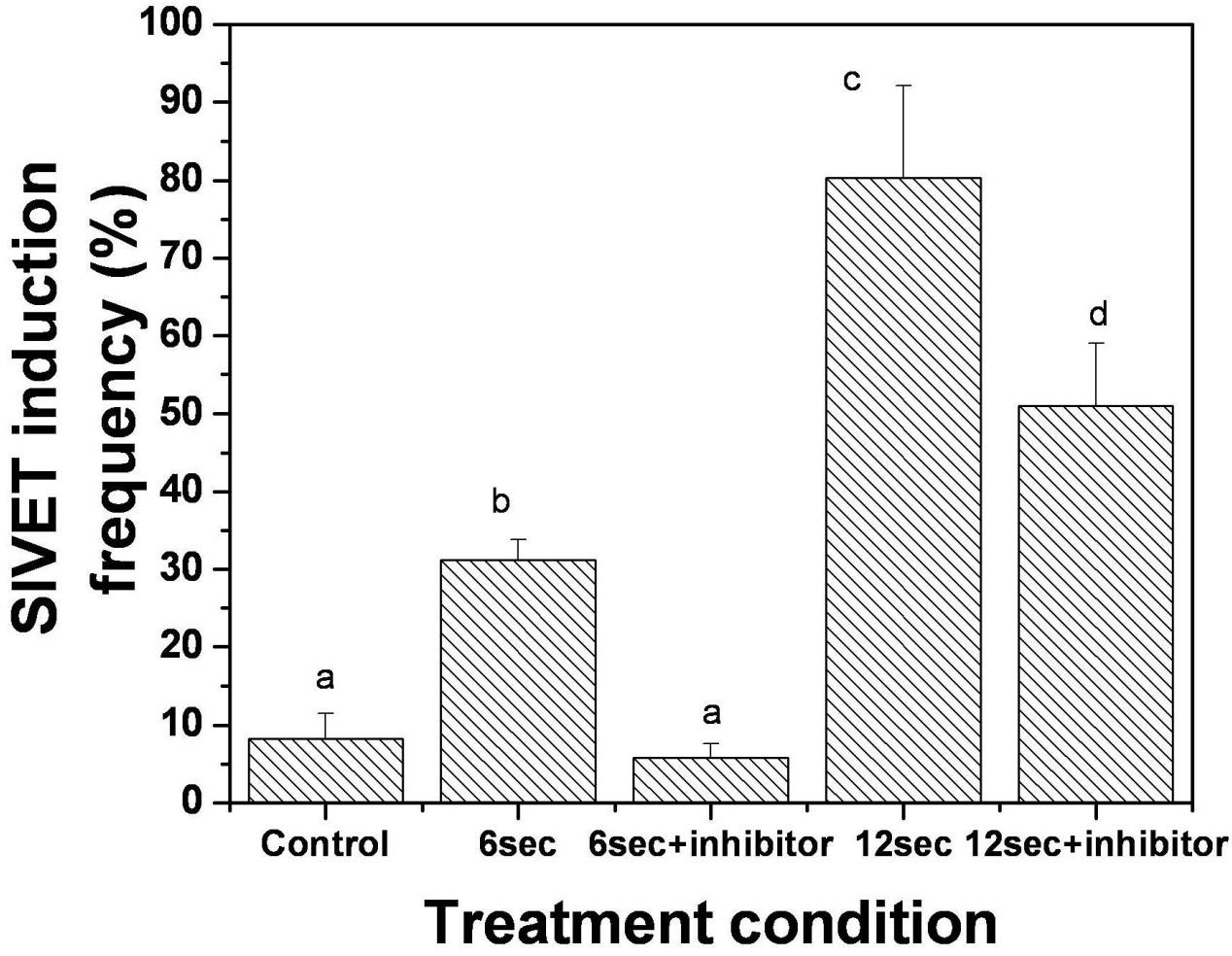

Fig.4.15: SIVET induction frequency in *E. coli* SG104 after UV exposure. The different letter on bars indicates that the means are significantly different at $p<0.05$.

4.3.2.2.3 Mutation frequency in E. coli wt, ΔrecA and ΔumuD strains after gamma/ UV radiation exposure

The rpoB (RNA polymerase)/Rif^r (rifampicin resistance) based assay was carried out to calculate the mutation frequency of radiation exposed cells. The number of Rif^r mutants/100 million cells was found to be 52 and 391 in case of *E.coli* MG1655 culture exposed to 90 Gy dose of gamma radiation and 12 sec UV exposure (lamp power: 8W; intensity: 220 μWcm^{-2}), respectively (Table 4.1). On the contrary the number of Rif^r cells dropped significantly to 4 and 18 in *E. coli* Δ*recA* and Δ*umuD* strains exposed to 90 Gy radiation (Table 4.2). *E. coli* Δ*recA* cells were unable to survive after UV exposure (12 sec). Increase in the number of Rif^r mutants in UV exposed *E. coli* cells could be possibly contributed by different molecular events including the error prone pathway of SOS response.

Table 4.2: Mutation frequency in *E. coli* strains after gamma/ UV radiation exposure

Treatment condition	Number of Rif^r mutants/100 million cells
E. coli wt (control; no exposure)	1.7 ± 1
E. coli wt + 90 Gy radiation	52 ± 11
E. coli Δ*umuD* + 90 Gy radiation	14 ± 3
E. coli Δ*umuD* (control; non-irradiated)	Nil
E. coli wt + UV exposure (12 sec)	391 ± 27

4.3.2.2.4 Status of caspase 3-like activity (CLA) and active caspase-3-like protein in situ by FITC-DEVD-FMK staining

The caspase-3-like activity (CLA) was found to increase in a dose dependent manner in UV exposed *E. coli* cells and was 1.7 fold higher in UV exposed (12 sec) cells than control (non treated) cells (Fig. 4.16A). FITC-DEVD-FMK, a fluorescent dye tagged with an irreversible caspase-3 inhibitor (DEVD-FMK) was also used for *in situ* labelling of *E.coli* cells exposed to UV (12 sec) to detect active caspase-3-like enzyme. Bright fluorescent filaments were observed in *E. coli* cultures treated with UV indicating the presence of active caspase-3-like protein in these cells (Fig. 4.16B and C). Similar observation was recently reported in a separate study [16]. Three different populations of cells were observed when they were stained with both FITC-DEVD-FMK and Propidium iodide (PI) (Fig. 4.16 C). Some cells (~34%) had taken up only the former dye and fluoresced green indicating live cells with active caspase-3-like protein. Around 31% cells fluoresced red indicating dead population. Interestingly, a few cells (~ 35%) were observed to fluoresce both red (in the middle segment of the filament) and green (towards the ends of the filament), suggesting that the cell death had begun in such filaments.

Figure 4.16

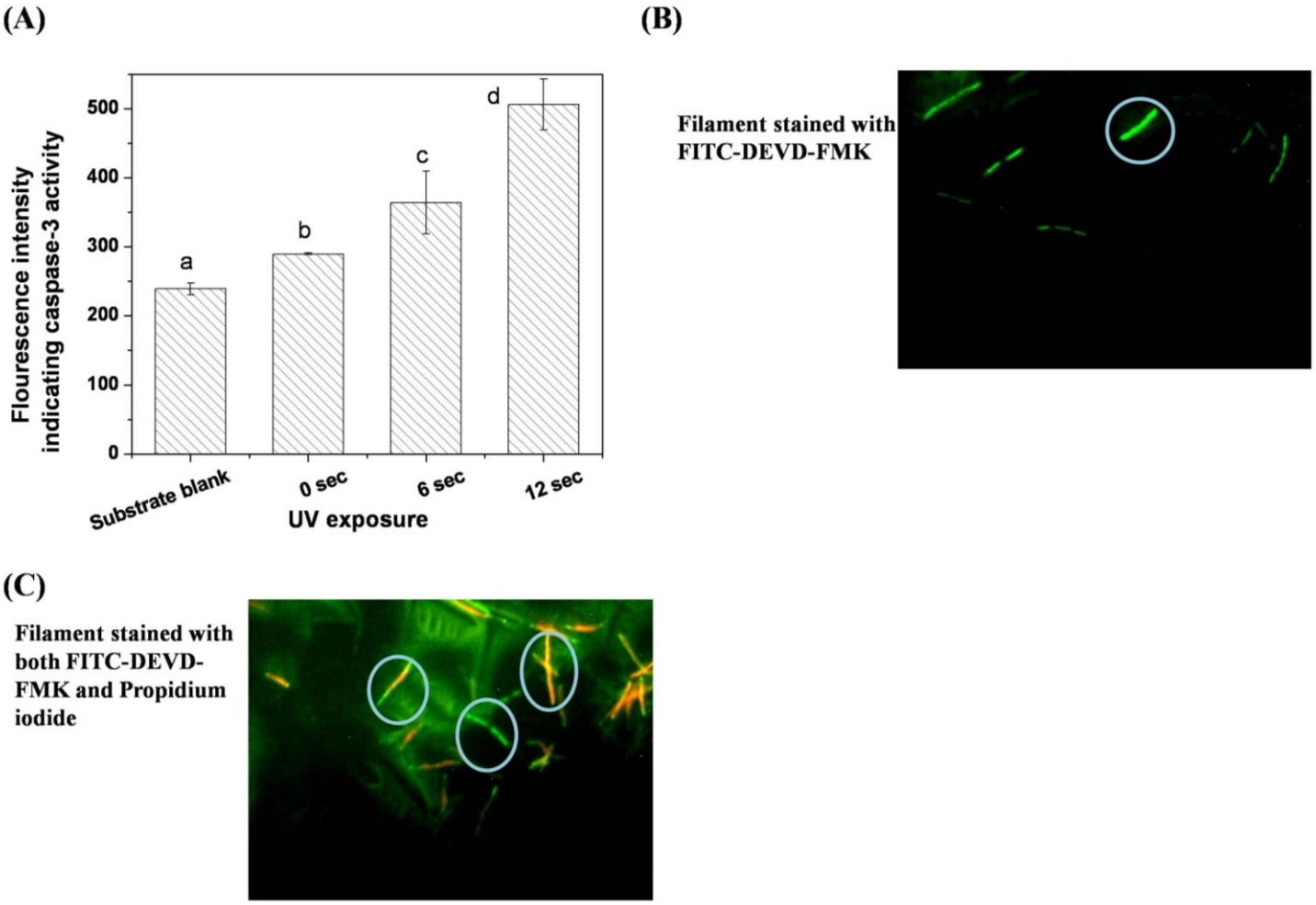

Fig.4.16: Caspase-3-like activity (CLA) in UV exposed cells: (A) Caspase-3-like activity assay in UV exposed cells. The different letter on bars indicates that the means are significantly different at $p<0.05$; **(B)** *in situ* staining of UV (12 sec) treated *E. coli* cells with fluorescent caspase-3 inhibitor (FITC-DEVD-FMK) and; **(C)** cells stained with FITC-DEVD-FMK and Propidium iodide (PI).

4.3.2.3 Phylogenetic analysis of caspase domain containing proteins in different bacteria

To the best of our knowledge, the current study reports for the first time the existence of radiation-induced caspase dependent programmed cell death in bacteria. Caspase-3 inhibitor was found to decrease SOS response in *E.* coli, the mechanism of which is still unclear. Findings indicated the presence of caspase-3 like protein in the bacteria investigated in this study. When a BLASTP search using *Aspergillus* metacaspase (accession no: EAL92173.1) as query sequence was performed, *E. coli* strains RN587 and TX1999 were found to have a caspase domain containing protein (EFZ73456.1 and EGX17538 respectively) with significant E (expect) value ($4x10^{-6}$ to $4x10^{-4}$). Further bioinformatic analysis showed the presence of several caspase domain containing proteins in microbes including *Xanthomonas campestris, Pseudomonas chlororaphis, Salmonella enterica, Bacillus subtilis, Beggiatoa, Colwellia psychrerythraea, Nostoc punctiforme* and *Vibrio parahaemolyticus.* Multiple sequence analysis indicated that most of these proteins are comparatively more closely related to *Aspergillus fumigatus* metacaspase than to human caspase-3 (Fig.4.17). Studying the mechanism of bacterial cell death would help in understanding the evolutionary linkage of this process and in devising possible strategies for controlling bacterial pathogenesis.

Figure 4.17

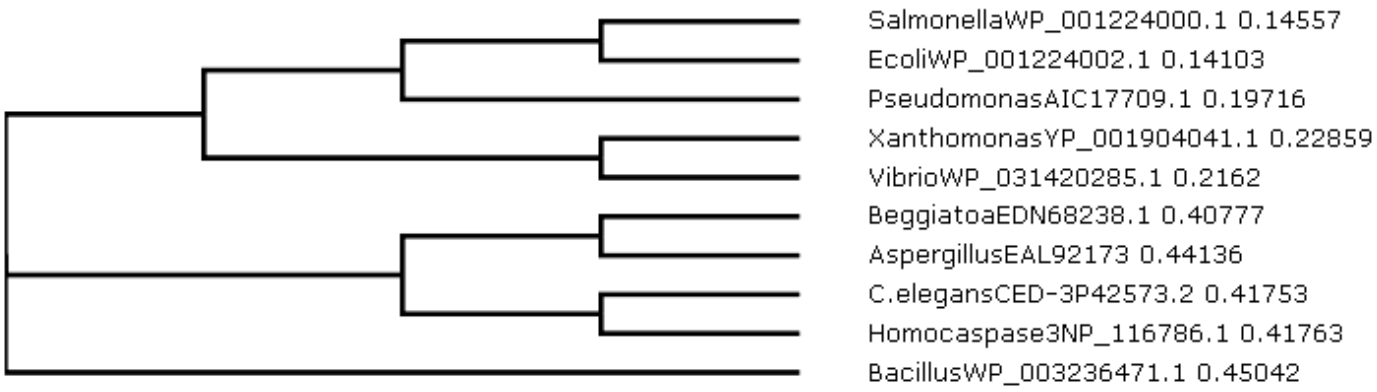

Fig.4.17: Evolutionary relationship between caspase domain containing proteins from different genera: Phylogram indicating evolutionary relatedness between *H. sapiens* caspase-3, *C. elegans* CED3, *Aspergillus* protein EAL92173, *Bacillus subtilis* protein WP_003236471.1, *E. coli* protein WP_001224002, *Salmonella eneterica* protein WP_001224000.1, *Pseudomonas chlororaphis* protein AIC17709, *Vibrio parahaemolyticus* protein WP_031420285, *Beggiatoa* EDN68238 and *Xanthomonas campestris* protein YP_001904041. The protein sequences were taken from NCBI protein database.

References

1. Sigler K, Chaloupka J, Brozmanova J, Stadler N, Hofer M (1999) Oxidative stress in microorganisms--I. Microbial vs. higher cells--damage and defenses in relation to cell aging and death. Folia Microbiol (Praha) 44: 587-624.

2. Sies H (1993) Strategies of antioxidant defense. Eur J Biochem 215: 213-219.

3. Nystrom T (2003) The free-radical hypothesis of aging goes prokaryotic. Cell Mol Life Sci 60: 1333-1341. 10.1007/s00018-003-2310-X [doi].

4. Elmore S (2007) Apoptosis: a review of programmed cell death. Toxicol Pathol 35: 495-516. 779478428 [pii];10.1080/01926230701320337 [doi].

5. Jordan BF, Sonveaux P (2012) Targeting tumor perfusion and oxygenation to improve the outcome of anticancer therapy. Front Pharmacol 3: 94. 10.3389/fphar.2012.00094 [doi].

6. Cooke MS, Mistry N, Ahmad J, Waller H, Langford L, Bevan RJ, Evans MD, Jones GD, Herbert KE, Griffiths HR, Lunec J (2003) Deoxycytidine glyoxal: lesion induction and evidence of repair following vitamin C supplementation in vivo. Free Radic Biol Med 34: 218-225. S0891584902012406 [pii].

7. Cabiscol E, Tamarit J, Ros J (2000) Oxidative stress in bacteria and protein damage by reactive oxygen species. Int Microbiol 3: 3-8.

8. Mimica-Dukic N, SN, Svircev E, Orcic D, Beara I, Lesjak M, Božin B (2012) The Effect of Plant Secondary Metabolites on Lipid Peroxidation and Eicosanoid Pathway. Lipid Peroxidation 193-210.

9. Daly MJ (2009) A new perspective on radiation resistance based on Deinococcus radiodurans. Nat Rev Microbiol 7: 237-245. nrmicro2073 [pii];10.1038/nrmicro2073 [doi].

10. Farr SB, Kogoma T (1991) Oxidative stress responses in Escherichia coli and Salmonella typhimurium. Microbiol Rev 55: 561-585.

11. Humphrey T (2004) Salmonella, stress responses and food safety. Nat Rev Microbiol 2: 504-509. 10.1038/nrmicro907 [doi];nrmicro907 [pii].

12. Zuber P (2009) Management of oxidative stress in Bacillus. Annu Rev Microbiol 63: 575-597. 10.1146/annurev.micro.091208.073241 [doi].

13. Mols M, Abee T (2011) Primary and secondary oxidative stress in Bacillus. Environ Microbiol 13: 1387-1394. 10.1111/j.1462-2920.2011.02433.x [doi].

14. Jungnitz H, West NP, Walker MJ, Chhatwal GS, Guzman CA (1998) A second two-component regulatory system of Bordetella bronchiseptica required for bacterial resistance to oxidative stress, production of acid phosphatase, and in vivo persistence. Infect Immun 66: 4640-4650.

15. Erental A, Sharon I, Engelberg-Kulka H (2012) Two programmed cell death systems in Escherichia coli: an apoptotic-like death is inhibited by the mazEF-

mediated death pathway. PLoS Biol 10: e1001281. 10.1371/journal.pbio.1001281 [doi];PBIOLOGY-D-11-02298 [pii].

16. Dwyer DJ, Camacho DM, Kohanski MA, Callura JM, Collins JJ (2012) Antibiotic-induced bacterial cell death exhibits physiological and biochemical hallmarks of apoptosis. Mol Cell 46: 561-572. S1097-2765(12)00349-8 [pii];10.1016/j.molcel.2012.04.027 [doi].

17. Mousavi SA, Robson GD (2004) Oxidative and amphotericin B-mediated cell death in the opportunistic pathogen Aspergillus fumigatus is associated with an apoptotic-like phenotype. Microbiology 150: 1937-1945. 10.1099/mic.0.26830-0 [doi];150/6/1937 [pii].

18. Carmona-Gutierrez D, Eisenberg T, Buttner S, Meisinger C, Kroemer G, Madeo F (2010) Apoptosis in yeast: triggers, pathways, subroutines. Cell Death Differ 17: 763-773. cdd2009219 [pii];10.1038/cdd.2009.219 [doi].

19. Jimenez V, Paredes R, Sosa MA, Galanti N (2008) Natural programmed cell death in T. cruzi epimastigotes maintained in axenic cultures. J Cell Biochem 105: 688-698. 10.1002/jcb.21864 [doi].

20. Nasirudeen AM, Hian YE, Singh M, Tan KS (2004) Metronidazole induces programmed cell death in the protozoan parasite Blastocystis hominis. Microbiology 150: 33-43.

21. Giansanti V, Dona F, Tillhon M, Scovassi AI (2010) PARP inhibitors: new tools to protect from inflammation. Biochem Pharmacol 80: 1869-1877. S0006-2952(10)00296-0 [pii];10.1016/j.bcp.2010.04.022 [doi].

22. Jeggo PA (1998) DNA repair: P. Curr Biol 8: R49-R51. S0960-9822(98)70032-6 [pii].

23. Woodhouse BC, Dianov GL (2008) Poly ADP-ribose polymerase-1: an international molecule of mystery. DNA Repair (Amst) 7: 1077-1086. S1568-7864(08)00118-3 [pii];10.1016/j.dnarep.2008.03.009 [doi].

24. Peralta-Leal A, Rodriguez-Vargas JM, Aguilar-Quesada R, Rodriguez MI, Linares JL, de Almodovar MR, Oliver FJ (2009) PARP inhibitors: new partners in the therapy of cancer and inflammatory diseases. Free Radic Biol Med 47: 13-26. S0891-5849(09)00208-1 [pii];10.1016/j.freeradbiomed.2009.04.008 [doi].

25. Michel B (2005) After 30 years of study, the bacterial SOS response still surprises us. PLoS Biol 3: e255. 05-PLBI-P-0386 [pii];10.1371/journal.pbio.0030255 [doi].

26. Autret S, Levine A, Holland IB, Seror SJ (1997) Cell cycle checkpoints in bacteria. Biochimie 79: 549-554. S0300-9084(97)82002-0 [pii].

27. Kuzminov A (1999) Recombinational repair of DNA damage in Escherichia coli and bacteriophage lambda. Microbiol Mol Biol Rev 63: 751-813, table.

28. Zgur-Bertok D (2013) DNA damage repair and bacterial pathogens. PLoS Pathog 9: e1003711. 10.1371/journal.ppat.1003711 [doi];PPATHOGENS-D-13-01803 [pii].

29. Aravind L, Walker DR, Koonin EV (1999) Conserved domains in DNA repair proteins and evolution of repair systems. Nucleic Acids Res 27: 1223-1242. gkc255 [pii].

30. Justice SS, Hunstad DA, Cegelski L, Hultgren SJ (2008) Morphological plasticity as a bacterial survival strategy. Nat Rev Microbiol 6: 162-168. nrmicro1820 [pii];10.1038/nrmicro1820 [doi].

31. Al Mamun AA, Gautam S, Humayun MZ (2006) Hypermutagenesis in mutA cells is mediated by mistranslational corruption of polymerase, and is accompanied by replication fork collapse. Mol Microbiol 62: 1752-1763.

32. Gautam S, Kalidindi R, Humayun MZ (2012) SOS induction and mutagenesis by dnaQ missense alleles in wild type cells. Mutat Res 735: 46-50. S0027-5107(12)00126-1 [pii];10.1016/j.mrfmmm.2012.05.004 [doi].

33. Livny J, Friedman DI (2004) Characterizing spontaneous induction of Stx encoding phages using a selectable reporter system. Mol Microbiol 51: 1691-1704. 3934 [pii].

34. Raju KK, Gautam S, Sharma A (2006) Molecules involved in the modulation of rapid cell death in Xanthomonas. J Bacteriol 188: 5408-5416. 188/15/5408 [pii];10.1128/JB.00056-06 [doi].

35. Gautam S, Sharma A (2002) Rapid cell death in Xanthomonas campestris pv. glycines. J Gen Appl Microbiol 48: 67-76.

36. Gautam S, Sharma A (2002) Involvement of caspase-3-like protein in rapid cell death of Xanthomonas. Mol Microbiol 44: 393-401. 2837 [pii].

37. Gautam S., Sharma A, Kobayashi I (2005) Programmed cell death in microorganisms. Survival and Death in Bacteria Research Sign Post Press, India .

38. Gautam S., Sharma A (2005) Programmed cell death: an overview. Advances in biochemistry and biotechnology 122-157.

39. Hakansson AP, Roche-Hakansson H, Mossberg AK, Svanborg C (2011) Apoptosis-like death in bacteria induced by HAMLET, a human milk lipid-protein complex. PLoS One 6: e17717. 10.1371/journal.pone.0017717 [doi].

40. LOWRY OH, ROSEBROUGH NJ, FARR AL, RANDALL RJ (1951) Protein measurement with the Folin phenol reagent. J Biol Chem 193: 265-275.

41. Saxena S, Gautam S, Maru G, Kawle D, Sharma A (2012) Suppression of error prone pathway is responsible for antimutagenic activity of honey. Food Chem Toxicol 50: 625-633. S0278-6915(12)00012-9 [pii];10.1016/j.fct.2012.01.003 [doi].

42. Vincent F, Tibi A, Goury V, Darbord JC (1990) Combined treatment using irradiation and heat: Susceptibility of bacillus, salmonella, staphylococcus and clostridium. International Journal of Radiation Applications and Instrumentation Part C Radiation Physics and Chemistry 35: 279-283.

43. Ning SB, Guo HL, Wang L, Song YC (2002) Salt stress induces programmed cell death in prokaryotic organism Anabaena. J Appl Microbiol 93: 15-28. 1651 [pii].

44. Sahoo S, Rao KK, Suraishkumar GK (2006) Reactive oxygen species induced by shear stress mediate cell death in Bacillus subtilis. Biotechnol Bioeng 94: 118-127. 10.1002/bit.20835 [doi].

45. Koonin EV, Aravind L (2002) Origin and evolution of eukaryotic apoptosis: the bacterial connection. Cell Death Differ 9: 394-404. 10.1038/sj/cdd/4400991 [doi].

46. Jimenez C, Capasso JM, Edelstein CL, Rivard CJ, Lucia S, Breusegem S, Berl T, Segovia M (2009) Different ways to die: cell death modes of the unicellular chlorophyte Dunaliella viridis exposed to various environmental stresses are mediated by the caspase-like activity DEVDase. J Exp Bot 60: 815-828. ern330 [pii];10.1093/jxb/ern330 [doi].

47. O'Donovan N, Crown J, Stunell H, Hill AD, McDermott E, O'Higgins N, Duffy MJ (2003) Caspase 3 in breast cancer. Clin Cancer Res 9: 738-742.

48. Schotte P, Declercq W, Van HS, Vandenabeele P, Beyaert R (1999) Non-specific effects of methyl ketone peptide inhibitors of caspases. FEBS Lett 442: 117-121. S0014-5793(98)01640-8 [pii].

49. Toyooka K, Tai XG, Park CS, Yashiro Y, Hamaoka T, Fujiwara H (1998) A caspase inhibitor protects thymocytes from diverse signal-mediated apoptosis but not from clonal deletion in fetal thymus organ culture. Immunol Lett 63: 83-89. S0165-2478(98)00059-5 [pii].

50. Kim KY, Seol JY, Jeon GA, Nam MJ (2003) The combined treatment of aspirin and radiation induces apoptosis by the regulation of bcl-2 and caspase-3 in human cervical cancer cell. Cancer Lett 189: 157-166. S0304383502005190 [pii].

51. Michelin S, del Rosario PM, Dubner D, Gisone P (2004) Increased activity and involvement of caspase-3 in radiation-induced apoptosis in neural cells

precursors from developing rat brain. Neurotoxicology 25: 387-398. 10.1016/j.neuro.2003.08.009 [doi];S0161-813X(03)00169-4 [pii].

52. Naito M, Nagashima K, Mashima T, Tsuruo T (1997) Phosphatidylserine externalization is a downstream event of interleukin-1 beta-converting enzyme family protease activation during apoptosis. Blood 89: 2060-2066.

53. Janion C (2008) Inducible SOS response system of DNA repair and mutagenesis in Escherichia coli. Int J Biol Sci 4: 338-344.

54. Darzynkiewicz Z, Galkowski D, Zhao H (2008) Analysis of apoptosis by cytometry using TUNEL assay. Methods 44: 250-254. S1046-2023(07)00217-4 [pii];10.1016/j.ymeth.2007.11.008 [doi].

55. Costa SB, Campos AC, Pereira AC, de Mattos-Guaraldi AL, Junior RH, Rosa AC, Asad LM (2014) Adherence to abiotic surface induces SOS response in Escherichia coli K-12 strains under aerobic and anaerobic conditions. Microbiology 160: 1964-1973. mic.0.075317-0 [pii];10.1099/mic.0.075317-0 [doi].

Chapter 5: Summary and Conclusion

5.1 Summary and Conclusion

PCD similar to that found in eukaryotes was reported in *Xanthomonas campestris* pv. *glycines* (Xcg), the causal agent of the bacterial pustule disease of soybean (*Glycine max*), from this laboratory [1,2]. PCD in Xcg was found to be induced in protein rich media {like, Luria-Bertani (LB), nutrient broth (NB), and casein medium} but not in carbohydrate rich starch medium, which was usually employed for maintenance of this organism. The growth medium was found to play an important role in governing the metabolism of *Xanthomonas* and in inducing PCD in this organism. This was evident from the observed reduction in generation time from 126 min in starch minimal medium (PNIM) to 90 min in Luria Bertani (LB) broth (i.e. PIM). But this increase in growth rate was not without its harmful effects and the cells grown in PIM were observed to undergo PCD in the post exponential phase. Hence, the trigger(s) for PCD in *Xanthomonas* grown in PIM was investigated in this study. Based on the findings of this work, a possible mechanism of PCD in *Xanthomonas* is proposed in Fig. 5.1.

A protein rich medium (like LB) lacking a carbohydrate source serves as a ready source of amino acids and peptides of which glutamate and proline are in predominance [3]. *Xanthomonas* has been reported to produce extracellular proteases [4]. These proteases help in breaking down the peptides to free amino acids which can be taken up by the cell.

These amino acids can serve both as a source of carbon and nitrogen in the cell. All amino acids except proline are known to enter the central metabolic pathway, the tricarboxylic acid (TCA) cycle through transamination. This surge in availability of amino acids is presumed to increase the NADH derived from TCA cycle resulting in metabolic stress. Meanwhile, high intracellular levels of proline were found to increase PutA (proline oxidase) activity, an enzyme solely dedicated to the oxidation of this secondary amino acid (Fig. 5.1). Both, metabolic stress and enhanced PutA activity were observed to play a decisive role in the PCD of this bacterium. The reductants NADH and $FADH_2$ derived from TCA cycle and PutA activity, respectively, are channelized to ETC increasing the electron flux (Fig. 5.1). Although electron transport occurs with great efficiency, a small percentage of electrons are prematurely leaked to oxygen, resulting in the formation of the toxic superoxide radical ($O_2^{\cdot-}$) and subsequently other ROS. Similar findings have been reported in eukaryotes too [5,6]. It has been demonstrated earlier that $FADH_2$ produced during the oxidation of proline to glutamate transfers electrons directly to ubiquinone of ETC, thus fuelling electron leakage and contributing to the ROS pool of the cell [7]. In this study, the PutA activity in *Xanthomonas* was observed to be inhibited by ETC inhibitors rotenone and antimycin. It was also observed that the oxidation of proline by PutA led to ROS generation and PCD in *Xanthomonas* (Fig 5.1). ROS have also been reported to play a significant role in PCD of *E. coli, Bacillus subtilis, S. pneumoniae* and *S. aureus* [8–11]. Additionally, DNA damage and PS externalization have been reported in the PCD of *E. coli* [8,9,11].

Metabolic stress induced apoptosis has been well studied in animal cell lines [12]. Moreover, several other diseases like phenylketonuria, Lesch-Nyhan syndrome and alcaptonuria in humans are also caused due to metabolic imbalance. Cancer is also considered a paradigm of metabolic imbalance associated disease. Dysfunctional mitochondrial metabolism and

accumulation of certain TCA cycle metabolites have been reported to promote aberrant signaling in tumor cells. The pro-oncogenic role of certain TCA cycle enzymes like succinate dehydrogenase, fumarate hydratase, isocitrate dehydrogenase, and α-ketoglutarate dehydrogenase has also been demonstrated [13].

Interestingly, Proline oxidase (POX) is regarded as a tumor suppressor protein in humans and any anomaly in its functioning results in cancer. POX activation in higher systems has been reported to induce both intrinsic and extrinsic pathways of apoptosis by regulating the redox homeostasis of the cell and has been observed to activate caspase-3, 8 and 9 [7,14–17]. Similar findings in relation to PutA have been observed in this study.

To evaluate the conserved existence of PCD-like process in other bacteria besides *Xanthomonas, Bacillus subtilis, Bordetella bronchiseptica, Escherichia coli* and *Salmonella enterica* sv. Typhimurium were also studied. Radiation was used as a means to generate ROS. Since eukaryotes are known to undergo radiation induced PCD involving caspase activation [18], it was interesting to investigate whether radiation-induced cell death (RICD) in bacteria was programmed or not. Hence, it was interesting to study the nature of cell death after gamma radiation treatment in *Xanthomonas* and some other bacteria (*B.subtilis, B. bronchiseptica, E.coli* and *S. enterica* sv. Typhimurium). *Xanthomonas* was found to be the most radiosensitive of all. Radiation exposed cells of all these bacteria were found to express markers of PCD i.e. ROS generation, activation of caspase-3-like protein and PS externalization. Moreover, in *E. coli* the cell permeable caspase-3 inhibitor was found to inhibit SOS induction significantly suggesting that PCD and SOS induction might be interlinked.

In conclusion, the growth medium induced acceleration of metabolism in *Xanthomonas* was responsible for generation of surplus reductants, leading to electron leakage from ETC, and hence excessive ROS formation. Eventually cells succumbed to this metabolism driven oxidative stress. Proline oxidation by PutA was also found to be an important contributing factor to the ROS pool. Furthermore, other triggers of oxidative stress like exposure to gamma or UV radiation also induced programmed cell death in bacteria.

5.2 Key Findings of the Study

- Involvement of PutA in bacterial PCD: activation of PutA in PIM grown Xcc cells generated high ROS levels causing DNA damage and eventually cell death indicating a conserved role of this protein in PCD.
- Caspase-3-like enzyme activity was found to be present in other bacteria like *E. coli*, *S.enterica* sv. Typhimurium, *B. subtilis* and *B. bronchiseptica* besides *Xanthomonas.*
- ROS generated due to radiation exposure was observed to cause caspase-3 dependent PCD in these bacteria
- Caspase-3 and endonuclease inhibitors were found to decrease SOS induction in radiation exposed *E. coli* cells

5.3 Future Perspectives

As *Xanthomonas* represents one of the major groups of bacterial plant pathogens, understanding the balance between its survival and death could not only provide significant clues to microbial growth control and regulation but also have broad practical significance in agriculture. Since the process of PCD has been found to be evolutionarily conserved,

understanding its mechanism in a bacterial system like *Xanthomonas* will be helpful in deciphering the evolutionary linkage of this process. As a number of proteins orchestrate PCD in a eukaryotic cell, it is possible that a similar mechanism might be functioning in a bacterial cell too. Investigating the key proteins driving this phenomenon and their regulation in bacteria will improve our understanding about this process.

PCD in other bacteria (including food borne pathogens *E. coli* and *Salmonella*) in response to gamma radiation observed in this study provides an interesting lead. Exploring the mechanism by which caspase-3 inhibitor prevents SOS induction in *E. coli* will improve the understanding of DNA damage repair and PCD process in bacteria.

Figure 5.1

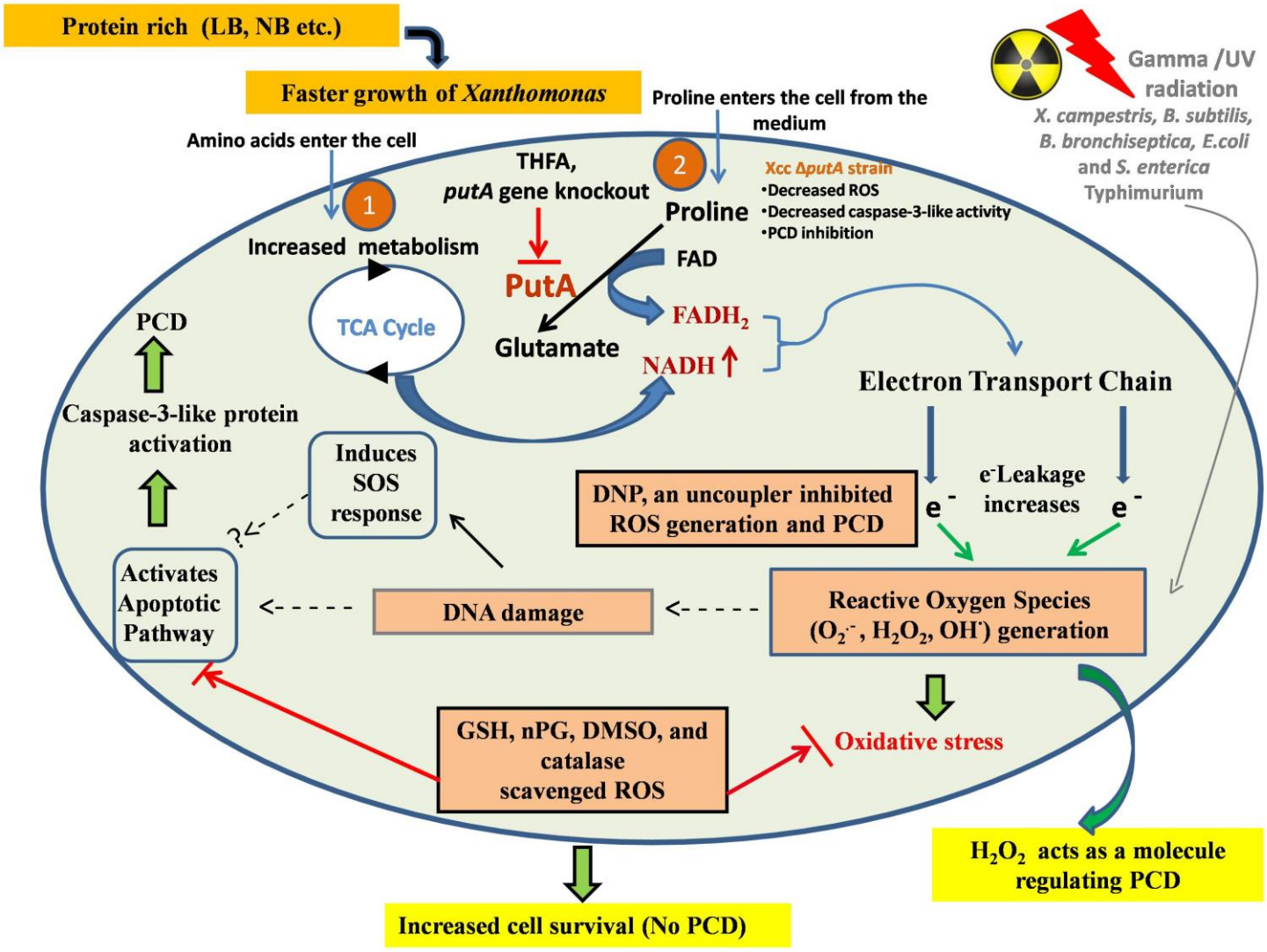

Fig.5.1: Proposed mechanism of PCD in *Xanthomonas* cells under metabolic stress or *E.coli* and other bacteria upon oxidative stress

References

1. Gautam S, Sharma A (2002) Rapid cell death in Xanthomonas campestris pv. glycines. J Gen Appl Microbiol 48: 67-76.

2. Gautam S, Sharma A (2002) Involvement of caspase-3-like protein in rapid cell death of Xanthomonas. Mol Microbiol 44: 393-401. 2837 [pii].

3. Sezonov G, Joseleau-Petit D, D'Ari R (2007) Escherichia coli physiology in Luria-Bertani broth. J Bacteriol 189: 8746-8749. JB.01368-07 [pii];10.1128/JB.01368-07 [doi].

4. Syed AN (1998) Molecular mechanisms of plant pathogen interactions. Ph D thesis, Mumbai University .

5. Murphy MP (2009) How mitochondria produce reactive oxygen species. Biochem J 417: 1-13. BJ20081386 [pii];10.1042/BJ20081386 [doi].

6. Turrens JF (2003) Mitochondrial formation of reactive oxygen species. J Physiol 552: 335-344. 10.1113/jphysiol.2003.049478 [doi];jphysiol.2003.049478 [pii].

7. Liu W, Phang JM (2012) Proline dehydrogenase (oxidase) in cancer. Biofactors 38: 398-406. 10.1002/biof.1036 [doi].

8. Erental A, Sharon I, Engelberg-Kulka H (2012) Two programmed cell death systems in Escherichia coli: an apoptotic-like death is inhibited by the mazEF-mediated death pathway. PLoS Biol 10: e1001281. 10.1371/journal.pbio.1001281 [doi];PBIOLOGY-D-11-02298 [pii].

9. Dwyer DJ, Camacho DM, Kohanski MA, Callura JM, Collins JJ (2012) Antibiotic-induced bacterial cell death exhibits physiological and biochemical hallmarks of apoptosis. Mol Cell 46: 561-572. S1097-2765(12)00349-8 [pii];10.1016/j.molcel.2012.04.027 [doi].

10. Sahoo S, Rao KK, Suraishkumar GK (2006) Reactive oxygen species induced by shear stress mediate cell death in Bacillus subtilis. Biotechnol Bioeng 94: 118-127. 10.1002/bit.20835 [doi].

11. Thomas VC, Sadykov MR, Chaudhari SS, Jones J, Endres JL, Widhelm TJ, Ahn JS, Jawa RS, Zimmerman MC, Bayles KW (2014) A central role for carbon-overflow pathways in the modulation of bacterial cell death. PLoS Pathog 10: e1004205. 10.1371/journal.ppat.1004205 [doi];PPATHOGENS-D-13-03034 [pii].

12. Mathew R, Karantza-Wadsworth V, White E (2007) Role of autophagy in cancer. Nat Rev Cancer 7: 961-967. nrc2254 [pii];10.1038/nrc2254 [doi].

13. DeBerardinis RJ, Thompson CB (2012) Cellular metabolism and disease: what do metabolic outliers teach us? Cell 148: 1132-1144. S0092-8674(12)00232-2 [pii];10.1016/j.cell.2012.02.032 [doi].

14. Liu Y, Borchert GL, Surazynski A, Hu CA, Phang JM (2006) Proline oxidase activates both intrinsic and extrinsic pathways for apoptosis: the role of ROS/superoxides, NFAT and MEK/ERK signaling. Oncogene 25: 5640-5647. 1209564 [pii];10.1038/sj.onc.1209564 [doi].

15. Phang JM, Donald SP, Pandhare J, Liu Y (2008) The metabolism of proline, a stress substrate, modulates carcinogenic pathways. Amino Acids 35: 681-690. 10.1007/s00726-008-0063-4 [doi].

16. Liu Y, Borchert GL, Donald SP, Diwan BA, Anver M, Phang JM (2009) Proline oxidase functions as a mitochondrial tumor suppressor in human cancers. Cancer Res 69: 6414-6422. 0008-5472.CAN-09-1223 [pii];10.1158/0008-5472.CAN-09-1223 [doi].

17. Hu CA, Donald SP, Yu J, Lin WW, Liu Z, Steel G, Obie C, Valle D, Phang JM (2007) Overexpression of proline oxidase induces proline-dependent and mitochondria-mediated apoptosis. Mol Cell Biochem 295: 85-92. 10.1007/s11010-006-9276-6 [doi].

18. Elmore S (2007) Apoptosis: a review of programmed cell death. Toxicol Pathol 35: 495-516. 779478428 [pii];10.1080/01926230701320337 [doi].